# Lightweight Concrete: Transfer and Development Length of Prestressing Strands

Publication FHWA-HIF-19-018

February 2019

Research, Development, and Technology
Turner-Fairbank Highway Research Center
6300 Georgetown Pike
McLean, VA 22101-2296

U.S. Department of Transportation
Federal Highway Administration

# FOREWORD

Broad-based advancements in concrete materials have led to significant enhancements in the performance of lightweight concrete (LWC). Although the value of using LWC within the constructed infrastructure is clear, decades-old performance perceptions continue to hinder wider use of the concrete. Additionally, the lack of modern updates to structural design provisions for LWC has perpetuated additional barriers to the use of LWC. In 2007, the Federal Highway Administration (FHWA) investigated the structural performance of modern LWCs. The study described in this report engaged the academic, public sector, and private sector communities to compile the body of knowledge on LWC while also conducting nearly 100 full-scale structural tests on lightweight concretes.

This report presents the results of transfer length measurement and development length tests on high-strength LWC prestressed girders as well as a compilation of data available from the literature. It also provides potential revisions to the *American Association of State Highway and Transportation Officials Load and Resistance Factor Design Bridge Design Specifications*, with a focus on transfer and development length of prestressing strands in LWC.

Cheryl Allen Richter, P.E., Ph.D.
Director, Office of Infrastructure
Research and Development

# TECHNICAL REPORT DOCUMENTATION PAGE

| | | |
|---|---|---|
| 1. Report No.<br>FHWA-HIF-19-018 | 2. Government Accession No. | 3. Recipient's Catalog No. |
| 4. Title and Subtitle<br>Lightweight Concrete: Transfer and Development Length of Prestressing Strands | | 5. Report Date<br>February 2019<br>6. Performing Organization Code: |
| 7. Author(s)<br>Gary G. Greene and Benjamin A. Graybeal | | 8. Performing Organization Report No. |
| 9. Performing Organization Name and Address<br>Office of Infrastructure Research & Development<br>Federal Highway Administration<br>6300 Georgetown Pike<br>McLean, VA 22101-2296 | | 10. Work Unit No.<br>11. Contract or Grant No. |
| 12. Sponsoring Agency Name and Address<br>Office of Infrastructure Research & Development<br>Federal Highway Administration<br>6300 Georgetown Pike<br>McLean, VA 22101-2296 | | 13. Type of Report and Period Covered<br>Final Report: 2010-2015<br>14. Sponsoring Agency Code<br>HRDI-40 |

15. Supplementary Notes

This document was developed by research staff at the Turner-Fairbank Highway Research Center. Portions of the work were completed by PSI, Inc. under contract DTFH61-10-D-00017. Gary Greene formerly of PSI, Inc., who was the lead contract researcher on FHWA's lightweight concrete research efforts, and Ben Graybeal of FHWA, who manages the FHWA Structural Concrete Research Program, developed this document.

16. Abstract

Much of the fundamental basis for the current lightweight concrete provisions in the AASHTO LRFD Bridge Design Specifications is based on research of lightweight concrete (LWC) from the 1960s. The LWC that was part of this research used traditional mixes of coarse aggregate, fine aggregate, portland cement, and water. Broad-based advancement in concrete technology over the past 50 years has given rise to significant advancements in concrete mechanical and durability performance.

This document describes the results of transfer length measurements and development length tests on high-strength LWC prestressed girders that were conducted as part of an overall FHWA research project on LWC. The FHWA test results are included in a strand bond database with over 250 LWC specimens and 350 NWC specimens available in the literature. An analysis of the database was used to develop potential revisions to provisions related to LWC and NWC within Section 5 of the AASHTO LRFD Bridge Design Specifications. The framework for addressing LWC in the specifications that was proposed previously as a part of this research effort is applied to the design expressions for strand transfer length and development length. The framework includes a revision to the definition of LWC and a revised expression for predicting concrete elastic modulus.

| | |
|---|---|
| 17. Key Words<br>LWC, lightweight concrete, bridge design, LRFD design specifications, transfer length, development length, strand bond | 18. Distribution Statement<br>No restrictions. This document is available through the National Technical Information Service, Springfield, VA 22161. |

| | | | |
|---|---|---|---|
| 19. Security Classif. (of this report)<br>Unclassified | 20. Security Classif. (of this page)<br>Unclassified | 21. No. of Pages<br>206 | 22. Price<br>N/A |

Form DOT F 1700.7 (8-72) Reproduction of completed page authorized

# SI* (MODERN METRIC) CONVERSION FACTORS

## APPROXIMATE CONVERSIONS TO SI UNITS

| Symbol | When You Know | Multiply By | To Find | Symbol |
|---|---|---|---|---|
| | | **LENGTH** | | |
| in | inches | 25.4 | millimeters | mm |
| ft | feet | 0.305 | meters | m |
| yd | yards | 0.914 | meters | m |
| mi | miles | 1.61 | kilometers | km |
| | | **AREA** | | |
| $in^2$ | square inches | 645.2 | square millimeters | $mm^2$ |
| $ft^2$ | square feet | 0.093 | square meters | $m^2$ |
| $yd^2$ | square yard | 0.836 | square meters | $m^2$ |
| ac | acres | 0.405 | hectares | ha |
| $mi^2$ | square miles | 2.59 | square kilometers | $km^2$ |
| | | **VOLUME** | | |
| fl oz | fluid ounces | 29.57 | milliliters | mL |
| gal | gallons | 3.785 | liters | L |
| $ft^3$ | cubic feet | 0.028 | cubic meters | $m^3$ |
| $yd^3$ | cubic yards | 0.765 | cubic meters | $m^3$ |
| | | NOTE: volumes greater than 1000 L shall be shown in $m^3$ | | |
| | | **MASS** | | |
| oz | ounces | 28.35 | grams | g |
| lb | pounds | 0.454 | kilograms | kg |
| T | short tons (2000 lb) | 0.907 | megagrams (or "metric ton") | Mg (or "t") |
| | | **TEMPERATURE (exact degrees)** | | |
| °F | Fahrenheit | 5 (F-32)/9<br>or (F-32)/1.8 | Celsius | °C |
| | | **ILLUMINATION** | | |
| fc | foot-candles | 10.76 | lux | lx |
| fl | foot-Lamberts | 3.426 | $candela/m^2$ | $cd/m^2$ |
| | | **FORCE and PRESSURE or STRESS** | | |
| lbf | poundforce | 4.45 | newtons | N |
| $lbf/in^2$ | poundforce per square inch | 6.89 | kilopascals | kPa |

## APPROXIMATE CONVERSIONS FROM SI UNITS

| Symbol | When You Know | Multiply By | To Find | Symbol |
|---|---|---|---|---|
| | | **LENGTH** | | |
| mm | millimeters | 0.039 | inches | in |
| m | meters | 3.28 | feet | ft |
| m | meters | 1.09 | yards | yd |
| km | kilometers | 0.621 | miles | mi |
| | | **AREA** | | |
| $mm^2$ | square millimeters | 0.0016 | square inches | $in^2$ |
| $m^2$ | square meters | 10.764 | square feet | $ft^2$ |
| $m^2$ | square meters | 1.195 | square yards | $yd^2$ |
| ha | hectares | 2.47 | acres | ac |
| $km^2$ | square kilometers | 0.386 | square miles | $mi^2$ |
| | | **VOLUME** | | |
| mL | milliliters | 0.034 | fluid ounces | fl oz |
| L | liters | 0.264 | gallons | gal |
| $m^3$ | cubic meters | 35.314 | cubic feet | $ft^3$ |
| $m^3$ | cubic meters | 1.307 | cubic yards | $yd^3$ |
| | | **MASS** | | |
| g | grams | 0.035 | ounces | oz |
| kg | kilograms | 2.202 | pounds | lb |
| Mg (or "t") | megagrams (or "metric ton") | 1.103 | short tons (2000 lb) | T |
| | | **TEMPERATURE (exact degrees)** | | |
| °C | Celsius | 1.8C+32 | Fahrenheit | °F |
| | | **ILLUMINATION** | | |
| lx | lux | 0.0929 | foot-candles | fc |
| $cd/m^2$ | $candela/m^2$ | 0.2919 | foot-Lamberts | fl |
| | | **FORCE and PRESSURE or STRESS** | | |
| N | newtons | 0.225 | poundforce | lbf |
| kPa | kilopascals | 0.145 | poundforce per square inch | $lbf/in^2$ |

*SI is the symbol for the International System of Units. Appropriate rounding should be made to comply with Section 4 of ASTM E380.
(Revised March 2003)

## TABLE OF CONTENTS

## LIST OF FIGURES

## LIST OF TABLES

## LIST OF ABBREVIATIONS AND NOTATIONS

### ABBREVIATIONS

| | |
|---|---|
| AASHTO | American Association of State Highway and Transportation Officials |
| AMS | average maximum strain |
| ASTM | American Society for Testing and Materials |
| BT | bulb tee |
| CL | Centerline |
| CSS | concrete surface strain |
| COV | coefficient of variation |
| DEMEC | demountable mechanical strain gauge |
| ERS | electrical resistance strain gauge |
| ESCSI | Expanded Shale, Clay, and Slate Institute |
| FHWA | Federal Highway Administration |
| HG | girder concrete mixture containing Haydite lightweight aggregate |
| LRFD | load-and-resistance factor design, the design philosophy used by current AASHTO bridge design specification |
| LVDT | linear variable differential transformer |
| LWC | lightweight concrete |
| Max. | maximum |
| Min. | minimum |
| NCHRP | National Cooperative Highway Research Program |
| No. | number |
| NWC | normal weight concrete |
| PCI | Precast/Prestressed Concrete Institute |

| | |
|---|---|
| RC | reinforced concrete |
| SCOBS | Subcommittee on Bridges and Structures, a part of the overall AASHTO organizational structure |
| SCP | Standard Concrete Products |
| SDC | specified density concrete |
| SG | girder concrete mixture containing Stalite lightweight aggregate |
| SMR | triple-mirror prism in a spherical steel ball followed by the FARO non-contact laser tracking system |
| T-10 | Concrete Design technical committee in SCOBS |
| TFHRC | Turner-Fairbank Highway Research Center |
| TLD | taut-line deflection |
| UG | girder concrete mixture containing Utelite lightweight aggregate |

## NOTATIONS

| | | |
|---|---|---|
| $a$ | = | shear span or depth of equivalent rectangular stress block |
| $A_{ps}$ | = | area of the longitudinal prestressing steel |
| $A_v$ | = | area of the shear reinforcement within the spacing s |
| $b$ | = | width of the compression face of a rectangular member |
| $b_v$ | = | effective web width |
| $d_b$ | = | nominal diameter of a prestressing strand |
| $d_v$ | = | effective shear depth |
| $d_p$ | = | distance from compression face to the centroid of the prestressing steel |
| $E_c$ | = | modulus of elasticity of concrete |
| $E_{ci}$ | = | modulus of elasticity of concrete at transfer |

$f'_c$ = concrete compressive strength in reference to material test values and specified compressive strength in reference to articles of the AASHTO LRFD Bridge Design Specification

$f'_{ci}$ = concrete compressive strength at time of prestressing in reference to material test values and specified compressive strength at time of prestressing in reference to articles of the AASHTO LRFD Bridge Design Specification

$f_{cpe}$ = compressive stress in the concrete at the extreme tensile fiber after all prestress losses have occurred

$f_{ct}$ = concrete splitting tensile strength

$f_{po}$ = parameter taken as the modulus of elasticity of prestressing steel multiplied by the locked-in difference in strain between the prestresing steel and the surrounding concrete

$f_{pc}$ = compressive stress at the centroid of the concrete after all prestress losses have occurred

$f_{pe}$ = effective stress in the prestressing steel after losses

$f_{ps}$ = average stress in prestressing steel at the time for which the nominal resistance of member is required

$f_{pbt}$ = stress in prestressing steel immediately prior to transfer

$f_{pt}$ = stress in prestressing steel immediately after transfer

$f_{pu}$ = tensile strength of prestressing steel in reference to material tests values and specified tensile strength of prestressing steel in reference to articles of the AASHTO LRFD Bridge Design Specification

$f_{px}$ = design stress in pretensioned strand at nominal flexural strength at section of member under consideration

$f_{yt}$ = specified yield strength of the shear reinforcement

h = member height

k = prestresssing factor

$K_1$ = correction factor for source of aggregate

L = span length

| | | |
|---|---|---|
| $n$ | = | number of data values |
| $\ell_d$ | = | development length |
| $\ell_e$ | = | embedment length which is the bonded length of strand provided from the end of the girder to the critical section |
| $\ell_{e,1}$ | = | embedment length of the first girder end tested |
| $\ell_{e,2}$ | = | embedment length of the second girder end tested |
| $\ell_{fb}$ | = | flexural bond length |
| $\ell_{px}$ | = | distance from free end of pretensioned strand to section of member under consideration |
| $\ell_t$ | = | transfer length |
| $\widehat{\ell_t}$ | = | predicted transfer length |
| $\ell_{ti}$ | = | transfer length determined using measurements taken immediately after prestress transfer |
| $\ell_{t,test}$ | = | transfer length determined using measurements taken prior to testing to failure |
| $m$ | = | measured transfer length divided by normalizing parameters |
| $\bar{m}$ | = | mean of a group of measured transfer length divided by the same normalizing parameters |
| $M$ | = | applied moment |
| $M_{cr}$ | = | flexural cracking moment |
| $M_{test}$ | = | ultimate moment |
| $M_n$ | = | nominal flexural resistance |
| $R^2$ | = | coefficient of determination |
| $s$ | = | spacing of the shear reinforcement |
| $V_{cr}$ | = | applied shear force at web cracking |

$V_p$ = component of the effective prestressing force in the direction of the applied shear, positive if resisting the applied shear

$w_c$ = concrete unit weight

$\bar{y}$ = mean of all of the $y_i$ values

$y_i$ = individual value on the vertical axis

$\hat{y}_i$ = predicted vertical-axis value corresponding to $y_i$

$\Delta f_p$ = difference between $f_{ps}$ and $f_{pe}$

$\varepsilon_t$ = strain measured in the stirrups by electrical resistance strain gauges

$\varepsilon_{ty}$ = stirrup yield strain

$\varepsilon_x$ = calculated longitudinal strain at the mid-depth of the member

$\kappa$ = multiplier for strand development length

$\lambda$ = lightweight concrete modification factor

$\rho_v$ = transverse reinforcement ratio ($A_v/b_vs$)

# CHAPTER 1. INTRODUCTION

## INTRODUCTION

Much of the fundamental basis for the lightweight concrete provisions in the AASHTO LRFD Bridge Design Specifications prior to the 2015 Interim Revisions[1] was based on research of lightweight concrete (LWC) from the 1960s.[2-5] The LWC that was part of this research used traditional mixes of coarse aggregate, fine aggregate, portland cement, and water. Broad-based advancement in concrete technology over the past 50 years has given rise to significant advancements in concrete mechanical and durability performance. Research during the past 30 years including the recent National Cooperative Highway Research Program (NCHRP) studies on different aspects of high-strength concrete has resulted in revisions to the AASHTO LRFD Specifications to capitalize on the benefits of high-strength normal weight concrete (NWC). However, as described by Russell[6], many of the design equations in the AASHTO LRFD Specifications are based on data that do not include tests of LWC specimens, particularly with regard to structural members with compressive strengths in excess of 6 ksi (41 MPa).

The Federal Highway Administration (FHWA) at the Turner-Fairbank Highway Research Center (TFHRC) has executed a research program investigating the performance of LWC with concrete compressive strengths in the range of 6 to 10 ksi (41 to 69 MPa) and equilibrium densities between 0.125 kcf to 0.135 kcf (2000 to 2160 kg/m$^3$). The research program used LWC with three different lightweight aggregates that are intended to be representative of those available in North America. The program included tests from 27 precast/prestressed LWC girders to investigate topics including transfer length and development length of prestressing strand, the time-dependent prestress losses, and shear strength of LWC. The development and splice length of mild steel reinforcement used in girders and decks made with LWC was also investigated using 40 reinforced concrete (RC) beams. While much of the research program focused on structural behavior, it also included a material characterization component wherein the compressive strength, elastic modulus, and splitting tensile strength of the concrete mixes used in the structural testing program were assessed. One key outcome of the research program is to recommend changes to the AASHTO LRFD Bridge Design Specifications relevant to LWC.

This document describes the results of transfer length measurements on 18 prestressed girders and development length tests on 12 prestressed girders used to evaluate the bond of prestressing strands in high-strength LWC. The LWC prestressed girders tested in this study are included in a database of transfer length measurements and development length tests on LWC and NWC specimens that was collected from test results available in the literature. This document describes the database and the analysis of the database. Design expressions in the current edition of the AASHTO LRFD Bridge Design Specifications[7] and prediction expressions found in the literature are compared to the database. Potential revisions to the AASHTO LRFD Bridge Design Specifications relating to LWC and NWC are presented.

## OBJECTIVE

There are three objectives for this document. The first objective is to describe the results of transfer length measurements and development length tests on LWC prestressed girders conducted at TFHRC. The second objective is to describe a database including the TFHRC test results and to describe the analysis of the database. The third objective is to develop and present potential revisions to the AASHTO LRFD Bridge Design Specifications relating to the transfer and development length of prestressing strands, with a focus on the performance of LWC.

## OUTLINE OF DOCUMENT

Introductory material in Chapter 2 summarizes the properties of LWC, the treatment of LWC in the AASHTO LRFD Bridge Design Specifications, the mechanism of bond transfer, the factors affecting transfer and development length, and the design expressions for transfer and development length in the AASHTO LRFD Bridge Design Specifications and in the literature. Chapter 3 describes the transfer length measurements and development length tests of LWC prestressed girders, summarizes the test results, and provides a discussion of the results. A description of the strand bond database is given in Chapter 4 and includes statistical information about the database. Chapter 5 includes an analysis of the database and comparisons of the transfer length, flexural bond length, and development length determined by prediction expressions to the measured lengths for specimens in the database. Potential revisions to the AASHTO LRFD Bridge Design Specifications are included in Chapter 6. Chapter 7 provides concluding remarks. References to the papers and reports used in the strand bond database are included in Chapter 8.

The units for stress and elastic modulus are ksi and the units for unit weight are kcf for all expressions unless stated otherwise. SI units are given in parentheses for values in the text and conversion factors are provided for values in the tables.

## SUMMARY OF PRELIMINARY RECOMMENDATIONS

Several revisions to the AASHTO LRFD Bridge Design Specifications related to the transfer and development length of prestressing strand in LWC and NWC are proposed in this document. The revisions involve separate expressions for the transfer length of LWC members and NWC members, the expression for strand development length, and the expression for design strand stress.

The revisions proposed in this document are based on the recommendations made in previous documents that are a part of this research effort[8-10] and were originally included in the 2015 Interim Revisions[11] to the AASHTO LRFD Bridge Design Specifications and the AASHTO LRFD Bridge Construction Specifications. The previous recommendations relate to the definition of LWC, concrete elastic modulus, and a modification factor for LWC. The definition

of LWC was revised to include concrete with lightweight aggregates up to a unit weight of 0.135 kcf (2160 kg/m$^3$), which is considered the lower limit for NWC. Also, the terms “sand-lightweight concrete” and “all-lightweight concrete” were removed in the definition to allow other types of LWC mixtures. A concrete density modification factor was included to allow a more unified approach of accounting for the mechanical properties of LWC.

The concrete density modification factor was evaluated in expressions for predicting transfer length and development length in Chapter 5. The proposed code language presented in Chapter 6 does not include the LWC modification factor.

# CHAPTER 2. BACKGROUND

## INTRODUCTION

This chapter provides background information relevant to the focus of the research effort. This information begins with a description of the mechanical properties of LWC, the gap of equilibrium densities in previous editions of the AASHTO LRFD Specifications, and the LWC modification factor. The rest of the chapter covers the bond strength of prestressing strand. The information on bond strength includes bond transfer mechanisms, factors that influence transfer length and development length, and a summary of previous research on the bond of prestressing strands in LWC. Expressions for predicting the transfer and development length of strands from the literature and in the AASHTO LRFD Bridge Design Specification are described.

## MECHANICAL PROPERTIES OF LWC

The aggregate in LWC can either be manufactured or natural, with a cellular pore system providing for a lower density particle. The density of lightweight aggregate is approximately half of that of normal weight rock. The reduced dead weight of the LWC has many benefits in building and bridge construction such as smaller, lighter members, longer spans, and reduced substructures and foundations requirements.[11]

As compared to NWC, LWC tends to exhibit a reduction in tensile strength. This difference is generally attributed to the characteristics of the lightweight aggregate. The performance of concrete structures is affected by the tensile strength of concrete in several significant ways. The reduced tensile strength of LWC can affect the shear strength, cracking strength at the release of prestress, and bond strength of prestressed and non-prestressed reinforcement.[11]

## EQUILIBRIUM DENSITY GAP IN PREVIOUS EDITIONS OF AASHTO LRFD

The definition for LWC in the AASHTO LRFD Specifications prior to the 2015 revisions of the 7th edition[1] covered concrete having lightweight aggregate and an air-dry unit weight less than or equal to 0.120 kcf (1920 kg/m$^3$). Normal weight concrete was defined as having a unit weight from 0.135 to 0.155 kcf (2160 to 2480 kg/m$^3$). Concretes in the gap of densities between 0.120 and 0.135 kcf (1920 to 2160 kg/m$^3$) are commonly referred to as "specified density concrete" and were not directly addressed by the AASHTO LRFD Bridge Design Specifications. Specified density concrete (SDC) typically contains a mixture of normal weight and lightweight coarse aggregate.

Modifications to AASHTO LRFD Bridge Design Specifications were made in the 2015 revisions of the 7th edition[11] to remove the SDC-related ambiguity, to give the designer the freedom of specifying a slightly lower density than NWC, and to allow for appropriate design with SDC. The inclusion of SDC into AASHTO LRFD required modifications to the definition of LWC and NWC and modifications to design expressions.

## TRANSFER LENGTH

The AASHTO LRFD Bridge Design Specifications define transfer length as the length over which the pretensioning force is transferred to the concrete by bond and friction in a pretensioned member.[7] An accurate estimation of the transfer length is important for several reasons: calculation of the concrete stresses at transfer and under service loads, design of anchorage zone reinforcement for strut-and-tie models, and design of shear reinforcement which requires knowledge of the level of precompression in the concrete.[13]

The extreme concrete fiber stress is determined at the time of prestress transfer and at the Service Limit State. Overestimation of the transfer length is unconservative in the determination of fiber stresses.[14]

The nominal resistance of tension ties in strut-and-tie models is dependent on the stress in the prestressing steel. An underestimation of the transfer length would result in an overestimation of the effective prestress. The result is a potentially unconservative estimation of the tie resistance.[14]

Transfer is also important in determining the shear resistance because the concrete compressive stress due to prestressing increases the member's shear resistance. Underestimation of the transfer length would result in an overestimation of the level precompression due to prestressing and a potentially unconservative estimation of the shear resistance.[14]

### TRANSFER BOND MECHANISMS

There are three general mechanisms that contribute to the transfer of the prestressing: adhesion, friction, and mechanical resistance.[15,16] The role of adhesion between the strand and concrete plays a minimal role because of the relative slip between the two materials. The two most significant mechanisms that contribute to prestress transfer bond are friction and mechanical resistance.[14]

During the pretensioning process, the strands are stretched resulting in reduction of the diameter proportional to Poisson's ratio. After concrete casting and prestress transfer, the loss of all stress at the end of the strand results in an enlargement of the strand diameter due to Poisson's effect. The strand diameter is reduced by development of stress in the strand. This results in the end of the strand being wedge-shaped. Radial compressive stresses in the concrete around the strand result in friction being developed between the strand and concrete. The expansion of the strand, radial compressive stress, and resulting frictional bond stresses are commonly referred to as the "Hoyer Effect."[17]

A small amount of relative slip between the concrete and the helical shape of the seven-wire strand develops bearing stresses at the interface between the strand and the surrounding concrete. These bearing stresses result in mechanical resistance between the strand and concrete. The twist

at the strand's free end is unrestrained, resulting in a minimal contribution of mechanical resistance at the end of the member.[18] The Hoyer Effect develops frictional bond stresses and also serves to restrain twist in the strand. As a result, the bond developed by mechanical resistance is more significant away from the free end of the strand.[19]

## FACTORS INFLUENCING TRANSFER LENGTH

There are many variables known to affect transfer length. Transfer length has been shown by previous research to be proportional to strand diameter.[14,16,20-22] Transfer length is also strongly influence by the stress level in the strand.[16,21] Other variables that can affect the transfer length include surface condition of the steel (clean, oiled, rusted), time-dependent effects (concrete creep and shrinkage, strand relaxation), method of release (flame cut, gradual release), and concrete properties (compressive strength, tensile strength, and modulus of elasticity).[13,19,21,23] In many previous investigations the transfer length was measured at release of the prestress. Previous research has shown that the transfer length does not change significantly after release.[23]

Research on small specimens with only a few strands has shown that strands that were flame cut had longer transfer lengths than strands that were released gradually.[21] Research has shown that flame cutting the strands of large AASHTO-type girders with multiple strands causes less of an increase in transfer length than flame cutting the strands of small, single-strand members.[19]. This is due to the greater mass of concrete being more capable of distributing the energy and stress induced by flame cutting.

## INFLUENCE OF CONCRETE PROPERTIES

The stresses generated in the concrete due to the Hoyer Effect are relatively small and the concrete remains elastic. In this short region near the end of the strand, the radial compressive stress depends directly on the elastic modulus of the concrete. Beyond this region, the circumferential tensile stress of concrete is exceeded and concrete does not behave elastically. Studies have shown that the inelastic region extends along 90 percent of the transfer length for NWC.[13,14] In the inelastic region, the radial compressive stress depends on both the elastic modulus and the tensile capacity of concrete.[13]

Both the elastic modulus and tensile capacity of LWC are commonly less than normal weight concrete of the same compressive strength. Previous test specimens using LWC have had varied results as to the whether AASHTO bridge design specifications gave accurate predictions of the transfer length.[24-26]

## PREDICTIVE EXPRESSIONS FOR TRANSFER LENGTH

The following section includes a description of several expressions for predicting transfer length. Included are design expressions in the AASHTO LRFD Bridge Design Specifications, AASHTO

Standard Specifications for Highway Bridges, and the ACI 318 Building Code. Expressions developed by researchers for use with NWC and LWC are also included.

### *AASHTO Specifications*

The Standard Specifications for Highway Bridges, 16th Edition[27] (AASHTO 16th) recommends the expression in Eq. 1 for transfer length. The expression in Eq. 2 is recommended by the AASHTO LRFD Bridge Design Specifications, 4th Edition[1] (AASHTO LRFD) resulting in a calculated transfer length that is 20 percent longer than the one calculated by Eq. 1.

$$\ell_t = 50 d_b \quad \text{(Eq. 1)}$$

$$\ell_t = 60 d_b \quad \text{(Eq. 2)}$$

### *ACI Building Code*

The expression for transfer length in the ACI 318-14 Building Code[28] is given by Eq. 3. This expression was derived by Mattock[29] who assumed a uniform bond stress of 400 psi based on the research of Hanson and Kaar[16]. The expression in Eq. 3 was developed for Grade 250 prestressing strand (i.e., 250 ksi (1720 MPa) ultimate strength). Assuming a 150 ksi (1030 MPa) effective stress ($f_{pe}$), then Eq. 3 simplifies to the expression in Eq. 1.

Since the development of Eq. 1, construction practice has changed and Grade 270 strand (i.e., 270 ksi (1860 MPa) ultimate strength) is currently most commonly used. If a 180 ksi (1240 MPa) effective stress is assumed for the Grade 270 strands, then this represents a 20 percent increase in the effective stress over the stress assumed for the Grade 250 strand. Assuming the same uniform bond stress of 400 psi, Eq. 2 incorporates the 20 percent increase in effective stress over Eq. 1.

$$\ell_t = \frac{f_{pe} d_b}{3} \quad \text{(Eq. 3)}$$

### *Mitchell et al.*

The expression in Eq. 4 was the result of research by Mitchell, Cook, Khan and Tham[22] on 22 precast, pretensioned normal weight concrete beams to investigate the effect of the concrete compressive strength and strand diameter on transfer and development length. The beams had a small cross section with a single strand and the prestress was released gradually. The compressive strength at release varied from 3.0 ksi to 7.3 ksi (20.7 to 50.3 MPa), and the nominal strand diameters varied from 0.375 inch to 0.62 inch (9.5 mm to 16 mm).

$$\ell_t = 0.33 f_{pt} d_b \sqrt{\frac{3}{f'_{ci}}} \quad \text{(Eq. 4)}$$

***Zia and Mostafa***

The empirical expression for transfer length developed by Zia and Mostafa[21] is given by Eq. 5 and was based on data available in the literature. The data was from normal weight concrete specimens with nominal strand diameters that ranged from 0.25 inch to 0.75 inch (6.4 mm to 19 mm). The investigators stated that their expression was applicable to concrete strengths ranging from 2.0 to 8.0 ksi (13.8 to 55.2 MPa).

$$\ell_t = 1.5\frac{f_{pt}d_b}{f'_c} - 4.6 \qquad \text{(Eq. 5)}$$

***Buckner***

Buckner[20] performed a review of the literature related to transfer and development length and he analyzed the data from several studies that were published in the early 1990s. As part of his analysis, he developed Eq. 6 based on the data from normal weight specimens that had only one 0.5 inch (13 mm) nominal diameter fully bonded seven-wire strand. Buckner's study indicated an influence of the modulus of elasticity of concrete ($E_{ci}$) on transfer length.

$$\ell_t = \frac{1250f_{pt}d_b}{E_{ci}} \qquad \text{(Eq. 6)}$$

***Thatcher et al.***

The study by Thatcher, Heffington, Lolozs, Sylva, Breen, and Burns[24] also indicated an influence of the modulus of elasticity on transfer length. The study included transfer length measurements on six AASHTO Type I girders with 0.5 inch (13 mm) nominal diameter seven-wire strands. Concrete strength at release ranged from 4.9 ksi to 5.6 ksi (33.8 to 38.6 MPa). The concrete mix used expanded clay coarse aggregate and natural sand. Their expression for transfer length is given by Eq. 7 and is 72 percent of the value calculated by Eq. 6.

$$\ell_t = \frac{900f_{pt}d_b}{E_{ci}} \qquad \text{(Eq. 7)}$$

***Meyer et al.***

A study was performed on high-strength lightweight concrete by Meyer, Kahn, Lai and Kurtis[25]. The study included transfer length measurements on six AASHTO Type II girders with 0.6 inch (15 mm) nominal diameter seven-wire strands. Concrete strength at transfer ranged from 6.3 ksi to 9.6 ksi (43.4 to 66.2 MPa). The concrete mix used expanded slate coarse aggregate and natural sand. Their expression for transfer length is given by Eq. 8 and includes a modification factor for concrete strength at transfer multiplied by the transfer length given in the AASHTO Standard Specification (Eq. 1).

$$\ell_t = 50 d_b \sqrt{\frac{6000}{f'_{ci}}} \qquad \text{(Eq. 8)}$$

in Eq. 8, the units of stress are in psi

***Ramirez and Russell***

Ramirez and Russell[30] developed the expression for transfer length given by Eq. 9 as part of NCHRP project 12-60. The transfer length was measured on a total of 43 rectangular-shaped beams and eight I-shaped beams. Strand from four different manufacturers was included in the study. Seven-wire stand sizes of 0.5 inch (13 mm) and 0.6 inch (15 mm) were used. Concrete strength at release ranged from 4 ksi to 10 ksi (28 to 69 MPa).

The transfer length predicted by Eq. 9 gives the same predicted transfer length as that of Eq. 1 for concrete with a compressive strength at release of 4 ksi (28 MPa). The predicted transfer length remains the same for concrete with a compressive strength at release greater than 9 ksi (62 MPa) due to the limiting value of $40d_b$.

$$\ell_t = \frac{120 d_b}{\sqrt{f'_{ci}}} \geq 40 d_b \qquad \text{(Eq. 9)}$$

***Barnes et al.***

A study of 36 AASHTO Type I girders with 0.6 inch (15 mm) nominal diameter strand was performed by Barnes et al.[14] The normal weight concrete girders had target compressive strengths ranging from 5 to 15 ksi (34.5 to 103 MPa). The study investigated strand surface condition, prestress release methods, and debonding. The researchers recommended the expression by Mitchell et al., given by Eq. 4, as an upper bound of the measured transfer lengths. The researchers proposed the expression given by Eq. 10 as a lower-bound of the measured transfer lengths. The expression was recommended for determining transfer lengths as part of calculations of concrete stress at service loads.

$$\ell_t = \frac{0.33 f_{pt} d_b}{\sqrt{f'_{ci}}} \qquad \text{(Eq. 10)}$$

**DEVELOPMENT LENGTH**

The AASHTO LRFD Bridge Design Specifications define development length as the distance required to develop the specified strength of prestressing strand.[7] Inadequate development length could result in strand slip before the strand reaches its calculated nominal strength ($f_{ps}$). This in turn could result in the member not attaining the calculated nominal resistance for flexure or shear. Previous tests on the development length of LWC specimens have shown varied results

as to whether the AASHTO LRFD Bridge Design Specifications gave accurate predictions of the development length.[24-26,31,32]

The development length of prestressing strand is comprised of the transfer length plus the additional length required to develop the strand stress at nominal moment capacity ($f_{ps}$). This additional length is commonly referred to as the "flexural bond length." This extra bond resistance is primarily attributed to mechanical resistance.[13,19]

The origins of bond stresses along the transfer length are different from those along the development length. While transfer bond stresses are due to flow of force from the strand to the surrounding concrete at the application of the pretensioning force, the bond stresses induced along the flexural bond length are due to the application of externally applied loads onto the member. The applied loads induce internal shear force and bending moments in a beam and after cracking these internal forces induce stress in the strand. The bond stresses induced along the flexural bond length of prestressing strand are analogous to the bond stresses that develop in mild steel reinforcement.[13,19]

The externally applied loads cause cracking in the member as the tensile stress is exceeded. The cracks originate near the region of maximum moment. As the load is increased, new cracks open closer to the support. Away from the regions of the high bending moment and cracking, the stress in the strand is near the effective stress after losses ($f_{pe}$). At the flexural cracks, the strand stress is much higher. Between and flexural cracks, the strand stress is reduced due to mechanical resistance of the concrete surrounding the strand, but the stresses are still higher than $f_{pe}$. Assuming sufficient strand anchorage, a level of applied loading can be reached that will cause $f_{ps}$ in the strand.[13,19]

Compared to the transfer bond strength, the bond strength between the strand and the concrete in flexural bond length is reduced due to cracking. If the external loads cause flexural cracking in the transfer length, then general strand slip could result.[13,19]

## PREDICTIVE EXPRESSIONS FOR DEVELOPMENT LENGTH

The following section includes a description of several expressions for predicting development length. Included are design expressions in the AASHTO LRFD Bridge Design Specifications and the ACI 318 Building Code. Expressions developed by researchers for use with NWC and LWC are also included.

### *ACI Building Code*

The expression in the ACI 318-14 Building Code[28] is given by Eq. 11. This expression is in the form of the sum of the transfer length ($\ell_t$) and flexural bond length ($\ell_{fb}$). The transfer length expression was previously given as Eq. 3. An expression for development length in the form given by the middle two terms of Eq. 11 was originally proposed by Hanson and Kaar[16]. The expression was then simplified by Mattock[29] to the form given by the right-hand term.

$$\ell_d = \ell_t + \ell_{fb} = \frac{f_{pe}}{3} d_b + (f_{ps} - f_{pe}) d_b = \left(f_{ps} - \frac{2}{3} f_{pe}\right) d_b \quad \text{(Eq. 11)}$$

***AASHTO Specifications***

The AASHTO LRFD Specifications[7] require prestressing strand to be bonded beyond the critical section a distance not less than the development length ($\ell_d$) given by Eq. 12. This expression is Eq. 11 with the additional κ-factor to account for the reduced bond characteristics of some strand. The κ-factor has a value of 1.6 for members with a depth greater than 24 in and a value of 1.0 for other members.

$$\ell_d = \kappa \left(f_{ps} - \frac{2}{3} f_{pe}\right) d_b \quad \text{(Eq. 12)}$$

***Ramirez and Russell***

The rectangular and I-shaped beams used to measure transfer length were also tested for development length. The expression proposed by Ramirez and Russell[30] is given by Eq. 13. The expression includes their proposed expression for transfer length, given by Eq. 9, plus an additional term for the flexural bond strength.

$$\ell_d = \ell_t + \ell_{fb} = \left[\frac{120 d_b}{\sqrt{f'_c}} + \frac{225 d_b}{\sqrt{f'_c}}\right] \geq 100 d_b \quad \text{(Eq. 13)}$$

***Meyer et al.***

The six high-strength lightweight concrete AASHTO Type II girders used by Meyer, Kahn, Lai and Kurtis to measure transfer length were also tested to evaluate the development length. The expression proposed by Meyer et al.[25] is given by Eq. 14.

$$\ell_d = \left(50 \sqrt{\frac{5000}{f'_c}} + f_{ps} - f_{pe}\right) d_b \quad \text{(Eq. 14)}$$

***Mitchell et al.***

Mitchell, Cook, Khan, and Tham tested twenty-two prestressed rectangular beams to evaluate their development length. The expression proposed by Mitchell et al.[22] is given by Eq. 15.

$$\ell_d = 0.33 f_{se} d_b \sqrt{\frac{3}{f'_{ci}}} + (f_{ps} - f_{pe}) d_b \sqrt{\frac{4.5}{f'_c}} \quad \text{(Eq. 15)}$$

## TRANSFER AND DEVELOPMENT LENGTH OF STRAND IN LWC

The following is a summary of research on the transfer and development length of prestressing strands in LWC girders.

### MEYER ET AL.

Meyer, Kahn, Lai and Kurtis[25] evaluated the transfer and development length of six AASHTO Type II girders with 0.6 inch (15 mm) diameter seven-wire strands. The concrete mix used expanded slate coarse aggregate and natural sand. Concrete compressive strength at transfer ranged from 6.3 to 9.6 ksi (43.4 to 66.2 MPa) and the compressive strength at time of test ranged from 8.9 to 10.8 ksi (63.4 to 74.5 MPa).

The researchers found that the AASHTO LRFD expression for transfer length (Eq. 2) overestimated all of the measured transfer lengths. The mean ratio of the measured-to-predicted transfer length was 1.42 for the AASHTO LRFD expression.

Their tests on development length found that the AASHTO LRFD expression (Eq. 12) with the κ-factor taken as 1.0 overestimated all of the measured development lengths. The mean ratio of the measured-to-predicted development length was 1.19 for the AASHTO LRFD expression.

### THATCHER ET AL.

The study by Thatcher, Heffington, Lolozs, Sylva, Breen, and Burns[24] also indicated an influence of the modulus of elasticity on transfer length. The study included transfer length measurements on six AASHTO Type I girders with 0.5 inch (13 mm) diameter seven-wire strands. Two concrete mixes were developed as part of the study using lightweight aggregate available in Texas. Design strengths for the two mixes were 6 ksi and 8 ksi (41 to 55 MPa). The 6 ksi (41 MPa) mix had a compressive strength at release of 4.9 ksi (33.8 MPa) and a long-term strength of 8.1 ksi (55.8 MPa). The 8 ksi (55 MPa) mix had a release strength of 5.6 ksi (38.6 MPa) and a long-term strength of 7.9 ksi (54.5 MPa).

The measured transfer length was reported to be as high as 40 percent greater than the transfer length predicted by the AASHTO LRFD Specifications (Eq. 2). The researchers reported that the development length was less than 60 inches (1520 mm) for the 0.5 inch (13 mm) diameter strands and the development length was overestimated by the AASHTO LRFD expression (Eq. 12 with the κ-factor taken as 1.0).

### COUSINS ET AL.

Cousins, Roberts-Wollmann, and Brown[26] evaluated the transfer and development length of eight LWC T-beams. The six beams had a depth of 17 inches (432 mm) and used seven-wire 0.5 inch (13 mm) diameter strand. Two beams used 0.6 inch (15 mm) diameter seven-wire strand and had a depth of 24 inches (610 mm). Six beams used expanded slate coarse aggregate and two used expanded shale. The concrete strengths at transfer ranged from 5.0 to 5.9 ksi (34.5 to

40.7 MPa). The 56-day or 90-day concrete strength ranged from at 8.3 to 9.0 ksi (57.2 to 62.1 MPa).

The researchers found that the measured transfer lengths were less than those predicted by the AASHTO LRFD Specifications (Eq. 2) and by Ramirez and Russell (Eq. 9). The researchers reported that the tested development lengths were also less than the development length predicted by either the AASHTO LRFD Specifications (Eq. 12 with the κ-factor taken as 1.0) or by Ramirez and Russell (Eq. 13).

## FACTOR FOR LWC TENSILE STRENGTH

The tendency for LWC to have a reduced tensile strength was not treated consistently in the AASHTO LRFD Specifications prior to the 2015 revisions of the 7th edition.[1] The approach adopted in the 2015 revisions[11] provides a more uniform treatment of LWC tensile strength by adding the definition of a modification factor for LWC, λ-factor, to Section 5.4 which is then referenced in other articles. Then λ-factor has been added to design expressions where the $\sqrt{f'_c}$ term is used to represent concrete tensile strength.

A modification factor for LWC was previously developed from tests on LWC[8] and applied to the prediction of bar stress developed in lap splices of mild steel reinforcement[9] and nominal shear resistance[10]. The modification factor is based on the splitting tensile strength when available and the unit weight otherwise. An expression for the modification factor for LWC that is based on unit weight is convenient to designers because this is a quantity, like compressive strength, that is determined during the design phase. The expression for the modification factor for LWC (λ-factor) based on unit weight is given by Eq. 16. The expression for the λ-factor based on splitting tensile strength ($f_{ct}$) is given by Eq. 17.

$$\text{For } w_c \leq 0.100 \text{ kcf: } \lambda = 0.75 \quad \text{(Eq. 16a)}$$

$$\text{For } 0.100 < w_c < 0.135 \text{ kcf: } \lambda = 7.5 w_c \leq 1.00 \quad \text{(Eq. 16b)}$$

$$\text{For } w_c \geq 0.135 \text{ kcf: } \lambda = 1.00 \quad \text{(Eq. 16c)}$$

$$\lambda = 4.7 \frac{f_{ct}}{\sqrt{f'_c}} \leq 1.00 \quad \text{(Eq. 17)}$$

# CHAPTER 3. RESEARCH ON TRANSFER AND DEVELOPMENT LENGTH OF PRESTRESSING STRANDS IN LWC AT TFHRC

## INTRODUCTION

This research program focused on LWC with compressive strengths in the range of 6 to 10 ksi (41 to 69 MPa) and equilibrium densities between 0.125 kcf and 0.135 kcf (2000 and 2160 kg/m$^3$). The LWC used in this research program can be considered high-strength specified density concrete (SDC). The research program used LWC with three different lightweight aggregates to produce 27 precast/prestressed LWC girders and 40 reinforced concrete splice beam specimens. The Russell synthesis report[(6)] recognized the lack of mild steel bond test data and shear test data for LWC. While this research program focused on structural behavior, it also had a material characterization component that is described in another document[(8)] and included mechanical property tests on the concrete mixes used in the structural testing program. Mechanical tests included the compressive strength, elastic modulus, and splitting tensile strength. The concrete unit weight was determined using several methods. More details can be found in another document covering material properties of LWC tested by FHWA.[(8)] The 40 splice beam specimens that were tested by FHWA and used to evaluate the development length of mild steel reinforcement are described in a second document.[(9)] A third document describes the 30 shear tests on precast/prestressed girders that were completed by FHWA.[(10)]

The details of the FHWA research program involving the transfer and development length of prestressing strand in LWC are given in this section. This section summarizes the LWC mix design selection process, the specimen fabrication at the precaster's facility, and the material property testing. The girder design, test setup, transfer length measurements, and test results for the 24 development length tests on 12 LWC girders are discussed in detail. The transfer length results include the effect of the number of strands, stirrup spacing, strand size, and duration of prestressing on the measured transfer length. The development length results include the effect of the number of strands, stirrup spacing, and strand size. The strand transfer length, flexural bond length, and development length are compared to design expressions in the AASHTO LRFD Specifications and design expressions in the literature.

## RESEARCH SIGNIFICANCE

There is a limited amount of test data on the transfer and development length of prestressing strand in high-strength LWC. This research project includes transfer length measurements on 18 girders and 24 development length tests on this type of concrete. These tests on transfer and development length are combined with the results of other tests on LWC to determine the effect of lightweight aggregates. Design expressions for strand transfer length, flexural bond length, and development length are compared to design expressions in the AASHTO LRFD Specifications and other design expressions in the literature. A new expression for strand transfer length that accounts for the reduced stiffness of LWC is validated using tests on LWC.

## LWC MIX DESIGNS

The Expanded Shale, Clay, and Slate Institute (ESCSI) assisted FHWA in obtaining specified density mixes that had been used in production. One of the criteria for this research project was to use lightweight aggregate sources that were geographically distributed across the United States. Additional selection criteria included mixes using a large percentage of the coarse aggregate as lightweight coarse aggregate, mixes using natural sand as the fine aggregate, and mixes with a target equilibrium density between 0.125 and 0.135 kcf (2000 and 2160 kg/m$^3$). In order to make sure that the behavior of the concrete would be controlled by the lightweight aggregate, only mixes with greater than 50 percent of the coarse aggregate as lightweight aggregate were considered. The concrete density needed to be in the range of densities not currently covered by the AASHTO LRFD Bridge Design Specifications[1] because of the limited amount of test data in this density range. The literature has shown that silica fume can increase LWC compressive strength[33-36] and has also been shown to improve bond of mild steel reinforcement and prestressing strand.[33] As a result, mixes that included silica fume were not selected for this experimental study so that the results would be representative of mechanical properties for more common specified density concretes.

Three mix designs were selected with a design compressive strength greater than 6.0 ksi (41.3 MPa) to represent concrete that could be used for bridge girders. Another mix design was selected that had a design compressive strength less than 6.0 ksi (41.3 MPa) to represent concrete that could be used for a bridge deck.

The mix designs selected are shown in Table 1. Each uses partial replacement of the coarse aggregate with lightweight aggregate to achieve their reduced unit weight. The lightweight aggregates in the mixes were Haydite, expanded shale from Ohio, Stalite, expanded slate from North Carolina, and Utelite, expanded shale from Utah. The normal weight coarse aggregate was No. 67 Nova Scotia granite. Natural river sand was used as the fine aggregate. Type III portland cement was used to obtain the high early strengths typically required in high-strength precast girders. Admixtures included a water reducer, an air entrainer, and a high range water reducer.

**Table 1. Selected Concrete Mix Designs.**

| Design Values and Component Materials | unit | Haydite Girder (HG) | Stalite Girder (SG) | Utelite Girder (UG) |
|---|---|---|---|---|
| Design 28-Day Strength | ksi | 6.0 | 10.0 | 7.0 |
| Design Release Strength | ksi | 3.50 | 7.5 | 4.2 |
| Target Unit Weight | kcf | 0.130 | 0.126 | 0.126 |
| Lightweight Coarse Aggregate | kips | 0.80 | 0.88 | 0.74 |
| Normal Weight Coarse | kips | 0.52 | 0.25 | 0.39 |
| Normal Weight Sand | kips | 1.19 | 1.22 | 1.27 |
| Class F Fly Ash | kips | - | - | 0.15 |
| Type III Portland Cement | kips | 0.75 | 0.80 | 0.60 |
| Water | kips | 0.27 | 0.25 | 0.26 |
| Water Reducer | oz | 19 | 19 | 19 |
| Air Entrainer | oz | 2 | 2 | 2 |
| High Range Water Reducer | oz | 34 | 34 | 34 |
| Water / Cementitious Materials | | 0.36 | 0.31 | 0.34 |

Units: 1.0 ksi = 6.89 MPa, 0.001 kcf = 16.01 kg/m$^3$, 1.0 kip = 4.45 kN, 1.0 oz = 29.6 mL

## EXPERIMENTAL PROGRAM

The experimental program consisted of transfer length measurements on 18 girders and 24 development length tests on 12 prestressed concrete girders made using three different LWC mixes. Key test parameters included the lightweight aggregate, the strand size, the total prestressing force, and the amount of shear reinforcement. Four girders designs were developed to evaluate the effect of the key parameters. The end of each girder had the same amount of reinforcement: shear, confinement, and bursting. A set of four girders was cast for each of three different concrete mixes intended to represent typical LWC for girders. Table 2 gives the nominal details for the four girder end designs that were AASHTO Type II girders (Type II).

A naming scheme was developed for the 24 girder tests that included the concrete mix, girder design, and girder end. The concrete mixes were designated A through C and were UG, HG, and SG, respectively. The girder design number was used in the naming scheme. An “L” or a “D” was used to denote a test near the live or dead end of the girder, respectively. The end of the girder closer to the prestressing bed bulkhead where the strands were jacked is known as the live end, and the end towards the bulkhead with the stationary anchorage is known as the dead end.

The transfer and development length girders were designed as part of a larger study that included the shear resistance of prestressed LWC girders. A total of nine different girder designs were used in the overall research program. The first four designs were Type II girders what were tested to failure to evaluate development length of prestressing strand. Girder Designs 5-9 were

AASHTO Type II girders and AASHTO/PCI BT-54 girder for the evaluation of shear performance.

TEST SPECIMENS

Girder Designs 1 through 4 were Type II girders. The same amount of shear reinforcement (stirrups) was used in the test regions near the live (L) and dead (D) ends of the girder. The design details for each girder end are shown in Table 2. A sketch of each girder design showing the cross section, strand pattern, and mild steel reinforcement is shown in Figure 1 through Figure 4 for Girder Designs 1 through 4, respectively. Girder Design 1 was considered the control girder in respects to strand size, amount of strands, and amount of shear reinforcement. Girder Design 2 had a greater amount of prestressing strand and a corresponding increase in shear reinforcement. The amount of shear reinforcement was reduced in Girder Design 3. Larger 0.6 inch (15 mm) diameter strands were used in Girder Design 4. The total area of prestressing was slightly greater in Girder Design 4, so the amount of shear reinforcement was also increased slightly compared to the control girder design.

**Table 2. Design Details of the AASHTO Type II Girders.**

| | | No. of Strands | | Double Stirrups | |
|---|---|---|---|---|---|
| Girder Test | Strand Size (inch) | Bottom | Top | Bar Size | Spacing (inch) |
| 1 | 0.5 | 10 | 2 | 5 | 8 |
| 2 | 0.5 | 18 | 4 | 5 | 5 |
| 3 | 0.5 | 10 | 2 | 5 | 10 |
| 4 | 0.6 | 8 | 2 | 5 | 9 |

Units: 1.0 inch = 25.4 mm

The end of each girder had additional reinforcement as required by the AASHTO LRFD Specifications. No. 6 rebar was added between the strands in the bottom flange to satisfy the requirements of Article 5.8.3.5 for additional longitudinal reinforcement. Additional transverse reinforcement (as stirrups) was provided as splitting resistance in the pretensioned anchorage zone per Article 5.10.10.1. Confinement reinforcement was provided around the strands to satisfy Article 5.10.10.2.

The girders were designed with an amount of shear reinforcement that was intended to ensure that a flexural failure would occur prior to a shear failure. For the design of the girders, a concrete compressive strength ($f'_c$) of 10 ksi (69 MPa) was assumed for all girders and no modification of the shear resistance for LWC was used.

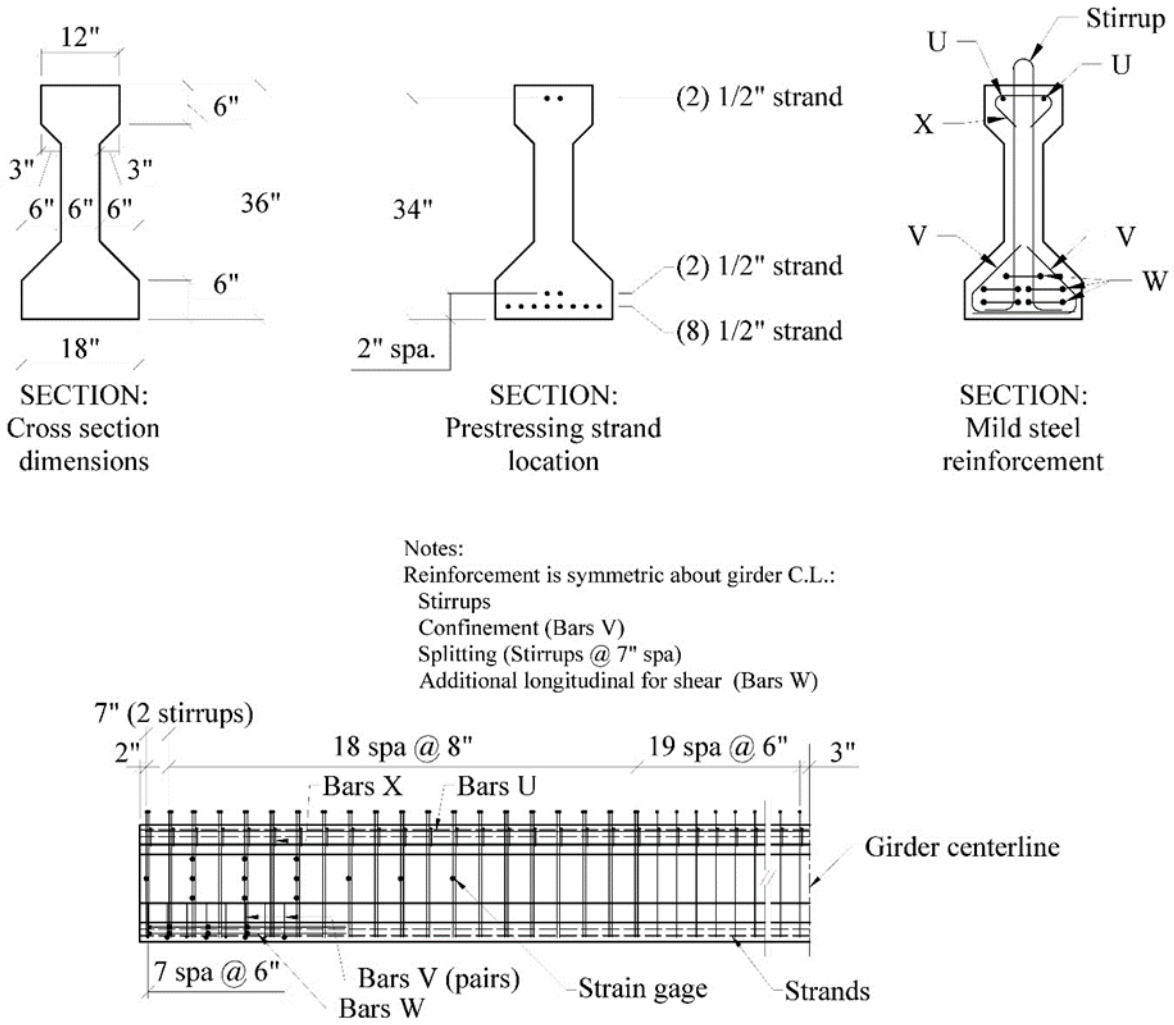


**Figure 1. Illustration. Beam Design 1.**

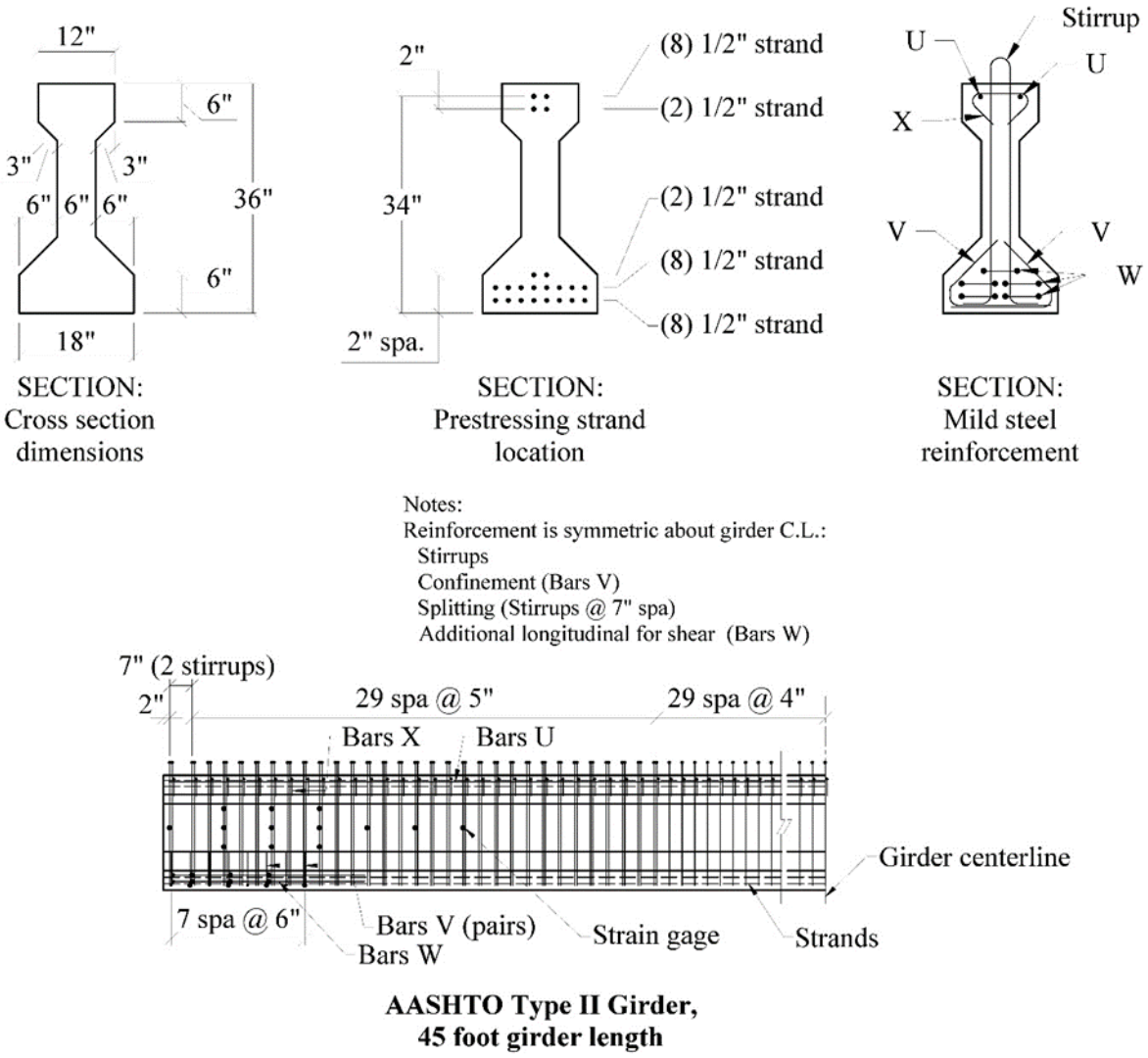


**Figure 2. Illustration. Beam Design 2.**

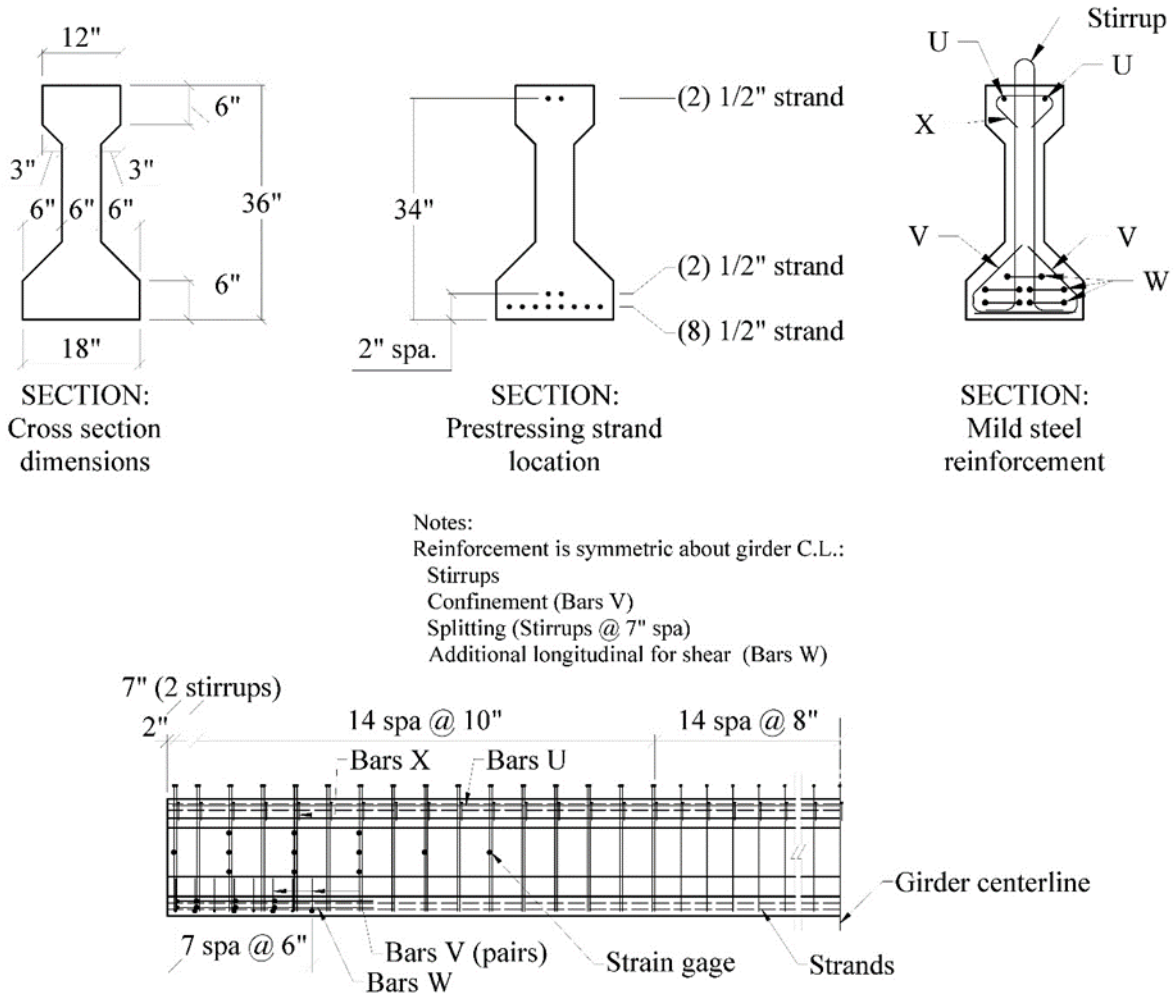


**Figure 3. Illustration. Beam Design 3.**

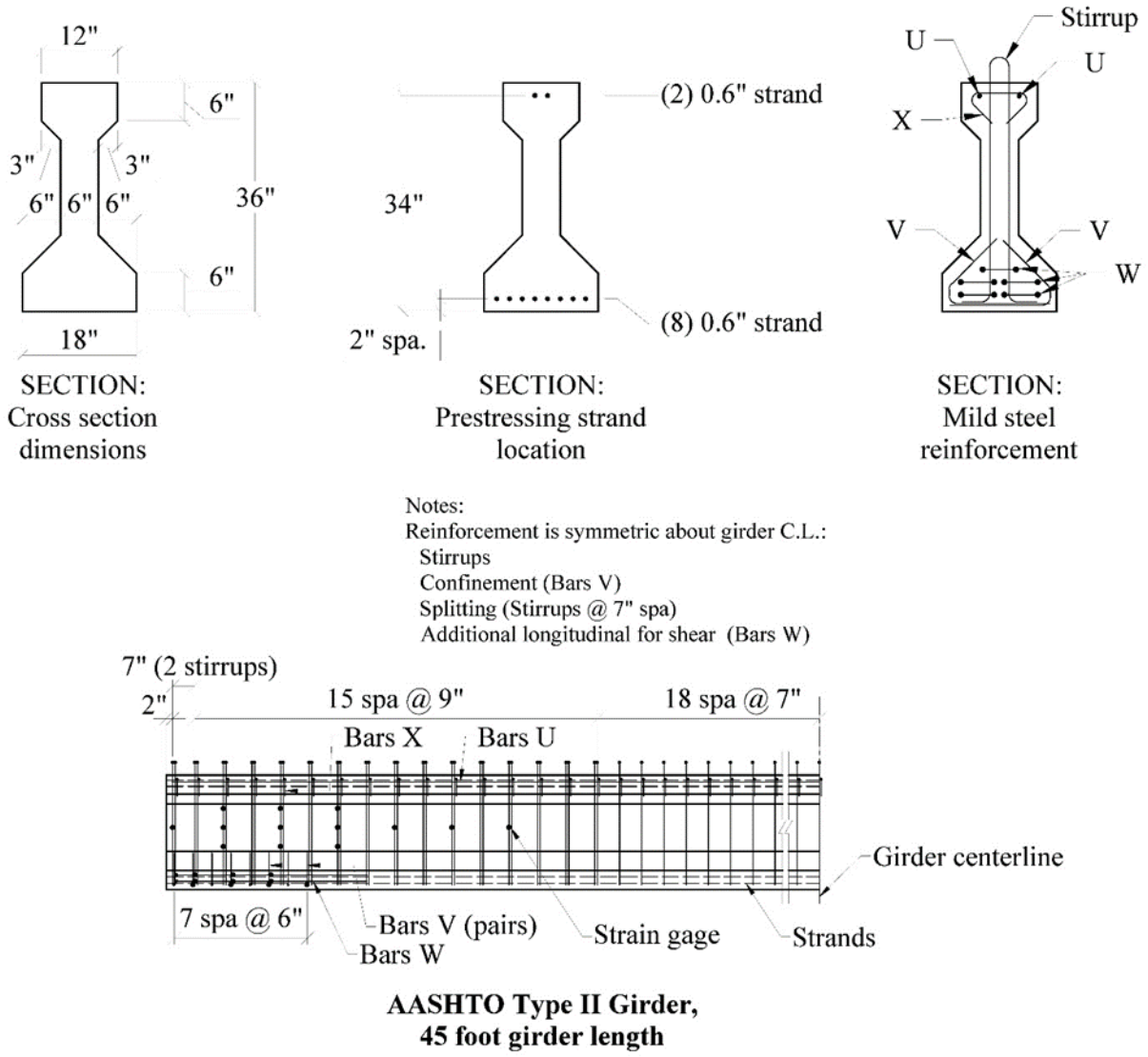


**Figure 4. Illustration. Beam Design 4.**

SPECIMEN FABRICATION

The girders were fabricated at the Standard Concrete Products (SCP) plant in Mobile, Alabama. The fabricator was asked to prescriptively produce the concrete mixes, without trying to adjust them for target strengths or unit weight. This was intended to remove batch-to-batch variations as a variable in the study. The lightweight aggregates were stored in three piles at the plant and watered continuously using a sprinkler on each pile as shown in Figure 5.


**Figure 5. Photo. Lightweight Aggregate Stockpiles at Precaster's Facility with Continuous Sprinklers.**

The girders were produced in seven production runs over a seven-week period between May 8, 2008 and June 23, 2008. A production run consisted of tensioning the strands, tying cages, casting concrete, and releasing the prestress. The girder fabricator only had enough length of side forms to cast three girders simultaneously, so concrete was cast on two different days for production runs 4 and 5. The fabricator organized the girders into casting production runs as given in Table 3. Girders with the same strand pattern were cast together. Note that the numbering of the production runs varied slightly in a preliminary paper describing the transfer length measurements.[37] The currently numbering system reflects the chronological order of the first concrete casting in each production run.

**Table 3. Girder Production Runs and Pretension Release Method.**

| Cross Section | Production Run | Cast Date | Release Date | Release Method | Girder Design and LW Aggregate† |
|---|---|---|---|---|---|
| AASHTO Type II | 2 | 5/21/2008 | 5/22/2008 | Flame Cut | 5, 1, 3 (SG) |
| | 4 - Cast 1 | 5/30/2008 | 6/4/2008 | Detension | 5, 1, 3 (UG) |
| | 4 - Cast 2 | 6/3/2008 | 6/4/2008 | Detension | 5, 1, 3 (HG) |
| | 5 - Cast 1 | 6/9/2008 | 6/11/2008 | Detension | 7, 2 (SG); 2 (UG) |
| | 5 - Cast 2 | 6/10/2008 | 6/11/2008 | Detension | 7 (UG); 2, 7 (HG) |
| | 6 | 6/14/2008 | 6/16/2008 | Detension | 4 (UG, HG, SG) |
| | 7 | 6/20/2008 | 6/23/2008 | Detension | 6 (UG, HG, SG) |
| AASHTO/PCI BT-54 | 1 | 5/14/2008 | 5/17/2008 | Flame Cut | 8 (UG, HG, SG) |
| | 3 | 5/29/2008 | 5/31/2008 | Flame Cut | 9 (UG, HG, SG) |

Notes:
† Girder Design number followed by mix in parentheses

CONCRETE PROPERTIES

Concrete for the three girder mixes was supplied by the precaster. After mixing, the precaster's personnel performed testing of the fresh concrete properties and produced 4 x 8 inch (102 x 203 mm) cylinders for quality control purposes. The fresh concrete properties, concrete batch weights, and compressive strength tests performed by the precaster's personnel are in another document covering material properties of the LWC tested within this research program.[8]

Independently, research personnel made 4 x 8 inch (102 x 203 mm) cylinders following ASTM C31[38] for mechanical property testing and density measurements. Compression tests were performed according to ASTM C39[39] to determine the compressive strength at release of prestressing, 28 days, and at girder testing. Neoprene pads were used inside steel caps at each end of the cylinders. The indirect tensile strength was measured using the splitting tensile test described in ASTM C 496.[40] The elastic modulus was determined following ASTM C469[41] using one of the cylinders intended for compressive strength testing. Typically, one cylinder was tested first for compressive strength to determine the proper load level for determining the elastic modulus. The air-dry density was calculated using the measured cylinder weight and measured cylinder lengths and diameters to calculate an average volume. The mechanical properties of the LWC used in the prestressed girders used to evaluated strand development length are given in Table 4 and the measured unit weights are given in Table 5. The compressive strengths, splitting tensile strengths, modulus of elasticity, and air-dry densities shown are based on the average of three cylinders.

**Table 4. Mean Girder Concrete Properties for Girder Design 1 to 4 by Mix Design.**

| | Compressive Strength (ksi) | | | Splitting Tensile Strength (ksi) | | | Modulus of Elasticity (ksi) | | |
|---|---|---|---|---|---|---|---|---|---|
| Mix Design | Release | 28 Day | Test Day | Release | 28 Day | Test Day | Release | 28 Day | Test Day |
| HG | 6.7 | 9.5 | 10.4 | 0.590 | 0.720 | 0.770 | 3,690 | 4,420 | 4,320 |
| SG | 6.8 | 9.7 | 10.6 | 0.600 | 0.680 | 0.720 | 3,790 | 4,140 | 4,360 |
| UG | 6.4 | 8.6 | 10.1 | 0.590 | 0.680 | 0.760 | 3,590 | 4,080 | 4,150 |

Units: 1.0 ksi = 6.89 MPa

**Table 5. Girder Concrete Unit Weight for Girder Design 1 to 4 by Mix Design.**

| Mix Design | Unit Weight (kcf) | | |
|---|---|---|---|
| | Release | 28 Day | Test Day |
| HG | 0.132 | 0.132 | 0.130 |
| SG | 0.124 | 0.125 | 0.123 |
| UG | 0.132 | 0.130 | 0.127 |

Units: 0.001 kcf = 16.01 kg/m$^3$

REINFORCING BAR PROPERTIES

The reinforcing bars were ASTM A615, Grade 60. The mechanical properties were tested under displacement control in a 100 kip (445 kN) testing machine. Two bars were tested for each nominal size used in the prestressed girders. Strain was measured with an 8 inch (203 mm) extensometer. When the extensometer reached a measured strain of 2.0 percent at the beginning of the assumed strain-hardening regime, the test was paused to remove the extensometer. The test was then continued until the bar fractured. The yield strength was determined using the 0.2 percent offset method. The average yield strength and the ultimate strength of two bars used as stirrups, confinement reinforcement, and as girder end longitudinal reinforcement are given in Table 6. Test data and stress-strain relationships from individual bars are given in Appendix A.

**Table 6. Reinforcing Bar Properties.**

| Bar Usage, Nominal and Measured Property | Stirrup | Girder End Longitudinal Reinforcement | Confinement Reinforcement |
|---|---|---|---|
| Bar Size | 5 | 6 | 4 |
| Nominal Diameter (inch) | 0.625 | 0.625 | 0.500 |
| Nominal Area (in$^2$) | 0.31 | 0.44 | 0.44 |
| Yield Strength$^\dagger$ (ksi) | 72.8 | 65.8 | 65.8 |
| Ultimate Strength (ksi) | 113.1 | 107.1 | 107.5 |

Notes: $^\dagger$ Calculated using 0.2 percent offset method

Units: 1.0 inch = 25.4 mm, 1.0 in$^2$ = 645 mm$^2$, 1.0 ksi = 6.89 MPa

PRESTRESS RELEASE

The AASHTO Type II girders and AASTHO/PCI BT-54 girders were produced in different pretensioning beds. The bulkhead against which the strands are jacked is known as the “live end.” The other bulkhead is known as the “dead end.” The girders were cast near the dead end bulkhead of the 400–500 ft (120–150 m) long pretensioning beds and filled less than half of the

total length of the beds. This meant that there was several hundred feet of free strand between the last girder and the live end of the prestressing bed.

The strand pretension was released by flame cutting for the first three production runs. For flame cutting, workers used acetylene torches to simultaneously cut the same strand at the girder ends and between each girder. At a foreman's signal, the workers began cutting the same strand at each location. The strands are progressively cut, starting with the top strands, and then working from the outside of the bottom flange toward the center of the girder. Each strand gave an audible "bang" after it was cut and all the cuts along a strand typically varied by several seconds. When only two strands remained, the girders would separate at the location where the first cut was made. This was due to the remaining strand being unable to carry the force of the two uncut strands that remained between all the other girder ends. This caused the girders to slide away from the location without any connected strands. Release of prestress using the flame cutting technique was typically completed in 30 minutes.

The AASHTO Type II girders of Run 3 slid when the last two strands were cut. The fabricator decided to use the "detensioning" method due to safety concerns for the remaining production runs. For the detensioning method, the strand stress is significantly reduced prior to flame cutting. The strands were detensioned one at a time at the jacking end of the prestressing bed. Release of prestress using the detensioning method was typically completed in 2-3 hours.

### NWC CONCRETE DECK

An 8-inch (200 mm) thick composite NWC deck was cast onto each LWC girder at TFHRC in order to move the neutral axis above the web and top flange. The concrete used in the decks had a specified compressive strength of 4 ksi (28 MPa). The mean compressive strength of the NWC decks was 3.96 ksi (27.3 MPa) at 28 days and 5.68 ksi (39.2 MPa) at test day. The decks had two orthogonal mats of reinforcing, as specified in Article 9.7.3 of the AASHTO LRFD Specifications for bridge decks. The deck reinforcement is shown in typical cross sections in Figure 6.

## TRANSFER LENGTH

Transfer length measurements were made on a total of 18 girders. These included Girder Designs 1 through 4 and Girder Designs 8 and 9. The twelve girders that were designs 1 through 4 are described in detail in this report and were AASHTO Type II girders tested to failure for development length determination. The six girders that were designs 8 and 9 were described in detail in a previous document[10] and were AASHTO/PCI BT-54 girders tested to failure to evaluate shear resistance. Two different types of transfer length measurement were made on the girders: concrete surface strain (CSS) and strand draw-in measurements. Only the CSS measurements were analyzed and the resulting strain profiles and transfer lengths are presented in this document. The strand draw-in measurements were not taken on all of the girders due to time constraints and difficulty making the measurements in the field.

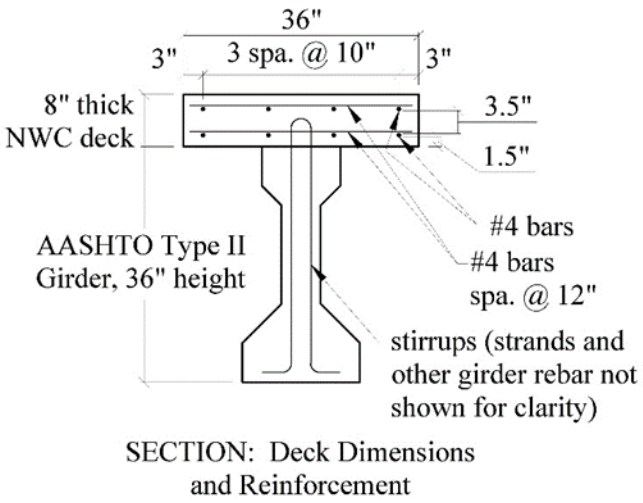


**Figure 6. Illustration. NWC Deck Cast onto the LWC Girders.**

This section describes the method used to measure the concrete surface strain, the method used to analyze the concrete strains to determine the transfer length, and then provides an analysis of the transfer lengths. The analysis included evaluating the effects of the main variables, evaluating parameters typically used to predict transfer length, and then comparing expressions used to predict transfer length.

TRANSFER LENGTH MEASUREMENT

The transfer length was "measured" using the CSS method. This method uses a Demountable Mechanical Strain Gauge (DEMEC) to read the distance between two target points (DEMEC points) in the concrete. The average strain at the surface of the concrete girders is calculated by taking the difference between readings made before and after the release of the prestressing. The CSS gives a reasonable estimate of the strain in the prestressing strand due to strain compatibility.[19] The strain measurements typically start near zero at the end of the girder and increase approximately linearly until they reach a constant value. A plot of the CSS with respect to the distance from the girder end is the strain profile. An ideal strain profile shows a plateau beginning at the theoretical transfer length.

The DEMEC points were brass inserts spaced at 2 inch (51 mm) that were screwed to a 0.25 inch (6.4 mm) thick steel strip that was bolted to the inside of the side forms. The points were located at the centroid of the bottom layer of prestressing strand. After the concrete was cast and set, the side forms and steel strips were removed to expose the brass inserts cast into the side of the girder. The DEMEC points cast into the end of an AASHTO Type II girder are shown in Figure 7.

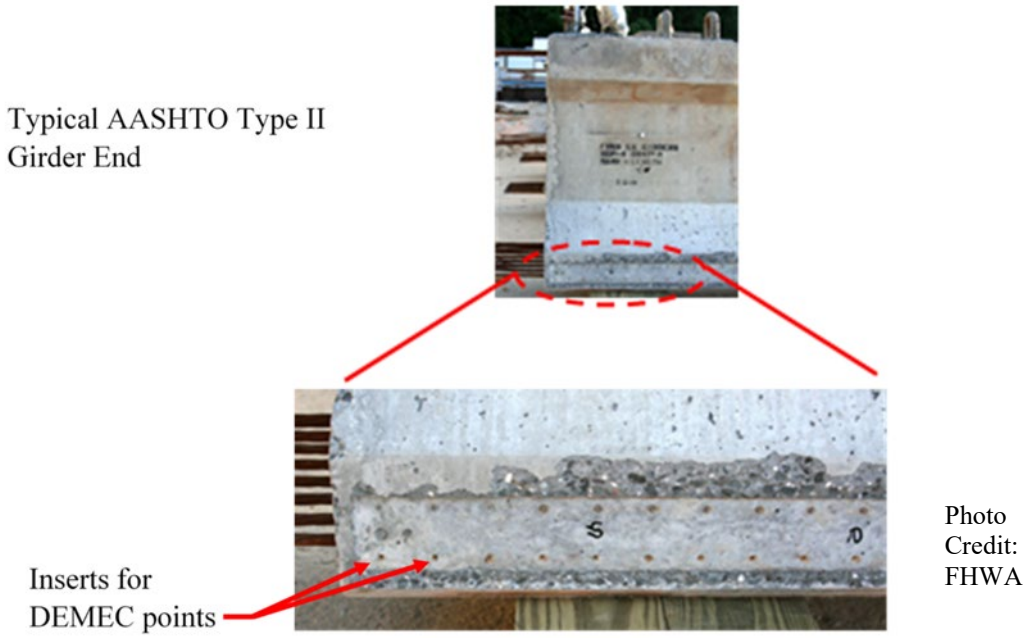


**Figure 7. Illustration. Compound Figure Showing DEMEC Points on Girder End.**

The DEMEC instrument is shown in Figure 8 and consisted of a small hand-held frame that holds a fixed conical pin at one end and second conical pin on a slider at the other end. The slider was oriented to allow the second pin to travel along a linear path from the fixed pin. A spring pushed the slider away from the fixed pin. A Mitutoyo digital dial indicator model IDA-112ME with a reading to the nearest 0.0001 inch (0.0025 mm) measured the movement of the slider. DEMEC reading are known to be very sensitive to the technique used by the operator to make the reading.[25,31] For this reason, measurements were made by two different operators, and the difference between two operator readings was limited to 0.0010 inch (0.0254 mm), although typical readings had a difference that was less than 0.0005 inch (0.013 mm). Prior to the first reading and after every ten readings, the DEMEC instrument was calibrated using an 8 inch (203 mm) gauge bar made from Invar (Figure 8). Invar is a nickel-iron alloy with low coefficient of thermal expansion.

Multiple measurements were made along each group of points. Each measurement spanned four DEMEC points and represents the average strain across the 8 inch (203 mm) gauge length. The instrument was moved to the next set of points, approximately 2 inches (51 mm), and the next measurement was made. Measurements were made along a length of 60 inches (1520 mm) at each girder end. The initial measurements were made for all the girders prior to release of the prestressing. It took approximately 30 minutes for two individuals to make measurements at all four ends of a single girder. A second set of measurements were made started immediately following release of the strand pretensioning. A final set of measurements were made several days prior to testing to failure, approximately 1–2 years after casting.

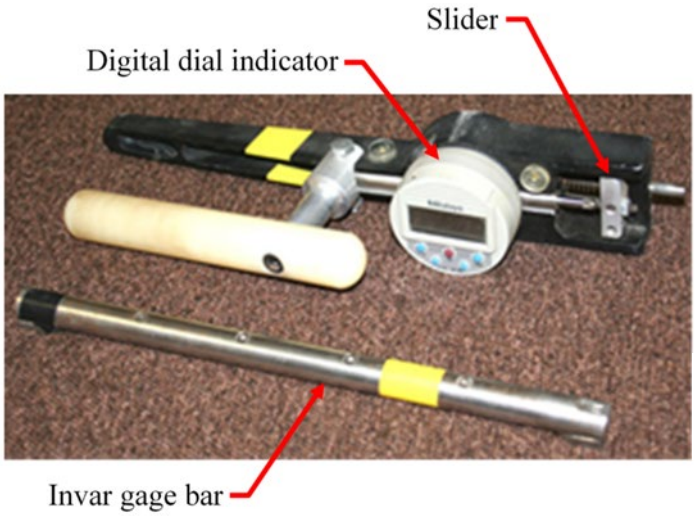


Photo Credit: FHWA

**Figure 8. Photo. DEMEC Instrument and Gauge Bar.**

## TRANSFER LENGTH DETERMINATION

The measurements from the two operators taking the readings were averaged together. The strain was calculated by taking the difference between the initial and final measurements, and then dividing by the gauge length adjusted for the initial measurement. The adjusted gauge length was taken as 8 inches (203 mm) plus the initial measurement. The average data for each end of a girder (dead or live) was calculated by determining the mean of the calculated strain at points that were the same distance from the girder end. The average data for each girder was calculated by determining the mean of the calculated strain at points on all four sides that are the same distance from the girder end. The average data (individual end, averaged for end, averaged for girder) was "smoothed" by determining the mean of the strain at three consecutive points and applying their mean value to the middle point.

The transfer length was calculated using the 95 percent Average Maximum Strain Method (95 percent AMS). This method was developed by Russell and Burns[19] and has also been used by researchers in several recent investigations to evaluate the CSS data for transfer length.[20,25,26,31] The 95 percent AMS method involves calculating the mean strain along the strain plateau (i.e., the average maximum strain or "AMS"), constructing a line on the strain profile at the strain equal to 95 percent of the AMS, then determining the transfer length at the intersection of the 95 percent AMS line and the smoothed girder strain profile.

The strain profiles for three girders are shown in Figure 9, Figure 10, and Figure 11. The figures show the 95 percent AMS line, the length of the strain plateau used to calculate the maximum strain, and the distance from the girder end determined to be the transfer length. The strain profile for Girder B1 is shown in Figure 9. B1 was an AASTHO Type II girder, used the HG mix, and had 0.5 inch (13 mm) diameter strand. Figure 10 shows the strain profile for girder A4,

an AASTHO Type II girder with 0.6 inch (15 mm) diameter strand that used the UG mix. The strain profile for an AASHTO/PCI BT-54 girder, C8, with 0.5 inch (13 mm) diameter strand and the SG mix is shown in Figure 11. The strain profiles for all of the girders are contained in Appendix D.

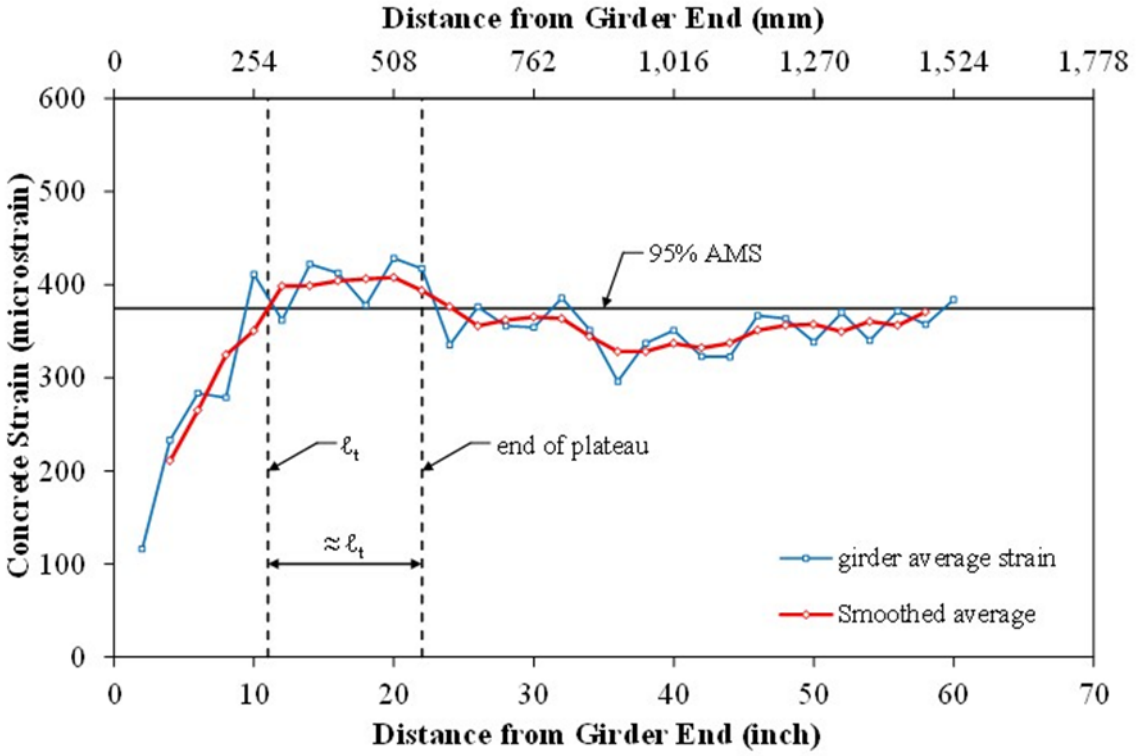


**Figure 9. Graph. Strain Profile and Transfer Length Determination for Girder B1.**

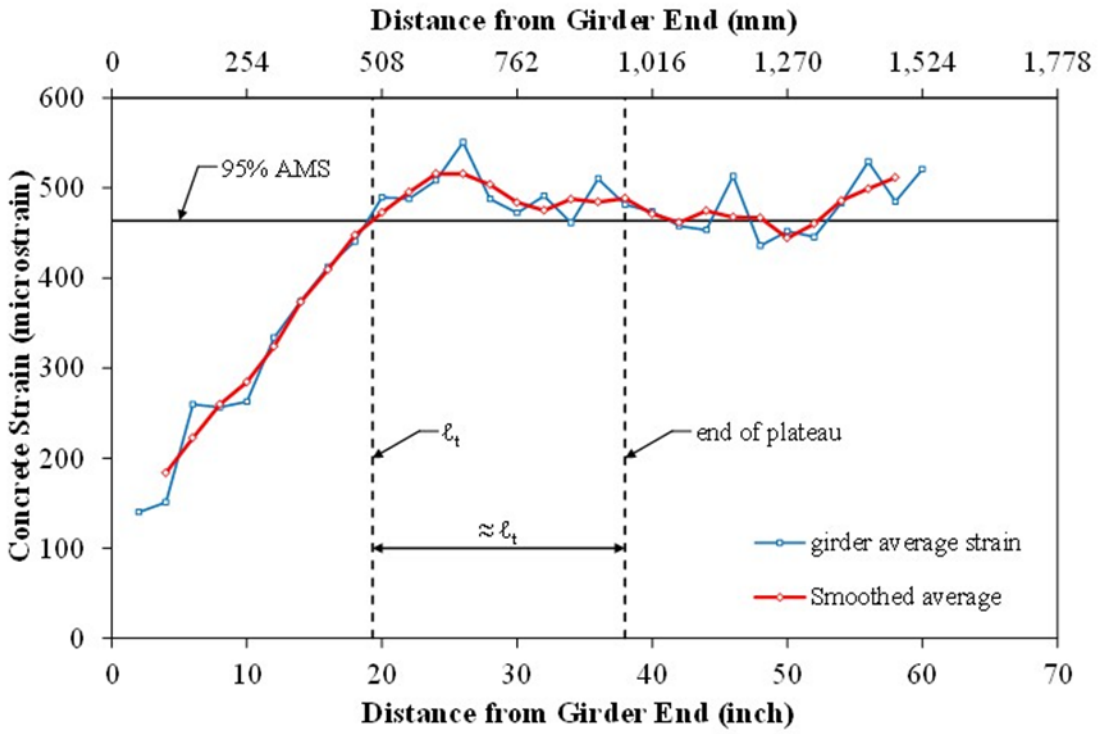


**Figure 10. Graph. Strain Profile and Transfer Length Determination for Girder A4.**

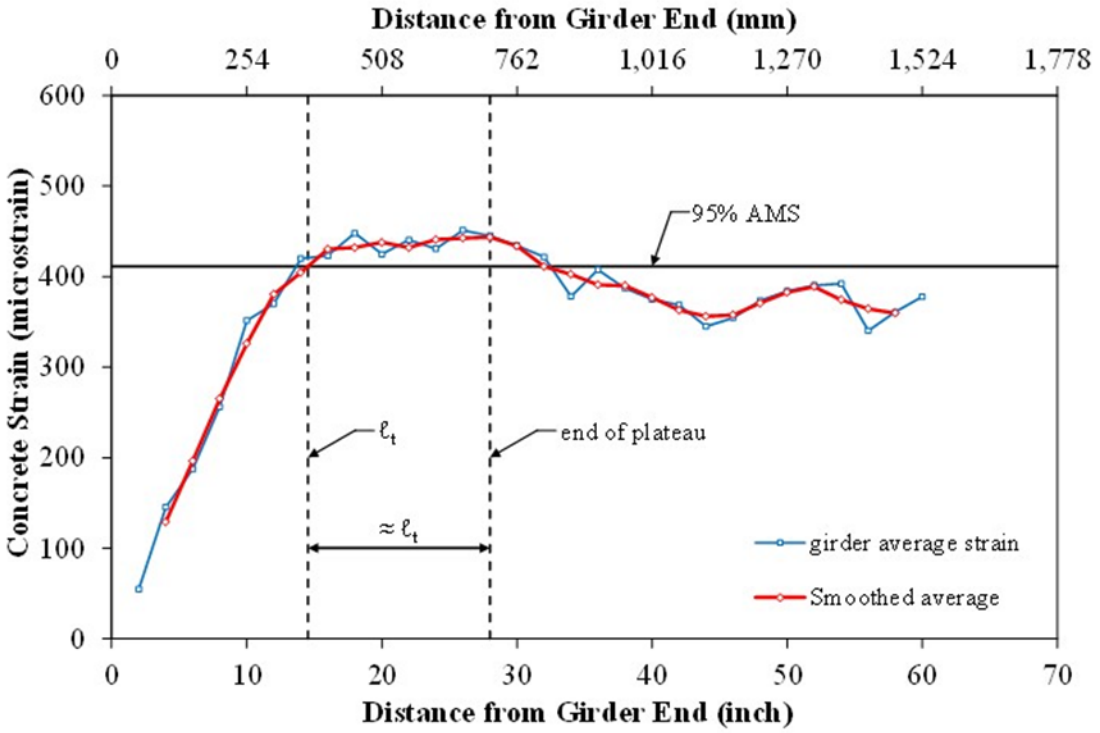


**Figure 11. Graph. Strain Profile and Transfer Length Determination for Girder C8.**

The strain profiles shown in Figure 9 through Figure 11 exhibit a nearly linear increase in strain to a peak (or narrow plateau), followed by a slow decrease in strain. The decrease in strain is most likely due to the self-weight of the girder. The calculated change in flexural tensile strain due to self-weight from 18 to 60 inches (460 to 1520 mm) from the girder end is approximately 150 microstrain for a BT-54 girder with an elastic modulus of 4000 ksi (28 GPa). This is of similar magnitude to the drop in compressive strain shown in the strain profiles. Research on transfer length using AASHTO girders did not report compensating for self-weight.[19,24,25] Buckner[20] used the strain profile data from previous tests on AASHTO-type girders to show that compensating for self-weight only slightly increases the transfer length (approximately 5 percent).[19,48]

The strain profiles were not compensated for self-weight to be consistent with several recent studies.[19,24,25] However, the decreasing trend of the strains after peak does affect the calculated AMS. An AMS that included all 60 inches (1520 mm) of measured strains would be much lower that an AMS that included only the strains near the peak, and would result in a much smaller transfer length using the 95 percent AMS method. In this study, the length of the plateau was taken as equal to the calculated transfer length. As a result, only the data over a region approximately equal to the calculated transfer length was used. This method consistently gave transfer lengths that were longer than when considering the data over the full length of 60 inch (1520 mm) for most girders.

The transfer length determined for the 18 girders is given in Table 7 for the AASHTO Type II girders and in Table 8 for the AASHTO/PCI BT-54 girders. The transfer length determined using measurements taken immediately after prestress release ($\ell_{ti}$) and the transfer length determined using measurements taken prior to testing to failure ($\ell_{t,test}$) are given. The tables also give the ratio of transfer length to nominal strand diameter, the concrete compressive strength ($f'_{ci}$) and elastic modulus ($E_{ci}$) at prestress transfer, the concrete unit weight ($w_c$), and the calculated effective stress in the prestressing ($f_{pe}$). The effective prestress was calculated using the approximate estimate of time-dependent losses in Article 5.9.5.3 of the AASHTO LRFD Bridge Design Specifications.

**Table 7. Summary of Transfer Length, and Concrete Strength, Elastic Modulus, Unit Weight at Prestress Transfer, and Effective Prestress for AASHTO Type II Girders.**

| Girder Test† | Measured transfer length at prestress transfer, $\ell_{ti}$ (inch) | Measured transfer length at girder test, $\ell_{t,test}$ (inch) | Ratio of $\ell_{ti}$ to strand size | Ratio of $\ell_{t,test}$ to strand size | Concrete compressive strength at transfer, $f'_{ci}$ (ksi) | Concrete elastic modulus at transfer, $E_{ci}$ (ksi) | Concrete unit weight at transfer, $w_c$ (kcf) | Effective stress in prestressing‡, $f_{pe}$ (ksi) |
|---|---|---|---|---|---|---|---|---|
| A1 | 7.9 | 8.1 | 15.7 | 16.3 | 7.11 | 3560 | 0.131 | 174 |
| B1 | 11.0 | 11.4 | 22.0 | 22.7 | 6.21 | 3550 | 0.132 | 172 |
| C1 | 9.4 | 12.9 | 18.8 | 25.7 | 6.35 | 3630 | 0.126 | 173 |
| A2 | 11.1 | 10.6 | 22.2 | 21.1 | 6.22 | 3790 | 0.133 | 159 |
| B2 | 8.5 | 10.2 | 16.9 | 20.3 | 6.66 | 3730 | 0.134 | 160 |
| C2 | 8.8 | 8.9 | 17.6 | 17.8 | 7.12 | 3670 | 0.123 | 161 |
| A3 | 11.9 | 8.7 | 23.8 | 17.3 | 7.11 | 3560 | 0.131 | 174 |
| B3 | 11.5 | 10.1 | 23.0 | 20.1 | 6.21 | 3550 | 0.132 | 172 |
| C3 | 19.9 | 20.5 | 39.7 | 40.9 | 6.35 | 3630 | 0.126 | 173 |
| A4 | 19.3 | 19.1 | 32.1 | 31.8 | 5.86 | 3410 | 0.131 | 168 |
| B4 | 15.3 | 19.4 | 25.5 | 32.4 | 7.31 | 3780 | 0.131 | 173 |
| C4 | 21.2 | 22.4 | 35.3 | 37.3 | 6.80 | 4070 | 0.123 | 173 |

Notes:

† Specimen name of form $#, where: $ is A for UG mix, B for HG mix, C for SG mix, # is girder design

‡ Determined using approximate estimate of time-dependent losses in AASHTO LRFD Bridge Design Specifications

Units: 1.0 inch = 25.4 mm, 1.0 ksi = 6.89 MPa

**Table 8. Summary of Transfer Length, and Concrete Strength, Elastic Modulus, Unit Weight at Prestress Transfer, and Effective Prestress for AASHTO/PCI BT-54 Girders.**

| Girder Test† | Measured transfer length at prestress transfer, $\ell_{ti}$ (inch) | Measured transfer length at girder test, $\ell_{t,test}$ (inch) | Ratio of $\ell_{ti}$ to strand size | Ratio of $\ell_{t,test}$ to strand size | Concrete compressive strength at transfer, $f'_{ci}$ (ksi) | Concrete elastic modulus at transfer, $E_{ci}$ (ksi) | Concrete unit weight at transfer, $w_c$ (kcf) | Effective stress in prestressing‡, $f_{pe}$ (ksi) |
|---|---|---|---|---|---|---|---|---|
| A8 | 15.1 | 13.0 | 30.2 | 26.0 | 6.08 | 3570 | 0.133 | 173 |
| B8 | 12.0 | 11.9 | 23.9 | 23.7 | 7.50 | 1540 | 0.134 | 160 |
| C8 | 14.5 | 10.7 | 29.1 | 21.4 | 8.20 | 3950 | 0.127 | 177 |
| A9 | 21.4 | 19.6 | 42.8 | 39.3 | 5.80 | 3480 | 0.130 | 159 |
| B9 | 12.6 | 13.1 | 25.2 | 26.2 | 7.44 | 4110 | 0.134 | 165 |
| C9 | 12.9 | 13.6 | 25.8 | 27.3 | 7.72 | 3560 | 0.125 | 164 |

Notes:
† Specimen name of form $#, where: $ is A for UG mix, B for HG mix, C for SG mix, # is girder design
‡ Determined using approximate estimate of time-dependent losses in AASHTO Specifications
Units: 1.0 inch = 25.4 mm, 1.0 ksi = 6.89 MPa

## TRANSFER LENGTH ANALYSIS

An analysis of the transfer lengths determined from the DEMEC data taken on the 18 girders described in this report. The analysis is divided into three sections. A statistical analysis was performed to evaluate the mean transfer for the main experimental variables. The transfer lengths were compared graphically to parameters typically used to predict transfer length. The transfer lengths were normalized by expressions used to predict transfer length. Test-to-prediction ratios were determined for several prediction expressions including those in the AASHTO LRFD Bridge Design Specification.

### *Mean Transfer Length*

Table 9 gives the mean transfer length for all 18 girders and for each girder design. In Table 10 the mean transfer lengths are compared by girder concrete mix, strand size, and girder size. The mean transfer length is given for the measurements taken immediately after prestress release ($\ell_{ti}$) and the measurements taken prior to testing to failure ($\ell_{t,test}$). The table gives the ratio of $\ell_{t,test}$ to $\ell_{ti}$ to indicate the change in transfer length with time. The maximum transfer length, minimum transfer length, and coefficient of variation (COV) of the transfer lengths are also given. The

COV is an indication of how close the individual transfer length values were to the mean transfer length and a smaller COV value indicates less scatter.

The effect of the main experimental variables on transfer length can be observed by examining the mean transfer lengths given in Table 9 and Table 10. The main experimental variables were number of strands, amount of transverse reinforcement, lightweight aggregate, strand size, and girder size. The number of strands was varied from Girder Design 1 to Girder Design 2. The mean $\ell_{ti}$ in Table 9 for the girders of Design 1 and 2 were similar, indicating that the additional strands in Girder Design 2 did cause an increase in mean $\ell_{ti}$. The amount of stirrups was varied from Girder Design 1 to Girder Design 3. The girders of Design 3, with a reduced amount of stirrups, had a mean $\ell_{ti}$ of 53 percent greater than the mean $\ell_{ti}$ of Design 1. Table 10 gives a comparison of the girders designs with 0.5 inch (13 mm) nominal diameter strands (Designs 1-3) to Girder Design 4 with 0.6 inch (15 mm) nominal diameter strands. Consistent with previous research, there was significant increase in the transfer of the larger strands.[16] The mean transfer length of the nine AASHTO Type II girders was 25 percent less that the transfer length of the six AASHTO/PCI BT-54 girders as given in Table 10. As shown in Table 3, Girder Designs 8 and 9 were flame cut to release the prestressing. Almost all the AASHTO Type II girders were detensioned, and previous research has shown that flame cutting tends to produce slightly longer measured transfer lengths.[14]

The mean $\ell_{t,test}$-to-$\ell_{ti}$ ratio for all 18 girders was 1.01 indicating an slight increase of transfer length with time. The ratios ranged from 0.73 to 1.37 indicating considerable scatter in the ratio. The slight increase transfer length with time is consistent with previous research.[23]

**Table 9. Summary of Transfer Length at Prestress Transfer and Prior to Test by Girder Design.**

| Girder Specimens† | Property‡ | Mean | COV | Max. | Min. |
|---|---|---|---|---|---|
| All Girders (18) | $\ell_{ti}$ (inch) | 13.57 | 0.32 | 21.41 | 7.87 |
| | $\ell_{t,test}$ (inch) | 13.56 | 0.34 | 22.40 | 8.14 |
| | $\ell_{t,test}$ / $\ell_{ti}$ | 1.01 | 0.16 | 1.37 | 0.73 |
| Girder Design 1 (3) | $\ell_{ti}$ (inch) | 9.42 | 0.17 | 11.00 | 7.87 |
| | $\ell_{t,test}$ (inch) | 10.78 | 0.22 | 12.85 | 8.14 |
| | $\ell_{t,test}$ / $\ell_{ti}$ | 1.15 | 0.17 | 1.37 | 1.03 |
| Girder Design 2 (3) | $\ell_{ti}$ (inch) | 9.46 | 0.15 | 11.09 | 8.47 |
| | $\ell_{t,test}$ (inch) | 9.87 | 0.09 | 10.56 | 8.91 |
| | $\ell_{t,test}$ / $\ell_{ti}$ | 1.05 | 0.12 | 1.20 | 0.95 |
| Girder Design 3 (3) | $\ell_{ti}$ (inch) | 14.42 | 0.33 | 19.86 | 11.51 |
| | $\ell_{t,test}$ (inch) | 13.07 | 0.49 | 20.47 | 8.67 |
| | $\ell_{t,test}$ / $\ell_{ti}$ | 0.88 | 0.17 | 1.03 | 0.73 |
| Girder Design 4 (3) | $\ell_{ti}$ (inch) | 18.60 | 0.16 | 21.20 | 15.29 |
| | $\ell_{t,test}$ (inch) | 20.30 | 0.09 | 22.40 | 19.06 |
| | $\ell_{t,test}$ / $\ell_{ti}$ | 1.11 | 0.13 | 1.27 | 0.99 |
| Girder Design 8 (3) | $\ell_{ti}$ (inch) | 13.86 | 0.12 | 15.08 | 11.96 |
| | $\ell_{t,test}$ (inch) | 11.86 | 0.10 | 13.02 | 10.70 |
| | $\ell_{t,test}$ / $\ell_{ti}$ | 0.86 | 0.15 | 0.99 | 0.74 |
| Girder Design 9 (3) | $\ell_{ti}$ (inch) | 15.64 | 0.32 | 21.41 | 12.59 |
| | $\ell_{t,test}$ (inch) | 15.45 | 0.24 | 19.64 | 13.08 |
| | $\ell_{t,test}$ / $\ell_{ti}$ | 1.00 | 0.08 | 1.06 | 0.92 |

Notes:

† No. of specimens given in parentheses

‡ Measured transfer length at prestress transfer ($\ell_{ti}$), Measured transfer length at girder test ($\ell_{t,test}$)

Units: 1.0 inch = 25.4 mm

**Table 10. Summary of Transfer Length at Prestress Transfer and Prior to Test by Girder Mix Design, Nominal Strand Size, and Girder Type.**

| Girder Specimens† | Property‡ | Mean | COV | Max. | Min. |
|---|---|---|---|---|---|
| All Girders (18) | $\ell_{ti}$ (inch) | 13.57 | 0.32 | 21.41 | 7.87 |
| UG Mix (6) | $\ell_{ti}$ (inch) | 14.44 | 0.36 | 21.41 | 7.87 |
| HG Mix (6) | $\ell_{ti}$ (inch) | 11.80 | 0.19 | 15.29 | 8.47 |
| SG Mix (6) | $\ell_{ti}$ (inch) | 14.45 | 0.36 | 21.20 | 8.82 |
| Girder Design 1-3, 0.5 inch strand (9) | $\ell_{ti}$ (inch) | 11.10 | 0.32 | 19.86 | 7.87 |
| Girder Design 4, 0.6 inch strand (3) | $\ell_{ti}$ (inch) | 18.60 | 0.16 | 21.20 | 15.29 |
| Girder Design 1-3, Type II (9) | $\ell_{ti}$ (inch) | 11.10 | 0.32 | 19.86 | 7.87 |
| Girder Design 8-9, BT-54 (6) | $\ell_{ti}$ (inch) | 14.75 | 0.24 | 21.41 | 11.96 |

Notes:
† Specimen name of form $#, where: $ is A for UG mix, B for HG mix, C for SG mix, # is girder design; No. of specimens given in parentheses
‡ Measured transfer length at prestress transfer ($\ell_{ti}$), Measured transfer length at girder test ($\ell_{t,test}$)
Units: 1.0 inch = 25.4 mm

### *Analysis of Parameters used for Transfer Length Prediction*

The transfer lengths measured immediately after prestress release ($\ell_{ti}$) are presented graphically in Figure 12 through Figure 19. The figures are presented in pairs. The first figure in each pair gives the transfer lengths identified by girder design number. The second figure in each pair gives the transfer length identified by girder concrete mix. The figures compare transfer length to parameters used by researchers to predict transfer length.[20,22,25,29] Figure 12 and Figure 13 compare transfer length to concrete compressive strength at the time of prestress transfer ($f'_{ci}$). Figure 14 and Figure 15 compare transfer length to concrete unit weight ($w_c$). Transfer length is compared to concrete elastic modulus at the time of prestress transfer in Figure 16 and Figure 17. The measured transfer length was also compared to the calculated effective stress in the prestressing ($f_{pe}$) in Figure 18 and Figure 19.

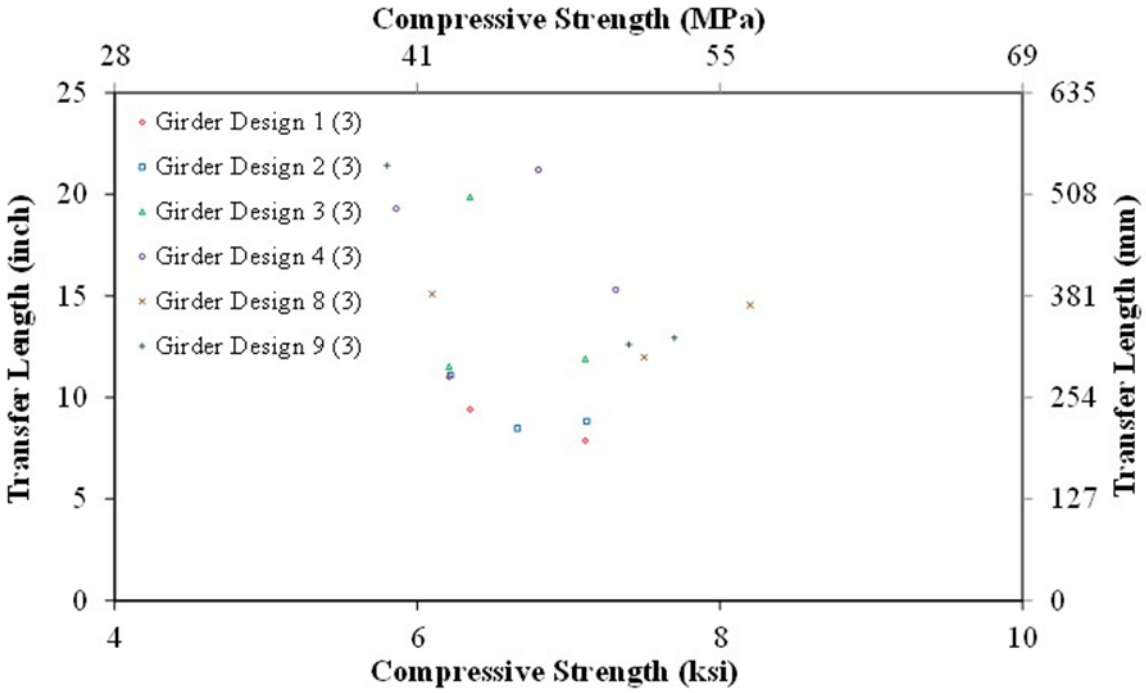


**Figure 12. Graph. Transfer Length at Prestress Transfer Compared to Compressive Strength at Transfer by Girder Design.**

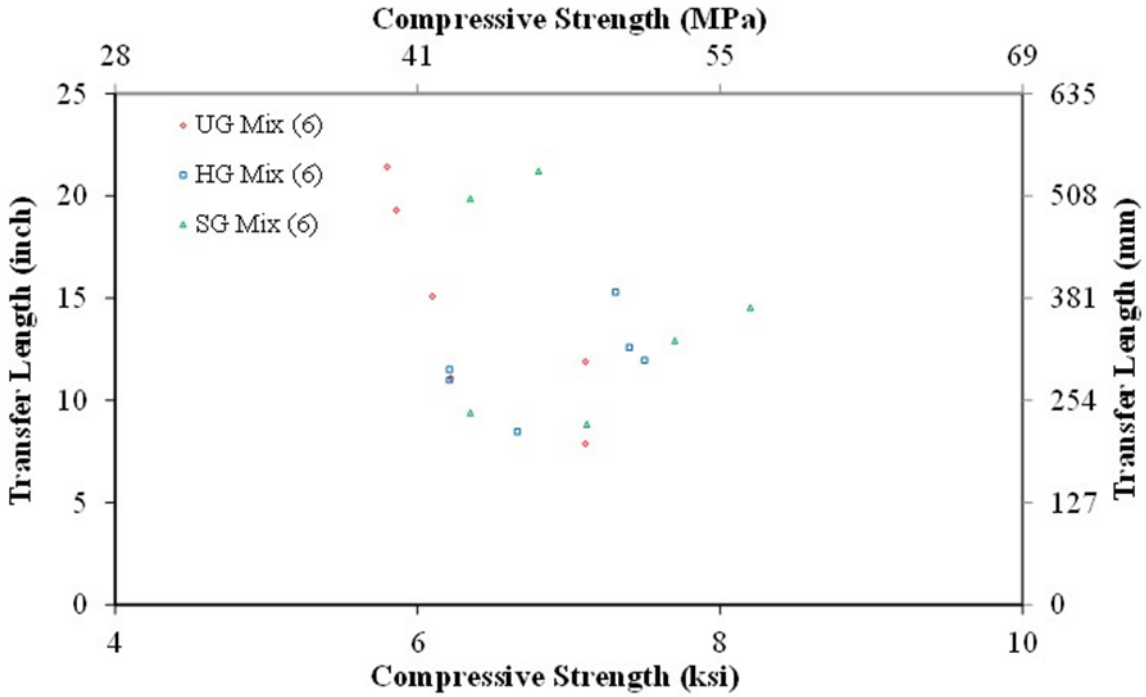


**Figure 13. Graph. Transfer Length at Prestress Transfer Compared to Compressive Strength at Transfer by Girder Concrete Mix.**

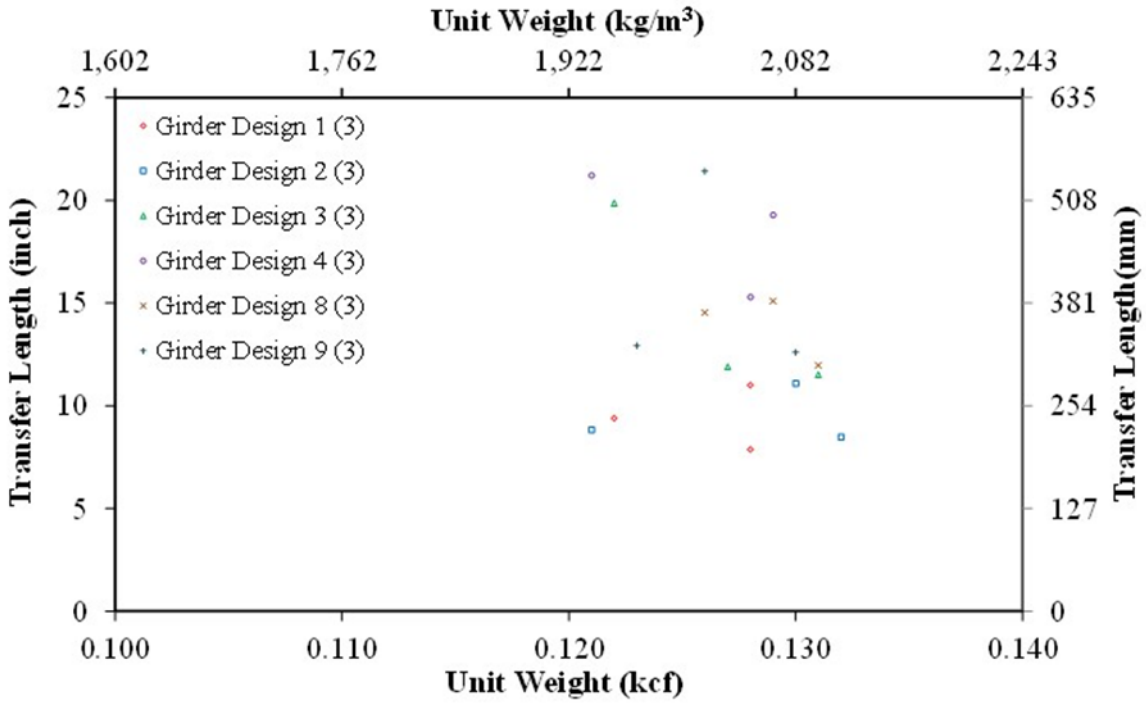


**Figure 14. Graph. Transfer Length at Prestress Transfer Compared to Unit Weight by Girder Design.**

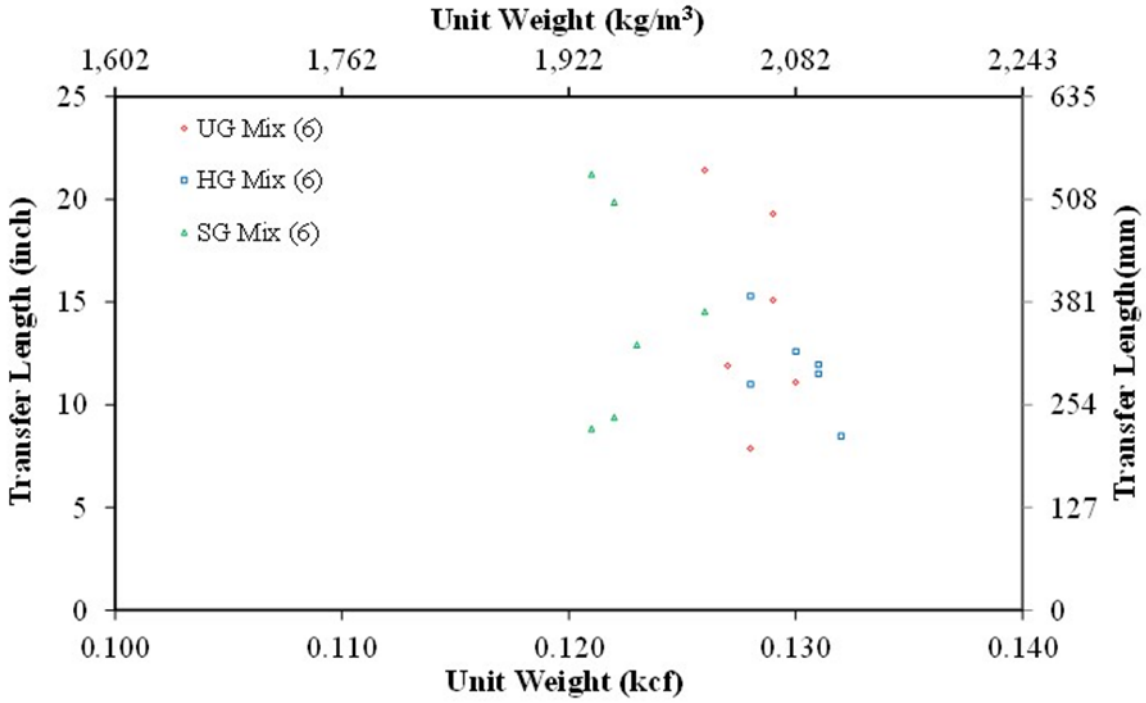


**Figure 15. Graph. Transfer Length at Prestress Transfer Compared to Unit Weight by Girder Concrete Mix.**

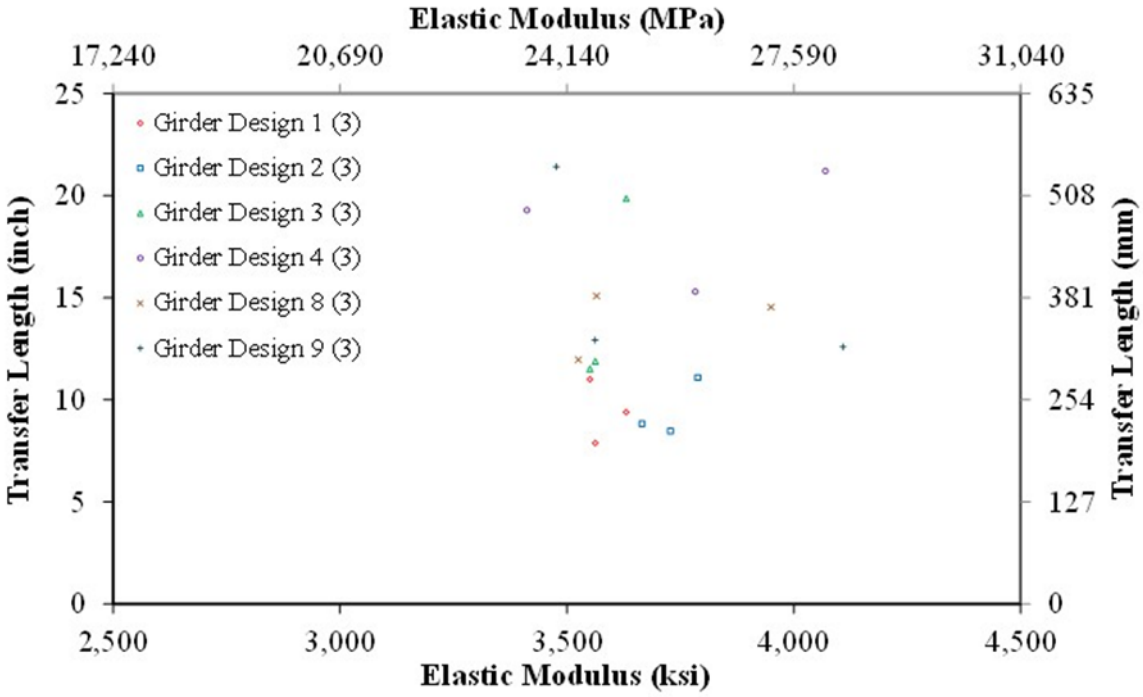


**Figure 16. Graph. Transfer Length at Prestress Transfer Compared to Elastic Modulus at Transfer by Girder Design.**

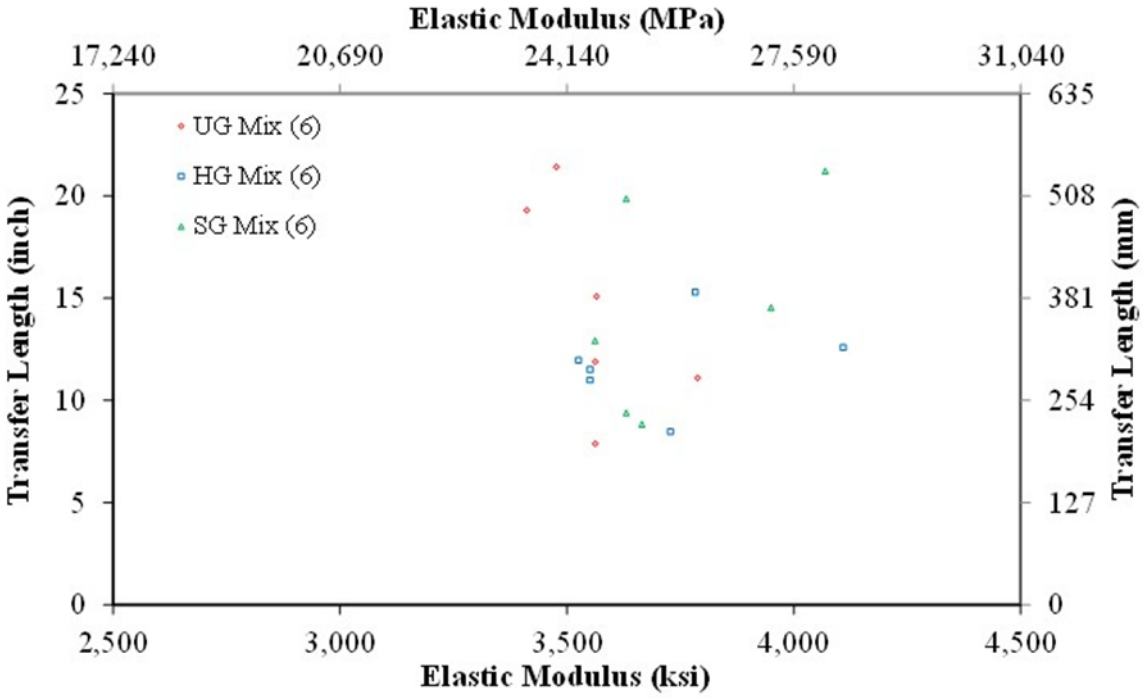


**Figure 17. Graph. Transfer Length at Prestress Transfer Compared to Elastic Modulus at Transfer by Girder Concrete Mix.**

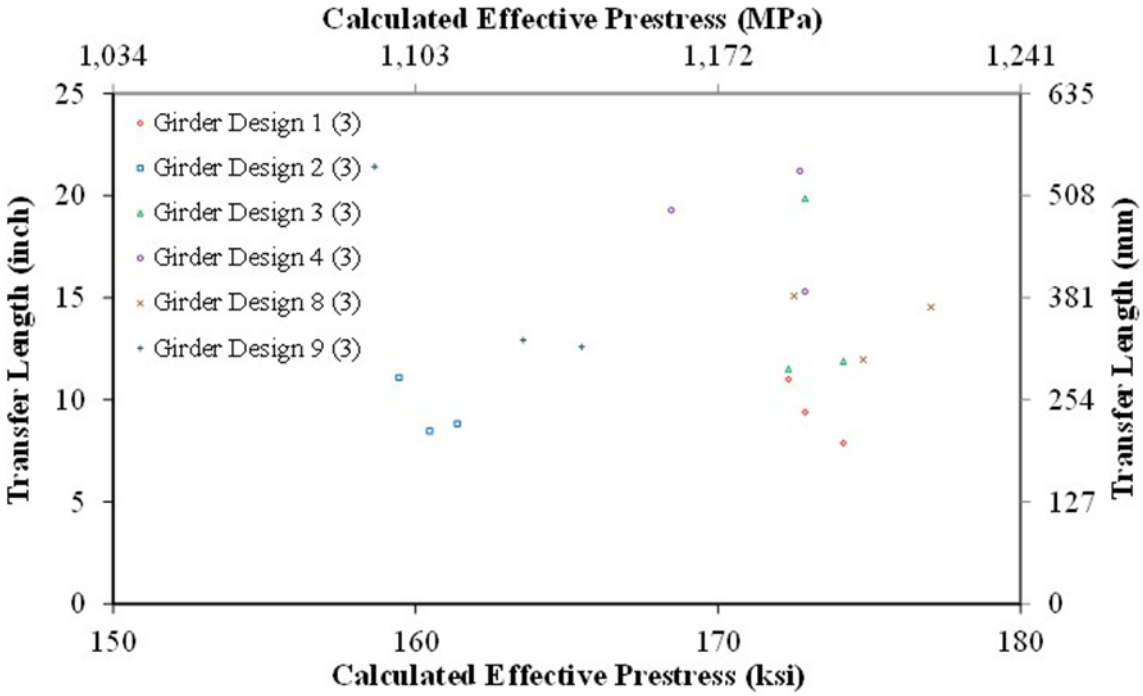


**Figure 18. Graph. Transfer Length at Prestress Transfer Compared to Calculated Effective Prestress by Girder Design.**

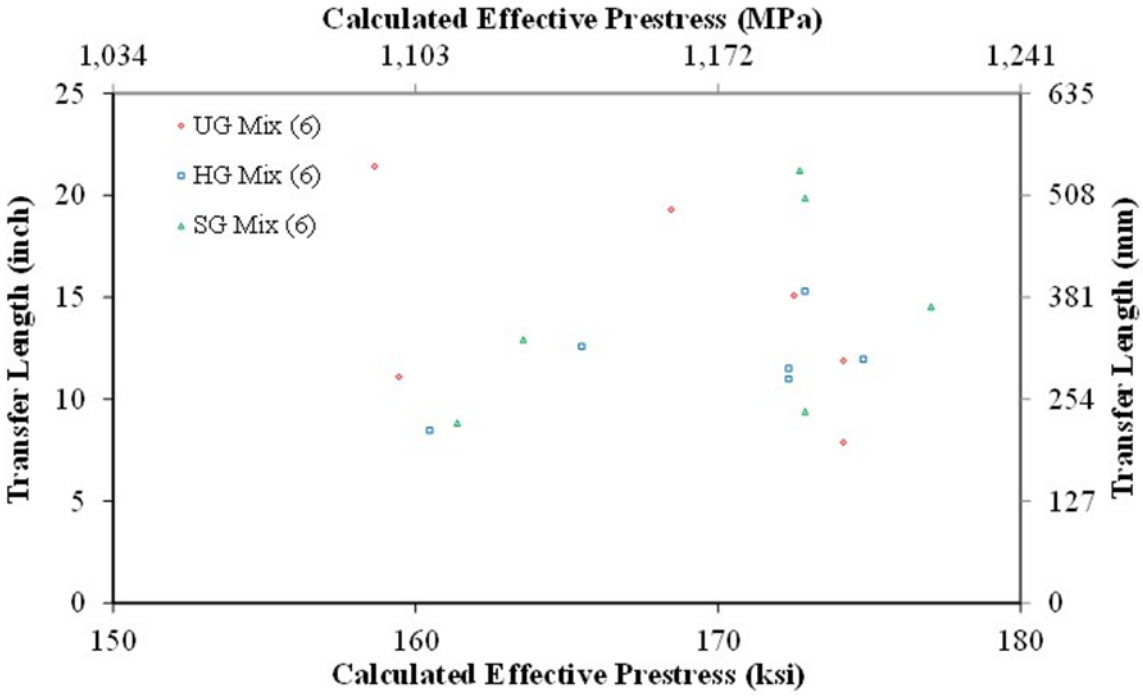


**Figure 19. Graph. Transfer Length at Prestress Transfer Compared to Calculated Effective Prestress by Girder Concrete Mix.**

### *Normalized Transfer Length*

The transfer lengths determined using the measurements taken immediately after prestress release ($\ell_{ti}$) were normalized by parameters described by researchers in the literature as being important in the prediction of transfer length.[20,22,25,29] These parameters include nominal strand diameter, effective strand stress, concrete compressive strength, and concrete elastic modulus. The normalized transfer lengths are shown graphically in Figure 20 through Figure 31. In each figure, the transfer lengths are shown in series by girder design number. The figures are presented in pairs. The first figure in each pair compares the normalized transfer length to concrete compressive strength at the time of prestress transfer ($f'_{ci}$). The second figure of each pair compares the normalized transfer length to concrete unit weight ($w_c$).

In Figure 20 and Figure 21 transfer length is normalized by nominal strand diameter ($d_b$). This method of normalizing transfer length is in the form of the expression for transfer length given by the AASHTO Standard Specifications for Highway Bridges (Eq. 1) and the AASHTO LRFD Bridge Design Specification (Eq. 2). Horizontal lines at values of 50 and 60 represent the prediction given by Standard Specifications for Highway Bridges (AASHTO STD) and AASHTO LRFD Bridge Design Specification (AASHTO LRFD) expressions. All of the data are below the horizontal lines indicating an overestimation of the transfer length by both expressions.

The transfer length is normalized by nominal strand diameter multiplied by the calculated effective prestress ($d_b f_{pe}$) in Figure 22 and Figure 23. A horizontal line at a value of 1/3 indicates the prediction given by the Hanson and Kaar expression (Eq. 3) that is the basis for the expression in the ACI 318 Building Code. All of the data are below the horizontal prediction line indicating an overestimation of the transfer length.

The transfer lengths in Figure 24 and Figure 25 are normalized by the ratio of nominal strand diameter to the square root of concrete compressive strength at time of transfer ($d_b/\sqrt{f'_{ci}}$). The prediction of transfer length given by Meyer et al. (Eq. 8) is shown as a horizontal line at $50\sqrt{6}$. All of the data are below the horizontal prediction line indicating an overestimation of the transfer length.

Figure 26 and Figure 27 show the transfer lengths normalized by $f_{pt}d_b/\sqrt{f'_{ci}}$. Predictions of transfer length by Mitchell et al. (Eq. 4) and Barnes et al. (Eq. 10) are indicated by horizontal lines at values of $0.3\sqrt{33}$ and 0.17. All of the points are below the prediction given by Mitchell et al. indicating all of the data are overestimated. The expression proposed by Barnes et al. was intended to be a lower bound prediction of transfer length. All of the data are above the prediction by Barnes et al. indicating the intended underestimation of transfer length.

The building and bridge design specifications do not explicitly include the concrete elastic modulus in the prediction expressions for transfer length. A study completed by Buckner for FHWA[20] and a study by Thatcher et al. on LWC[24] included the concrete modulus of elasticity at prestress transfer ($E_{ci}$) in the prediction expression. Figure 28 and Figure 29 show transfer

length normalized by $d_b/E_{ci}$. The expressions by Buckner (Eq. 6) and Thatcher et al. (Eq. 7) included a term for stress in the prestressing strands. The horizontal lines shown in the figures included an assumed 150 ksi (1030 MPa) for strand stress. All of the data were below the line at 1250×150/1000 representing the Buckner expression. All but three data points were above the line at 900×150/1000 representing the Thatcher et al. expression.

The normalization of transfer length by $f_{pt}d_b/E_{ci}$ is shown in Figure 30 and Figure 31. These figures give a more direct evaluation of the Buckner and Thatcher et al. expressions. Horizontal lines at 1250/1000 and 900/1000 represent the predictions by the Buckner and Thatcher et al. expressions, respectively. All of the data are below both the Buckner and Thatcher et al. prediction.

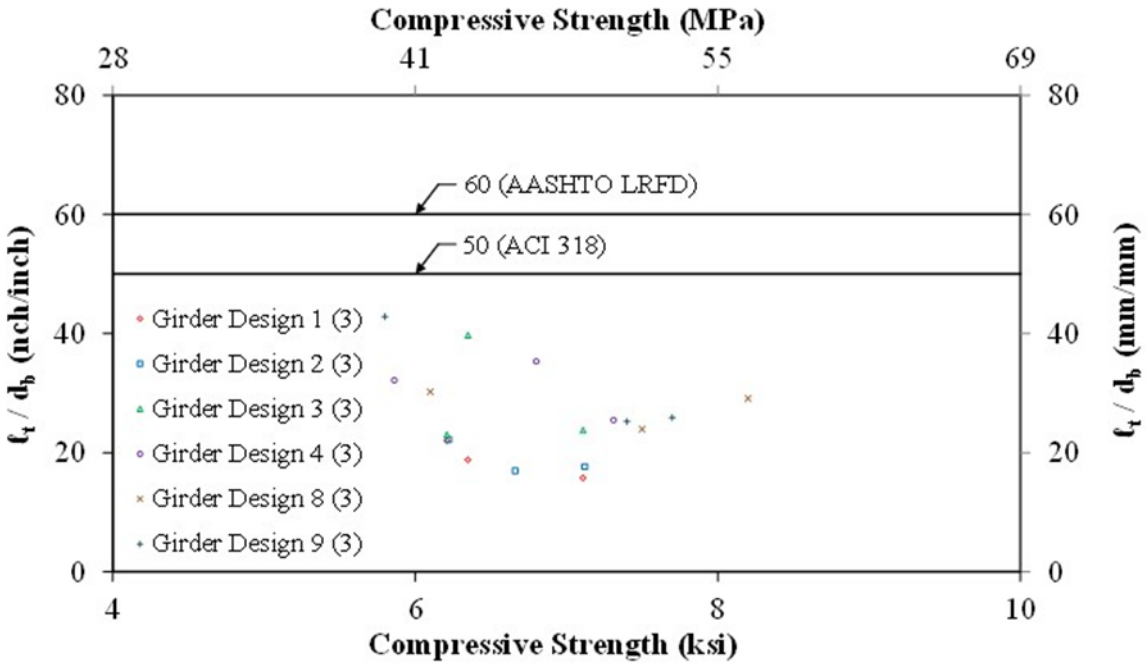


**Figure 20. Graph. Normalized Transfer Length ($\ell_t/d_b$) Compared to Compressive Strength by Girder Design.**

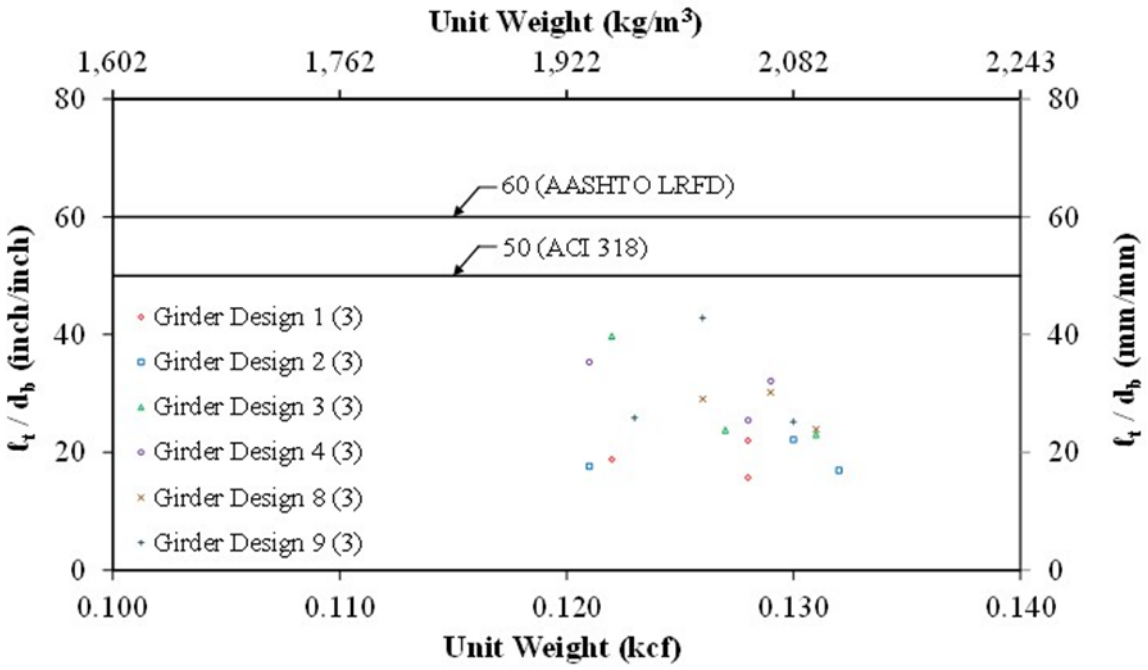


**Figure 21. Graph. Normalized Transfer Length ($\ell_t/d_b$) Compared to Unit Weight by Girder Design.**

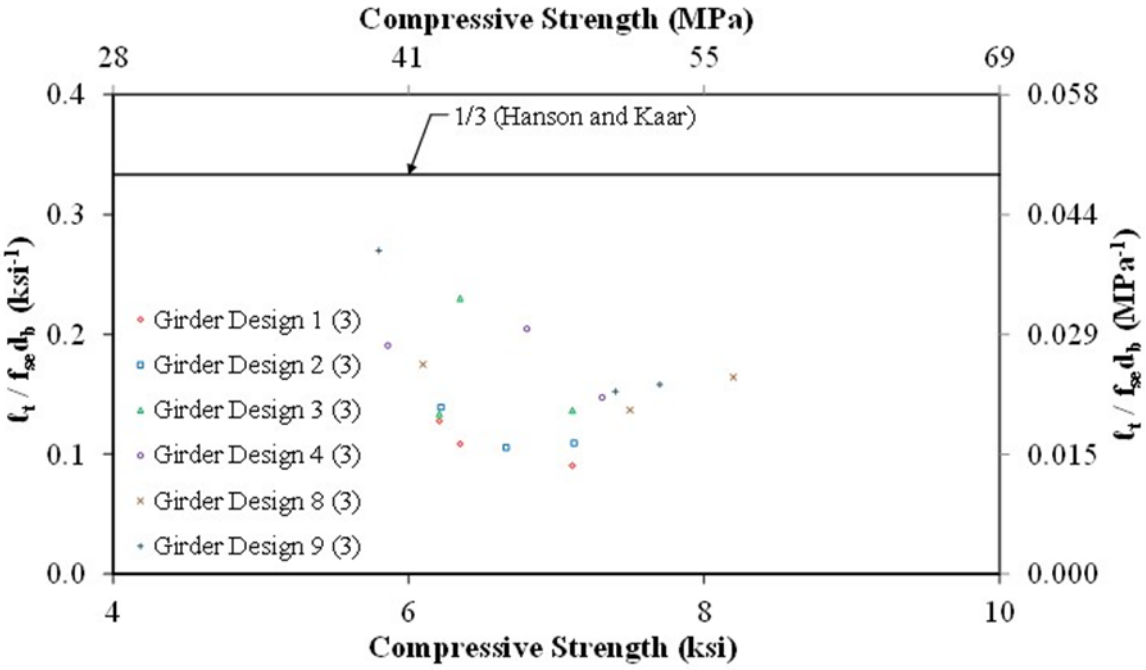


**Figure 22. Graph. Normalized Transfer Length ($\ell_t/f_{se}d_b$) Compared to Compressive Strength by Girder Design.**

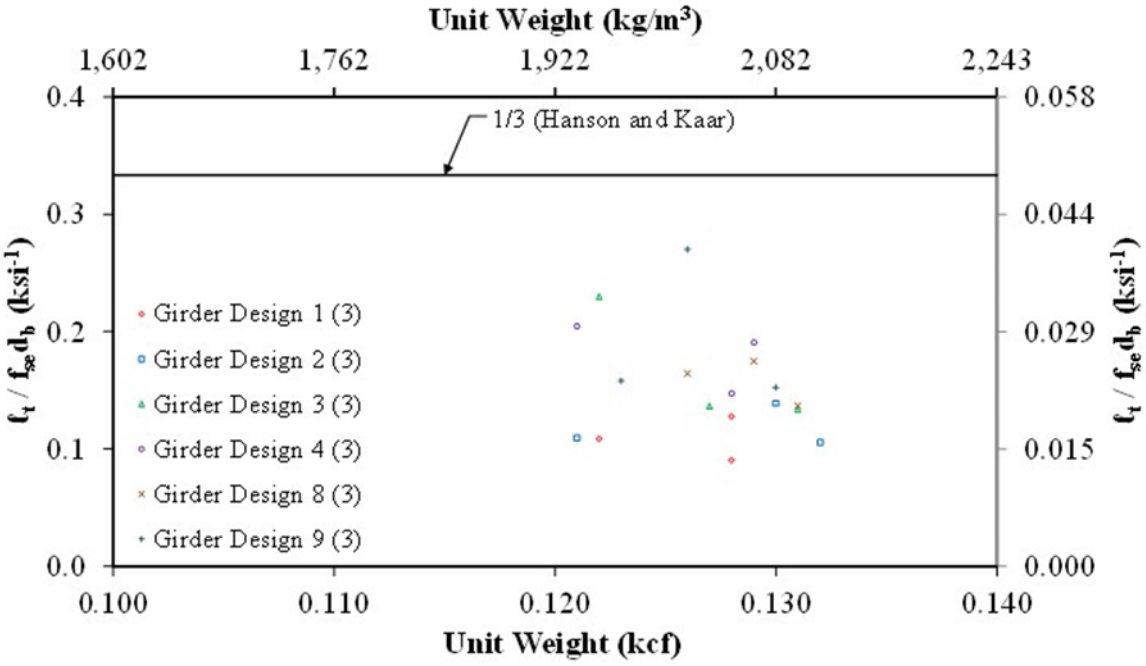


**Figure 23. Graph. Normalized Transfer Length ($\ell_t/f_{se}d_b$) Compared to Unit Weight by Girder Design.**

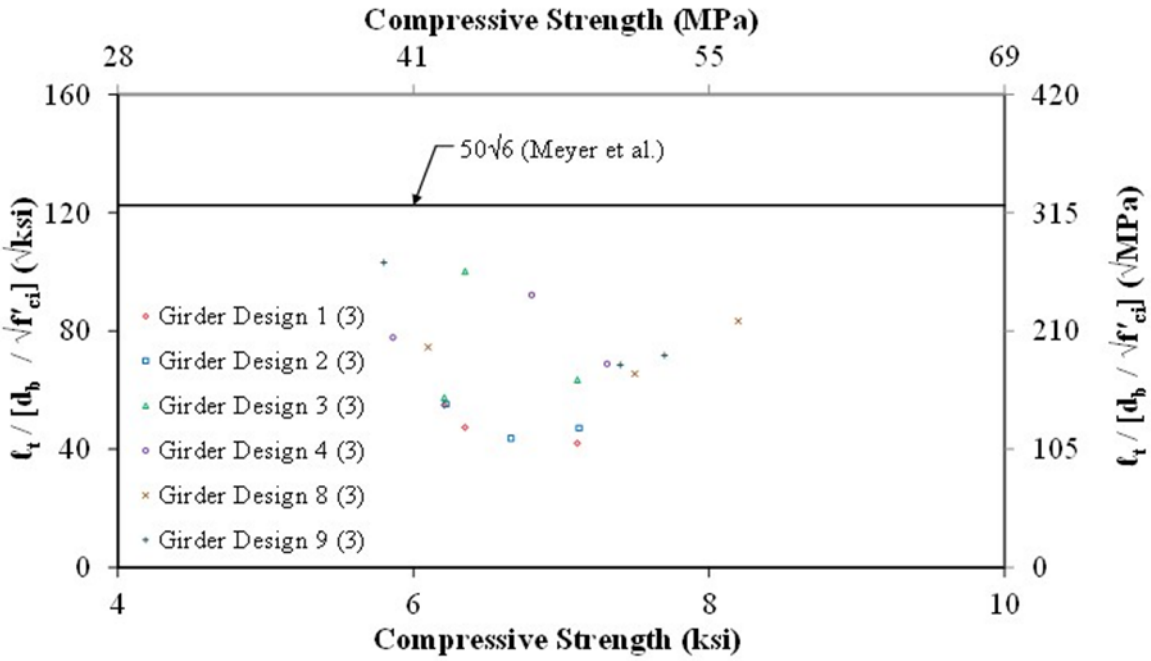


**Figure 24. Graph. Normalized Transfer Length ($\ell_t/[d_b/\sqrt{f'_{ci}}]$) Compared to Compressive Strength by Girder Design.**

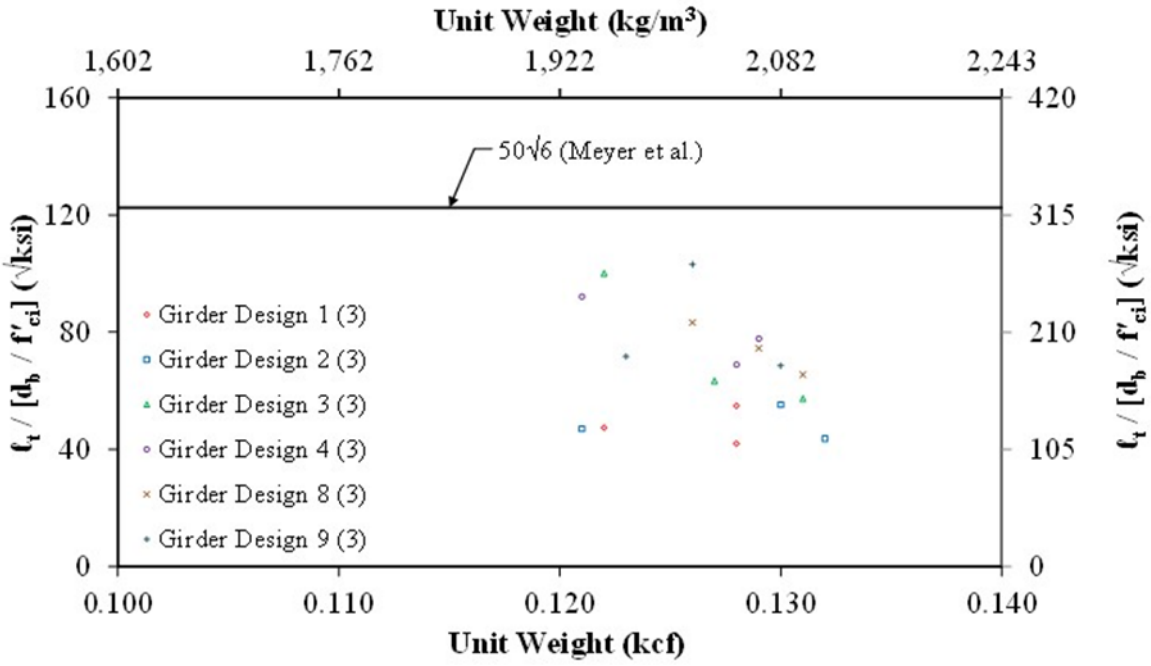


**Figure 25. Graph. Normalized Transfer Length ($\ell_t/[d_b/\sqrt{f'_{ci}}]$) Compared to Unit Weight by Girder Design.**

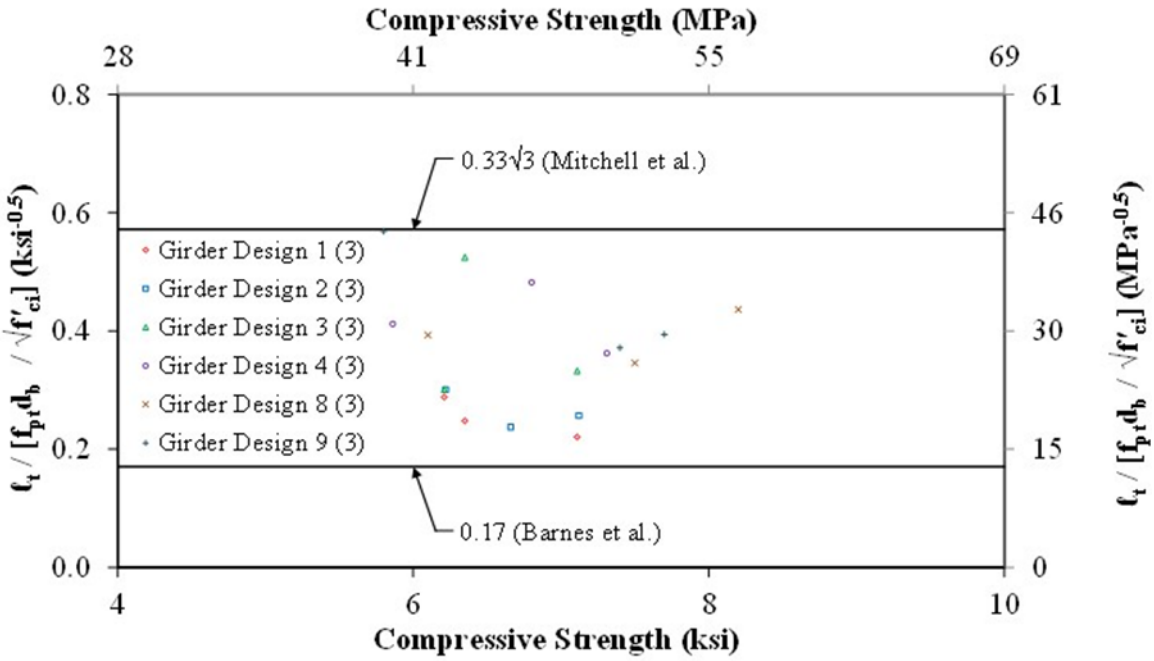


**Figure 26. Graph. Normalized Transfer Length ($\ell_t/[f_{pt}d_b/\sqrt{f'_{ci}}]$) Compared to Compressive Strength by Girder Design.**

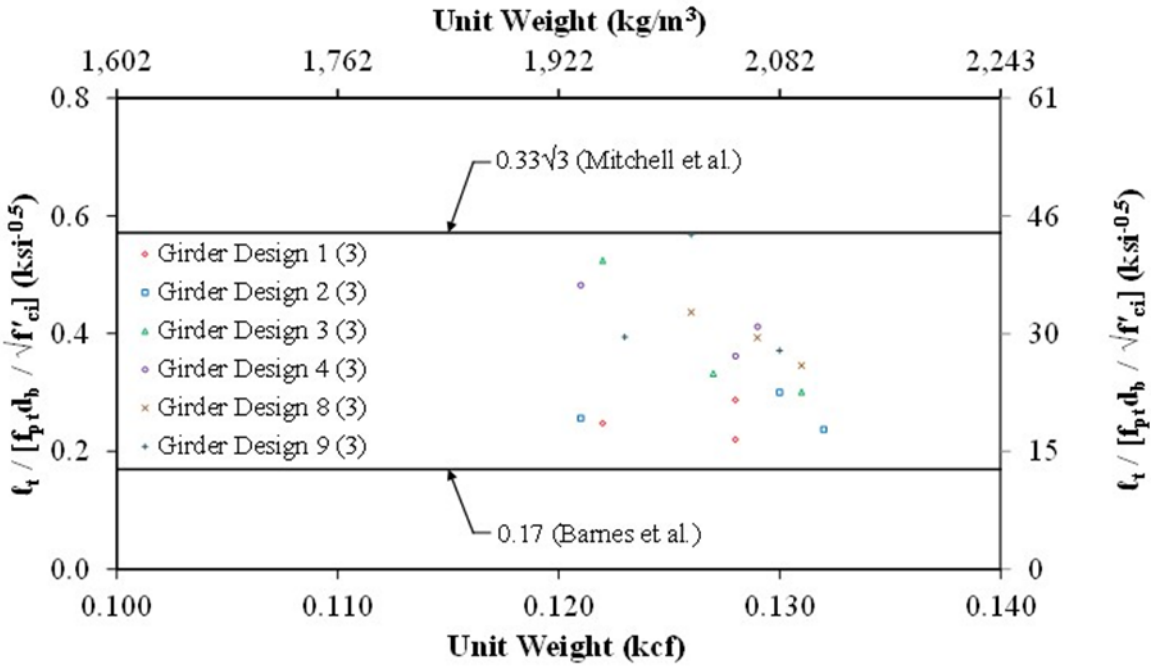


**Figure 27. Graph. Normalized Transfer Length ($\ell_t/[f_{pt}d_b/\sqrt{f'_{ci}}]$) Compared to Unit Weight by Girder Design.**

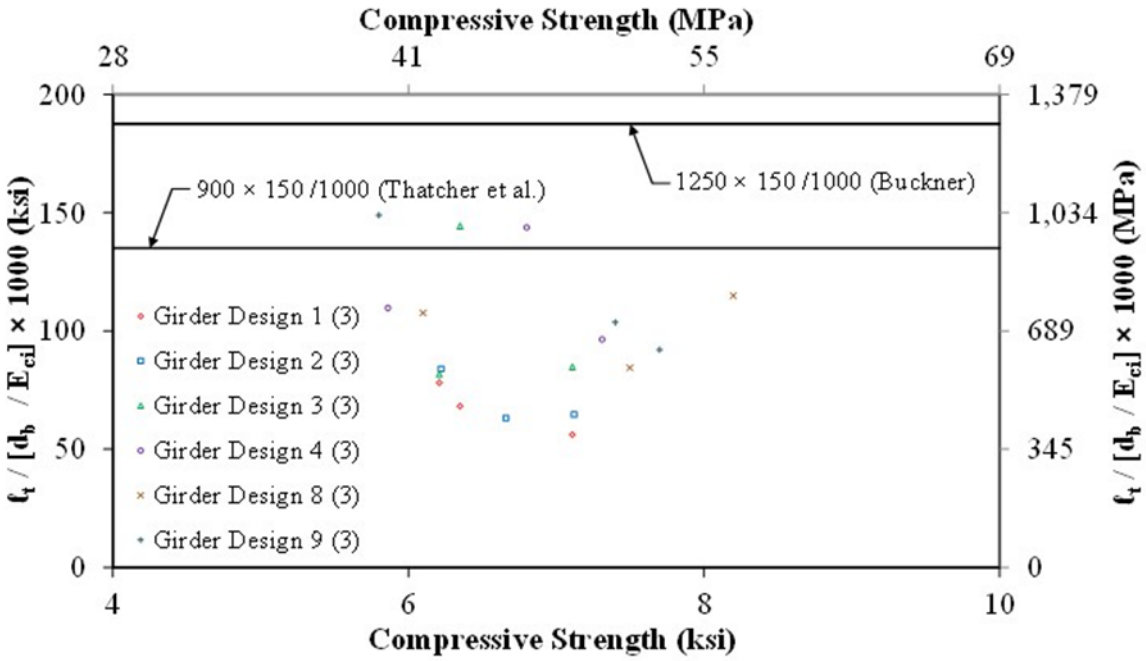


**Figure 28. Graph. Normalized Transfer Length ($\ell_t/[d_b/E_{ci}]$) Compared to Compressive Strength by Girder Design.**

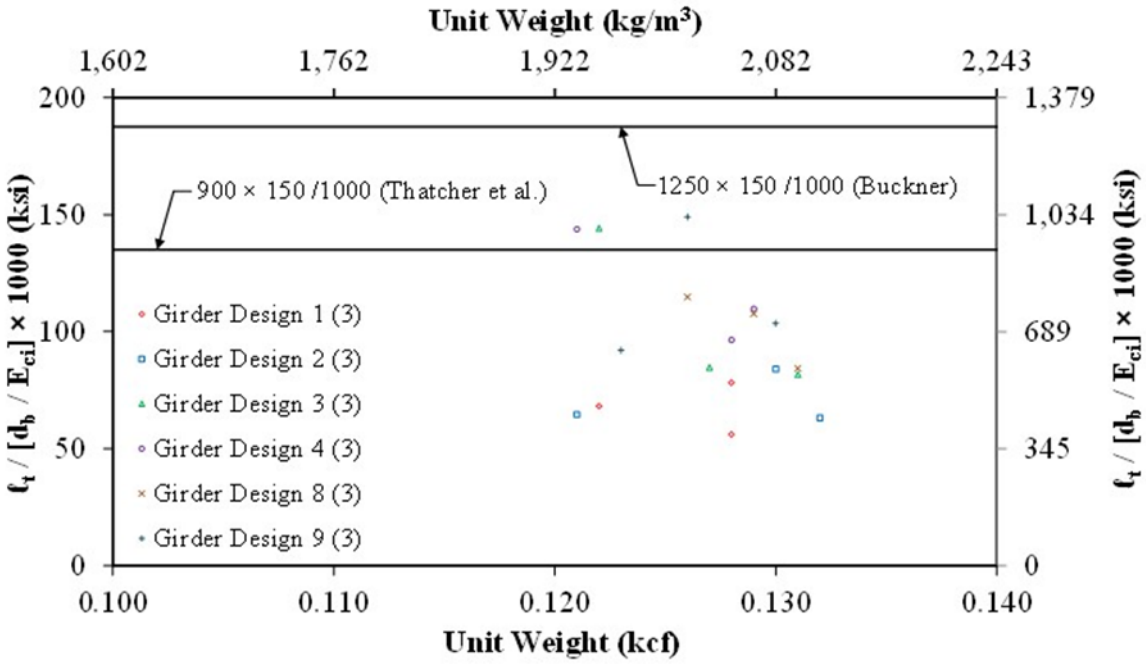


**Figure 29. Graph. Normalized Transfer Length ($\ell_t/[d_b/E_{ci}]$) Compared to Unit Weight by Girder Design.**

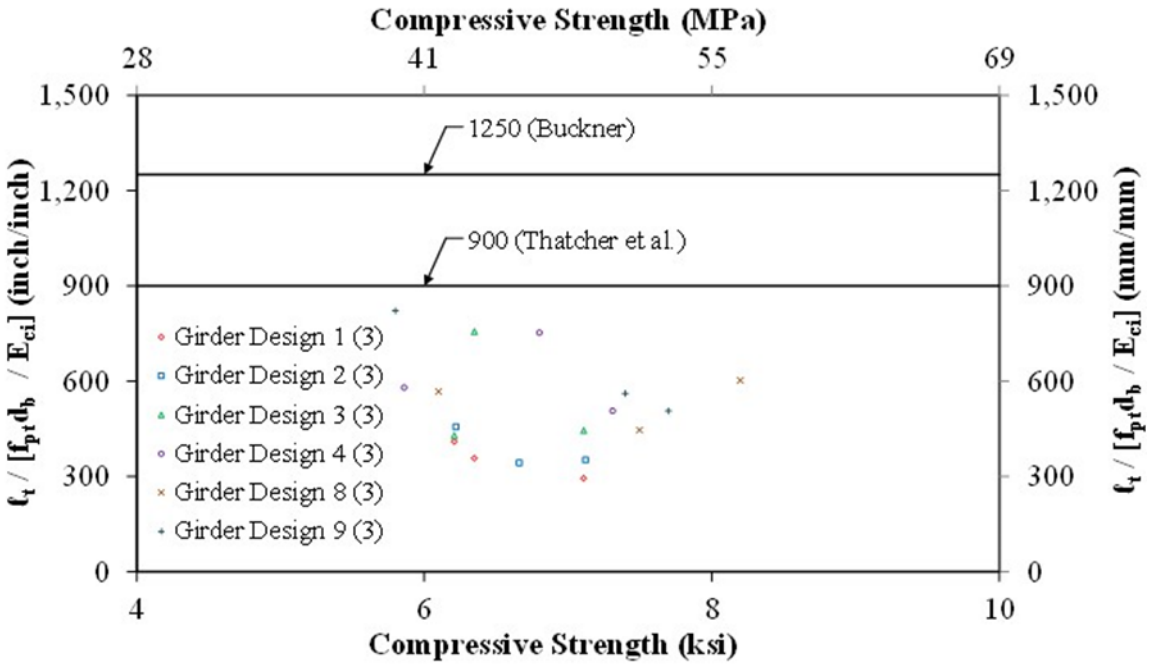


**Figure 30. Graph. Normalized Transfer Length ($\ell_t/[f_{pt}d_b/E_{ci}]$) Compared to Compressive Strength by Girder Design.**

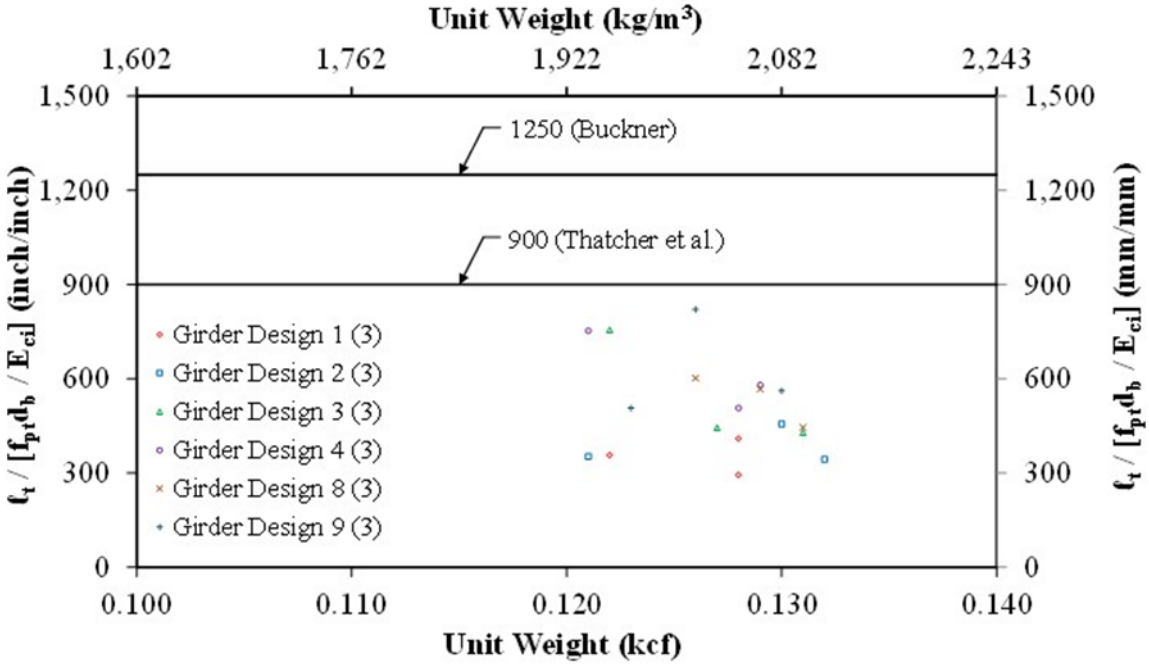


**Figure 31. Graph. Normalized Transfer Length ($\ell_t/[f_{pt}d_b/E_{ci}]$) Compared to Unit Weight by Girder Design.**

### *Transfer Length Predictions*

The transfer length determined from measurements taken immediately after prestress release ($\ell_{ti}$) was compared to the transfer length predicted by several expressions including the one in the AASHTO LRFD Bridge Design Specifications. The measured transfer lengths were compared to the predicted transfer lengths using a test-to-prediction ratio with the measured $\ell_{ti}$ being referred to as the "test."

Table 11 gives the test-to-prediction ratios for nine expressions for predicting transfer length described previously in this report. The mean ratios for all 18 LWC girders described in this report are given in Table 11. The COV, maximum ratio, minimum ratio, and percent of ratios less than 1.0 are also given in the table. Ratios less than 1.0 indicate a prediction that overestimates the transfer length. There is significant scatter in all of the predicted transfer lengths as indicated in the high COV for the expressions that ranged from 0.27 to 0.32. The largest scatter is given by the expression in the AASHTO LRFD Bridge Design Specifications (Eq. 2) and the smallest scatter is given by the Meyer et al. (Eq. 8) and Ramirez and Russell (Eq. 9) expressions. All expressions except those by Mitchell et al. and Barnes et al. overestimated all of the transfer lengths. The Mitchell et al. expression (Eq. 4) underestimated two data points. The Barnes et al. expression (Eq. 10) is described as a lower-bound prediction of transfer length[14] and underestimated all of the data points.

The transfer length test-to-prediction ratios are evaluated for the main experimental variables of concrete mix, nominal strand diameter, and girder size in Table 12, Table 13, and Table 14. The transfer length test-to-prediction ratios are separated by concrete mix design in Table 12. This table shows that the scatter in the prediction of transfer lengths (i.e., higher COV) for girders with the HG mix was significantly less than for girders of the other two mixes. The mean ratios for the girders with the HG mix were also lower for each prediction expression. Table 13 separates the girders by nominal strand diameter. The scatter in the ratios for girders with 0.6 inch (15 mm) diameter strand was significantly less that for the girders with 0.5 inch (13 mm) diameter strand. The mean ratios for each expression were higher for the girders with 0.6 inch (15 mm) diameter strand. This indicates that the magnitude of increase in measured transfer length of the larger diameter strands was underestimated by the prediction expressions. The measured transfer lengths were grouped by girder size in Table 14. The scatter in the ratios for the larger AASHTO/PCI BT-54 girders was less that the scatter in the smaller AASHTO Type II girders. The mean ratios were also slightly larger for the BT-54 girders indicating that the measured transfer lengths were longer than the Type II girders even though they had the same size strand. As described previously in this report, this is likely due to the method of prestress release.

**Table 11. Test-to-Prediction Ratio of Transfer Length for All Girders.**

| Girder Specimens[†] | Design Expression[‡] | Mean | COV | Max. | Min. | Percent < 1.0 |
|---|---|---|---|---|---|---|
| All TFHRC Girders (18) | AASHTO Std. | 0.522 | 0.291 | 0.856 | 0.315 | 100% |
| | AASHTO LRFD | 0.452 | 0.320 | 0.714 | 0.262 | 100% |
| | ACI 318 | 0.463 | 0.298 | 0.810 | 0.271 | 100% |
| | Meyer et al. | 0.552 | 0.274 | 0.842 | 0.343 | 100% |
| | Ramirez and Russell | 0.563 | 0.274 | 0.859 | 0.350 | 100% |
| | Mitchell et al. | 0.701 | 0.277 | 1.140 | 0.423 | 89% |
| | Barnes et al. | 2.351 | 0.277 | 3.824 | 1.418 | 0% |
| | Buckner | 0.379 | 0.294 | 0.588 | 0.222 | 100% |
| | Thatcher et al. | 0.526 | 0.294 | 0.817 | 0.308 | 100% |

Notes:

[†] No. of specimens given in parentheses

[‡] AASHTO Standard Spec. (Eq. 1), AASHTO LRFD (Eq. 2), ACI 318 (Eq. 3), Meyer et al. (Eq. 8), Ramirez and Russell (Eq. 9), Mitchell et al. (Eq. 4), Barnes et al. (Eq. 10), Buckner (Eq. 6), Thatcher et al. (Eq. 7)

**Table 12. Test-to-Prediction Ratio of Transfer Length by Girder Mix Design.**

| Girder Specimens[†] | Design Expression[‡] | Mean | COV | Max. | Min. | Percent < 1.0 |
|---|---|---|---|---|---|---|
| UG Mix (6) | AASHTO Std. | 0.556 | 0.339 | 0.856 | 0.315 | 100% |
| | AASHTO LRFD | 0.481 | 0.358 | 0.714 | 0.262 | 100% |
| | ACI 318 | 0.501 | 0.367 | 0.810 | 0.271 | 100% |
| | Meyer et al. | 0.566 | 0.304 | 0.842 | 0.343 | 100% |
| | Ramirez and Russell | 0.578 | 0.304 | 0.859 | 0.350 | 100% |
| | Mitchell et al. | 0.730 | 0.332 | 1.140 | 0.423 | 83% |
| | Barnes et al. | 2.447 | 0.332 | 3.824 | 1.418 | 0% |
| | Buckner | 0.389 | 0.319 | 0.588 | 0.222 | 100% |
| | Thatcher et al. | 0.540 | 0.319 | 0.817 | 0.308 | 100% |
| HG Mix (6) | AASHTO Std. | 0.455 | 0.138 | 0.510 | 0.339 | 100% |
| | AASHTO LRFD | 0.393 | 0.188 | 0.510 | 0.282 | 100% |
| | ACI 318 | 0.402 | 0.124 | 0.457 | 0.317 | 100% |
| | Meyer et al. | 0.488 | 0.164 | 0.563 | 0.357 | 100% |
| | Ramirez and Russell | 0.498 | 0.164 | 0.574 | 0.364 | 100% |
| | Mitchell et al. | 0.617 | 0.153 | 0.726 | 0.478 | 100% |
| | Barnes et al. | 2.070 | 0.153 | 2.436 | 1.602 | 0% |
| | Buckner | 0.334 | 0.168 | 0.409 | 0.249 | 100% |
| | Thatcher et al. | 0.464 | 0.168 | 0.568 | 0.346 | 100% |
| SG Mix (6) | AASHTO Std. | 0.555 | 0.318 | 0.794 | 0.353 | 100% |
| | AASHTO LRFD | 0.482 | 0.359 | 0.707 | 0.294 | 100% |
| | ACI 318 | 0.487 | 0.302 | 0.689 | 0.326 | 100% |
| | Meyer et al. | 0.601 | 0.306 | 0.817 | 0.384 | 100% |
| | Ramirez and Russell | 0.613 | 0.306 | 0.834 | 0.392 | 100% |
| | Mitchell et al. | 0.756 | 0.290 | 1.016 | 0.480 | 83% |
| | Barnes et al. | 2.536 | 0.290 | 3.406 | 1.610 | 0% |
| | Buckner | 0.413 | 0.339 | 0.570 | 0.256 | 100% |
| | Thatcher et al. | 0.574 | 0.339 | 0.791 | 0.355 | 100% |

Notes:

[†] No. of specimens given in parentheses

[‡] AASHTO Standard Spec. (Eq. 1), AASHTO LRFD (Eq. 2), ACI 318 (Eq. 3), Meyer et al. (Eq. 8), Ramirez and Russell (Eq. 9), Mitchell et al. (Eq. 4), Barnes et al. (Eq. 10), Buckner (Eq. 6), Thatcher et al. (Eq. 7)

**Table 13. Test-to-Prediction Ratio of Transfer Length by Nominal Strand Diameter.**

| Girder Specimens[†] | Design Expression[‡] | Mean | COV | Max. | Min. | Percent < 1.0 |
|---|---|---|---|---|---|---|
| Girder Designs 1 thru 3 with 0.5 inch dia. strand (9) | AASHTO Std | 0.444 | 0.323 | 0.794 | 0.315 | 100% |
| | AASHTO LRFD | 0.370 | 0.323 | 0.662 | 0.262 | 100% |
| | ACI (Hanson and | 0.394 | 0.309 | 0.689 | 0.271 | 100% |
| | Meyer et al. | 0.464 | 0.311 | 0.817 | 0.343 | 100% |
| | Ramirez and Russell | 0.473 | 0.311 | 0.834 | 0.350 | 100% |
| | Mitchell et al. | 0.589 | 0.296 | 1.016 | 0.423 | 89% |
| | Barnes et al. | 1.974 | 0.296 | 3.406 | 1.418 | 0% |
| | Buckner | 0.318 | 0.323 | 0.570 | 0.222 | 100% |
| | Thatcher et al. | 0.442 | 0.323 | 0.791 | 0.308 | 100% |
| Girder Design 4 with 0.6 inch dia. strand (3) | AASHTO Std. | 0.620 | 0.162 | 0.707 | 0.510 | 100% |
| | AASHTO LRFD | 0.620 | 0.162 | 0.707 | 0.510 | 100% |
| | ACI 318 | 0.543 | 0.165 | 0.614 | 0.442 | 100% |
| | Meyer et al. | 0.650 | 0.147 | 0.752 | 0.563 | 100% |
| | Ramirez and Russell | 0.664 | 0.147 | 0.768 | 0.574 | 100% |
| | Mitchell et al. | 0.815 | 0.145 | 0.936 | 0.699 | 100% |
| | Barnes et al. | 2.734 | 0.145 | 3.139 | 2.345 | 0% |
| | Buckner | 0.461 | 0.210 | 0.568 | 0.381 | 100% |
| | Thatcher et al. | 0.640 | 0.210 | 0.789 | 0.529 | 100% |

Notes:

[†] No. of specimens given in parentheses

[‡] AASHTO Standard Spec. (Eq. 1), AASHTO LRFD (Eq. 2), ACI 318 (Eq. 3), Meyer et al. (Eq. 8), Ramirez and Russell (Eq. 9), Mitchell et al. (Eq. 4), Barnes et al. (Eq. 10), Buckner (Eq. 6), Thatcher et al. (Eq. 7)

**Table 14. Test-to-Prediction Ratio of Transfer Length by Girder Depth.**

| Girder Specimens[†] | Design Expression[‡] | Mean | COV | Max. | Min. | Percent < 1.0 |
|---|---|---|---|---|---|---|
| Type II Girder Designs 1 thru 3 (9) | AASHTO Std. | 0.444 | 0.323 | 0.794 | 0.315 | 100% |
| | AASHTO LRFD | 0.370 | 0.323 | 0.662 | 0.262 | 100% |
| | ACI 318 | 0.394 | 0.309 | 0.689 | 0.271 | 100% |
| | Meyer et al. | 0.464 | 0.311 | 0.817 | 0.343 | 100% |
| | Ramirez and Russell | 0.473 | 0.311 | 0.834 | 0.350 | 100% |
| | Mitchell et al. | 0.589 | 0.296 | 1.016 | 0.423 | 89% |
| | Barnes et al. | 1.974 | 0.296 | 3.406 | 1.418 | 0% |
| | Buckner | 0.318 | 0.323 | 0.570 | 0.222 | 100% |
| | Thatcher et al. | 0.442 | 0.323 | 0.791 | 0.308 | 100% |
| BT-54 Girder Designs 8 and 9 (6) | AASHTO Std. | 0.590 | 0.235 | 0.856 | 0.478 | 100% |
| | AASHTO LRFD | 0.492 | 0.235 | 0.714 | 0.399 | 100% |
| | ACI 318 | 0.528 | 0.271 | 0.810 | 0.411 | 100% |
| | Meyer et al. | 0.635 | 0.178 | 0.842 | 0.535 | 100% |
| | Ramirez and Russell | 0.648 | 0.178 | 0.859 | 0.546 | 100% |
| | Mitchell et al. | 0.813 | 0.209 | 1.140 | 0.658 | 83% |
| | Barnes et al. | 2.724 | 0.209 | 3.824 | 2.205 | 0% |
| | Buckner | 0.429 | 0.208 | 0.588 | 0.333 | 100% |
| | Thatcher et al. | 0.595 | 0.208 | 0.817 | 0.463 | 100% |

Notes:

[†] No. of specimens given in parentheses

[‡] AASHTO Standard Spec. (Eq. 1), AASHTO LRFD (Eq. 2), ACI 318 (Eq. 3), Meyer et al. (Eq. 8), Ramirez and Russell (Eq. 9), Mitchell et al. (Eq. 4), Barnes et al. (Eq. 10), Buckner (Eq. 6), Thatcher et al. (Eq. 7)

## SUMMARY OF TRANSFER LENGTH EXPERIMENTAL RESULTS

The transfer length measurements were made on a total of 18 girders. These included twelve AASHTO Type II girders and six AASHTO/PCI BT-54 girders. The transfer length of each girder was determined from concrete surface strain measurements. Concrete strain profiles were determined from the strain measurements and the 95 percent Average Maximum Strain Method was used to determine the transfer length.

The effect of the main experimental variables on transfer length was observed by examining the mean transfer lengths. A similar mean transfer length was observed for girders with an increased number of strands. A 53 percent increase in the transfer length was observed for girders with a 25 percent increase in stirrup spacing. The mean transfer length of girders with 0.6 inch (15 mm) nominal diameter strand was 33 percent longer than the mean transfer length of girders with 0.5 inch (13 mm) nominal diameter strand.

A girder's transfer length was measured immediately after transfer of the prestressing and again before the girder was tested to failure. The mean ratio of the long-term to immediately measured transfer lengths was 1.01 indicating only a slight increase in transfer length with time.

The transfer length determined from measurements taken immediately after prestress release was compared to the transfer length predicted by several expressions including the AASHTO LRFD Bridge Design Specification. The largest scatter, as measured by the COV, was given by the expression in the AASHTO LRFD Specifications and the smallest scatter was given by the Meyer et al. and Ramirez and Russell expressions. All expressions except those by Mitchell et al. and Barnes et al. overestimated all of the transfer lengths. The Barnes et al. expression is described by its authors as a lower-bound prediction of transfer length and underestimated all of the data points. The mean ratios for each expression were higher for the girders with 0.6 inch (15 mm) diameter strand. This indicates that the magnitude of increase in measured transfer length of the larger diameter strands was underestimated by the prediction expressions.

## DEVELOPMENT LENGTH

The development length was evaluated on a total of 12 girders. These included the twelve girders of Designs 1 through 4 described in detail in this report. This section describes the method used to determine the development lengths, provides an analysis of the flexural bond lengths, and provides an analysis of the development lengths. The analysis included evaluating the effects of the main variables, evaluating parameters typically used to predict flexural bond length and development length, and then comparing expressions used to predict flexural bond length and development length.

### DEVELOPMENT LENGTH DETERMINATION

The development length ($\ell_d$) was determined by testing both ends of the girder specimens to flexural failure as shown in Figure 32. This is an indirect method employed in numerous studies.[13,19,24,25,30-32] The setup of the first test on the girder specimen is such that the strand embedment length is approximately equal to the development length determined using the expression in the AASHTO LRFD Bridge Design Specifications (Eq. 12). The embedment length ($\ell_e$) is the bonded length of strand provided from the end of the girder to the critical section which is typically the centerline of the applied load in structural tests. If the test on the first end resulted in a ductile flexural failure, then the tested embedment length ($\ell_{e,1}$) is assumed to be greater than the development length (i.e., $\ell_{e,1} > \ell_d$) and a shorter embedment length ($\ell_{e,2}$) is used for the second test on the girder specimen. If the test on the first end resulted in a significant strand slip, then the tested embedment length is assumed to be less than the calculated development length (i.e., $\ell_{e,1} < \ell_d$) and a longer embedment length ($\ell_{e,2}$) is used for the second test on the girder specimen. In this manner, tests on one girder specimen can "bracket" the development length; however, the development length cannot be specifically determined. Significant strand slip is defined as a measured slip exceeding 0.01 inch (0.25 mm). This is the slip that has been used by several researchers.[19,25,49] The second end test illustrated in Figure 32 was based on the assumption that the test on the first end resulted in a flexural failure. The illustration shows that the embedment length of the second end tested ($\ell_{e,2}$) was approximately 70 percent of the calculated development length.

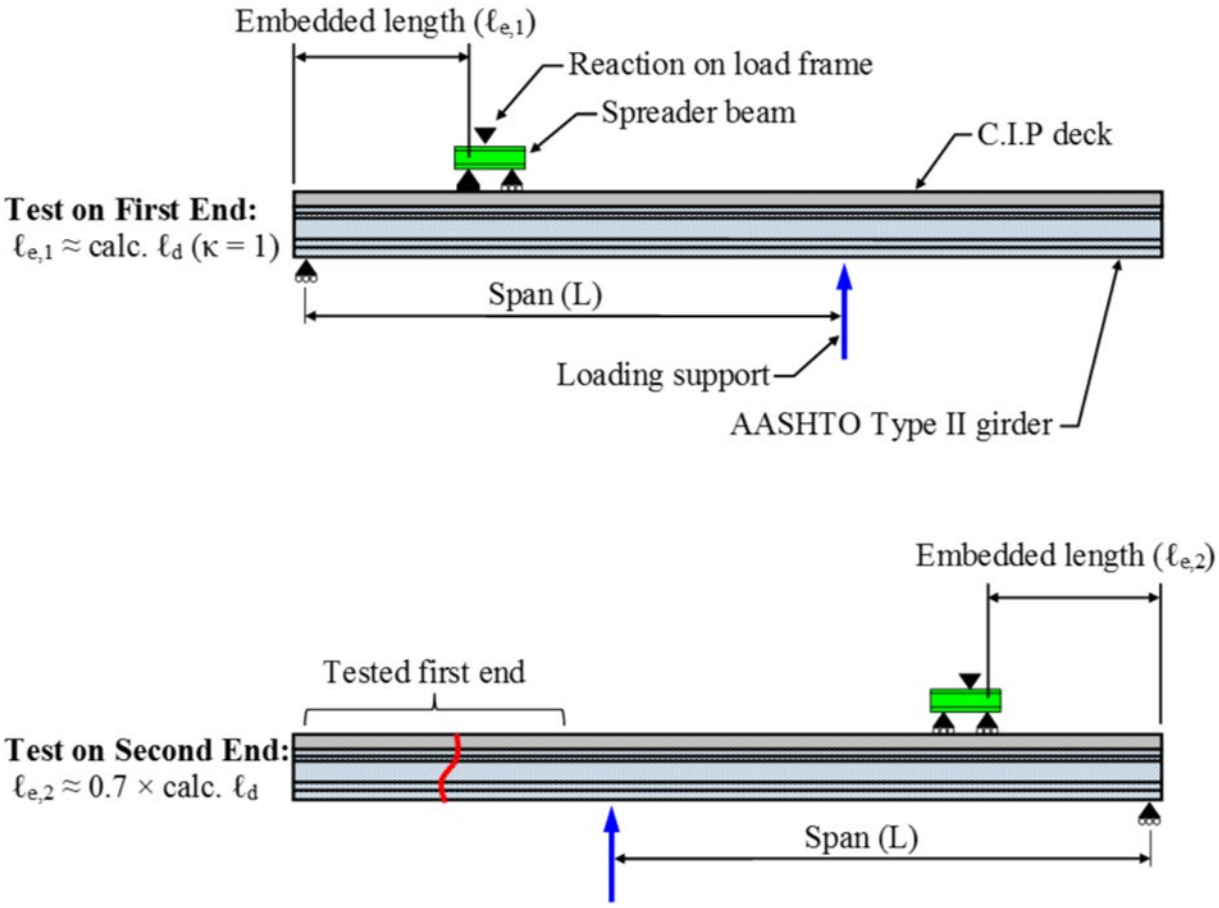


**Figure 32. Illustration. Compound Figure Showing Sequence of Tests to Determine Strand Development Length on Each Girder.**

TEST SETUP

A sketch of the test setup is shown in Figure 33. Figure 34 shows a photograph of the setup for test A3L after the completion of the test. Before a test, the end of the girder being tested was supported by a roller and the other end of the span the girder was supported by a hydraulic jack. These supports are referred to as the "roller support" and the "loading jack," respectively.

The roller support consisted of a 6 inch (152 mm) diameter steel roller and a 2 inch (51 mm) thick steel bearing plate. The bearing plate had a width of 12 inches (305 mm) and was long enough to fully support the width of the girder's bottom flange. Grout was placed between the girder and bearing plate to uniformly support the girder.

The loading jack is shown in Figure 35. The girder rested directly on another 2 inch (51 mm) thick and 12 inch (305 mm) wide steel bearing plate. A greased Teflon sheet was between the bearing plate and a roller assembly. The roller assembly consisted of a 6 inch (152 mm) diameter roller between two grooved plates. Below the roller assembly was a loadcell with a 300 kip

(1340 kN) capacity and then a hydraulic jack with a 1000 kip (4450 kN) capacity. If the full 10 inch (254 mm) stroke of the 1000 kip (4450 kN) primary actuator was inadequate to complete a test, two smaller auxiliary hydraulic actuators were used to temporarily support the girder while spacer plates were installed.

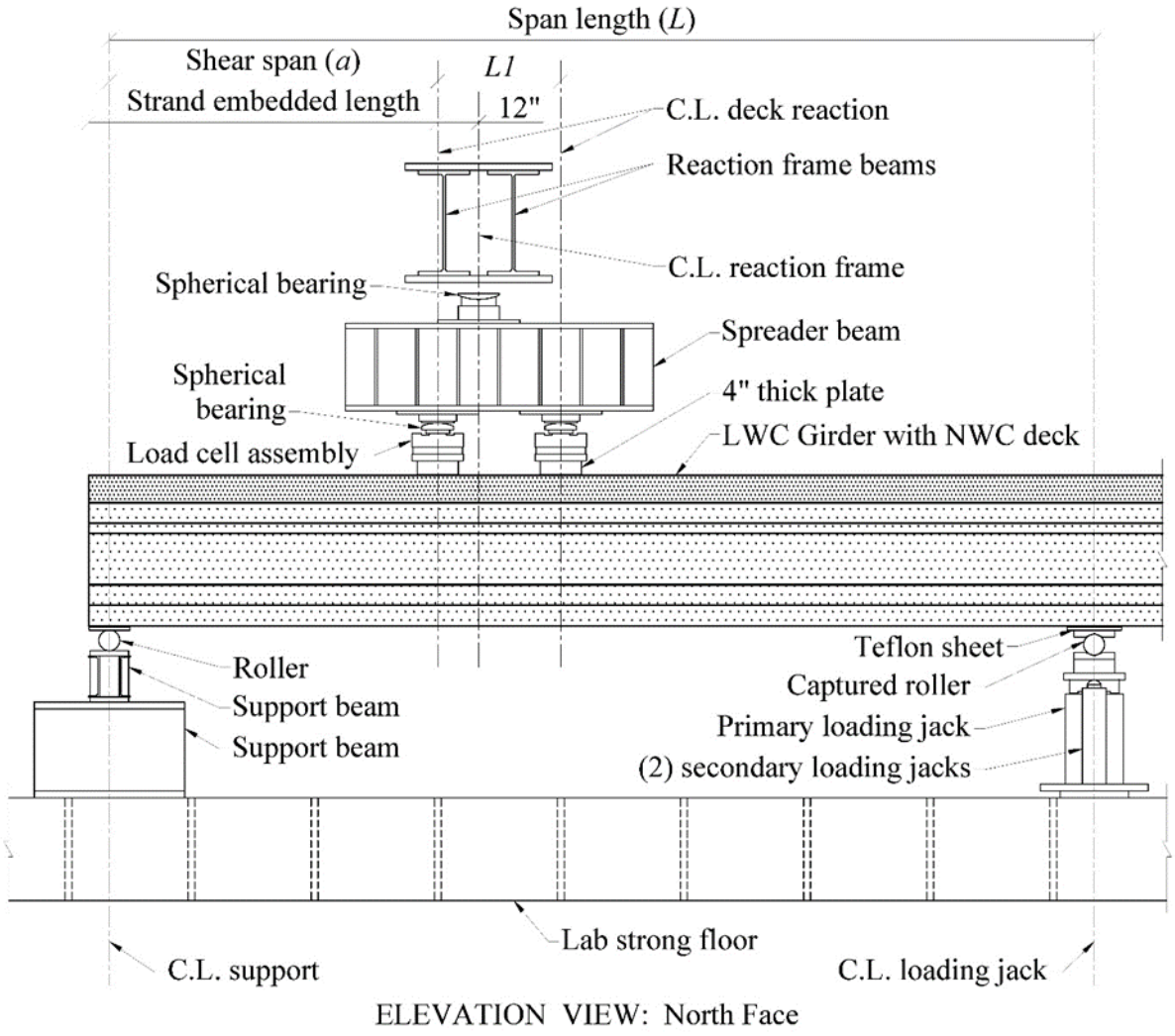


**Figure 33. Illustration. Setup for Girder Tests.**

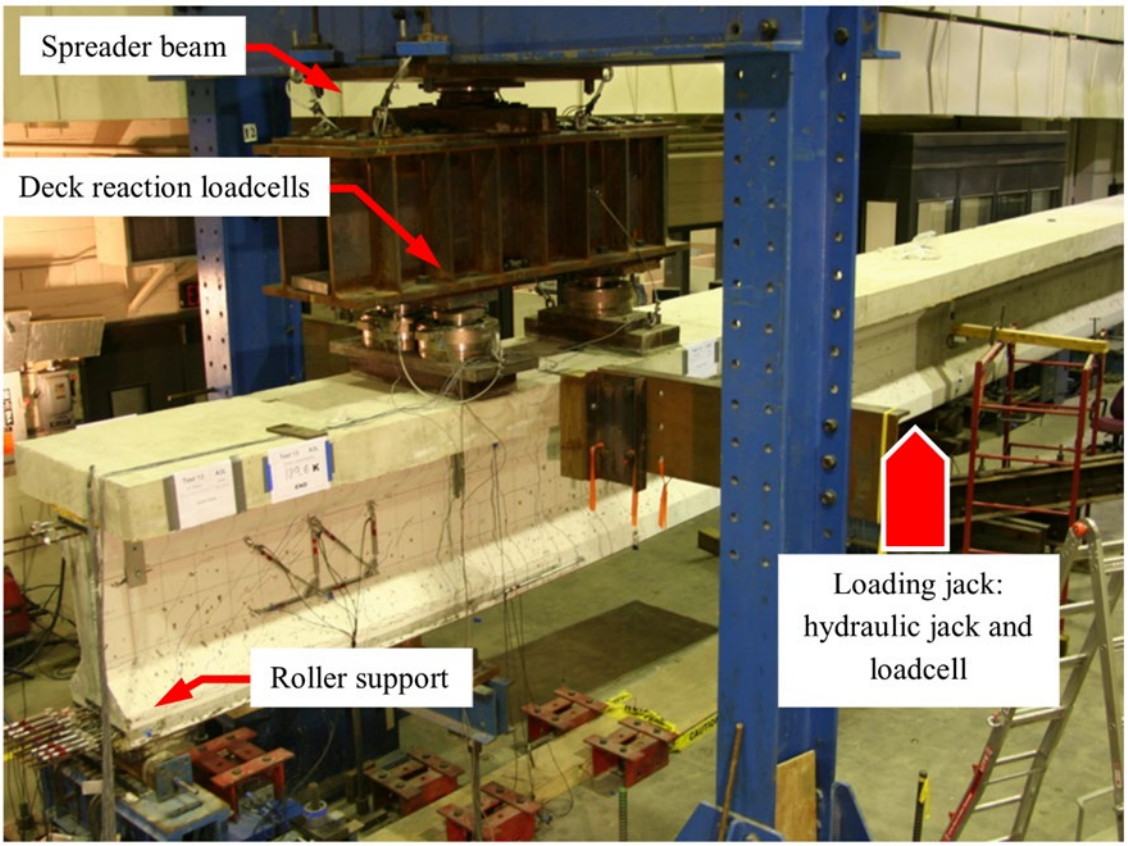


**Figure 34. Photo. Test Setup on Girder Test A3L.**

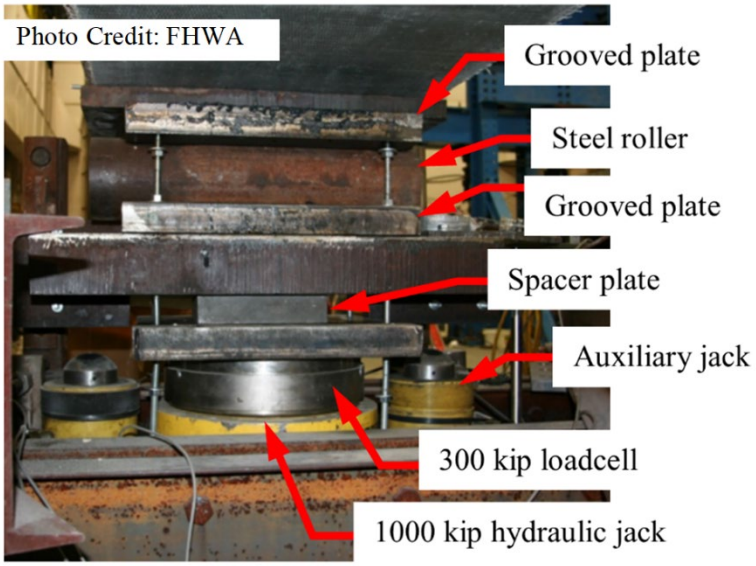


**Figure 35. Photo. Loading Jack.**

The load in the jack was controlled by a closed-loop servo-value system (Flextest-GT system). The feedback for the closed loop system was provided by the loadcell. The loading was applied by specifying the jack force in “load-control.”

When the jack applied load to the girder, it was reacted by a heavy load frame through a spreader beam, spherical bearing plates, and two pairs of 300 kip (1340 kN) loadcells on the deck that applied the reaction force into the girder. The loadcells were mounted to 4 inch (102 mm) thick bearing plates that were grouted to the top of the deck. Figure 33, Figure 34, and Figure 36 show the bearing plates, loadcells, and spreader beams. The locations of the loadcell pairs on the deck are referred to as the “deck reaction points” in this paper.

The distance from the roller support to the deck reaction points and the loading jack is given in Table 15. The distance between the centerline of the roller support and the closest deck reaction point is the shear span (a). The “test region” for each girder end was defined as the portion of the girder along the shear span. The distance from the roller support to the loading jack is the span length (L). The distance between the deck reaction points (L1) and the distance from the rolling support to the first anchor of the LVDT average strain rosette (L2) are given in Table 15. The variable dimensions a, L, L1, and L2 are shown in Figure 37.

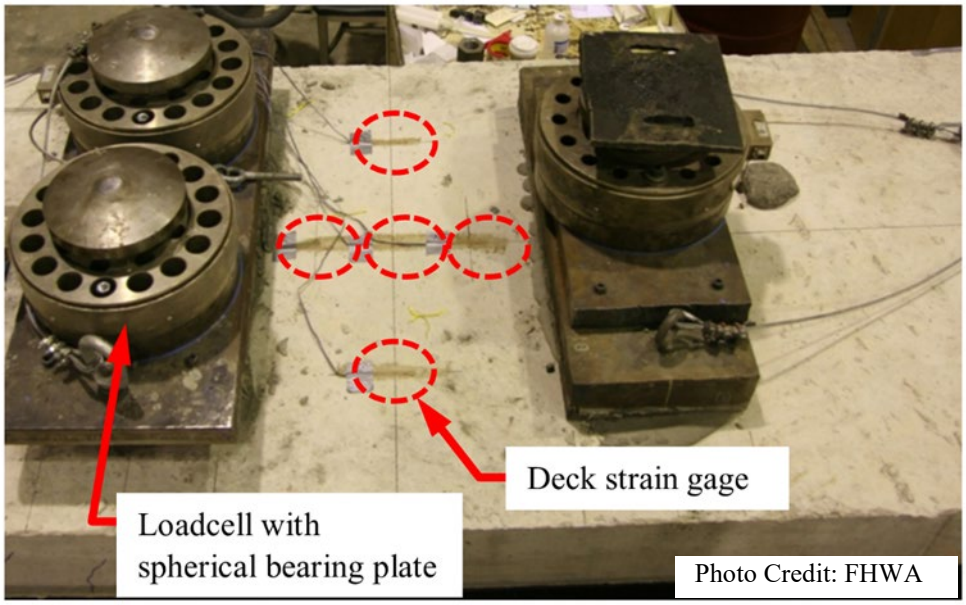


**Figure 36. Photo. Concrete Deck Anchors, Loadcells at Deck Reaction Points, and Deck Strain Gauges.**

**Table 15. Variable Dimensions in Figure 33 and Figure 37 for Girder Tests.**

| Girder Test† | Strand Size (inch) | Embedment Length, (inch) | Shear Span, a (inch) | Distance between deck loading points, L1 (inch) | Span Length, L (inch) | Distance from LVDT Rosette to C.L. Support, L2 (inch) |
|---|---|---|---|---|---|---|
| A1L | 0.5 | 72 | 66 | 48 | 270 | 21.9 |
| B1L | 0.5 | 72 | 66 | 48 | 270 | 21.9 |
| C1L | 0.5 | 75 | 69 | 36 | 273 | 21.9 |
| A1D | 0.5 | 54 | 48 | 48 | 228 | 21.9 |
| B1D | 0.5 | 54 | 48 | 48 | 228 | 21.9 |
| C1D | 0.5 | 54 | 48 | 36 | 210 | 21.9 |
| A2L | 0.5 | 72 | 66 | 48 | 270 | 22.5 |
| B2L | 0.5 | 72 | 66 | 48 | 270 | 22.5 |
| C2L | 0.5 | 75 | 69 | 36 | 273 | 22.5 |
| A2D | 0.5 | 54 | 48 | 48 | 228 | 22.5 |
| B2D | 0.5 | 54 | 48 | 48 | 228 | 22.5 |
| C2D | 0.5 | 54 | 48 | 36 | 210 | 22.5 |
| A3L | 0.5 | 72 | 66 | 48 | 270 | 21.6 |
| B3L | 0.5 | 72 | 66 | 48 | 270 | 21.6 |
| C3L | 0.5 | 75 | 69 | 36 | 273 | 21.6 |
| A3D | 0.5 | 54 | 48 | 48 | 228 | 21.6 |
| B3D | 0.5 | 54 | 48 | 48 | 228 | 21.6 |
| C3D | 0.5 | 54 | 48 | 36 | 210 | 21.6 |
| A4L | 0.6 | 84 | 78 | 48 | 306 | 21.5 |
| B4L | 0.6 | 84 | 78 | 48 | 306 | 21.5 |
| C4L | 0.6 | 84 | 78 | 48 | 306 | 21.5 |
| A4D | 0.6 | 60 | 54 | 48 | 234 | 21.5 |
| B4D | 0.6 | 60 | 54 | 48 | 234 | 21.5 |
| C4D | 0.6 | 60 | 54 | 48 | 234 | 21.5 |

Notes:

† Specimen name of form $#%, where: $ is A for UG mix, B for HG mix, C for SG mix, # is girder design; % is D for dead end or L for live end

Units: 1.0 inch = 25.4 mm

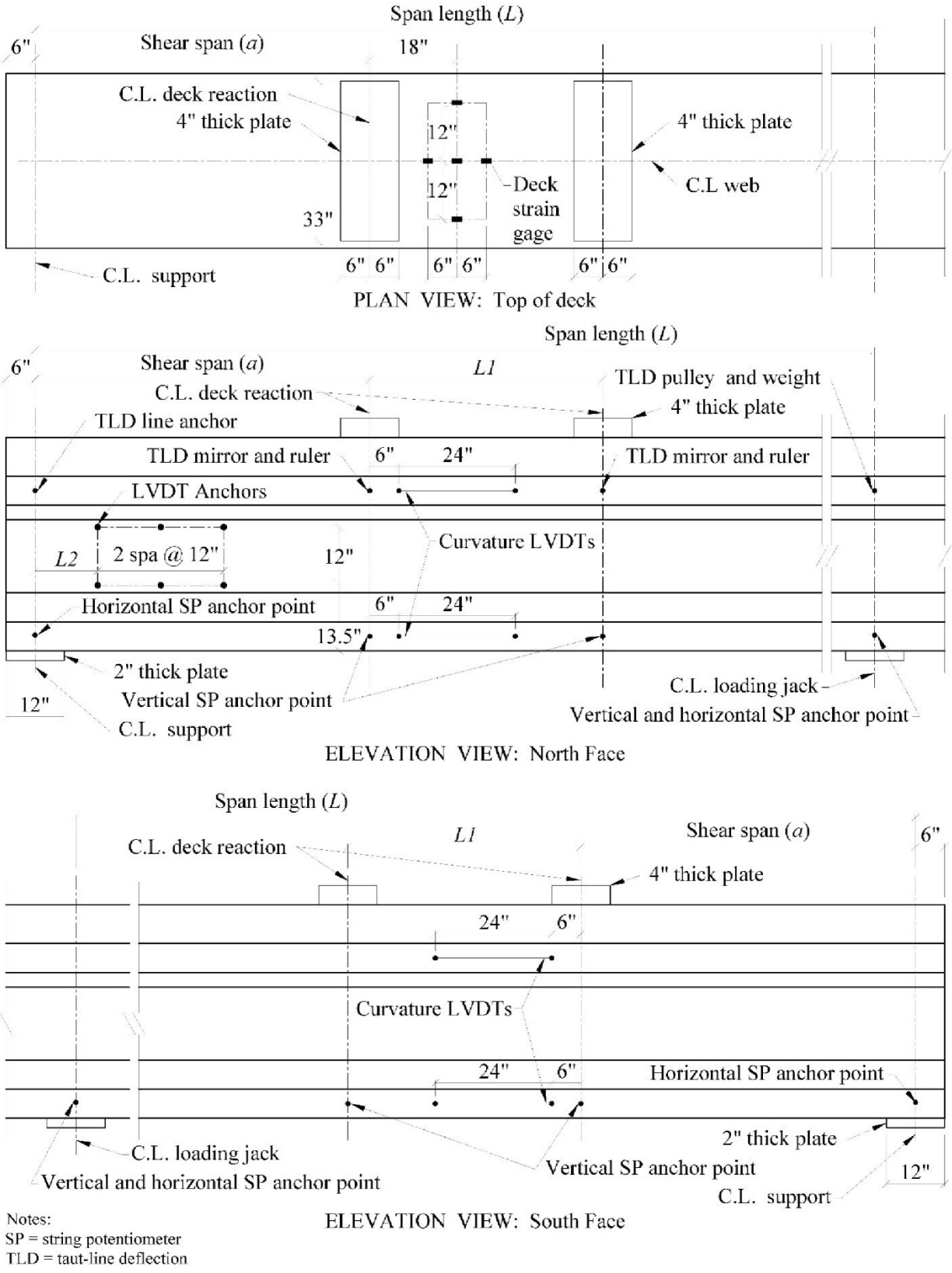


**Figure 37. Illustration. External Instrumentation for AASHTO Type II Girders.**

## INSTRUMENTATION

The girder tests were extensively instrumented to measure applied jack force, deck reaction forces, girder deformations, girder curvature, reinforcement strain, average concrete strain in the web, strand end slip, and concrete deck strain. The electronic instruments were connected to a data acquisition system that recorded data at a rate of 0.1 Hz.

Horizontal and vertical deflections were measured using string potentiometers. The locations of the anchor points for the string potentiometers on the exterior of the girder specimens are shown in Figure 37. Vertical deflections were measured using string potentiometers attached to the bottom flange directly below the deck reaction points. Vertical and horizontal deflections were measured using string potentiometers attached to the bottom flange directly over the loading jack. Horizontal deflections were measured using string potentiometers attached to the bottom flange directly over the roller support. These string potentiometers indirectly measured the deflection of the girder at the deck reaction points. The deflection at the deck reaction points was calculated as the measured change in vertical distance between the deck reaction anchor points and a straight line between the string potentiometer anchor points at the roller support and loading support. Girder deflection was directly measured at the deck reaction points using a taut-line deflection (TLD) system consisting of a weighted wire passing by pairs of rulers and mirrors attached to the top flange directly below the deck reaction points. The mirrors were used to correct for parallax before reading the deflection to the nearest 1/128 inch (0.20 mm) on the rulers. Photographs showing the components of the taut-line deflection system are in Figure 38.

Four LVDTs mounted to the top and bottom flanges were used to measured girder curvature between the deck reaction points. At the girder ends, LVDTs were attached to four strands on the bottom row to measure any slip between the strands and the end of the girder. Figure 39 shows an LVDT mounted to an exterior strand to measure strand slip.

Strain in the transverse reinforcement and strain in the end region reinforcement was measured using electrical resistance strain gauges (ERS). Figure 1 through Figure 4 show the locations of ERSs for the four girder designs. ERSs were also used to measure the strain on the top surface of the deck between the deck loading points. Figure 36 shows a photograph of the ERSs on the concrete deck and Figure 37 shows the location of the gauges.

Average concrete strain over several cracks was measured using two LVDT rosettes mounted to the web near the middle of the test region. A rosette consisted of three LVDTs oriented to measure the displacement in the horizontal, vertical, and diagonal (45 degrees) directions. ERSs only measure the local strain on a stirrup and will measure much larger strains when a crack opens near the gauge. An LVDT measuring the displacement across several cracks measures an average strain and can be used to calculate the angle of inclination of the diagonal compressive stresses. Figure 40 shows a photograph of the two LVDT rosettes.

The angle of the web-shear cracks was measured at the mid-height of the web using the “crack protractor” shown in Figure 41. A pencil line was drawn to estimate the path of the crack near

the mid-height of the web. A horizontal line on the protractor was aligned over the black horizontal line drawn at mid-height of the web. The axis of the protractor was centered over the intersection of the pencil line and the horizontal line. The protractor arm was rotated so that the tips of the protractor arm were aligned with the pencil line. The angle indicated by the tip of the protractor arm was read to the nearest 1.0 degree angle.

The widths of the cracks crossing the mid-height of the web were measured using a hand-held optical microscope. The microscope had 0.001 inch (0.025 mm) divisions. The location of the crack width reading was marked so that subsequent readings would be made at the same location.

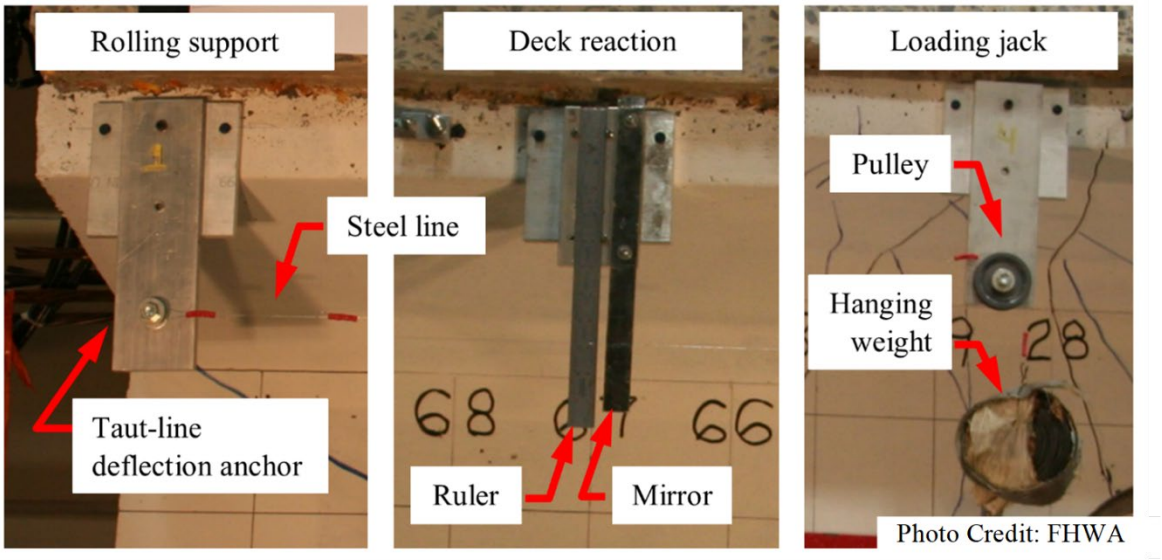


**Figure 38. Illustration. Compound Figure Showing Taut-Line Deflection Measurement System.**

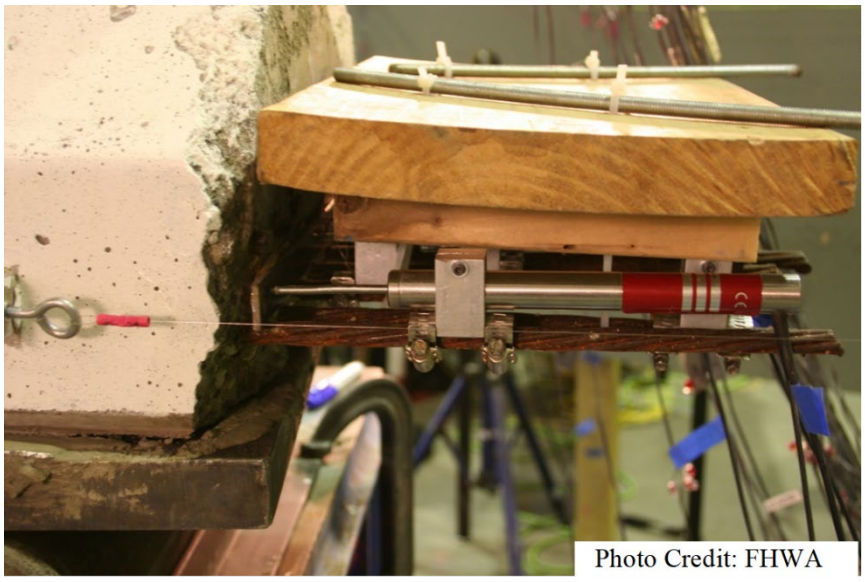


**Figure 39. Photo. LVDTs used to Measure Strand Slip.**

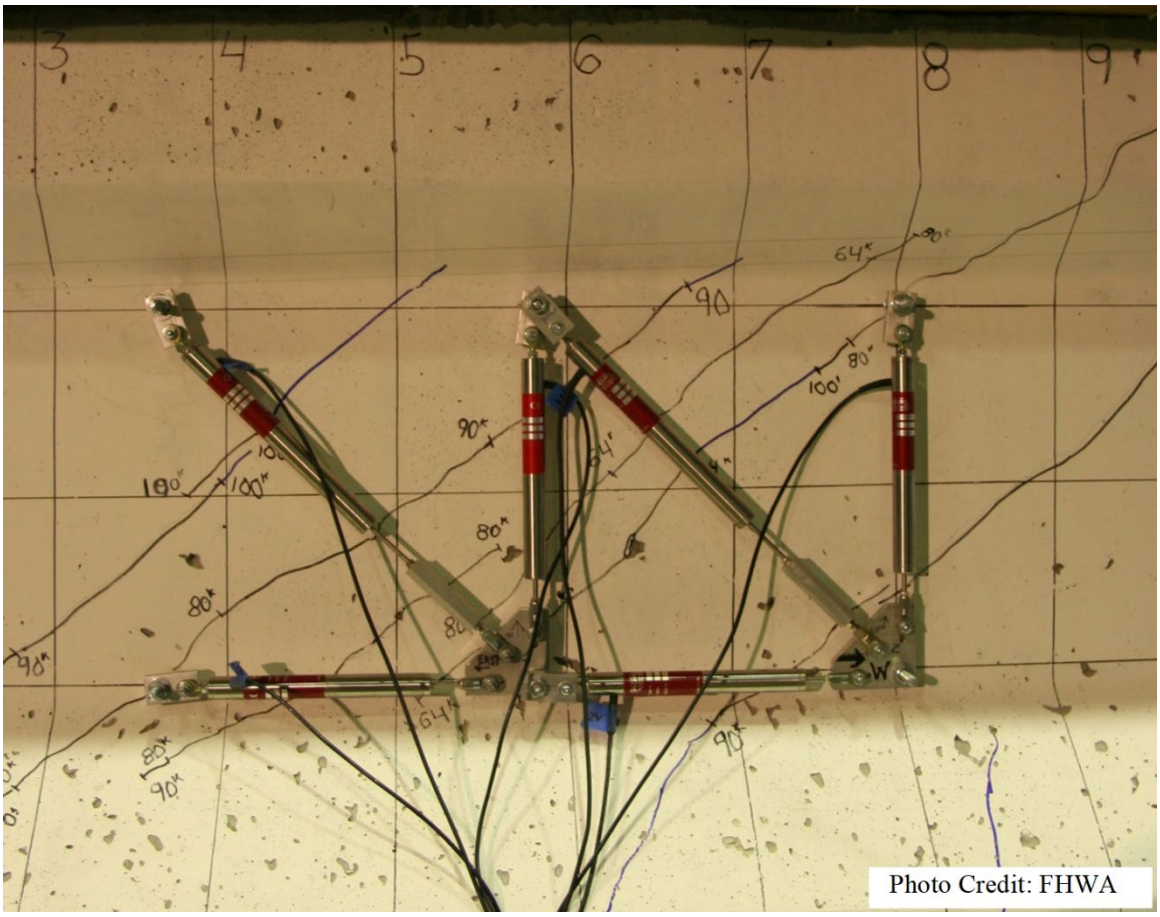


**Figure 40. Photo. LVDTs used to Measure Average Concrete Strain in a "Rosette."**

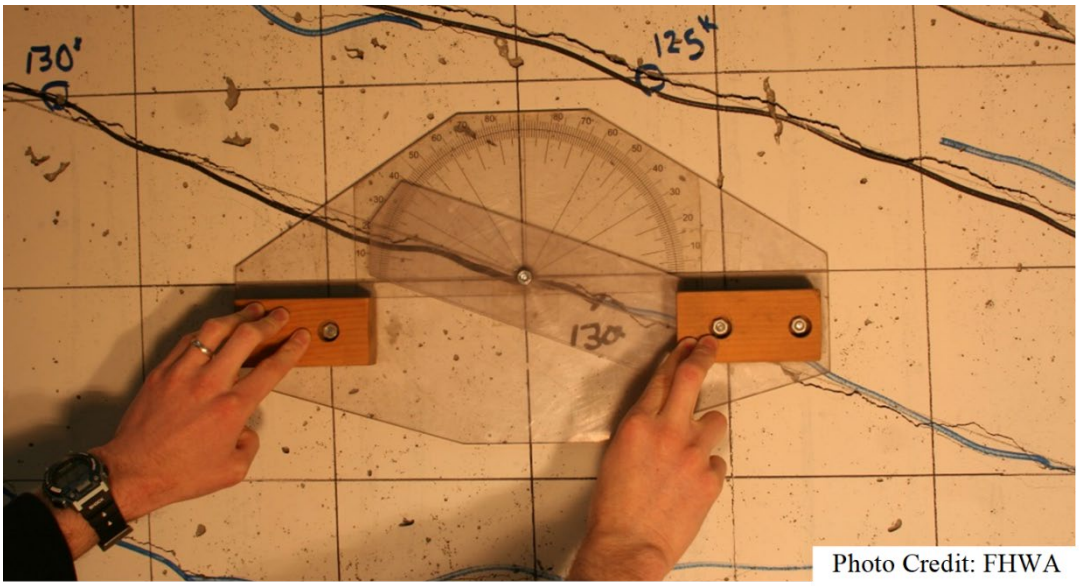


**Figure 41. Photo. Crack Angle Measurement using a Crack Protractor. The photograph shows diagonal cracks in the web of a prestressed concrete girder. A clear plastic crack protractor is held in place on top of one of the cracks demonstrating how the angle was measured.**

TEST PROCEDURE

Each test began in load control with the jack force increased in 5 kip (22 kN) increments up to approximately 80 percent of the load expected to cause web-shear cracking. Then the load increment was reduced to 2 kips (9 kN) until web-shear cracking occurred. The loading was paused at web-shear cracking in order to mark cracks, take photographs, measure deflections using the taut-line system, and measure crack widths and angles at the mid-height of the web. The loading was paused two or three times between web-cracking and 80 percent of the expected ultimate force to take measurements and photographs. After web-shear cracking, the loading was continued in 5 kip (22 kN) increments up to approximately 80 percent of the load expected to cause flexural cracking. The load increment was reduced again to 2 kips (9 kN) until flexural cracking occurred. At approximately 80 percent of the expected ultimate load, the loading was reduced to 2 kips (9 kN). This load rate was maintained until the load increment caused a significantly larger increment of displacement measured at the loading support. This was assumed to indicate yielding in the strands. The load rate was reduced again to 1 kip (4 kN) until crushing in the deck concrete between the loading supports was observed.

SUMMMARY OF TEST RESULTS

A summary of the girder specimens is given in Table 16 and includes the effective shear depth ($d_v$), ratio of the shear span to effective shear depth ($a/d_v$), concrete compressive strength ($f'_c$) at age of testing, the total area of prestressing strands ($A_{ps}$), and the stirrup strength ($\rho_v f_{yt}$). The effective shear depth was calculated using Article 5.8.2.9 in the AASHTO LRFD Bridge Design

Specifications. The $a/d_v$ ratios for the girder tests are given in Table 16. An $a/d_v$ ratio of less than 2.5 to 3.0 has been shown to increase the shear strength of a girder.[42,43] The stirrup strength is the product of the transverse reinforcement ratio given by Eq. 18 and the measured yield strength of the stirrups given in Table 6. Table 16 also gives the test number which corresponds to the order in which the girders were tested. The test number can be used to find detailed information on each girder specimen and the girder test results in Appendix D.

$$\rho_v = \frac{A_v}{b_v s} \qquad \text{(Eq. 18)}$$

A summary of the applied shear force, applied moment, level of stirrup yielding, and failure mode for the tested girders is given in Table 17. The table gives the applied shear force at web cracking ($V_{cr}$), and the applied moments at flexural cracking ($M_{cr}$) and at ultimate ($M_{test}$). The level of yielding at $M_{test}$ is given by the number of stirrups with a measured strain ($\varepsilon_t$) greater than the yield strain ($\varepsilon_{ty}$). The effect of girder self-weight was included in the determination of $M_{test}$. A flexural failure was observed by concrete deck crushing. The failure mode of strand slip was indicated by the maximum measured strand slip from LVDTs attached to the strands reaching a value of 0.010 inch (0.25 mm) before $M_{test}$. A shear failure mode was indicated by a sudden and brittle shear failure near the rolling support.

**Table 16. Summary of Effective Depth, Concrete Strength, Prestressing Steel, Effective Prestress, and Stirrup Strength, for AASHTO Type II Girders.**

| Girder Test† | Test No. | Effective shear depth, $d_v$ (inch) | Ratio shear span to shear depth, $a/d_v$ | Concrete compressive strength‡, $f'_c$ (ksi) | Total area of prestressing, $A_{ps}$ (inch$^2$) | Stirrup strength*, $\rho_v f_{yt}$ (ksi) |
|---|---|---|---|---|---|---|
| A1L | 15 | 32.70 | 2.02 | 9.1 | 1.84 | 1.82 |
| B1L | 16 | 32.70 | 2.02 | 9.7 | 1.84 | 1.82 |
| C1L | 2 | 32.70 | 2.11 | 10.8 | 1.84 | 1.82 |
| A1D | 20 | 32.70 | 1.47 | 9.1 | 1.84 | 1.82 |
| B1D | 21 | 32.70 | 1.47 | 9.7 | 1.84 | 1.82 |
| C1D | 4 | 32.70 | 1.47 | 10.8 | 1.84 | 1.82 |
| A2L | 17 | 31.91 | 2.07 | 10.5 | 3.37 | 2.91 |
| B2L | 24 | 31.91 | 2.07 | 11.4 | 3.37 | 2.91 |
| C2L | 3 | 31.91 | 2.16 | 9.9 | 3.37 | 2.91 |
| A2D | 22 | 31.91 | 1.50 | 10.5 | 3.37 | 2.91 |
| B2D | 23 | 31.91 | 1.50 | 11.4 | 3.37 | 2.91 |
| C2D | 5 | 31.91 | 1.50 | 9.9 | 3.37 | 2.91 |
| A3L | 13 | 32.70 | 2.02 | 10.7 | 1.84 | 1.46 |
| B3L | 14 | 32.70 | 2.02 | 9.8 | 1.84 | 1.46 |
| C3L | 1 | 32.70 | 2.11 | 11.1 | 1.84 | 1.46 |
| A3D | 18 | 32.70 | 1.47 | 10.7 | 1.84 | 1.46 |
| B3D | 19 | 32.70 | 1.47 | 9.8 | 1.84 | 1.46 |
| C3D | 6 | 32.70 | 1.47 | 11.1 | 1.84 | 1.46 |
| A4L | 8 | 32.04 | 2.43 | 10.0 | 2.15 | 1.62 |
| B4L | 7 | 32.04 | 2.43 | 10.0 | 2.15 | 1.62 |
| C4L | 9 | 32.04 | 2.43 | 9.7 | 2.15 | 1.62 |
| A4D | 10 | 32.04 | 1.69 | 10.0 | 2.15 | 1.62 |
| B4D | 12 | 32.04 | 1.69 | 10.0 | 2.15 | 1.62 |
| C4D | 11 | 32.04 | 1.69 | 9.7 | 2.15 | 1.62 |

Notes:

† Specimen name of form $#%, where: $ is A for UG mix, B for HG mix, C for SG mix, # is girder design, % is D for dead end or L for live end

‡ Test day compressive strength

* Shear reinforcement ratio, $\rho_v = A_v/b_v s$

Units: 1.0 inch = 25.4 mm, 1.0 ksi = 6.89 MPa

**Table 17. Shear Force at Web Cracking, Moment at Flexural Cracking and Ultimate, Strand Slip, Stirrups Yielding, and Failure Mode for AASHTO Type II Girders.**

| Girder Test† | Test No. | Shear Force at Web Cracking, $V_{cr}$ (ksi) | Moment at Flexural Cracking, $M_{cr}$ (k-ft) | Ultimate Moment, $M_{test}$ (k-ft) | Strand Slip at Ultimate Moment$ | No. of Stirrups with $\varepsilon_t \geq \varepsilon_{ty}$ at Ultimate Moment‡ | Failure Mode |
|---|---|---|---|---|---|---|---|
| A1L | 15 | 134 | 980 | 1640 | 0.001 | 0 | Flexural |
| B1L | 16 | 153 | 1160 | 1580 | 0.001 | 1 | Flexural |
| C1L | 2 | 131 | 1060 | 1540 | 0.001 | 0 | Flexural |
| A1D | 20 | 158 | 920 | 1630 | 0.001 | 0 | Flexural |
| B1D | 21 | 177 | 1100 | 1620 | 0.005 | 0 | Flexural |
| C1D | 4 | 132 | 1000 | 1580 | 0.015 | 0 | Flexural, Slip |
| A2L | 17 | 155 | 1620 | 2570 | 0.002 | 0 | Flexural |
| B2L | 24 | 207 | 1720 | 2550 | 0.003 | 0 | Flexural |
| C2L | 3 | 115 | 1690 | 2480 | 0.002 | 0 | Flexural |
| A2D | 22 | 137 | 1540 | 2400 | 0.001 | 0 | Shear |
| B2D | 23 | 188 | 1710 | 2540 | 0.032 | 0 | Flexural, Slip |
| C2D | 5 | 214 | 1540 | 2240 | 0.015 | 0 | Shear, Slip |
| A3L | 13 | 128 | 1060 | 1590 | 0.001 | 1 | Flexural |
| B3L | 14 | 142 | 1130 | 1620 | 0.001 | 0 | Flexural |
| C3L | 1 | 123 | 1130 | 1550 | 0.014 | 0 | Flexural, Slip |
| A3D | 18 | 136 | 920 | 1640 | 0.000 | 0 | Flexural |
| B3D | 19 | 172 | 1080 | 1620 | 0.000 | 2 | Flexural |
| C3D | 6 | 136 | 1060 | 1660 | 0.021 | 0 | Flexural, Slip |
| A4L | 8 | 164 | 1270 | 1850 | 0.000 | 0 | Flexural |
| B4L | 7 | 171 | 1290 | 1820 | 0.000 | 0 | Flexural |
| C4L | 9 | 148 | 1270 | 1820 | 0.002 | 0 | Flexural |
| A4D | 10 | 156 | 1210 | 1900 | 0.044 | 0 | Flexural, Slip |
| B4D | 12 | 179 | 1250 | 1830 | 0.020 | 0 | Flexural, Slip |
| C4D | 11 | 130 | 1160 | 1830 | 0.104 | 0 | Flexural, Slip |

Notes:

† Specimen name of form $#%, where: $ is A for UG mix, B for HG mix, C for SG mix, # is girder design, % is D for dead end or L for live end

‡ Determined using Article 5.8.2.9 of AASHTO LRFD Bridge Design Specifications

$ Shear force at web cracking not measured

Units: 1.0 inch = 25.4 mm, 1.0 ksi = 6.89 MPa

## FAILURE MODES

The mode of failure for the 24 tests on the ends of the girder specimens are given in Table 17. Fifteen girder end tests ended in a ductile flexural failure with wide flexural cracks and concrete crushing of the deck. The maximum measured strand slip in these 15 tests was less than 0.010 inch (0.25 mm). Seven tests on the girder ends resulted in a flexural failure but with strand slip greater than 0.010 inch (0.25 mm). The test on girder end C2D resulted in a shear failure with a measured maximum strand slip greater than 0.010 inch (0.25 mm). The only test ending in a shear failure without significant strand slip was the test on girder end A2D.

## EVALUATION OF DEVELOPMENT LENGTH

The development length was evaluated for each girder based on the results of the tests on the live and dead ends. This evaluation is shown in Table 18 for the specimens in Girder Designs 1 through 3 and in Table 19 for the specimens in Girder Design 4. The tables give the ratio of the ultimate moment ($M_{test}$) to the nominal moment capacity ($M_n$) determined using the AASHTO LRFD Bridge Design Specifications. The tables also give the strand slip at ultimate and the failure mode listed in the column corresponding to the embedment length of a test.

The tests on both ends of girders A1 and B1 resulted in flexural failures. The embedment lengths of the dead ends were shorter at 54 inches (1370 mm). This indicates that the development length of these two girders is less than 54 inches (1370 mm).

The test on the live end of girder C1 had an embedment length of 75 inches (1910 mm) and resulted in a flexural failure. A 54 inch (1370 mm) embedment length was tested for the dead end of girder C1 and resulted in a flexural failure with significant slip (i.e., maximum strand slip greater than 0.010 inch (0.25 mm)). As given in Table 18, the ratio of $M_{test}$ to $M_n$ ("moment ratio") for test C1D was 1.11 which is higher than the moment ratio for the live end of girder C1. Based on the moment ratio, the development length of this girder was also taken as less than 54 inch (1370 mm).

The six end tests on the three Girder Design 3 specimens had results similar to that of Girder Design 1. The tests on both ends of girders A3 and B3 resulted in flexural failures. The test on live end of C3 resulted in a flexural failure while the test on the dead end also experienced significant strand slip. The development length of all three Girder Design 3 specimens was taken as less than 54 inches (1370 mm).

The tests on the live ends of the three Girder Design 2 specimens resulted in flexural failures. The tests on A2 and B2 had an embedment length of 72 inches (1830 mm) and test C2 had a 75 inch (1910 mm) embedment length. The test on girder end A2D resulted in a shear failure without significant slip being measured. The test on C2D also resulted in a shear failure but with significant measured strand slip. This indicates that the development lengths of girders A2 and C2 are between 54 and 72 inches (1370 and 1830 mm). A flexural failure with significant strand slip was the result of the test on girder end B2D. The moment ratio of the test on B2D was 1.08

which is higher than the ratio for the live end. The development length of girder B2 was taken as less than 54 inches (1370 mm).

**Table 18. Evaluation of Development Length for Girder Designs 1 through 3.**

| Girder Test† | Test No. | $M_{test}/M_n$‡ | Strand Slip at Ultimate Moment$ | Failure Mode$ $\ell_e$ = 54 inch | Failure Mode$ $\ell_e$ = 72 inch | Failure Mode$ $\ell_e$ = 75 inch | Evaluation of Development Length by Girder Specimen* (dimensions in inches) |
|---|---|---|---|---|---|---|---|
| A1L | 15 | 1.17 | 0.001 | | F | | -- |
| B1L | 16 | 1.12 | 0.001 | | F | | -- |
| C1L | 2 | 1.09 | 0.001 | | | F | -- |
| A1D | 20 | 1.17 | 0.001 | F | | | A1: $\ell_d \leq 54$ |
| B1D | 21 | 1.15 | 0.005 | F | | | B1: $\ell_d \leq 54$ |
| C1D | 4 | 1.11 | 0.015 | F, S | | | C1: $\ell_d \leq 54$ |
| A2L | 17 | 1.09 | 0.002 | | F | | -- |
| B2L | 24 | 1.07 | 0.003 | | F | | -- |
| C2L | 3 | 1.04 | 0.002 | | | F | -- |
| A2D | 22 | 1.02 | 0.001 | V | | | A2: $54 \leq \ell_d \leq 72$ |
| B2D | 23 | 1.08 | 0.032 | F, S | | | B2: $\ell_d \leq 54$ |
| C2D | 5 | 0.94 | 0.015 | V, S | | | C2: $54 \leq \ell_d \leq 75$ |
| A3L | 13 | 1.12 | 0.001 | | F | | -- |
| B3L | 14 | 1.15 | 0.001 | | F | | -- |
| C3L | 1 | 1.10 | 0.014 | | | F, S | -- |
| A3D | 18 | 1.16 | 0.000 | F | | | A3: $\ell_d \leq 54$ |
| B3D | 19 | 1.14 | 0.000 | F | | | B3: $\ell_d \leq 54$ |
| C3D | 6 | 1.18 | 0.021 | F, S | | | C3: $\ell_d \leq 54$ |

Notes:

† Specimen name of form $#%, where: $ is A for UG mix, B for HG mix, C for SG mix, # is girder design, % is D for dead end or L for live end

‡ Ratio of ultimate moment to nominal moment capacity determined using AASHTO LRFD Bridge Design Specifications

$ Failure mode given only for the tested embedment length; Failure modes are flexure (F), strand slip (S), shear failure (V)

* Development length based on the test results of both dead and live ends

Units: 1.0 inch = 25.4 mm

Table 19 gives an evaluation of the development length tests on the Girder Design 4 specimens with the 0.6 inch (15 mm) nominal strand diameter. The tests on the live end of all three girders were at an embedment length of 84 inch (2130 mm) and resulted in a flexural failure without significant slip. The embedment length used for the test on the dead end was 60 inches (1520 mm) for all three girder end tests. All three tests resulted in a flexural failure with slip greater than 0.010 inch (0.25 mm). The development length of the three specimens was determined to be less than 60 inches (1520 mm).

**Table 19. Evaluation of Development Length for Girder Design 4.**

| Girder Test[†] | Test No. | $M_{test}/M_n$[‡] | Strand Slip at Ultimate Moment[$] | Failure Mode[$]: $\ell_e$ = 60 inch | Failure Mode[$]: $\ell_e$ = 84 inch | Evaluation of Development Length by Girder Specimen[*] (dimensions in inches) |
|---|---|---|---|---|---|---|
| A4L | 8 | 1.15 | 0.000 | | F | -- |
| B4L | 7 | 1.14 | 0.000 | | F | -- |
| C4L | 9 | 1.14 | 0.002 | | F | -- |
| A4D | 10 | 1.19 | 0.044 | F, S | | A4: $\ell_d \leq 60$ |
| B4D | 12 | 1.14 | 0.020 | F, S | | B4: $\ell_d \leq 60$ |
| C4D | 11 | 1.16 | 0.104 | F, S | | C4: $\ell_d \leq 60$ |

Notes:
[†] Specimen name of form $#%, where: $ is A for UG mix, B for HG mix, C for SG mix, # is girder design, % is D for dead end or L for live end
[‡] Ratio of ultimate moment to nominal moment capacity determined using AASHTO LRFD Bridge Design Specifications
[$] Failure mode given only for the tested embedment length. Failure modes are flexure (F), strand slip (S), shear failure (V)
[*] Development length based on the test results of both dead and live ends
Units: 1.0 inch = 25.4 mm

## FLEXURAL BOND LENGTH ANALYSIS

The transfer length is the length of bonded strand required to transfer the pretensioning force to the surrounding concrete. The flexural bond length is the additional length required to develop the stand stress at nominal moment capacity.[13,19] The development length is commonly described as the sum of the transfer length and the flexural bond length. Table 20 gives the transfer length determined from measurements taken prior to testing to failure ($\ell_{t,test}$) for each girder. The development length ($\ell_{d,test}$) and flexural bond length ($\ell_{fb}$) are also given in Table 20. The flexural bond length was taken as the difference between the experimentally determined development length and the measured transfer length.

The results of the development length evaluation are given in Table 18 and Table 19. The development length was expressed as range for girders with one tested end resulting in a shear failure. The experimentally determined development length used in subsequent analyses is given in Table 20 and is the larger embedment length of the range from Table 18 and Table 19.

Parameters that may influence flexural bond length are given Table 20. The table gives the concrete compressive strength at the time of development length test, the concrete elastic modulus determined at an age of 28 days. The nominal concrete unit weight determined from 4 x 8 inch (102 x 203 mm) cylinders used to determine the compressive strength is given in the table. The strand stress needed to be developed over the flexural bond length ($f_{ps} - f_{pe}$) was determined using the AASHTO LRFD Bridge Design Specifications and is given in the table.

**Table 20. Summary of Development Length, Flexural Bond Length, and Concrete Properties, and Strand Stress for AASHTO Type II Girders.**

| Girder Test† | Measured transfer length at girder test, $\ell_{t,test}$ (inch) | Evaluated development length, $\ell_{d,test}$ (inch) | Flexural bond length, $\ell_{fb,test}$ (inch) | Concrete compressive strength at girder test, $f'_c$ (ksi) | Concrete elastic modulus at 28 days, $E_c$ (ksi) | Concrete unit weight at girder test, $w_c$ (kcf) | Calculated $f_{ps} - f_{pe}$‡ (ksi) |
|---|---|---|---|---|---|---|---|
| A1 | 8.1 | 54 | 45.9 | 9.1 | 4320 | 0.128 | 88.6 |
| B1 | 11.4 | 54 | 42.6 | 9.7 | 4040 | 0.128 | 91.3 |
| C1 | 12.9 | 54 | 41.1 | 10.8 | 3890 | 0.122 | 90.8 |
| A2 | 10.6 | 72 | 61.4 | 10.5 | 4520 | 0.130 | 96.5 |
| B2 | 10.2 | 54 | 43.8 | 11.4 | 4420 | 0.132 | 96.2 |
| C2 | 8.9 | 75 | 66.1 | 9.9 | 4150 | 0.121 | 95.2 |
| A3 | 8.7 | 54 | 45.3 | 10.7 | 4320 | 0.127 | 89.5 |
| B3 | 10.1 | 54 | 43.9 | 9.8 | 4040 | 0.131 | 91.3 |
| C3 | 20.5 | 54 | 33.5 | 11.1 | 3890 | 0.122 | 90.3 |
| A4 | 19.1 | 60 | 40.9 | 10.0 | 3930 | 0.129 | 93.6 |
| B4 | 19.4 | 60 | 40.6 | 10.0 | 4130 | 0.128 | 89.2 |
| C4 | 22.4 | 60 | 37.6 | 9.7 | 3920 | 0.121 | 88.9 |

Notes:

† Specimen name of form $#, where: $ is A for UG mix, B for HG mix, C for SG mix, # is girder design

‡ Effective stress determined using approximate estimate of time-dependent losses in AASHTO Specifications

Units: 1.0 inch = 25.4 mm, 1.0 ksi = 6.89 MPa

### *Mean Flexural Bond Length*

Table 21 gives the mean flexural bond length ($\ell_{fb}$) for all 12 girders. The table also compares the flexural bond length by girder design, girder concrete mix, and strand size. The girder end tests A2 and C2 that ended in shear failure resulted in a longer evaluated development length and a corresponding longer flexural bond length. The tests on A2 and C2 give higher mean flexural bond length for Girder Design 2 and girder concrete mix UG and SG. The larger strand used in Girder Design 4 also resulted in a larger mean flexural bond length.

**Table 21. Summary of Flexural Bond Length by Girder Design, Mix Design, and Nominal Strand Size.**

| Girder Specimens† | Property‡ | Mean | COV | Max. | Min. |
|---|---|---|---|---|---|
| All Girders (12) | $\ell_{fb,test}$ (inch) | 45.24 | 0.21 | 66.09 | 33.53 |
| Girder Design 1 (3) | $\ell_{fb,test}$ (inch) | 44.04 | 0.06 | 45.86 | 40.94 |
| Girder Design 2 (3) | $\ell_{fb,test}$ (inch) | 48.65 | 0.23 | 61.44 | 40.56 |
| Girder Design 3 (3) | $\ell_{fb,test}$ (inch) | 40.01 | 0.14 | 43.85 | 33.53 |
| Girder Design 4 (3) | $\ell_{fb,test}$ (inch) | 48.28 | 0.32 | 66.09 | 37.60 |
| UG Mix (4) | $\ell_{fb,test}$ (inch) | 48.39 | 0.19 | 61.44 | 40.94 |
| HG Mix (4) | $\ell_{fb,test}$ (inch) | 42.74 | 0.04 | 43.94 | 40.56 |
| SG Mix (4) | $\ell_{fb,test}$ (inch) | 44.59 | 0.33 | 66.09 | 33.53 |
| Girder Design 1-3, 0.5 inch strand (9) | $\ell_{fb,test}$ (inch) | 44.23 | 0.17 | 61.44 | 33.53 |
| Girder Design 4, 0.6 inch strand (3) | $\ell_{fb,test}$ (inch) | 48.28 | 0.32 | 66.09 | 37.60 |

Notes:
† No. of specimens given in parentheses
‡ Measured transfer length at girder test ($\ell_{t,test}$), Measured flexural bond length ($\ell_{fb,test}$)
Units: 1.0 inch = 25.4 mm

### *Analysis of Parameters used for Flexural Bond Length Prediction*

The flexural bond lengths ($\ell_{fb}$) are presented graphically in Figure 42 through Figure 49. The figures are presented in pairs. The first figure in each pair gives the flexural bond lengths in series by girder design number. The second figure in each pair presents the results by girder concrete mix. The figures compare flexural bond length to parameters used by researchers to predict flexural bond length.[16,22,30] Figure 42 and Figure 43 compare flexural bond length to concrete compressive strength at the time of test ($f'_c$). Figure 44 and Figure 45 compare flexural bond length to concrete unit weight ($w_c$). Flexural bond length is compared to concrete elastic modulus at an age of 28 days in Figure 46 and Figure 47. The flexural bond length was also compared to the calculated strand stress needed to be developed over the flexural bond length ($f_{ps}$ - $f_{pe}$) in Figure 48 and Figure 49.

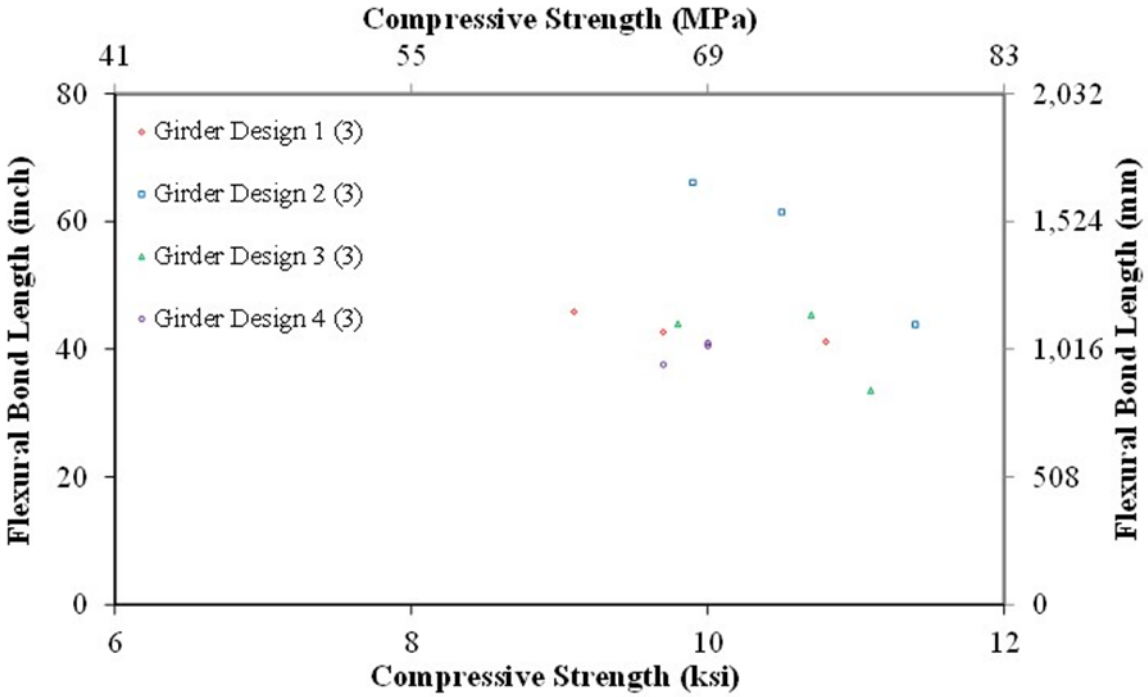


**Figure 42. Graph. Flexural Bond Length Compared to Compressive Strength by Girder Design.**

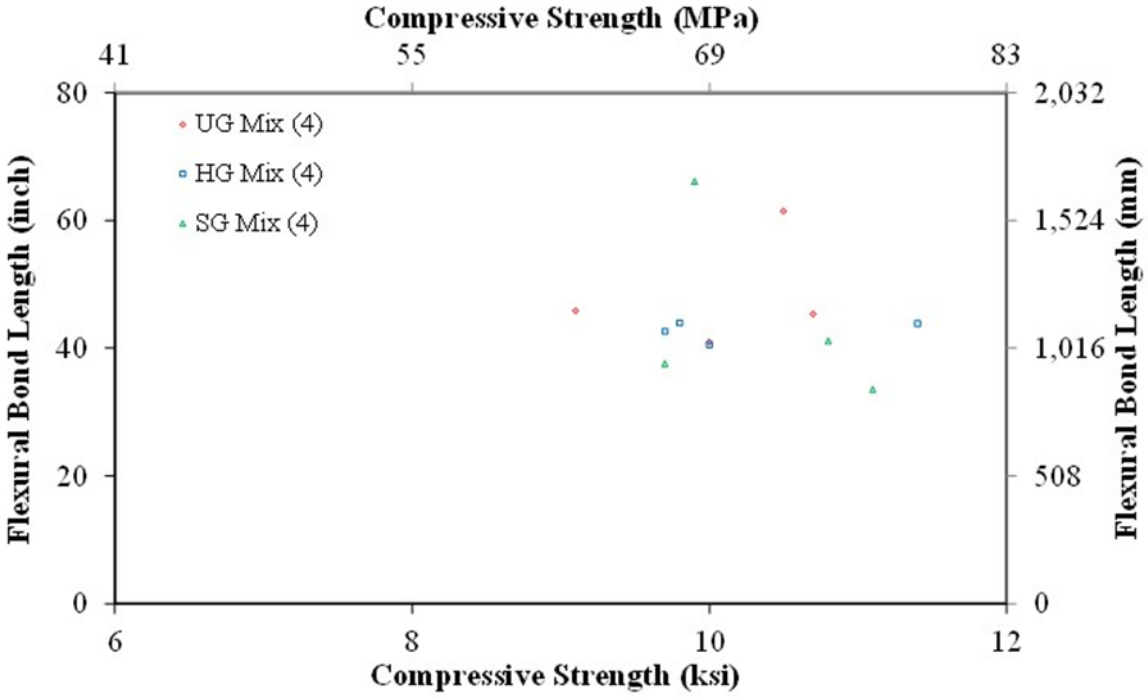


**Figure 43. Graph. Flexural Bond Length Compared to Compressive Strength by Girder Concrete Mix.**

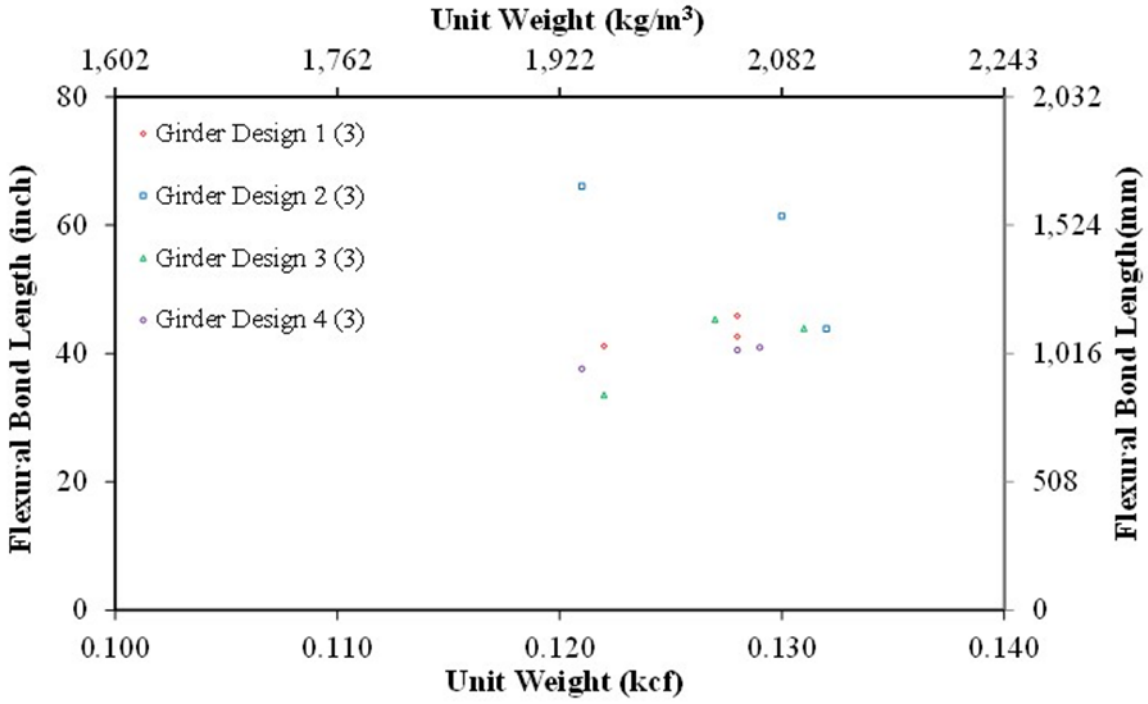


**Figure 44. Graph. Flexural Bond Length Compared to Unit Weight by Girder Design.**

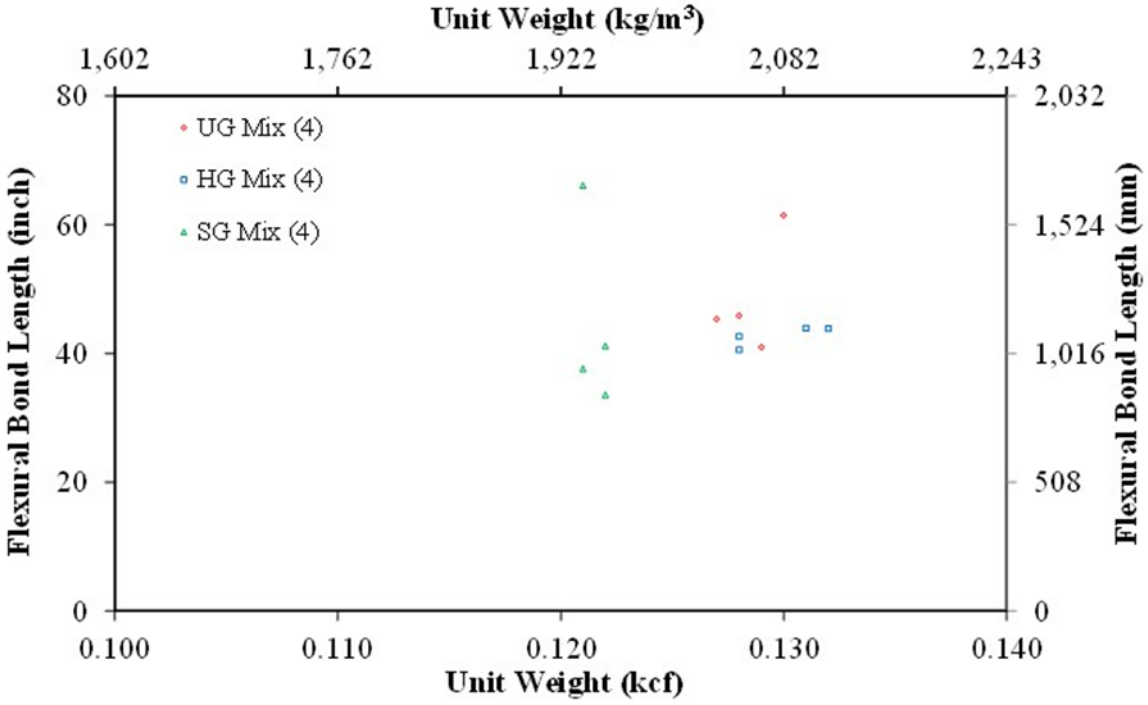


**Figure 45. Graph. Flexural Bond Length Compared to Unit Weight by Girder Concrete Mix.**

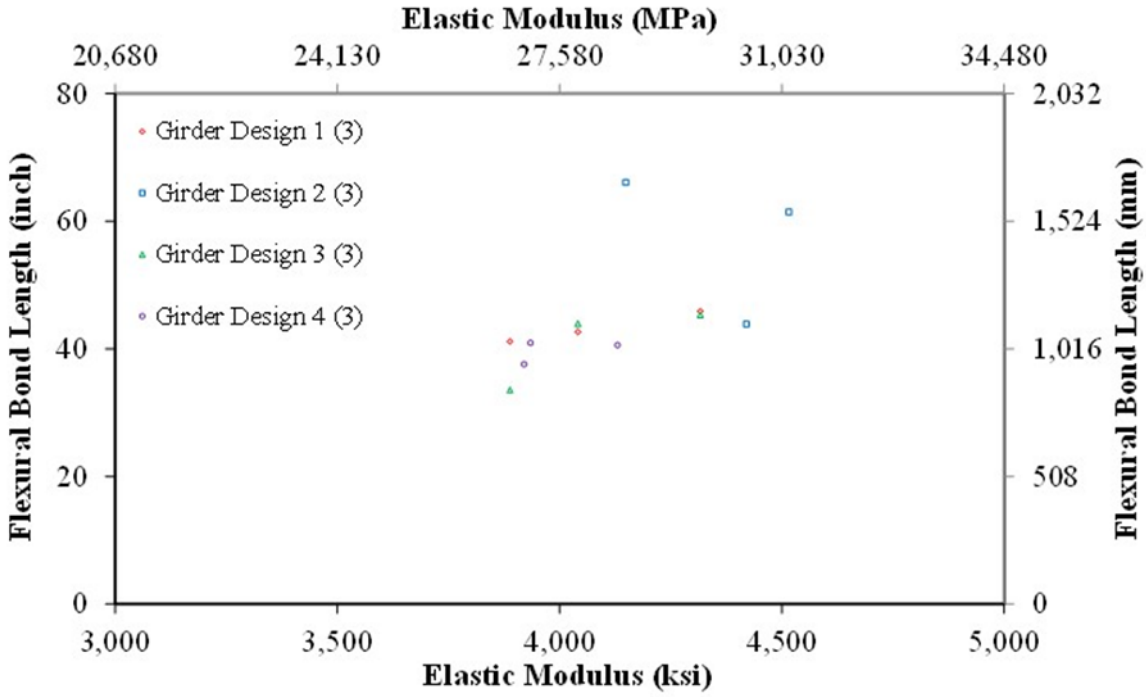


**Figure 46. Graph. Flexural Bond Length Compared to Elastic Modulus by Girder Design.**

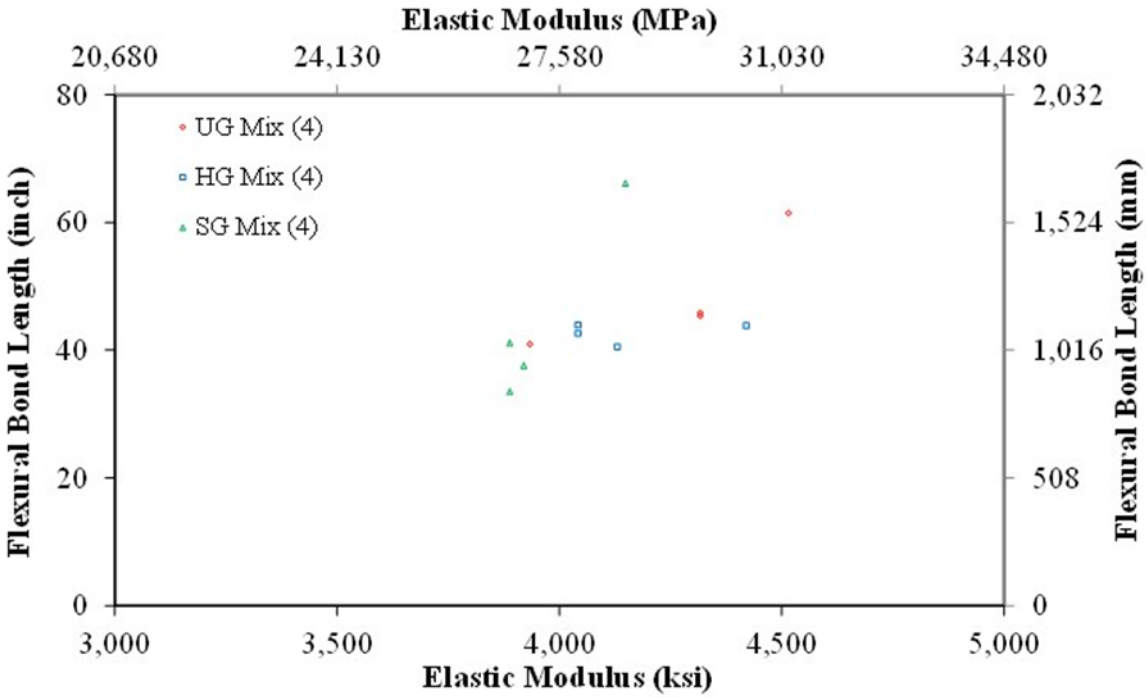


**Figure 47. Graph. Flexural Bond Length Compared to Elastic Modulus by Girder Concrete Mix.**

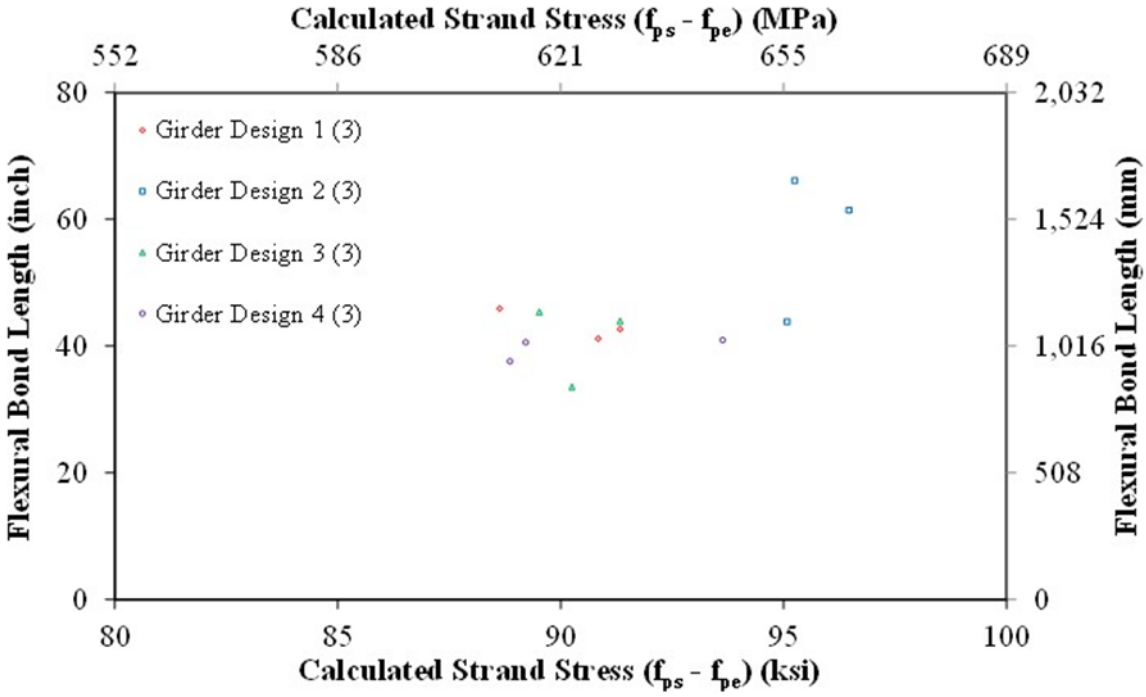


**Figure 48. Graph. Flexural Bond Length Compared to Calculated Strand Prestress by Girder Design.**

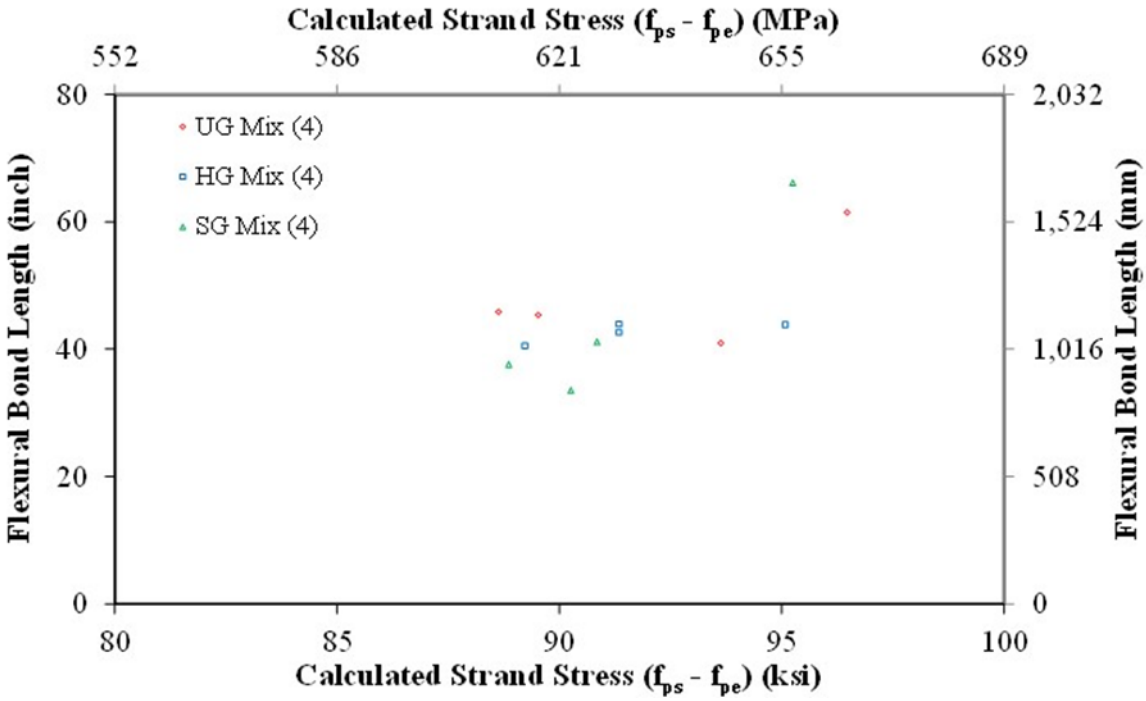


**Figure 49. Graph. Flexural Bond Length Compared to Calculated Strand Prestress by Girder Concrete Mix.**

### *Normalized Flexural Bond Length*

The flexural bond lengths ($\ell_{fb}$) determined from the transfer length measurements and evaluation of girder end tests were normalized by parameters described by researchers in the literature as being important in the prediction of flexural bond length.[16,22,30] These parameters include nominal strand diameter, strand stress, concrete compressive strength, and concrete elastic modulus. The normalized transfer lengths are shown graphically in Figure 50 through Figure 61. In each figure, the flexural bond lengths are shown in series by girder design number. The figures are presented in pairs. The first figure in each pair compares the normalized flexural bond length to concrete compressive strength at the time of test ($f'_c$). The second figure of each pair compares the normalized flexural bond length to concrete unit weight ($w_c$).

Expressions for development length are commonly written in the form of the addition of terms for the transfer length and flexural bond length.[16,22,25,30] The common parameters used to predict the flexural bond length are nominal strand diameter, strand stress needed to be developed over the flexural bond length ($f_{ps} - f_{pe}$), and concrete compressive strength ($f'_c$). The expression for flexural bond included in the AASHTO LRFD Specification is given by Eq. 19. It includes the parameters for strand diameter and strand stress. The expression for flexural bond length proposed by Ramirez and Russell includes the parameters of stand diameter and concrete compressive strength and is given by Eq. 20. All three parameters are included Eq. 21, which is the expression proposed by Mitchell et al. for flexural bond length.

$$\ell_{fb} = (f_{ps} - f_{pe})d_b \quad \text{(Eq. 19)}$$

$$\ell_{fb} = \frac{225d_b}{\sqrt{f'_c}} \quad \text{(Eq. 20)}$$

$$\ell_{fb} = (f_{ps} - f_{pe})d_b\sqrt{\frac{4.5}{f'_c}} \quad \text{(Eq. 21)}$$

The flexural bond length data in Figure 50 through Figure 61 represent an upper bound of the actual flexural bond length. This is due to the data being based on testing discrete embedment lengths to determine a range for strand development length. As a result, a more precise value for flexural bond length cannot be determined without additional testing to narrow the range of tested embedment lengths.

Flexural bond length is normalized by nominal strand diameter ($d_b$) in Figure 50 and Figure 51. All of the expressions include nominal strand diameter, but none use it alone. The mean calculated strand stress needed to be developed over the flexural bond length ($f_{ps} - f_{pe}$) for the 12 girder specimens is 91.8 ksi (633 MPa). A horizontal line in Figure 50 and Figure 51 at a value of 90 was used to represent the prediction by Eq. 19. The mean concrete compressive strength for the 12 girders is 10.2 ksi (70.3 MPa). A value of 10 ksi (69 MPa) was used in Eq. 20 to

approximate the prediction by the Ramirez and Russell expression. The prediction by the Mitchell et al. expression, given by Eq. 21, was approximated with the values of 90 ksi (620 MPa) for $f_{ps} - f_{pe}$ and 10 ksi (69 MPa) for $f'_c$. Horizontal lines at $225/\sqrt{10}$ and $90\sqrt{(4.5/10)}$ represent the predictions by Eq. 20 and Eq. 21, respectively. The flexural bond lengths determined from the two tests that ended in a shear failure are above all three horizontal prediction lines. The remaining data is near the AASHTO LRFD prediction or clearly below the prediction indicating an overestimation of the flexural bond length.

Figure 52 and Figure 53 show the flexural bond lengths normalized by $(f_{ps} - f_{pe})d_b$. A horizontal line at a value of 1.0 in each figure represents the prediction given by the AASHTO LRFD Bridge Design Specifications (Eq. 19). Except for the two tests failing in shear, most of the data is below the prediction line.

Flexural bond length is normalized by $d_b/\sqrt{f'_c}$ in Figure 54 and Figure 55. Only four data points are below the horizontal lines at 225 representing the prediction by Ramirez and Russell (Eq. 20).

None of the flexural bond data points are below the prediction line in Figure 56 and Figure 57. In these figures, flexural bond length is normalized by $(f_{ps} - f_{pe})d_b/\sqrt{f'_c}$. The prediction given by the Mitchell et al. expression (Eq. 21) is represented by horizontal lines at $\sqrt{4.5}$.

The parameter of concrete elastic modulus ($E_c$) has been used in prediction expressions for transfer length (Eq. 6 and Eq. 7). Flexural bond length normalized by $d_b/E_c$ is given in Figure 58 and Figure 59. Figure 60 and Figure 61 show flexural bond length normalized by $(f_{ps} - f_{pe})d_b/E_c$. No existing expression for flexural bond length that included $E_c$ was found in the literature. A simplified expression for $E_c$ in terms of $\sqrt{f'_c}$ has been in the AASHTO LRFD Bridge Design Specifications prior to the 2015 Interim Revisions.[1] This expression was substituted into the expression for flexural bond length given by Ramirez and Russell as shown in Eq. 22.

$$\ell_{fb} = \frac{225}{\sqrt{f_c'}} d_b \approx \frac{225}{E_c/1820} d_b = \frac{409{,}500}{E_c} d_b \qquad \text{(Eq. 22)}$$

Horizontal lines at 409,500 (i.e., 225×1850) in Figure 58 and Figure 59 represent the prediction by the Ramirez and Russell expression with the adjustment for $E_c$. All of the data except for the two points ending in shear failure are below the horizontal lines. In Figure 60 and Figure 61, the approximated value of 90 ksi (620 MPa) for $f_{ps} - f_{pe}$ was included in the Ramirez and Russell expression with the adjustment for $E_c$. Again, all of the data except for the two points ending in shear failure are below the horizontal lines.

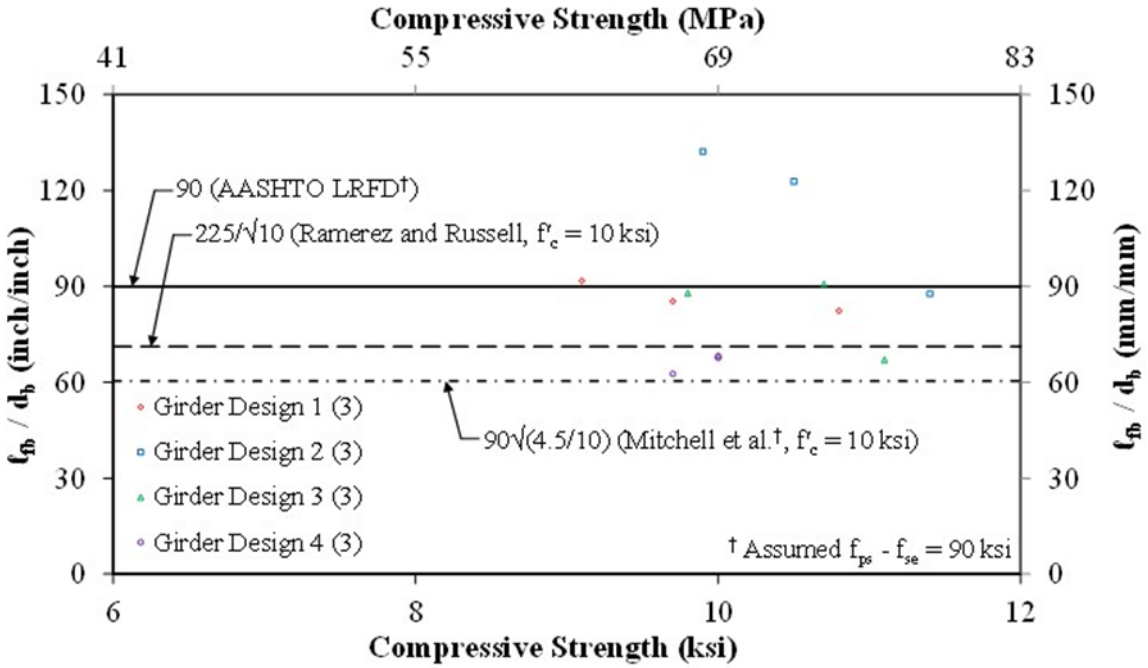


**Figure 50. Graph. Normalized Flexural Bond Length ($\ell_{fb}/d_b$) Compared to Compressive Strength by Girder Design.**

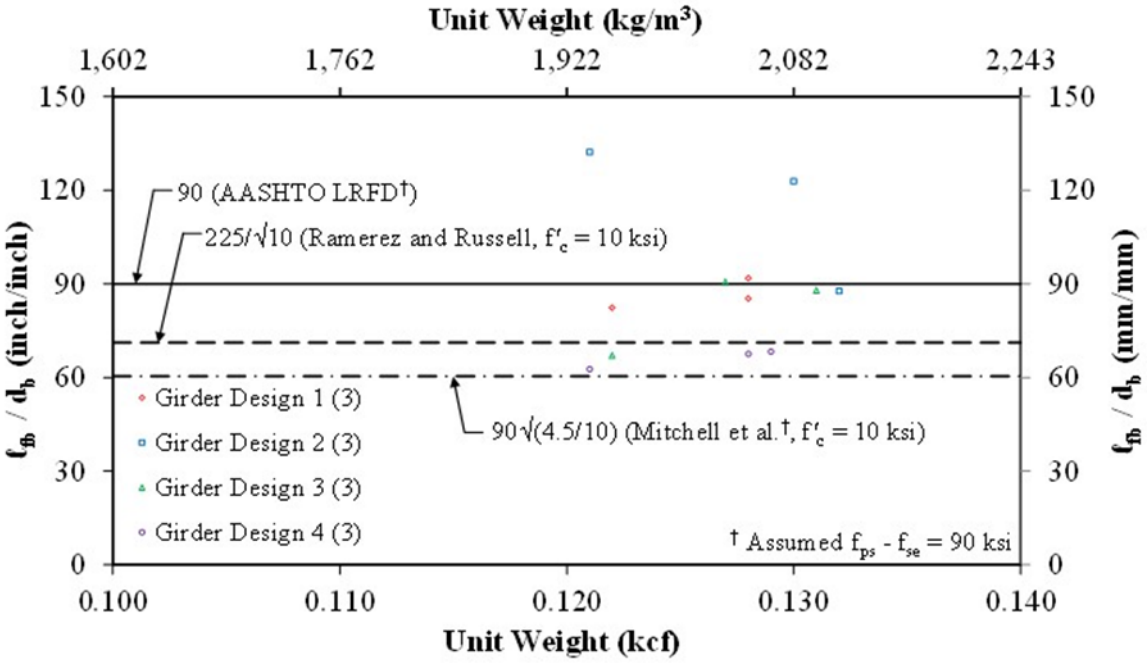


**Figure 51. Graph. Normalized Flexural Bond Length ($\ell_{fb}/d_b$) Compared to Unit Weight by Girder Design.**

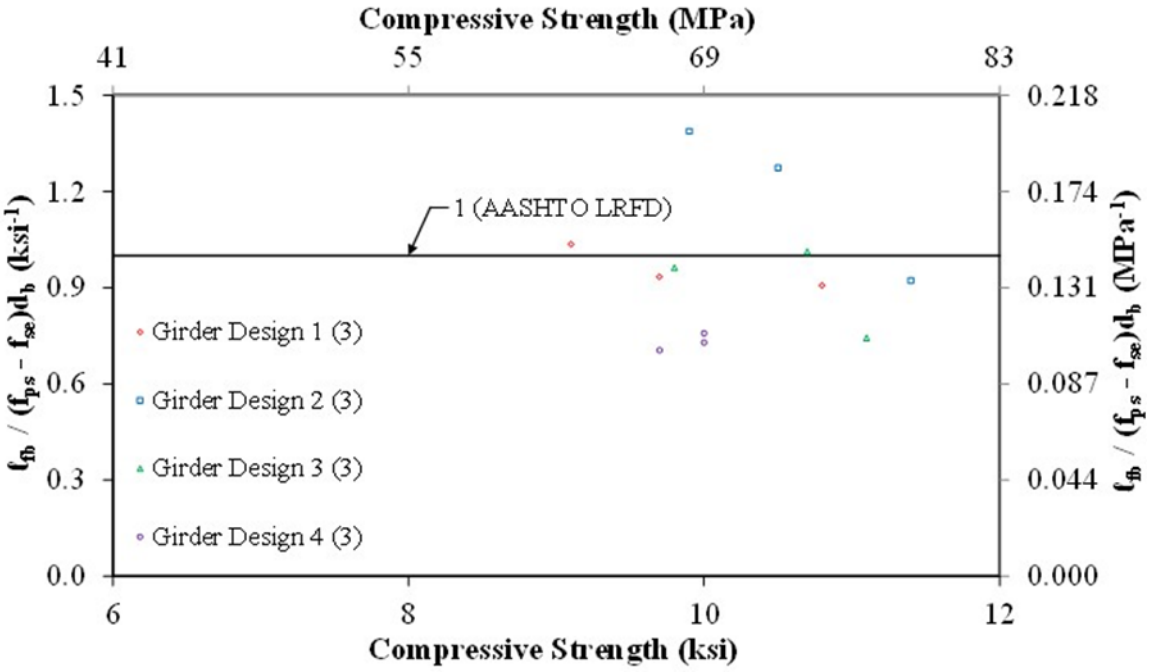


**Figure 52. Graph. Normalized Flexural Bond Length ($\ell_{fb} /(f_{ps} -f_{se})d_b$) Compared to Compressive Strength by Girder Design.**

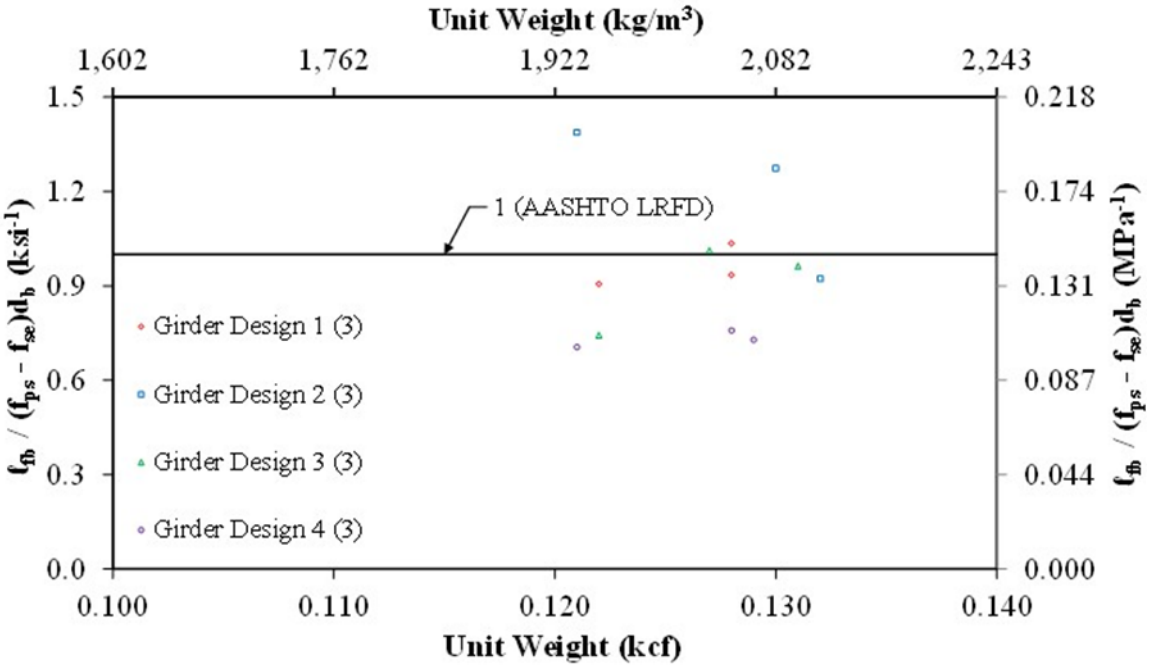


**Figure 53. Graph. Normalized Flexural Bond Length ($\ell_{fb} /(f_{ps} -f_{se})d_b$) Compared to Unit Weight by Girder Design.**

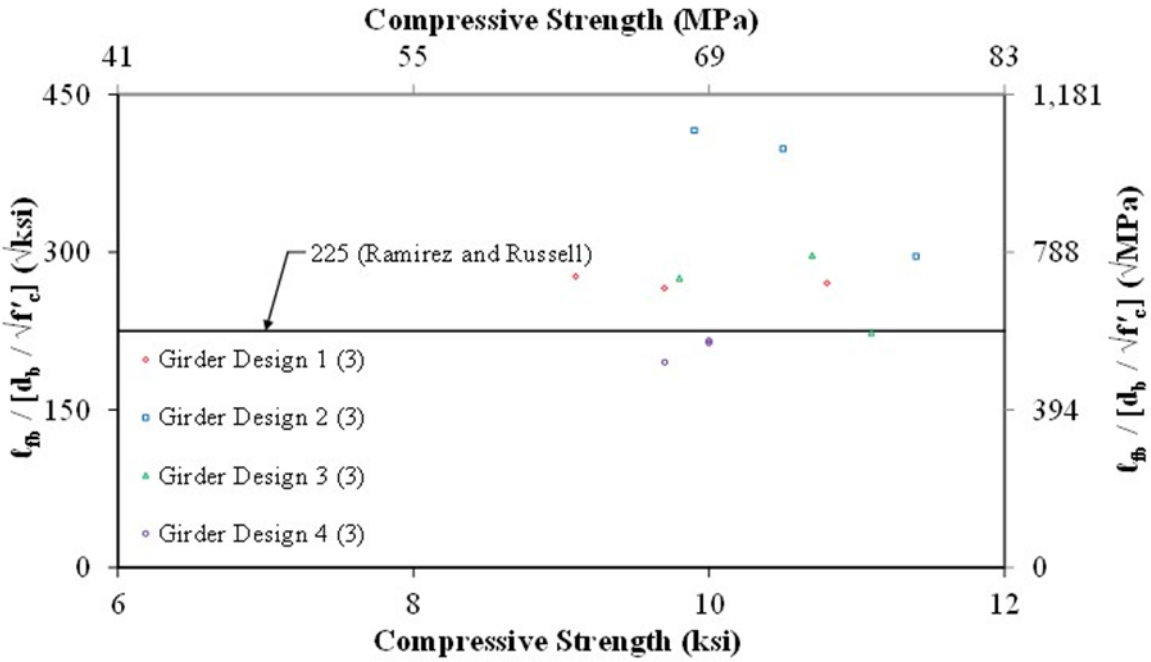


**Figure 54. Graph. Normalized Flexural Bond Length ($\ell_{fb}$ /[$d_b$/√$f'_{ci}$]) Compared to Compressive Strength by Girder Design.**

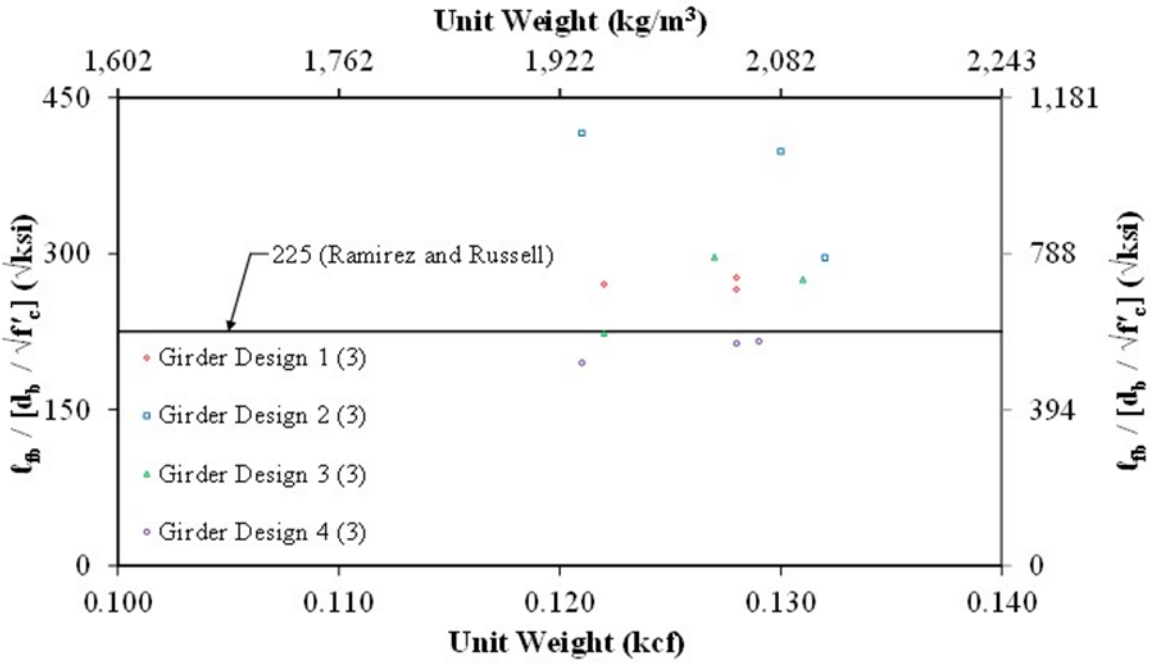


**Figure 55. Graph. Normalized Flexural Bond Length ($\ell_{fb}$ /[$d_b$/√$f'_{ci}$]) Compared to Unit Weight by Girder Design.**

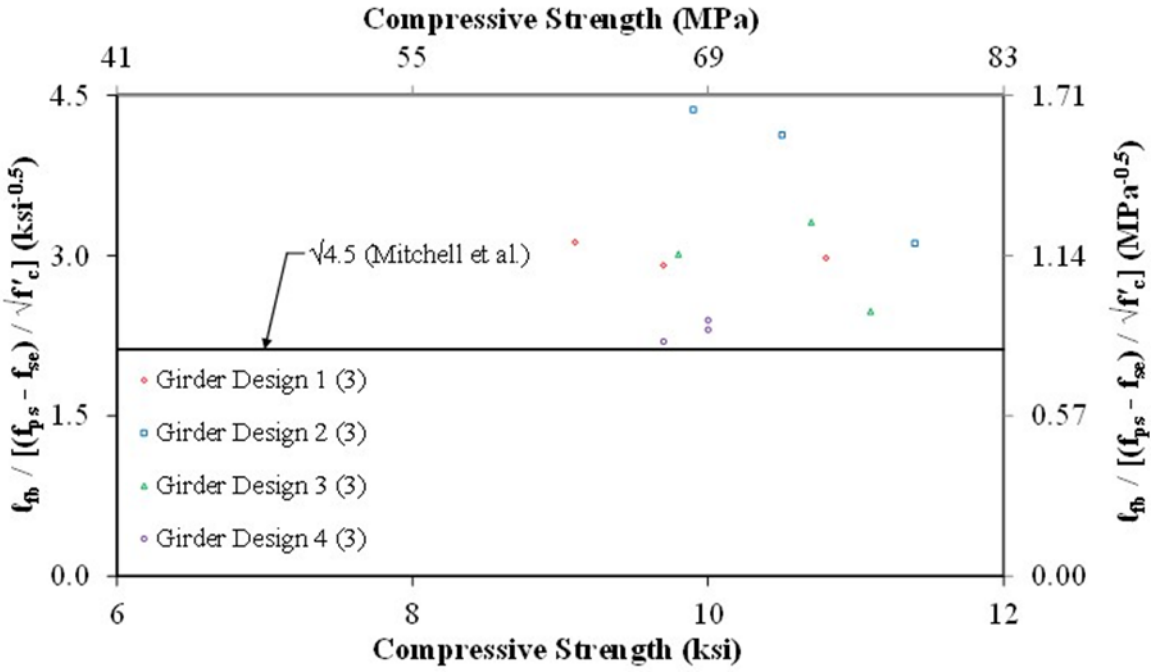


**Figure 56. Graph. Normalized Flexural Bond Length ($\ell_{fb}$ /[($f_{ps}$ -$f_{se}$)$d_b$/√$f'_{ci}$]) Compared to Compressive Strength by Girder Design.**

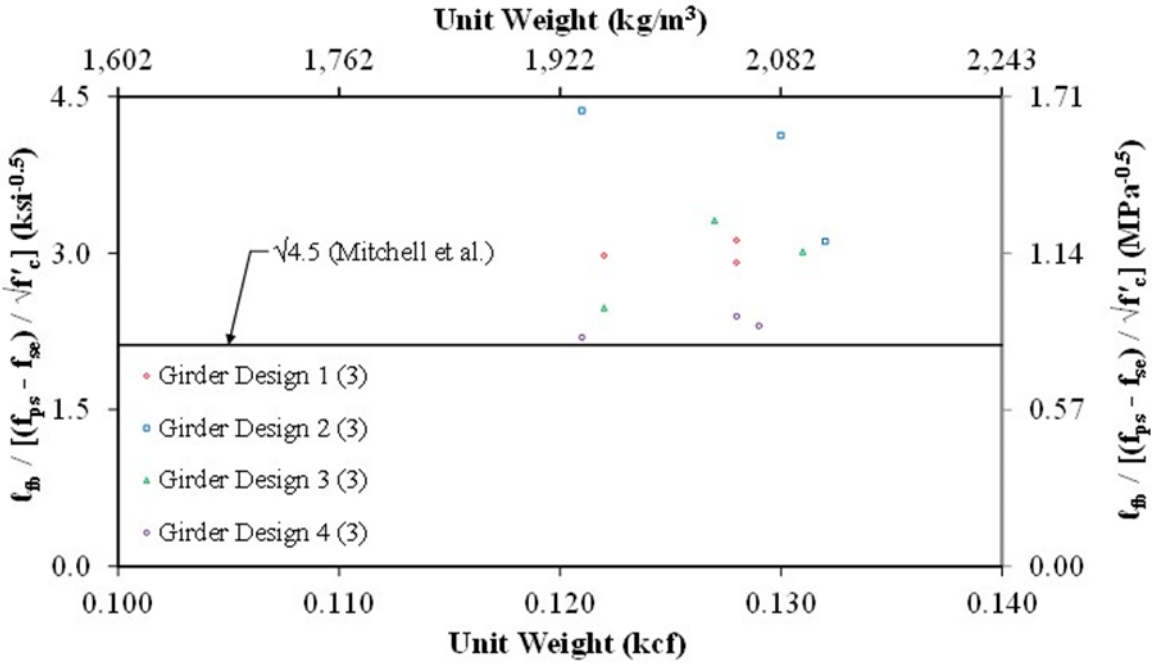


**Figure 57. Graph. Normalized Flexural Bond Length ($\ell_{fb}$ /[($f_{ps}$ -$f_{se}$)$d_b$/√$f'_{ci}$]) Compared to Unit Weight by Girder Design.**

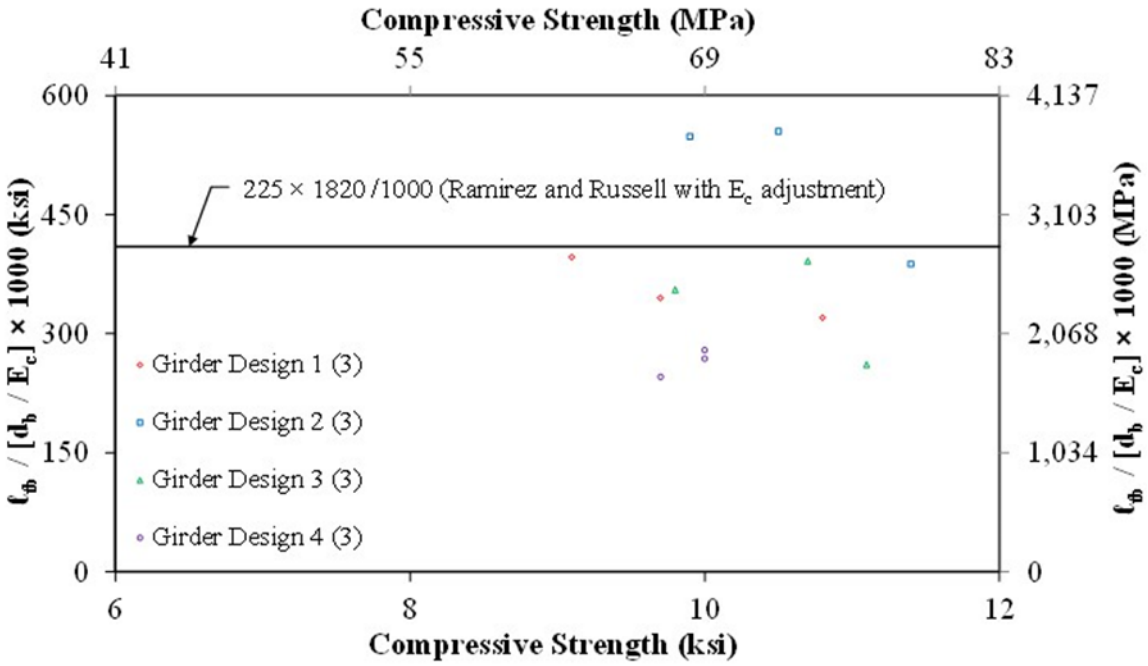


**Figure 58. Graph. Normalized Flexural Bond Length ($\ell_{fb}$ /[$d_b$/$E_c$]) Compared to Compressive Strength by Girder Design.**

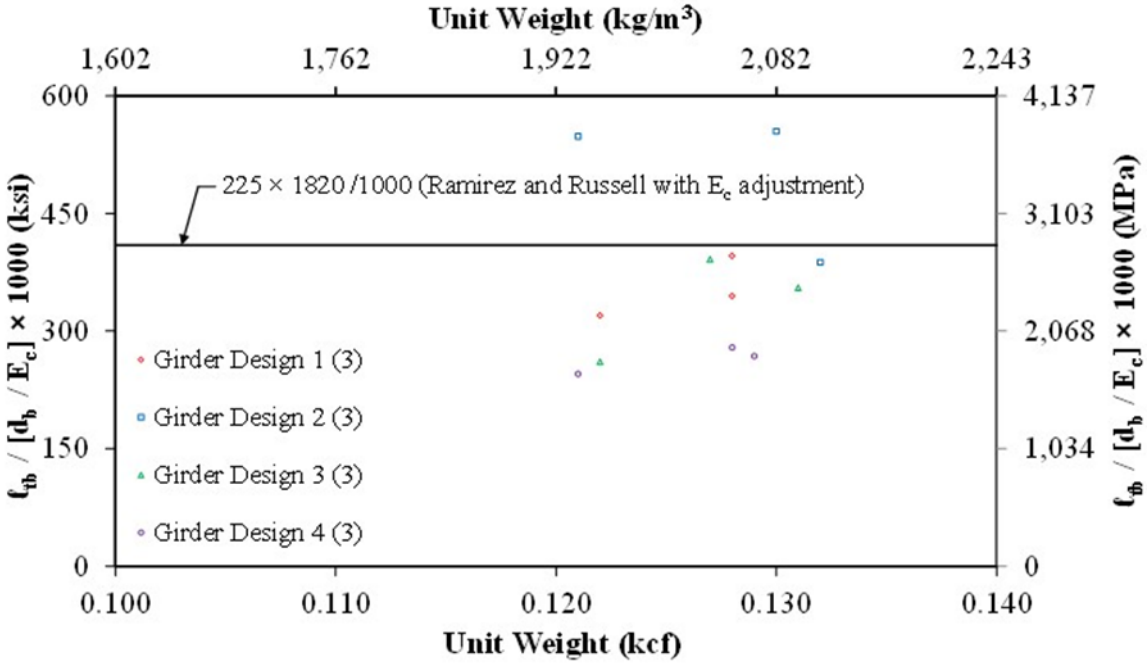


**Figure 59. Graph. Normalized Flexural Bond Length ($\ell_{fb}$ /[$d_b$/$E_c$]) Compared to Unit Weight by Girder Design.**

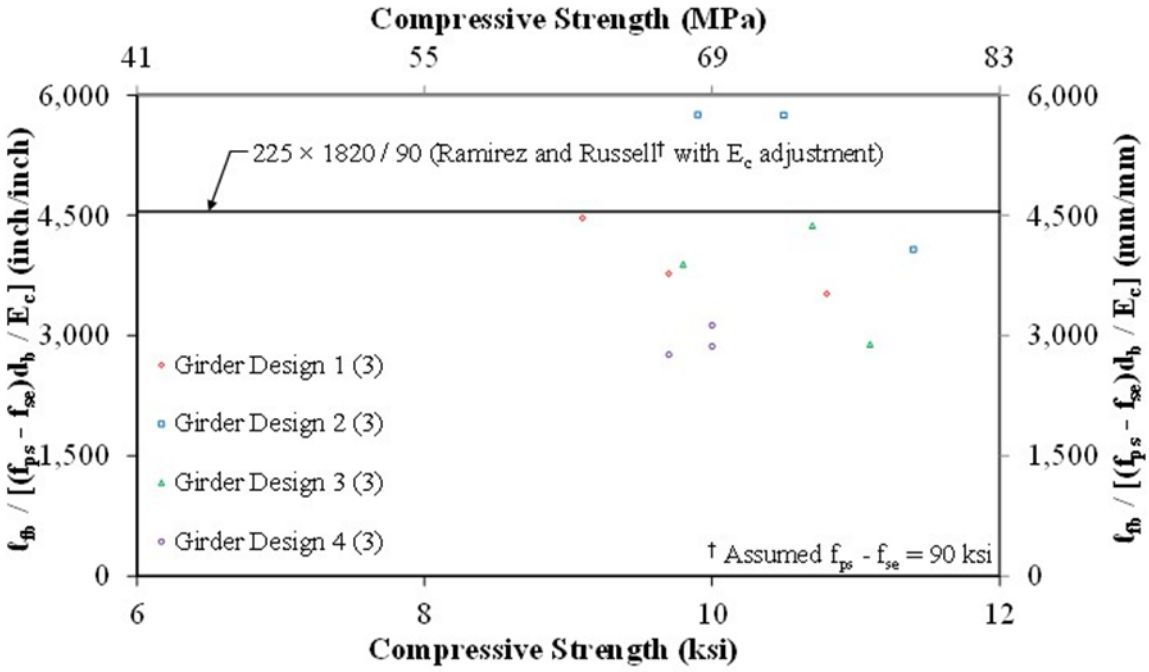


**Figure 60. Graph. Normalized Flexural Bond Length ($\ell_{fb}$ /[($f_{ps}$ -$f_{se}$)$d_b$/$E_c$]) Compared to Compressive Strength by Girder Design.**

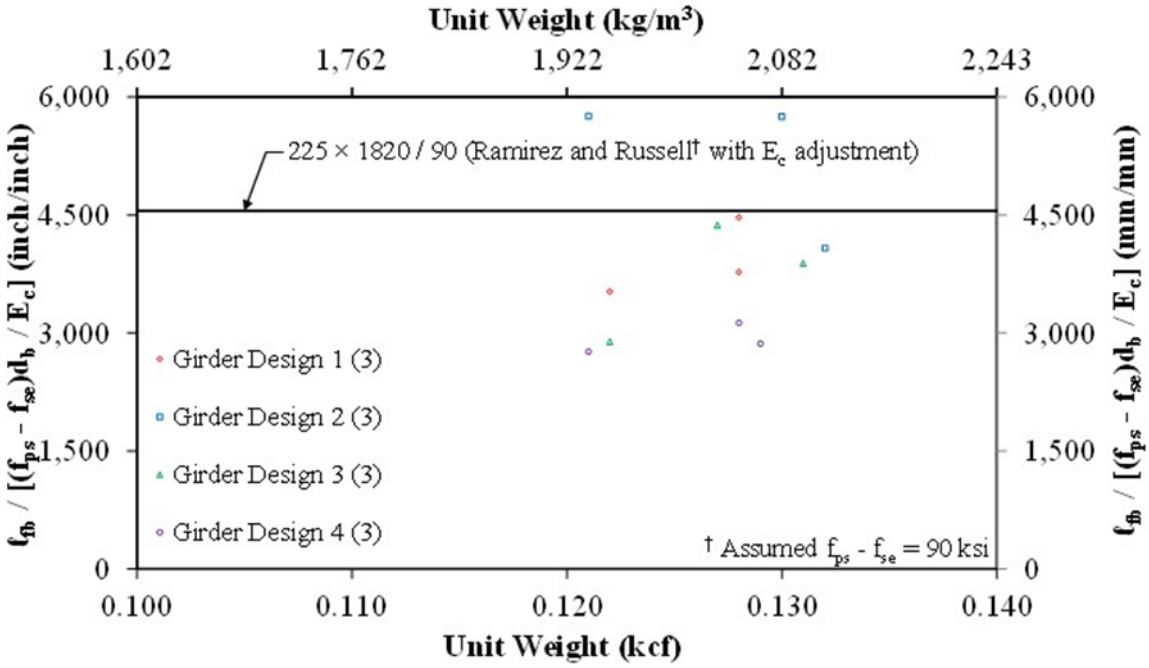


**Figure 61. Graph. Normalized Flexural Bond Length ($\ell_{fb}$ /[($f_{ps}$ -$f_{se}$)$d_b$/$E_c$]) Compared to Unit Weight by Girder Design.**

### *Flexural Bond Length Prediction*

The flexural bond lengths ($\ell_{fb}$) determined for the 12 LWC girder specimens were compared to the flexural bond lengths predicted by several expressions including the AASHTO LRFD Bridge Design Specifications. The measured flexural bond lengths were compared to the predicted transfer lengths using a test-to-prediction ratio with the measured $\ell_{fb}$ being referred to as the "test."

Table 22 gives the test-to-prediction ratios for three expressions for predicting flexural bond length described previously in this report. The mean ratios for all 12 LWC girders described in this report are given in Table 22. The COV, maximum ratio, minimum ratio, and percent of ratios less than 1.0 are also given in the table. A ratio less than 1.0 indicates a prediction that overestimates the flexural bond length. As discussed previously in this report, the flexural bond length data represent an upper bound of the actual flexural bond length. As a result, a ratio less than 1.0 (i.e., overestimated $\ell_{fb}$) is more significant than a ratio greater than 1.0. Additional testing with a shorter strand embedment length could have resulted in a short measured flexural bond length. The test-to-prediction ratio for such a test would have been lower.

The expression in the AASHTO LRFD Bridge Design Specifications (Eq. 19) had ratios less than 1.0 for 67 percent of the flexural bond length data. The Ramirez and Russell (Eq. 20) expression had ratios less than 1.0 for 33 percent of the data. All of the ratios were greater than 1.0 for the Mitchell et al. expression (Eq. 21).

The flexural bond length test-to-prediction ratios were evaluated for the main experimental variables of concrete mix and nominal strand diameter in Table 22. The test-to-prediction ratios were the lowest for the SG Mix, with the minimum ratios ranging from 0.71 to 1.04. The ratios were the highest for the HG Mix, with the minimum ratios ranging from 0.76 to 1.13. The test-to-prediction ratios were slightly lower for the girders with 0.5 inch (13 mm) nominal strand diameter. The minimum ratios ranged from 0.75 to 1.17 for the nine girders with 0.5 inch (13 mm) diameter strand and ranged from 0.70 to 1.04 for the three girders with 0.6 inch (15 mm) diameter strand.

**Table 22. Test-to-Prediction Ratio of Flexural Bond Length.**

| Girder Specimens[†] | Design Expression[‡] | Mean | COV | Max. | Min. | Percent < 1.0 |
|---|---|---|---|---|---|---|
| All TFHRC Girders (12) | AASHTO LRFD | 0.949 | 0.222 | 1.384 | 0.707 | 67% |
| | Ramirez and Russell | 1.238 | 0.247 | 1.848 | 0.867 | 33% |
| | Mitchell et al. | 1.429 | 0.221 | 2.053 | 1.038 | 0% |
| UG Mix (4) | AASHTO LRFD | 1.014 | 0.217 | 1.269 | 0.731 | 25% |
| | Ramirez and Russell | 1.319 | 0.255 | 1.770 | 0.959 | 25% |
| | Mitchell et al. | 1.519 | 0.229 | 1.939 | 1.090 | 0% |
| HG Mix (4) | AASHTO LRFD | 0.896 | 0.103 | 0.967 | 0.760 | 100% |
| | Ramirez and Russell | 1.167 | 0.133 | 1.316 | 0.950 | 25% |
| | Mitchell et al. | 1.350 | 0.110 | 1.462 | 1.133 | 0% |
| SG Mix (4) | AASHTO LRFD | 0.937 | 0.331 | 1.384 | 0.707 | 75% |
| | Ramirez and Russell | 1.228 | 0.355 | 1.848 | 0.867 | 50% |
| | Mitchell et al. | 1.419 | 0.317 | 2.053 | 1.038 | 0% |
| Girder Designs with 0.5 inch dia. strand (9) | AASHTO LRFD | 1.021 | 0.190 | 1.384 | 0.747 | 56% |
| | Ramirez and Russell | 1.342 | 0.210 | 1.848 | 0.993 | 11% |
| | Mitchell et al. | 1.543 | 0.181 | 2.053 | 1.173 | 0% |
| Girder Design with 0.6 inch dia. strand (3) | AASHTO LRFD | 0.733 | 0.036 | 0.760 | 0.707 | 100% |
| | Ramirez and Russell | 0.926 | 0.055 | 0.959 | 0.867 | 100% |
| | Mitchell et al. | 1.087 | 0.044 | 1.133 | 1.038 | 0% |

Notes:

[†] No. of specimens given in parentheses. Concrete mix included previously in specimen name: A for UG mix, B for HG mix, C for SG mix

[‡] AASHTO LRFD (Eq. 19), Ramirez and Russell (Eq. 20), Mitchell et al. (Eq. 21)

### *Development Length Prediction*

The development length ($\ell_d$) determined for the 12 LWC girder specimens were compared to the development lengths predicted by several expressions including the one in the AASHTO LRFD Bridge Design Specifications. The mean test-to-prediction ratios, COV of the ratios, maximum ratio, minimum ratio, and percent of ratios less than 1.0 are given in Table 23. A ratio less than 1.0 indicates a prediction that overestimates the development length. As discussed previously in this report for flexural bond length, the development length data also represent an upper bound of the actual development length. This is due to the data being based on testing discrete embedment lengths to determine a range for strand development length. Additional testing at embedment lengths less than the predicted development length (i.e., overestimating $\ell_d$) could potentially result in flexural failures. As a result, a ratio less than 1.0 (i.e., overestimated $\ell_d$) is more meaningful than a ratio greater than 1.0.

The first three girder ends were tested with an embedment length of 75 inches (1910 mm). This corresponded to approximately 100 percent of the $\ell_d$ predicted by the AASHTO LRFD Bridge Design Specifications based on preliminary calculations that used estimates of material properties. After these three tests, subsequent tests on the first end of the girders with 0.5 inch (13 mm) diameter strand used an embedment length of 72 inches (1830 mm) to ensure that embedment length would be less than the refined calculation of the $\ell_d$ predicted by the expression in the AASHTO LRFD Bridge Design Specifications. The second test on girder C3 resulted in a shear failure, therefore the development length was based on the 75 inch (1910 mm) embedment length of the first end tested. The test-to-prediction ratio determined using the prediction of $\ell_d$ using the AASHTO LRFD Bridge Design Specifications and the measured material properties is 1.005. In the discussion that follows, this ratio will not be interpreted as an underestimation of the expression in the AASHTO LRFD Bridge Design Specifications to predict $\ell_d$.

The test-to-prediction ratios for four expressions are given in Table 23. The development length was overestimated for all 12 LWC girders by the expression in the AASHTO LRFD Bridge Design Specifications (Eq. 12) with the $\kappa$-factor taken as 1.0. The expressions by Ramirez and Russell (Eq. 13) and Meyer et al. (Eq. 14) overestimated the prediction of $\ell_d$ for 83 percent of the data. The Mitchell et al. expression (Eq. 15) overestimated $\ell_d$ for 8 percent of the data.

The development length test-to-prediction ratios were evaluated for the main experimental variables of concrete mix and nominal strand diameter in Table 23. The ranges of minimum ratios were similar for each girder concrete mix: UG mix ranged from 0.67 to 0.98, HG mix ranged from 0.86 to 1.04, and the SG mix ranged from 0.68 to 1.02. The minimum ratios predicted by each expression for the 0.6 inch (15 mm) diameter strand were slightly less than the ratios for predicted for the 0.5 inch (13 mm) diameter strand.

**Table 23. Test-to-Prediction Ratio of Development Length.**

| Girder Specimens[†] | Design Expression[‡] | Mean | COV | Max. | Min. | Percent < 1.0 |
|---|---|---|---|---|---|---|
| All TFHRC Girders (12) | AASHTO LRFD | 0.760 | 0.141 | 1.005 | 0.669 | 92% |
| | Ramirez and Russell | 0.960 | 0.150 | 1.288 | 0.828 | 83% |
| | Mitchell et al. | 1.143 | 0.144 | 1.517 | 0.978 | 8% |
| | Meyer et al. | 0.832 | 0.131 | 1.092 | 0.717 | 83% |
| UG Mix (4) | AASHTO LRFD | 0.775 | 0.164 | 0.960 | 0.669 | 100% |
| | Ramirez and Russell | 0.976 | 0.177 | 1.225 | 0.828 | 75% |
| | Mitchell et al. | 1.161 | 0.171 | 1.443 | 0.978 | 25% |
| | Meyer et al. | 0.847 | 0.147 | 1.017 | 0.717 | 75% |
| HG Mix (4) | AASHTO LRFD | 0.716 | 0.031 | 0.728 | 0.682 | 100% |
| | Ramirez and Russell | 0.904 | 0.041 | 0.955 | 0.866 | 100% |
| | Mitchell et al. | 1.077 | 0.036 | 1.132 | 1.041 | 0% |
| | Meyer et al. | 0.784 | 0.018 | 0.796 | 0.768 | 100% |
| SG Mix (4) | AASHTO LRFD | 0.788 | 0.186 | 1.005 | 0.684 | 75% |
| | Ramirez and Russell | 1.000 | 0.196 | 1.288 | 0.846 | 75% |
| | Mitchell et al. | 1.192 | 0.186 | 1.517 | 1.019 | 0% |
| | Meyer et al. | 0.865 | 0.177 | 1.092 | 0.761 | 75% |
| Girder Design 1-3, 0.5 inch strand (9) | AASHTO LRFD | 0.787 | 0.142 | 1.005 | 0.725 | 89% |
| | Ramirez and Russell | 0.998 | 0.149 | 1.288 | 0.897 | 78% |
| | Mitchell et al. | 1.187 | 0.142 | 1.517 | 1.066 | 0% |
| | Meyer et al. | 0.860 | 0.131 | 1.092 | 0.778 | 78% |
| Girder Design 4, 0.6 inch strand (3) | AASHTO LRFD | 0.679 | 0.012 | 0.684 | 0.669 | 100% |
| | Ramirez and Russell | 0.846 | 0.022 | 0.866 | 0.828 | 100% |
| | Mitchell et al. | 1.013 | 0.032 | 1.041 | 0.978 | 33% |
| | Meyer et al. | 0.748 | 0.037 | 0.768 | 0.717 | 100% |

Notes:

[†] No. of specimens given in parentheses. Concrete mix included previously in specimen name: A for UG mix, B for HG mix, C for SG mix

[‡] AASHTO LRFD (Eq. 12), Ramirez and Russell (Eq. 13), Mitchell et al. (Eq. 15), Meyer et al. (Eq. 14)

## SUMMARY OF DEVELOPMENT LENGTH EXPERIMENTAL RESULTS

The ends of 12 AASHTO Type II girders were tested to determine the development length of prestressing strand. The strand embedment length of the first end tested on each girder was approximately equal to the development length determined using the expression in the AASHTO LRFD Bridge Design Specifications. The second end tested had a strand embedment length of approximately 70 percent of the calculated development length. The tests on each end were to determine whether the embedment length would cause a flexural failure without significant strand slip, or a flexural or shear failure with significant stand slip. This is an indirect method employed in numerous studies.[13,19,24,25,30-32]

The development length was evaluated for the 24 tests on the 12 girders. Girder end tests on two of the three specimens with the larger number of strand (Girder Design 2) ended in a shear failure. The tests on girder A2 and C2 with the shorter embedment length ended in shear failures, while the test on the end with the longer embedment length ended in flexural failure without significant strand slip. The rest of the girders with 0.5 inch (13 mm) nominal strand diameter had flexural failures and most of the tests did not have significant strand slip. The six tests on the three girders with 0.6 inch (15 mm) nominal strand diameter resulted in flexural failures. All three tests on the ends with the shorter embedment length had significant strand slip.

After the development length was determined for each girder, the flexural bond length was determined by subtracting the transfer length measured on the girder. The portion of the AASHTO LRFD expression for development length that represents the flexural bond length overestimated the measured flexural bond length for 67 percent of the girders. An overestimated flexural bond length indicates a conservative prediction. A similar expression by Ramirez and Russell overestimated the measured flexural bond length for 33 percent of the girders. An expression was substituted into the Ramirez and Russell expression to account for the modulus of elasticity of concrete. This modified expression overestimated the flexural bond lengths for all test but those on girder A2 and C2.

The development lengths for most of the tests were overestimated by the predictions given by the expression in the AASHTO LRFD Bridge Design Specifications, the Ramirez and Russell expression, and the Meyer et al. expression.

## SUMMARY OF EXPERIMENTAL RESULTS AND CONCLUDING REMARKS

The strand transfer length was measured on 18 prestressed girders and the strand development length was evaluated on 12 prestressed girders to investigate transfer and development length of strand in high-strength LWC. Key test parameters included the type of lightweight aggregate, the size of strand, the number of strands, the amount of shear reinforcement, and the girder depth. Four girders designs were developed to evaluate the effect of the key parameters for strand development length. Three different concrete mix designs using three different lightweight aggregates were used. The mix designs included two expanded shales and one expanded slate. The concrete mixes used a blend of lightweight and normal-weight coarse aggregate and normal-weight sand. These mixes were prescriptively produced at the precaster's facility and used to produce the 12 prestressed girders used to evaluate stand development length. The design compressive strength ranged from 6 to 10 ksi (41 to 69 MPa) and the target unit weight ranged from 0.126 to 0.130 kcf (2020 to 2080 kg/m$^3$). The resulting concrete had a range in 28-day compressive strength of 8.6 to 9.7 ksi (59.3 to 66.9 MPa) and an air-dry density range of 0.125 to 0.132 kcf (2000 to 2110 kg/m$^3$).

The transfer length measurements were made on a total of 18 girders. The transfer length of each girder was determined from concrete surface strain measurements. Concrete strain profiles were determined from the strain measurements and the 95 percent Average Maximum Strain Method was used to determine the transfer length. A 53 percent increase in the mean transfer length was observed for girders with a 25 percent increase in stirrup spacing. As expected, the mean transfer length of girders with 0.6 inch (15 mm) nominal diameter strand was 33 percent longer than the mean transfer length of girders with 0.5 inch (13 mm) nominal diameter strand. The mean ratio of the long-term to immediately measured transfer lengths was 1.01 indicating only a slight increase in transfer length with time.

The transfer length was overestimated by the expression in the AASHTO LRFD Bridge Design Specifications, the Meyer et al. expression, and Ramirez and Russell expressions. The Barnes et al. expression, which is described by its authors as a lower-bound prediction of transfer length, underestimated all of the measured transfer lengths. The mean ratios of the measured-to-predicted transfer length were higher for the girders with 0.6 inch (15 mm) nominal diameter strand than for the 0.5 inch (13 mm) nominal diameter strand. This indicates that the magnitude of increase in measured transfer length of the larger diameter strands was underestimated by the prediction expressions.

The development length was evaluated using 24 tests on the end-regions of 12 girders. Girder end tests on two of the three specimens with the larger number of strand (Girder Design 2) ended in a shear failure. This indicates that these specimens had a strand development length longer than the tested embedment length which was approximately 70 percent of the development length determined using the AASHTO LRFD Bridge Design Specifications. The remaining girder end tests resulted in flexural failures. Six of these tests had a strand slip greater than 0.010 inch (0.25 mm), which is the amount of slip considered to indicate a significant amount of slip.

Design expressions for flexural bond length and development length were compared to the evaluated lengths. The development lengths for most of the tests were overestimated by the predictions given by the expression in the AASHTO LRFD Bridge Design Specifications, the Ramirez and Russell expression, and the Meyer et al. expression. The flexural bond lengths were overestimated for 67 percent of the girders by the AASHTO LRFD Bridge Design expression, and overestimated for 33 percent of the girders by the Ramirez and Russell expression. A modified Ramirez and Russell expression to account for the reduced modulus of elasticity of the LWC overestimated the flexural bond lengths of all the girders except the two that failed in shear.

# CHAPTER 4. TFHRC PRESTRESSING STRAND BOND DATABASE

## INTRODUCTION

This chapter describes the information available in the TFHRC Prestressing Strand Bond Database ("TFHRC Database"). The database contains information about the transfer and development length of prestressing strand in LWC and NWC specimens. The type of information included in the database for each specimen is described. The number of each type of specimen and the types of concrete mixtures found for each specimen type is described. The chapter also includes statistical information by concrete mixture type and specimen type for the specimens in the TFHRC Database.

## TFHRC DATABASE

A thorough literature review was performed to find published journal papers, conference papers, technical reports, and university dissertations that included tests, analysis, or discussions of LWC. Over 500 references were found in the literature that mentioned LWC. These references were reviewed for transfer length measurements and development length tests on prestressed concrete specimens. The development length tests included in the database were limited to data from specimens that failed in flexure or strand slip. Development length tests that ended in a shear failure without observed strand slip were excluded from the database. The details of the specimens in each reference are described in the following section. Only test data from published reports was included in the database. A list of references for the specimens in the database is included in Chapter 8 and a list of all of the specimen names is included for the LWC specimens in Appendix B and the NWC specimens in Appendix C.

Three types of prestressing strand bond data were reported. There were references that reported only transfer length measurements and others that only reported tests to determine development length. References that reported transfer length measurements and development length tests on the same specimen were used to determine the available flexural bond length.

The specimens were separated into three groups: single-strand rectangular, multi-strand rectangular, and multi-strand I-beam or T-beam. The single-strand rectangular specimens had one prestressing strand and a rectangular cross section. The cross sections were typically much smaller than the other specimen types and the strand was located at either the mid-depth of the cross section or near the bottom face. Multi-strand rectangular specimens had between two and five strands in a rectangular cross section. The multi-strand I-beam or T-beam specimens had three or more strands and either an I-shaped or T-shaped cross section. Some of the specimens had cast-in-place (CIP) reinforced concrete deck cast on top of the prestressed section. The CIP decks were either LWC or NWC on the LWC specimens. All of the decks on the NWC specimens were NWC. Table 24 gives the number of transfer length measurements and

development length tests, separated into groups by LWC and NWC specimens, data type, and specimen type.

**Table 24. Number of Transfer Length Measurements and Development Length Tests by Concrete Mixture Type and Specimen Type in the TFHRC Database.**

| Concrete Mix Type | Data Type | Single-strand Rectangular | Multiple-strand Rectangular | Multiple-strand I-beam or T-beam | All Specimen Types |
|---|---|---|---|---|---|
| LWC | Transfer Length Only | 0 | 10 | 15 | 25 |
| | Development Length Only | 12 | 0 | 11 | 23 |
| | Transfer and Development Length | 24 | 40 | 60 | 124 |
| NWC | Transfer Length Only | 89 | 45 | 33 | 167 |
| | Development Length Only | 34 | 0 | 7 | 41 |
| | Transfer and Development Length | 0 | 37 | 129 | 166 |

There were 22 references with measured transfer lengths on LWC and NWC. Some references had measurements on both LWC and NWC specimens. Table 25 gives the number of references per specimen type and the number of measurements per reference. No transfer length measurements were found in the literature on LWC single-strand rectangular specimens. Table 25 shows that the measurements for each specimen type came from between 1 and 11 different references. Transfer length measurements on LWC single-strand rectangular specimens were each from only one reference. The small size of these specimens makes them of less practical importance than the larger multi-strand I-beam and T-beam specimens, which had the highest number of references and tests. While some references had many more measurements than other references, the mean number of measurements from a reference was greater than nine. This indicates that the measurements from one reference are not likely to improperly bias the analysis of the data.

**Table 25. Summary of the Number of References for Transfer Length Measurements in the TFHRC Database.**

| Concrete Type | Specimen Type | Total No. of Ref. | Total No. of Measurements | No. of Measurements per Reference | | |
|---|---|---|---|---|---|---|
| | | | | Max. | Min. | Mean |
| LWC | Single-strand rect. | 1 | 24 | 24 | 24 | 24.0 |
| | Multi-strand rect. | 3 | 50 | 34 | 4 | 16.7 |
| | Multi-strand I-beam or T-beam | 7 | 65 | 16 | 1 | 9.3 |
| NWC | Single-strand rect. | 3 | 89 | 40 | 22 | 29.7 |
| | Multi-strand rect. | 3 | 82 | 34 | 16 | 27.3 |
| | Multi-strand I-beam or T-beam | 11 | 145 | 40 | 2 | 13.2 |

There were 19 references with development length tests on LWC and NWC. Some references reported tests on both LWC and NWC specimens. Table 26 gives the number of references per specimen type and the number of measurements per reference. Table 26 shows that the measurements for each specimen type came from between 1 and 12 different references. Development length tests on NWC single-strand rectangular specimens were each from only one reference. The small size of these specimens makes them of less practical importance than the larger multi-strand I-beam and T-beam specimens, which had the highest number of references and tests. The mean number of tests from a reference was greater than 11 for multi-strand specimens. This indicates that the test results from one reference are not likely to improperly bias the analysis of the test data from the multi-strand specimens. Also, in the analysis of all of the LWC specimens or NWC specimens, the results from one reference are not likely to improperly bias the analysis.

**Table 26. Summary of the Number of References for Development Length Tests in the TFHRC Database.**

| Concrete Type | Specimen Type | Total No. of Ref. | Total No. of Tests | No. of Tests per Reference | | |
|---|---|---|---|---|---|---|
| | | | | Max. | Min. | Mean |
| LWC | Single-strand rect. | 2 | 36 | 24 | 12 | 18.0 |
| | Multi-strand rect. | 2 | 40 | 34 | 6 | 20.0 |
| | Multi-strand I-beam or T-beam | 6 | 71 | 22 | 4 | 11.8 |
| NWC | Single-strand rect. | 1 | 34 | 34 | 34 | 34.0 |
| | Multi-strand rect. | 2 | 37 | 21 | 16 | 18.5 |
| | Multi-strand I-beam or T-beam | 12 | 136 | 39 | 1 | 11.3 |

The information collected for each specimen included its concrete mix, associated concrete mechanical property tests, test specimen dimensions, transfer length measurements and/or development length test results. The recorded concrete mechanical tests included compressive strength and modulus of elasticity at prestress transfer and compressive strength and modulus of elasticity at time of test. Measured mechanical properties at 28 days or 56 days were used if the properties at time of test were not given. Concrete unit weight was recorded for LWC specimens and for any NWC specimens that was available. Concrete mix information was recorded including the type of coarse and fine aggregate, the use of chemical admixtures, and the use of supplementary cementitious materials.

The strand prestress immediately after transfer and the effective prestress were calculated using the approximate estimate of time-dependent losses in AASHTO LRFD Bridge Design Specifications Article 5.9.5.3. Measured concrete and steel material properties were used when reported. When material properties were not reported, nominal values were used as appropriate (e.g., strand ultimate strength) and predictions using expressions in the AASHTO LRFD Bridge Design Specifications were used as appropriate (e.g., for concrete modulus of elasticity).

The tests performed as part of the research program at TFHRC on LWC as described previously in this report are included in the TFHRC Database. The TFHRC specimens used specified density concrete with an I-shaped cross section and had an NWC deck.

TRANSFER LENGTH SPECIMENS

This section describes the information collected in the TFHRC Database for specimens with measured transfer lengths. All specimens in the database had fully bonded strands; there were no

debonded strands between the centerlines of the supports and no supplemental anchorage hardware at the ends of the specimens.

The transfer lengths recorded in the database were measured immediately after the time of prestress transfer. If this measurement was not available, the measurement taken at the fewest number of days after transfer was recorded. Only transfer lengths determined using the concrete surface strain method were included in the database. The method used to determine the transfer length from the concrete surface strain measurements was recorded. Transfer lengths determined from measurements of end slip were not included in the database.

Other information included in the database included the level of pretensioning, the method of prestress transfer, and the strand surface condition. The level of pretensioning, was typically given as a percentage of specified ultimate stress at strand jacking (e.g., 75 percent of 270 ksi (1860 MPa)). Other references reported a measured jacking stress or jacking force. The method of prestress transfer (e.g., “flame cut” or “gradual release”) was recorded. The condition of the strand (e.g., “bright” or “minimal weathering”) was recorded.

Table 27 gives a summary of the number of transfer length measurements for each concrete mixture type and specimen type in the TFHRC Database. The definitions of different types of lightweight concrete mixtures have been traditionally based on the use of lightweight or normal weight constituent materials. The types of concrete mixtures in the database included sand-lightweight and specified density. Sand-lightweight was defined as concrete with lightweight coarse aggregate and either sand or a mixture of sand and lightweight fine aggregate. Specified density was defined as concrete with a mixture of normal weight and lightweight coarse aggregate and either sand or lightweight fine aggregate. Specimens with all-lightweight concrete, which was defined as concrete with lightweight fine and coarse aggregate, were not found in the literature. NWC specimens had normal weight coarse and fine aggregate.

Table 28 gives the number of transfer length measurements on specimens with a given nominal strand size. The numbers of specimens in the table are grouped by concrete mix type and specimen type.

**Table 27. Number of Transfer Length Measurements by Concrete Type and Specimen Type in the TFHRC Database.**

| Concrete Mixture Type | Single-strand Rectangular | Multiple-strand Rectangular | Multiple-strand I-beam or T-beam | All Specimen Types |
|---|---|---|---|---|
| Sand-lightweight | 24 | 46 | 47 | 117 |
| Specified density | 0 | 4 | 18 | 22 |
| Summation LWC | 24 | 50 | 65 | 139 |
| NWC | 89 | 82 | 145 | 316 |
| LWC and NWC | 113 | 132 | 210 | 455 |

**Table 28. Number of Transfer Length Measurements by Concrete Type and Nominal Strand Size in the TFHRC Database.**

| Concrete Type | Nominal Strand Size | Single-strand Rectangular | Multiple-strand Rectangular | Multiple-strand I-beam or T-beam | All Specimen Types |
|---|---|---|---|---|---|
| LWC | 3/8 inch | 0 | 0 | 0 | 0 |
| | 1/2 inch | 24 | 12 | 46 | 82 |
| | 1/2 inch special | 0 | 3 | 0 | 3 |
| | 9/16 inch | 0 | 0 | 0 | 0 |
| | 0.6 inch | 0 | 35 | 19 | 54 |
| | 0.62 inch | 0 | 0 | 0 | 0 |
| NWC | 3/8 inch | 14 | 0 | 0 | 14 |
| | 1/2 inch | 48 | 38 | 55 | 141 |
| | 1/2 inch special | 0 | 0 | 8 | 8 |
| | 9/16 inch | 0 | 0 | 8 | 8 |
| | 0.6 inch | 15 | 44 | 74 | 133 |
| | 0.62 inch | 12 | 0 | 0 | 12 |

DEVELOPMENT LENGTH SPECIMENS

This section describes the information collected in the TFHRC Database for specimens that were loaded to failure as development length tests. All specimens included in the database had fully bonded strands beyond the supports.

The strand embedment length was recorded for each development length test. This is the length of the bonded strand from the end of the specimen near the support to the centerline of the first applied load on the specimen. The failure mode determined by the researcher reporting the test was recorded in the database. These were typically flexure, bond, or shear. Flexural failures that had significant strand-slip were noted as such. If strand-slip measurements were not indicated, significant strand slip was recorded if indicated as such by the researcher. If the researcher included measurements of strand slip, the slip was considered significant if it exceeded 0.01 inch (0.25 mm). Shear failures that were not indicated as having significant strand slip were not included in the database. Table 29 gives the number of development length tests in the TFHRC Database by concrete mix type, failure mode, and specimen type.

**Table 29. Number of Development Length Tests by Concrete Type and Nominal Strand Size in the TFHRC Database.**

| Concrete Type | Failure Mode (inch) | Single-strand Rectangular | Multiple-strand Rectangular | Multiple-strand I-beam or T-beam | All Specimen Types |
|---|---|---|---|---|---|
| LWC | Flexure | 34 | 22 | 49 | 105 |
| | Flexure & slip | 0 | 4 | 11 | 15 |
| | Bond | 2 | 14 | 11 | 27 |
| `NWC | Flexure | 19 | 26 | 60 | 105 |
| | Flexure & slip | 5 | 5 | 34 | 44 |
| | Bond | 10 | 6 | 42 | 58 |

Table 30 gives a summary of the number of development length measurements for each concrete mixture type and specimen type in the TFHRC Database. Only data for sand-lightweight, specified density, and normal weight concrete were found in the literature.

**Table 30. Number of Development Length Tests by Concrete Type and Specimen Type in the TFHRC Database.**

| Concrete Type | Single-strand Rectangular | Multiple-strand Rectangular | Multiple-strand I-beam or T-beam | All Specimen Types |
|---|---|---|---|---|
| Sand-lightweight | 24 | 40 | 42 | 106 |
| Specified density | 12 | 0 | 29 | 41 |
| Summation LWC | 36 | 40 | 71 | 147 |
| NWC | 34 | 37 | 136 | 207 |
| LWC and NWC | 70 | 77 | 207 | 354 |

The number of development length tests on specimens with a given nominal strand size are given in Table 31. The numbers of specimens in the table are grouped by use of concrete mix type and specimen type.

**Table 31. Number of Development Length Tests by Concrete Type and Nominal Strand Size in the TFHRC Database.**

| Concrete Type | Nominal Strand Size | Single-strand Rectangular | Multiple-strand Rectangular | Multiple-strand I-beam or T-beam | All Specimen Types |
|---|---|---|---|---|---|
| LWC | 3/8 inch | 0 | 0 | 0 | 0 |
| | 1/2 inch | 24 | 6 | 42 | 72 |
| | 1/2 inch special | 9 | 0 | 6 | 15 |
| | 9/16 inch | 0 | 0 | 0 | 0 |
| | 0.6 inch | 3 | 34 | 23 | 60 |
| | 0.62 inch | 0 | 0 | 0 | 0 |
| NWC | 3/8 inch | 10 | 0 | 0 | 10 |
| | 1/2 inch | 12 | 16 | 58 | 86 |
| | 1/2 inch special | 0 | 0 | 7 | 7 |
| | 9/16 inch | 0 | 0 | 8 | 8 |
| | 0.6 inch | 0 | 21 | 63 | 84 |
| | 0.62 inch | 12 | 0 | 0 | 12 |

## DISTRIBUTION OF STATISTICAL PARAMETERS FOR SPECIMENS IN THE TFHRC DATABASE

A series of tables and figures were created to give statistical information for the parameters that influence transfer length and development length of prestressing strand for the specimens in the TFHRC Database. In addition to the parameters that are known to influence the bond of prestressing strand, other parameters are included in the tables and figures that describe the specimens. The statistical information is given by specimen type. The information for LWC and NWC specimens with transfer length measurements is given in Table 32 and Table 33, respectively. Table 34 and Table 35 give the information for LWC and NWC specimens with development length tests. Table 36 and Table 37 give calculated strand prestress parameters. Figure 62 through Figure 69 show the statistical information graphically.

The statistical information given in the tables includes concrete material properties, specimen geometry parameters, and strand prestress. The tables also include the measured transfer lengths ($\ell_t$) and tested strand embedment lengths ($\ell_e$) for the specimens. For each parameter in the tables, the number of specimens with values, mean value, and range of values (i.e., maximum and minimum values) are given. The concrete material properties include the compressive strength ($f'_c$) at time of development length test, compressive strength ($f'_{ci}$) and elastic modulus ($E_{ci}$) at

time of prestress transfer, and unit weight ($w_c$). The specimen geometry parameters include the height of the cross section excluding a CIP deck (h), the number of strand ("No. strand"), and the total area of all prestressing strand in the cross section ($A_{ps}$). The strand prestress includes the calculated prestress immediately after prestress transfer ($f_{pt}$), the effective prestress after long-term losses ($f_{pe}$), and the strand stress at nominal flexural capacity ($f_{ps}$).

In Table 32 through Table 35 the parameters $f_{pt}$, $f_{pe}$, and $f_{ps}$ were given only if adequate information was reported to determine the jacking stress and if the concrete elastic modulus at the time of prestress transfer ($E_{ci}$) was reported. For the strand prestress parameters in Table 36 and Table 37, the jacking stress was assumed to be 75 percent of the strand ultimate stress if the jacking stress was not reported. Also, if $E_{ci}$ was not reported, it was determined using the expression for $E_c$ in the 6$^{th}$ edition AASHTO LRFD Bridge Design Specifications.[1] The strand stess parameters are given for all LWC specimens and all NWC specimens in Table 36. In Table 37 the strand stress parameters are given by specimen type.

Figure 62 and Figure 63 show transfer length ($\ell_t$) compared to concrete compressive strength at time of prestress transfer ($f'_{ci}$) by specimen type for LWC specimens and NWC specimens, respectively. Transfer length is compared to concrete elastic modulus at time of prestress transfer ($E_{ci}$) for LWC and NWC in Figure 64 and Figure 65. Figure 66 through Figure 69 are in pairs of LWC and NWC specimens and show the tested embedment length ($\ell_e$) compared to concrete compressive strength ($f'_c$) and elastic modulus ($E_c$) at time of development length test.

**Table 32. Transfer Length Measurements on LWC Specimens in the TFHRC Database.**

| Specimen Type | Property | No.† | Mean | Max. | Min. |
|---|---|---|---|---|---|
| Single-strand Rectangular: LWC | $f'_c$ (ksi) | 24 | 7.66 | 8.23 | 7.20 |
| | $f'_{ci}$ (ksi) | 6 | 5.30 | 5.37 | 5.16 |
| | $E_{ci}$ (ksi) | 24 | 2830 | 3150 | 2610 |
| | $w_c$ (kcf) | 24 | 0.120 | 0.123 | 0.115 |
| | h (inch) | 24 | 6.50 | 6.50 | 6.50 |
| | No. strand | 24 | 1.00 | 1 | 1 |
| | $A_{ps}$ (inch$^2$) | 24 | 0.153 | 0.153 | 0.153 |
| | $f_{pt}$ (ksi) | 24 | 179 | 188 | 170 |
| | $f_{pe}$ (ksi) | 24 | 161 | 168 | 153 |
| | $f_{ps}$ (ksi) | 24 | 25 | 26 | 23 |
| | $\ell_t$ (inch) | 24 | 18.6 | 29.0 | 11.0 |
| | $\ell_e$ (inch) | 24 | 69.5 | 77.0 | 62.0 |
| Multiple-strand I-beam or T-beam: LWC | $f'_c$ (ksi) | 50 | 6.85 | 12.06 | 5.00 |
| | $f'_{ci}$ (ksi) | 50 | 5.09 | 8.95 | 3.40 |
| | $E_{ci}$ (ksi) | 50 | 3053 | 4740 | 2300 |
| | $w_c$ (kcf) | 50 | 0.120 | 0.138 | 0.115 |
| | h (inch) | 50 | 11.36 | 12.00 | 4.00 |
| | No. strand | 50 | 2.00 | 2 | 2 |
| | $A_{ps}$ (inch$^2$) | 50 | 0.397 | 0.434 | 0.306 |
| | $f_{pt}$ (ksi) | 50 | 182 | 183 | 179 |
| | $f_{pe}$ (ksi) | 50 | 159 | 165 | 150 |
| | $f_{ps}$ (ksi) | 50 | 63 | 72 | 48 |
| | $\ell_t$ (inch) | 50 | 22.6 | 42.9 | 14.2 |
| | $\ell_e$ (inch) | 40 | 43.2 | 60.0 | 25.0 |
| Multiple-strand I-beam or T-beam: LWC | $f'_c$ (ksi) | 65 | 9.15 | 11.90 | 6.68 |
| | $f'_{ci}$ (ksi) | 65 | 6.47 | 9.64 | 4.78 |
| | $E_{ci}$ (ksi) | 64 | 3245 | 4109 | 2489 |
| | $w_c$ (kcf) | 65 | 0.121 | 0.132 | 0.114 |
| | h (inch) | 65 | 39.26 | 64.00 | 17.00 |
| | No. strand | 65 | 11.29 | 28 | 3 |
| | $A_{ps}$ (inch$^2$) | 65 | 2.039 | 6.120 | 0.459 |
| | $f_{pt}$ (ksi) | 64 | 182 | 191 | 167 |
| | $f_{pe}$ (ksi) | 64 | 164 | 177 | 148 |
| | $f_{ps}$ (ksi) | 60 | 305 | 810 | 75 |
| | $\ell_t$ (inch) | 65 | 20.3 | 40.7 | 7.9 |
| | $\ell_e$ (inch) | 50 | 68.2 | 96.0 | 34.0 |

Notes:
† Number of measured values for each transfer length measurement
Units: 1.0 inch = 25.4 mm, 1.0 ksi = 6.89 MPa, 0.001 kcf = 16.01 kg/m$^3$

**Table 33. Transfer Length Measurements on NWC Specimens in the TFHRC Database.**

| Specimen Type | Property | No.† | Mean | Max. | Min. |
|---|---|---|---|---|---|
| Single-strand Rectangular: NWC | $f'_c$ (ksi) | 68 | 8.39 | 12.90 | 4.50 |
| | $f'_{ci}$ (ksi) | 68 | 6.03 | 9.50 | 3.00 |
| | $E_{ci}$ (ksi) | 0 | -- | -- | -- |
| | $w_c$ (kcf) | 0 | -- | -- | -- |
| | h (inch) | 89 | 6.29 | 9.84 | 4.00 |
| | No. strand | 89 | 1.00 | 1 | 1 |
| | $A_{ps}$ (inch$^2$) | 89 | 0.164 | 0.231 | 0.085 |
| | $f_{pt}$ (ksi) | 0 | -- | -- | -- |
| | $f_{pe}$ (ksi) | 0 | -- | -- | -- |
| | $f_{ps}$ (ksi) | 0 | -- | -- | -- |
| | $\ell_t$ (inch) | 89 | 24.9 | 56.0 | 11.0 |
| | $\ell_e$ (inch) | 0 | -- | -- | -- |
| Multiple-strand Rectangular: NWC | $f'_c$ (ksi) | 82 | 8.91 | 14.61 | 5.40 |
| | $f'_{ci}$ (ksi) | 82 | 5.88 | 9.71 | 3.85 |
| | $E_{ci}$ (ksi) | 16 | 4745 | 4780 | 4710 |
| | $w_c$ (kcf) | 16 | 0.147 | 0.148 | 0.145 |
| | h (inch) | 82 | 11.09 | 13.00 | 9.00 |
| | No. strand | 82 | 2.71 | 5 | 2 |
| | $A_{ps}$ (inch$^2$) | 82 | 0.531 | 1.085 | 0.306 |
| | $f_{pt}$ (ksi) | 16 | 188 | 188 | 188 |
| | $f_{pe}$ (ksi) | 16 | 168 | 171 | 163 |
| | $f_{ps}$ (ksi) | 16 | 239 | 242 | 232 |
| | $\ell_t$ (inch) | 82 | 28.7 | 58.0 | 11.3 |
| | $\ell_e$ (inch) | 37 | 56.0 | 88.0 | 34.0 |
| Multiple-strand I-beam or T-beam: NWC | $f'_c$ (ksi) | 143 | 8.41 | 16.78 | 5.11 |
| | $f'_{ci}$ (ksi) | 137 | 5.85 | 11.03 | 3.36 |
| | $E_{ci}$ (ksi) | 40 | 5415 | 7500 | 4570 |
| | $w_c$ (kcf) | 10 | 0.147 | 0.149 | 0.146 |
| | h (inch) | 145 | 28.58 | 47.50 | 17.00 |
| | No. strand | 145 | 7.97 | 30 | 3 |
| | $A_{ps}$ (inch$^2$) | 145 | 1.651 | 6.510 | 0.459 |
| | $f_{pt}$ (ksi) | 40 | 191 | 194 | 187 |
| | $f_{pe}$ (ksi) | 40 | 172 | 181 | 158 |
| | $f_{ps}$ (ksi) | 40 | 249 | 266 | 229 |
| | $\ell_t$ (inch) | 145 | 20.9 | 44.0 | 10.6 |
| | $\ell_e$ (inch) | 114 | 75.7 | 120.0 | 45.0 |

Notes:
† Number of measured values for each transfer length measurement
Units: 1.0 inch = 25.4 mm, 1.0 ksi = 6.89 MPa, 0.001 kcf = 16.01 kg/m$^3$

**Table 34. Development Length Tests on LWC Specimens in the TFHRC Database.**

| Specimen Type | Property | No.† | Mean | Max. | Min. |
|---|---|---|---|---|---|
| Single-strand Rectangular | $f'_c$ (ksi) | 36 | 8.26 | 12.06 | 7.20 |
| | $f'_{ci}$ (ksi) | 18 | 6.33 | 8.95 | 5.16 |
| | $E_{ci}$ (ksi) | 36 | 3242 | 4740 | 2610 |
| | $w_c$ (kcf) | 36 | 0.125 | 0.138 | 0.115 |
| | h (inch) | 36 | 8.33 | 12.00 | 6.50 |
| | No. strand | 36 | 1.00 | 1 | 1 |
| | $A_{ps}$ (inch$^2$) | 36 | 0.162 | 0.217 | 0.153 |
| | $f_{pt}$ (ksi) | 36 | 185 | 198 | 170 |
| | $f_{pe}$ (ksi) | 36 | 169 | 186 | 153 |
| | $f_{ps}$ (ksi) | 36 | 27 | 40 | 23 |
| | $\ell_t$ (inch) | 24 | 18.6 | 29.0 | 11.0 |
| | $\ell_e$ (inch) | 36 | 71.9 | 85.4 | 62.0 |
| Multiple-strand Rectangular | $f'_c$ (ksi) | 40 | 6.58 | 8.31 | 5.00 |
| | $f'_{ci}$ (ksi) | 40 | 5.03 | 6.93 | 3.40 |
| | $E_{ci}$ (ksi) | 40 | 3076 | 3395 | 2300 |
| | $w_c$ (kcf) | 40 | 0.119 | 0.124 | 0.115 |
| | h (inch) | 40 | 12.00 | 12.00 | 12.00 |
| | No. strand | 40 | 2.00 | 2 | 2 |
| | $A_{ps}$ (inch$^2$) | 40 | 0.415 | 0.434 | 0.306 |
| | $f_{pt}$ (ksi) | 40 | 182 | 183 | 179 |
| | $f_{pe}$ (ksi) | 40 | 160 | 165 | 154 |
| | $f_{ps}$ (ksi) | 40 | 66 | 72 | 48 |
| | $\ell_t$ (inch) | 40 | 22.5 | 42.9 | 14.2 |
| | $\ell_e$ (inch) | 40 | 43.2 | 60.0 | 25.0 |
| Multiple-strand I-beam or T-beam | $f'_c$ (ksi) | 71 | 9.14 | 11.40 | 6.68 |
| | $f'_{ci}$ (ksi) | 71 | 6.20 | 9.64 | 3.71 |
| | $E_{ci}$ (ksi) | 67 | 3361 | 4740 | 2489 |
| | $w_c$ (kcf) | 71 | 0.123 | 0.138 | 0.114 |
| | h (inch) | 71 | 35.51 | 47.50 | 17.00 |
| | No. strand | 71 | 9.00 | 20 | 3 |
| | $A_{ps}$ (inch$^2$) | 71 | 1.578 | 3.366 | 0.459 |
| | $f_{pt}$ (ksi) | 67 | 184 | 193 | 167 |
| | $f_{pe}$ (ksi) | 67 | 166 | 180 | 149 |
| | $f_{ps}$ (ksi) | 67 | 264 | 543 | 75 |
| | $\ell_t$ (inch) | 60 | 18.8 | 40.7 | 7.9 |
| | $\ell_e$ (inch) | 71 | 67.8 | 96.0 | 34.0 |

Notes:
† Number of measured values for each transfer length measurement
Units: 1.0 inch = 25.4 mm, 1.0 ksi = 6.89 MPa, 0.001 kcf = 16.01 kg/m$^3$

**Table 35. Development Length Tests on NWC Specimens in the TFHRC Database.**

| Specimen Type | Property | No.† | Mean | Max. | Min. |
|---|---|---|---|---|---|
| Single-strand | $f'_c$ (ksi) | 34 | 8.43 | 12.90 | 4.50 |
| Rectangular | $f'_{ci}$ (ksi) | 34 | 5.65 | 7.31 | 3.00 |
| | $E_{ci}$ (ksi) | 0 | -- | -- | -- |
| | $w_c$ (kcf) | 0 | -- | -- | -- |
| | h (inch) | 34 | 8.51 | 9.84 | 6.89 |
| | No. strand | 34 | 1.00 | 1 | 1 |
| | $A_{ps}$ (inch$^2$) | 34 | 0.161 | 0.231 | 0.085 |
| | $f_{pt}$ (ksi) | 0 | -- | -- | -- |
| | $f_{pe}$ (ksi) | 0 | -- | -- | -- |
| | $f_{ps}$ (ksi) | 0 | -- | -- | -- |
| | $\ell_t$ (inch) | 34 | 20.0 | 31.6 | 11.9 |
| | $\ell_e$ (inch) | 34 | 40.9 | 73.4 | 22.6 |
| Multiple-strand | $f'_c$ (ksi) | 37 | 9.87 | 14.61 | 6.71 |
| Rectangular | $f'_{ci}$ (ksi) | 37 | 6.54 | 9.71 | 4.03 |
| | $E_{ci}$ (ksi) | 16 | 4745 | 4780 | 4710 |
| | $w_c$ (kcf) | 16 | 0.147 | 0.148 | 0.145 |
| | h (inch) | 37 | 12.00 | 12.00 | 12.00 |
| | No. strand | 37 | 2.00 | 2 | 2 |
| | $A_{ps}$ (inch$^2$) | 37 | 0.379 | 0.434 | 0.306 |
| | $f_{pt}$ (ksi) | 16 | 188 | 188 | 188 |
| | $f_{pe}$ (ksi) | 16 | 168 | 171 | 163 |
| | $f_{ps}$ (ksi) | 16 | 239 | 242 | 232 |
| | $\ell_t$ (inch) | 37 | 21.4 | 39.0 | 11.3 |
| | $\ell_e$ (inch) | 37 | 56.0 | 88.0 | 34.0 |
| Multiple-strand | $f'_c$ (ksi) | 136 | 8.44 | 16.78 | 5.11 |
| I-beam or T-beam | $f'_{ci}$ (ksi) | 128 | 5.77 | 11.03 | 3.36 |
| | $E_{ci}$ (ksi) | 39 | 5424 | 7500 | 4570 |
| | $w_c$ (kcf) | 11 | 0.147 | 0.149 | 0.145 |
| | h (inch) | 136 | 27.94 | 47.50 | 17.00 |
| | No. strand | 136 | 7.00 | 20 | 3 |
| | $A_{ps}$ (inch$^2$) | 136 | 1.427 | 4.340 | 0.459 |
| | $f_{pt}$ (ksi) | 39 | 191 | 194 | 187 |
| | $f_{pe}$ (ksi) | 39 | 172 | 181 | 158 |
| | $f_{ps}$ (ksi) | 39 | 249 | 266 | 229 |
| | $\ell_t$ (inch) | 129 | 21.3 | 42.0 | 10.6 |
| | $\ell_e$ (inch) | 136 | 77.6 | 167.5 | 45.0 |

Notes:
† Number of measured values for each transfer length measurement
Units: 1.0 inch = 25.4 mm, 1.0 ksi = 6.89 MPa, 0.001 kcf = 16.01 kg/m$^3$

**Table 36. Calculated Strand Stress for Development Length Tests for all LWC and NWC Specimens in the TFHRC Database.**

| Specimen Type | Property | No.† | Mean | Max. | Min. |
|---|---|---|---|---|---|
| All LWC | $f_{pbt}$ (ksi) | 111 | 200.1 | 203.0 | 179.1 |
| | $f_{pt}$ (ksi) | 111 | 183.6 | 192.6 | 166.7 |
| | $f_{pe}$ (ksi) | 111 | 164.1 | 179.7 | 148.5 |
| | $f_{ps}$ (ksi) | 111 | 251.2 | 274.2 | 223.7 |
| | $f_{ps}$ - $f_{pe}$ (ksi) | 111 | 87.0 | 116.1 | 67.9 |
| All NWC | $f_{pbt}$ (ksi) | 207 | 198.4 | 225.0 | 134.0 |
| | $f_{pt}$ (ksi) | 199 | 187.3 | 210.8 | 125.9 |
| | $f_{pe}$ (ksi) | 199 | 167.7 | 192.4 | 110.8 |
| | $f_{ps}$ (ksi) | 207 | 252.4 | 294.9 | 220.5 |
| | $f_{ps}$ - $f_{pe}$ (ksi) | 207 | 91.2 | 267.9 | 60.0 |

Notes:
† Number of measured values for each transfer length measurement
Units: 1.0 inch = 25.4 mm, 1.0 ksi = 6.89 MPa, 0.001 kcf = 16.01 kg/m$^3$

**Table 37. Calculated Strand Stress for Development Length Tests by Specimen Type in the TFHRC Database.**

| Specimen Type | Property | No.† | Mean | Max. | Min. |
|---|---|---|---|---|---|
| Single-strand rect.: | $f_{pbt}$ (ksi) | 36 | 194.7 | 202.5 | 181.8 |
| LWC | $f_{pt}$ (ksi) | 36 | 185.1 | 197.7 | 170.5 |
| | $f_{pe}$ (ksi) | 36 | 168.9 | 186.3 | 153.2 |
| | $f_{ps}$ (ksi) | 36 | 254.6 | 264.1 | 249.3 |
| | $f_{ps}$ - $f_{pe}$ (ksi) | 36 | 85.7 | 96.9 | 77.4 |
| Multi-strand rect.: | $f_{pbt}$ (ksi) | 40 | 202.5 | 202.5 | 202.5 |
| LWC | $f_{pt}$ (ksi) | 40 | 181.8 | 182.9 | 179.4 |
| | $f_{pe}$ (ksi) | 40 | 160.0 | 165.1 | 153.9 |
| | $f_{ps}$ (ksi) | 40 | 234.2 | 255.1 | 223.7 |
| | $f_{ps}$ - $f_{pe}$ (ksi) | 40 | 74.2 | 95.0 | 67.9 |
| Multi-strand | $f_{pbt}$ (ksi) | 71 | 198.7 | 203.0 | 179.1 |
| I-beam or T-beam: | $f_{pt}$ (ksi) | 71 | 184.6 | 192.6 | 166.7 |
| LWC | $f_{pe}$ (ksi) | 71 | 166.5 | 179.7 | 148.5 |
| | $f_{ps}$ (ksi) | 71 | 260.8 | 274.2 | 236.2 |
| | $f_{ps}$ - $f_{pe}$ (ksi) | 71 | 94.3 | 116.1 | 75.7 |
| Single-strand rect.: | $f_{pbt}$ (ksi) | 34 | 185.4 | 209.0 | 134.0 |
| NWC | $f_{pt}$ (ksi) | 34 | 177.8 | 199.8 | 125.9 |
| | $f_{pe}$ (ksi) | 34 | 160.3 | 176.8 | 110.8 |
| | $f_{ps}$ (ksi) | 34 | 251.1 | 265.0 | 238.6 |
| | $f_{ps}$ - $f_{pe}$ (ksi) | 34 | 90.8 | 131.7 | 79.0 |
| Multi-strand rect.: | $f_{pbt}$ (ksi) | 37 | 202.5 | 202.5 | 202.5 |
| NWC | $f_{pt}$ (ksi) | 37 | 189.6 | 193.1 | 185.3 |
| | $f_{pe}$ (ksi) | 37 | 171.5 | 181.4 | 159.8 |
| | $f_{ps}$ (ksi) | 37 | 248.2 | 259.8 | 232.2 |
| | $f_{ps}$ - $f_{pe}$ (ksi) | 37 | 76.6 | 86.1 | 65.4 |
| Multi-strand | $f_{pbt}$ (ksi) | 136 | 200.5 | 225.0 | 180.9 |
| I-beam or T-beam: | $f_{pt}$ (ksi) | 128 | 189.2 | 210.8 | 169.3 |
| NWC | $f_{pe}$ (ksi) | 128 | 168.6 | 192.4 | 151.1 |
| | $f_{ps}$ (ksi) | 136 | 254.0 | 294.9 | 220.5 |
| | $f_{ps}$ - $f_{pe}$ (ksi) | 136 | 95.2 | 267.9 | 60.0 |

Notes:
† Number of measured values for each transfer length measurement
Units: 1.0 inch = 25.4 mm, 1.0 ksi = 6.89 MPa, 0.001 kcf = 16.01 kg/m$^3$

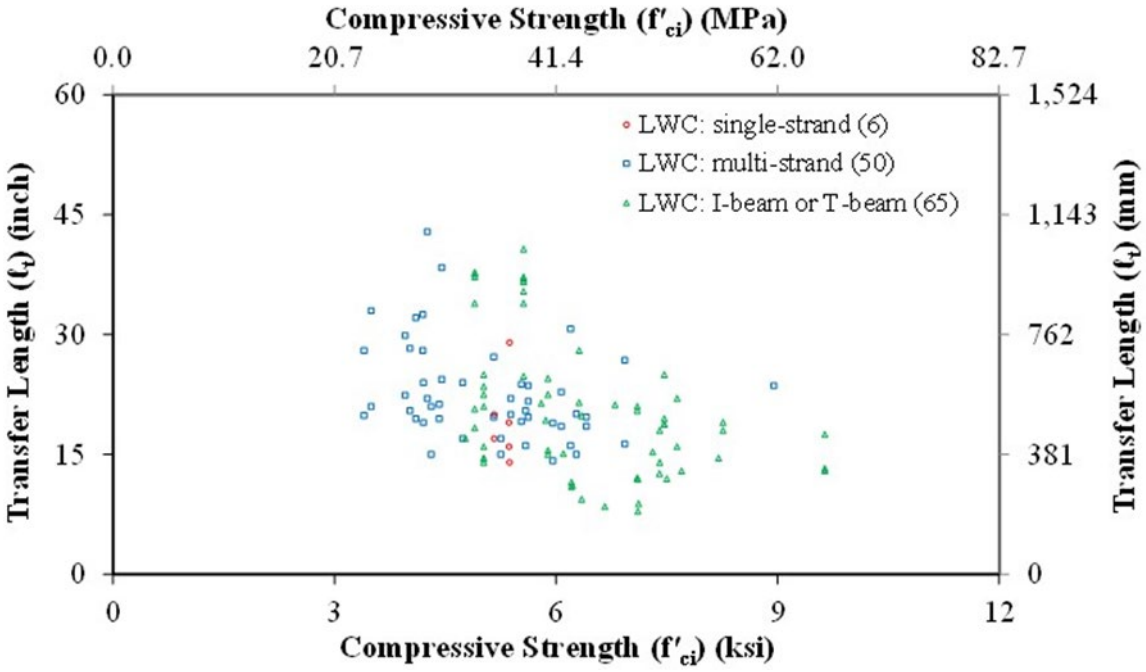


**Figure 62. Graph. Transfer Length Compared to Compressive Strength at Prestress Transfer by Specimen Type for LWC Specimens in the TFHRC Database.**

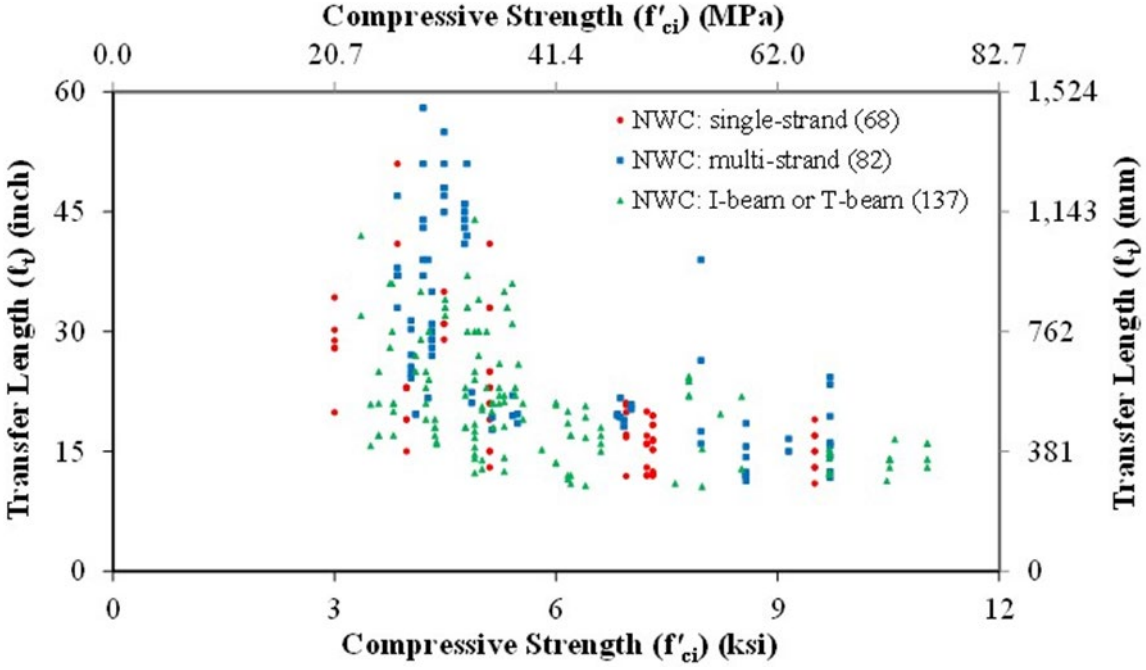


**Figure 63. Graph. Transfer Length Compared to Compressive Strength at Prestress Transfer by Specimen Type for NWC Specimens in the TFHRC Database.**

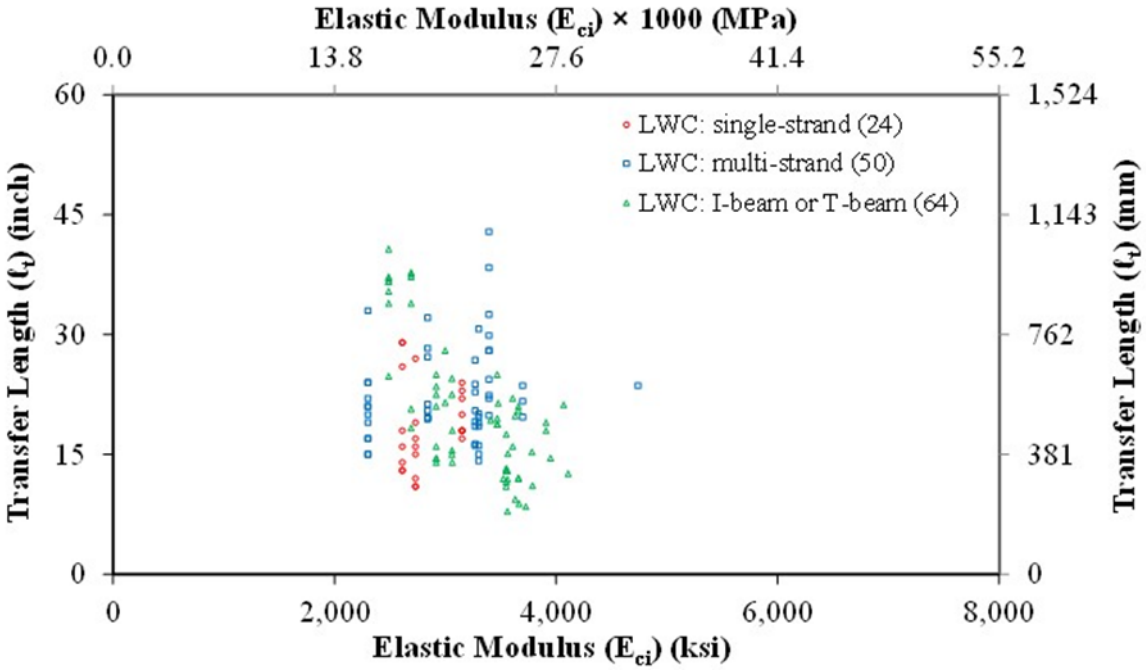


**Figure 64. Graph. Transfer Length Compared to Elastic Modulus at Prestress Transfer by Specimen Type for LWC Specimens in the TFHRC Database.**

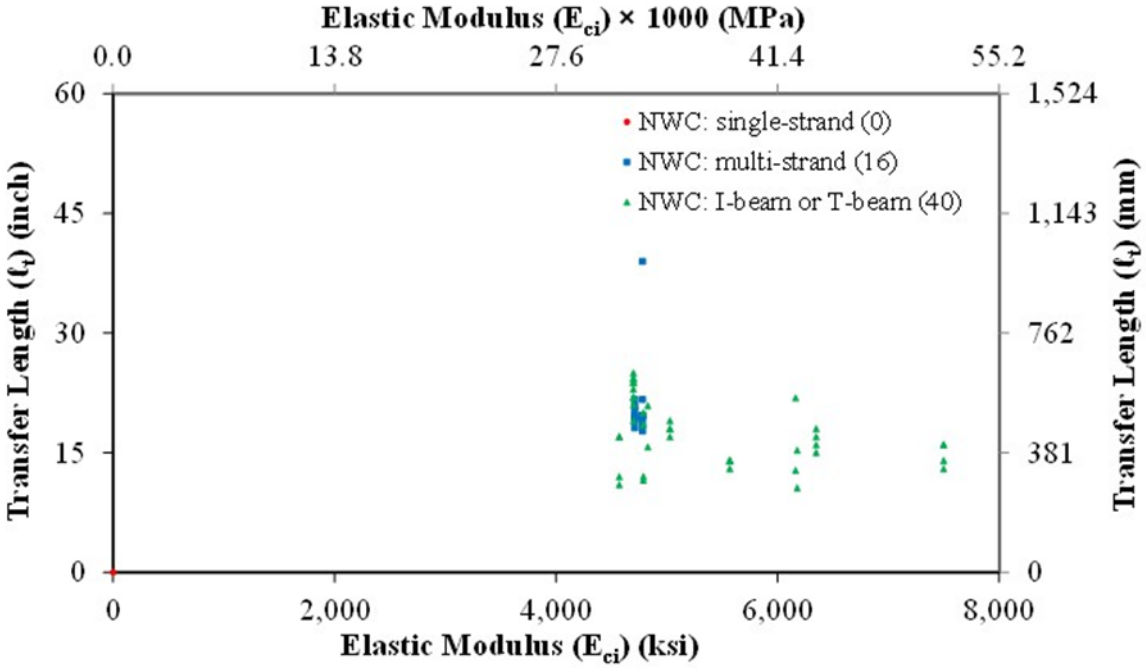


**Figure 65. Graph. Transfer Length Compared to Elastic Modulus at Prestress Transfer by Specimen Type for NWC Specimens in the TFHRC Database.**

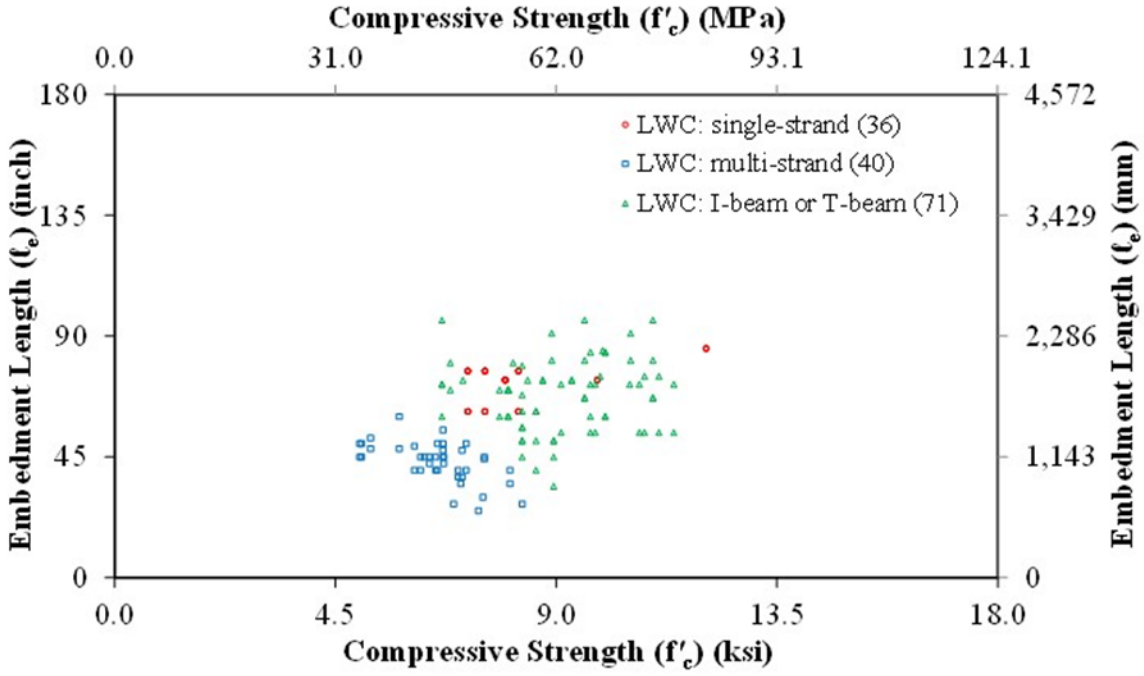


**Figure 66. Graph. Embedment Length Compared to Compressive Strength by Specimen Type for LWC Specimens in the TFHRC Database.**

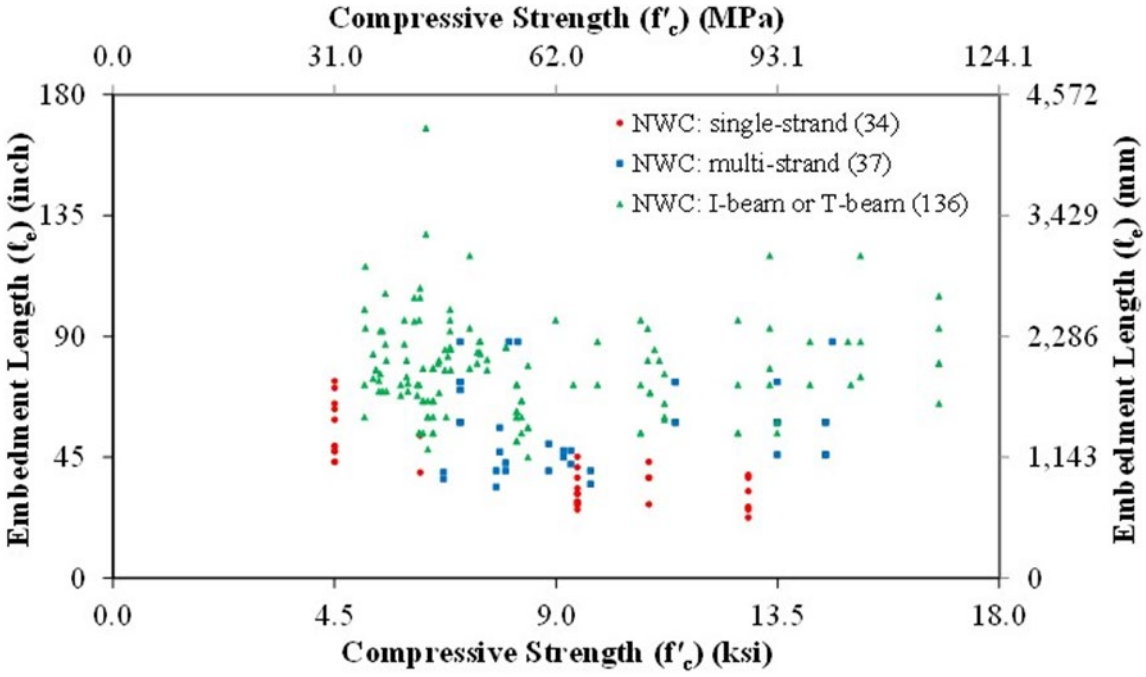


**Figure 67. Graph. Embedment Length Compared to Compressive Strength by Specimen Type for NWC Specimens in the TFHRC Database.**

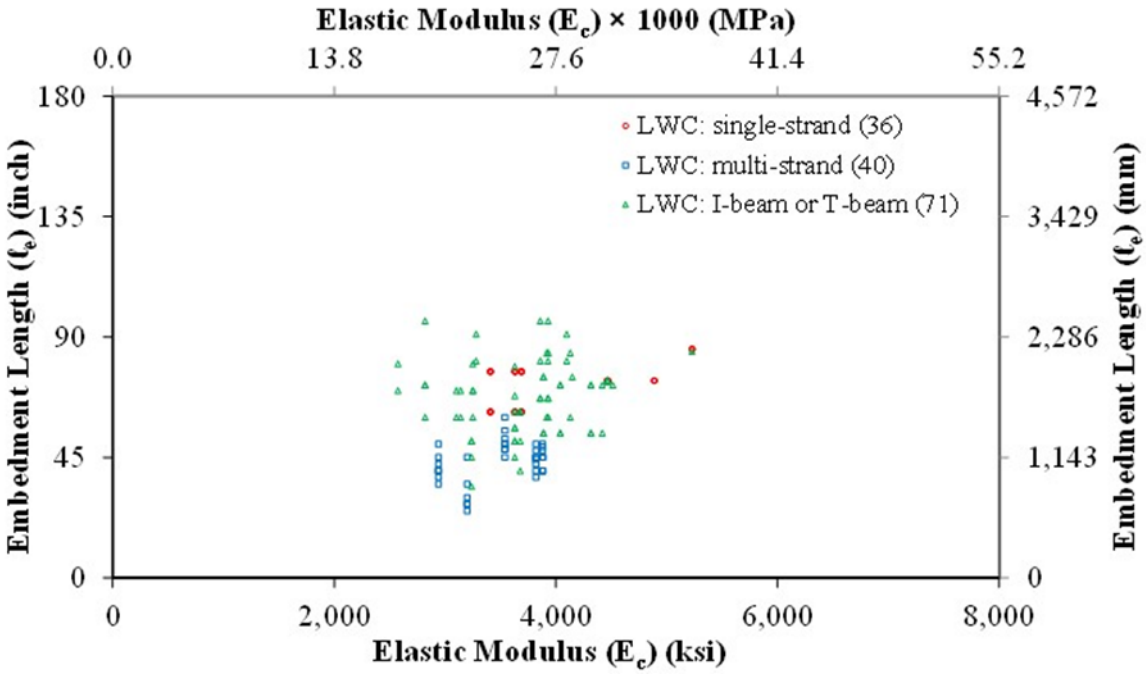


**Figure 68. Graph. Embedment Length Compared to Elastic Modulus by Specimen Type for LWC Specimens in the TFHRC Database.**

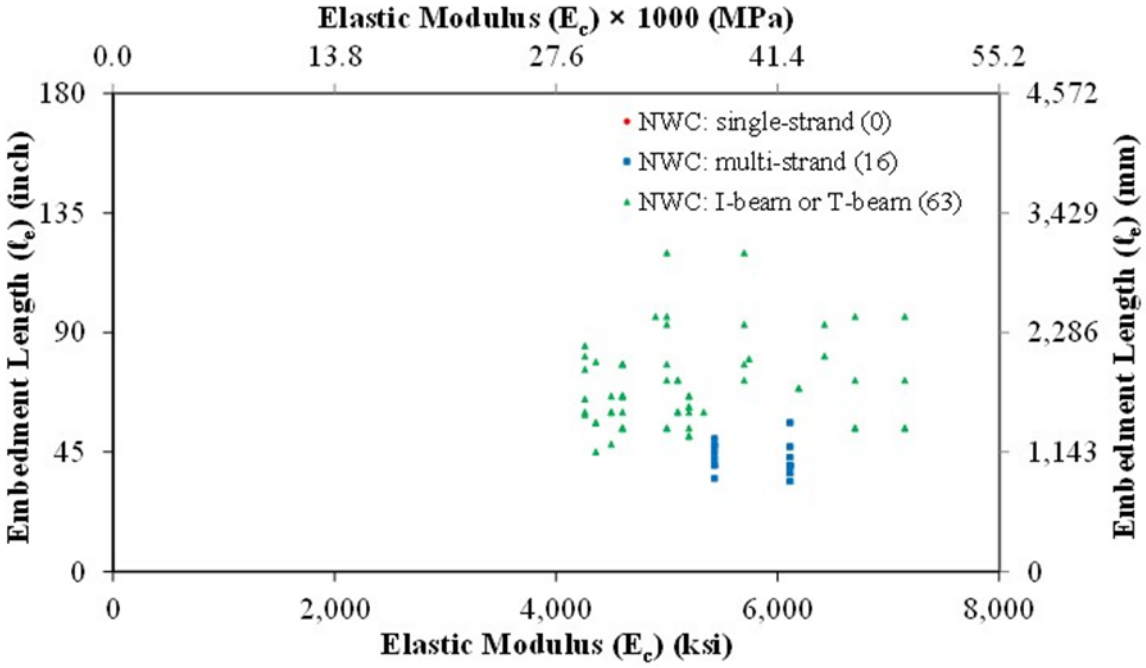


**Figure 69. Graph. Embedment Length Compared to Elastic Modulus by Specimen Type for LWC Specimens in the TFHRC Database.**

# CHAPTER 5. ANALYSIS OF THE BOND OF PRESTRESSING STRANDS FOR SPECIMENS IN THE TFHRC DATABASE

## INTRODUCTION

This chapter provides an analysis of the measured transfer lengths and tested embedment lengths for LWC specimens and NWC specimens in the TFHRC Database. In the first section, measured transfer lengths are analyzed. This analysis includes a graphical evaluation of normalized transfer lengths, a statistical analysis of the parameters used to predict transfer length, and comparisons with prediction expressions. The second section includes a graphical evaluation of flexural bond lengths. An analysis of development length is included in the third section. This analysis includes comparisons of embedment length test results with prediction expressions. The last section summarizes analyses included in the chapter and outlines the rational of the proposed changes to the AASHTO LRFD Bridge Design Specifications.

The quality of the prediction is given by its test-to-prediction ratio and the coefficient of variation (COV) describing the distribution of the ratios. A test-to-prediction ratio that is greater than unity indicates that the expression has under-estimated the measured value, while a ratio that is less than unity indicates an over-estimated value. The COV indicates the amount of scatter in the test-to-prediction ratio and a small COV is preferred.

The term "potential expression" in this document refers to a prediction expression that is being evaluated. The term "proposed expression" in the document refers to a prediction expression that is being proposed to AASHTO Subcommittee on Bridges and Structures (SCOBS) T-10 for consideration as a design expression in the AASHTO LRFD Bridge Design Specifications. Proposed expressions will also be included in the chapter of this document titled "Preliminary Recommendations for AASHTO LRFD Specifications."

## GRAPHICAL ANALYSIS OF NORMALIZED TRANSFER LENGTH

This section includes a comparison of the normalized transfer lengths for LWC and NWC specimens in the TFHRC Database. The purpose of the comparison is to examine the effect of different parameters on transfer length. Previous research has considered the following parameters to affect the transfer length of prestressing strand: concrete compressive strength ($f'_{ci}$) and elastic modulus ($E_{ci}$) at time of prestress transfer, strand prestress immediately after prestress transfer ($f_{pt}$), and nominal strand diameter ($d_b$).[14,16,20-22,24] A modification factor for LWC ($\lambda$-factor) based on unit weight has been recently adopted for use in the AASHTO LRFD Bridge Design Specifications. The expression for the $\lambda$-factor is given by Eq. 16. The analysis of transfer length in this section includes the $\lambda$-factor as a parameter.

The use the $\lambda$-factor to predict transfer length is reasonable based on its direct relationship to unit weight and reasonable correlation with splitting tensile strength.[8] The concrete tensile strength

has been correlated to compressive strength.[4,8] The concrete elastic modulus has been correlated to the concrete unit weight and compressive strength.[8,44,45] Previous research has indicated that transfer length is dependent upon the concrete elastic modulus in the region near the end of the strand and upon the tensile stress of concrete in the inelastic region beyond the elastic region. Research by Buckner[20] proposed using an apparent concrete elastic modulus ($E_c$) as a parameter to predict transfer length for NWC and research by Thatcher et al.[24] proposed using $E_{ci}$ as a parameter to predict the transfer length for LWC. The λ-factor alone or $\lambda\sqrt{f'_{ci}}$ are investigated here to describe the dependence of concrete tensile strength and concrete elastic modulus on transfer length.

The effect of the parameters on transfer length is analyzed in the figures and tables of this chapter. In order for a specimen to be included in a table or figure, the associated parameter had to be reported in the literature. All values that include $f'_{ci}$ or $E_{ci}$ had a reported concrete strength and/or elastic modulus at time of prestress transfer. All values that include $f_{pt}$ had a reported strand jacking stress, strand jacking force, or jacking stress as a percent of nominal strand tensile strength. All values that include the λ-factor had a reported concrete unit weight.

The parameters are evaluated by pairs of figures that compare normalized transfer length to concrete compressive strength at prestress transfer ($f'_{ci}$). In the first figure of each pair, transfer length is normalized by $d_b$. In the second figure of each, transfer length is normalized by $f_{pt}d_b$. The first pair of figures uses only the $d_b$ and $f_{pt}d_b$ parameters to normalized transfer length. The second pair of figures also includes $\sqrt{f'_{ci}}$ as an additional parameter. The effect of the parameter $E_{ci}$ is included in the third pair of figures. The fourth and fifth pair include λ and $\lambda\sqrt{f'_{ci}}$ as parameters.

In Figure 70, transfer length is normalized by nominal strand diameter ($d_b$). This method of normalizing transfer length is in the form of the expression for transfer length given by the AASHTO Standard Specifications for Highway Bridges (Eq. 1) and the AASHTO LRFD Bridge Design Specification (Eq. 2). Horizontal lines at values of 50 and 60 represent the prediction given by Standard Specifications for Highway Bridges (AASHTO STD) and AASHTO LRFD Bridge Design Specification (AASHTO LRFD) expressions. Nearly all of the data with a compressive strength greater than 6 ksi (41 MPa) are less than the horizontal line at a value of 50 indicating an overestimation of the transfer length by both expressions. For data with a compressive strength less than 6 ksi (41 MPa), 19 percent of the data from LWC specimens and 28 percent of the data from NWC specimens is greater than the horizontal line at a value of 60. This indicates that both expressions underestimated the transfer length for these data points.

The transfer length is normalized by $d_b f_{pt}$ in Figure 71. A horizontal line at a value of 1/3 approximates the prediction given by the Hanson and Kaar expression (Eq. 3) that is the basis for the expression in the ACI 318 Building Code.[28] The difference between the Hanson and Kaar expression and the value shown is that the effective prestress in the strand after all losses ($f_{pe}$) has been replaced with the prestress in the strand immediately after transfer ($f_{pt}$). The result is that

transfer length is being divided by a slightly larger number which will lower the value of the horizontal line. Still most of the data are below the horizontal prediction line indicating an overestimation of the transfer length. Note that there are fewer data points shown in Figure 71 than in Figure 70 because information about strand jacking stress was not reported for some of the specimens.

The transfer lengths in Figure 72 are normalized by $d_b/\sqrt{f'_{ci}}$. The prediction of transfer length given by Meyer et al. (Eq. 8) is shown as a horizontal line at $50\sqrt{6}$. Nearly all of the data with a compressive strength greater than 6 ksi (41 MPa) are less than the line at $50\sqrt{6}$ and 20 percent of the LWC data and 30 percent of the NWC data below 6 ksi (41 MPa) are above the line. The data below the horizontal line at a value of $50\sqrt{6}$ indicate an overestimation of the transfer length and the data above the line indicate an underestimation.

Figure 73 shows the transfer lengths normalized by $f_{pt}d_b/\sqrt{f'_{ci}}$. Predictions of transfer length by Mitchell et al. (Eq. 4) and Barnes et al. (Eq. 10) are indicated by horizontal lines at values of $0.3\sqrt{33}$ and 0.17, respectively. Some of the data are above the prediction given by Mitchell et al. indicating that the transfer length is overestimated for these data points. The expression proposed by Barnes et al. was intended to be a lower bound prediction of transfer length. All of the data are above the prediction by Barnes et al. indicating the intended underestimation of transfer length.

The overall trend of the data in Figure 70 and Figure 71 is that normalized transfer length decreases slightly as compressive strength increases. The parameter $\sqrt{f'_{ci}}$ is included with the parameters used to normalize transfer length in Figure 72 and Figure 73 and the downward trend of transfer length with increasing compressive strength is no longer apparent.

Figure 74 shows transfer length normalized by $d_b/E_{ci}$. The expressions by Buckner (Eq. 6) and Thatcher et al. (Eq. 7) included a term for stress in the prestressing strands. The horizontal lines shown in the figures included an assumed 150 ksi (1030 MPa) for strand stress. Nearly all of the data for LWC specimens are below the line at $1250\times150/1000$ representing the Buckner expression. Nearly all of the limited data for NWC specimens with a reported $E_{ci}$ are also below the line representing the Buckner expression.

The normalization of transfer length by $f_{pt}d_b/E_{ci}$ is shown in Figure 75. This figure gives a more direct evaluation of the Buckner and Thatcher et al. expressions. Horizontal lines at 1250/1000 and 900/1000 give the predictions by the Buckner and Thatcher et al. expressions, respectively. All but one NWC data point and all but one LWC data point are below the Buckner prediction.

Figure 76 through Figure 79 include the λ-factor as a parameter for normalization. Figure 76 and Figure 77 are comparable to Figure 70 and Figure 71. Similarly, Figure 78 and Figure 79 are comparable to Figure 72 and Figure 73. Inclusion of the λ-factor in Figure 76 caused the number of LWC data with a compressive strength less than 6 ksi (41 MPa) that are above the prediction given by the expression in the AASHTO LRFD Bridge Design Specifications to only be reduced

from 19 percent to 18 percent. The AASHTO LRFD Bridge Design Specifications prediction is given by the horizontal line at a value of 60. The inclusion of the λ-factor with $\sqrt{f'_{ci}}$ in Figure 79 caused the number of LWC data with a compressive strength less than 6 ksi (41 MPa) that are above the prediction given by the Mitchell et al. expression (i.e., the line at $0.33\sqrt{3}$) to be reduced from 55 percent to 41 percent.

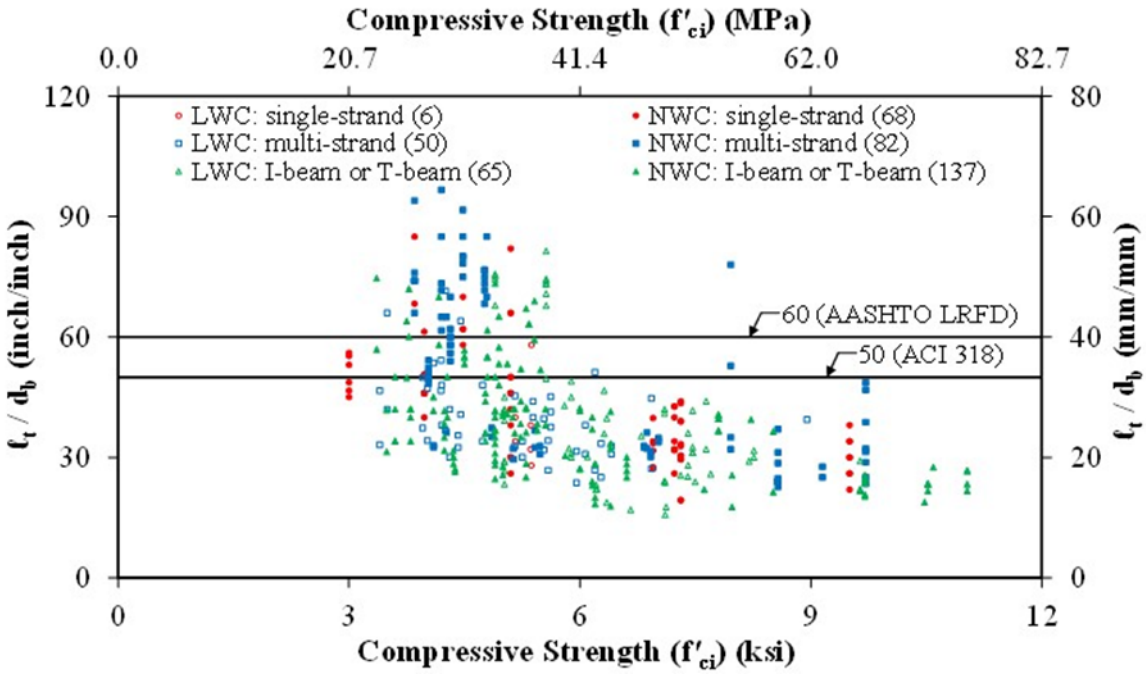


**Figure 70. Graph. Normalized Transfer Length ($\ell_t/d_b$) Compared to Compressive Strength ($f'_{ci}$) by Specimen Type in the TFHRC Database.**

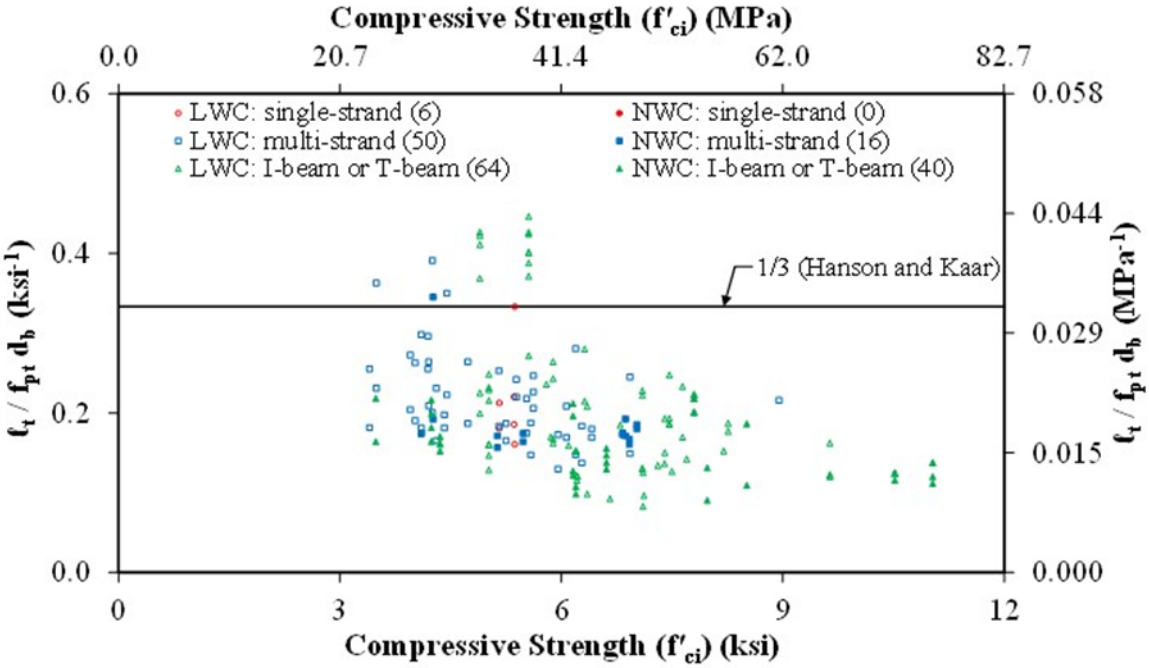


**Figure 71. Graph. Normalized Transfer Length ($\ell_t/f_{pt}d_b$) Compared to Compressive Strength ($f'_{ci}$) by Specimen Type in the TFHRC Database.**

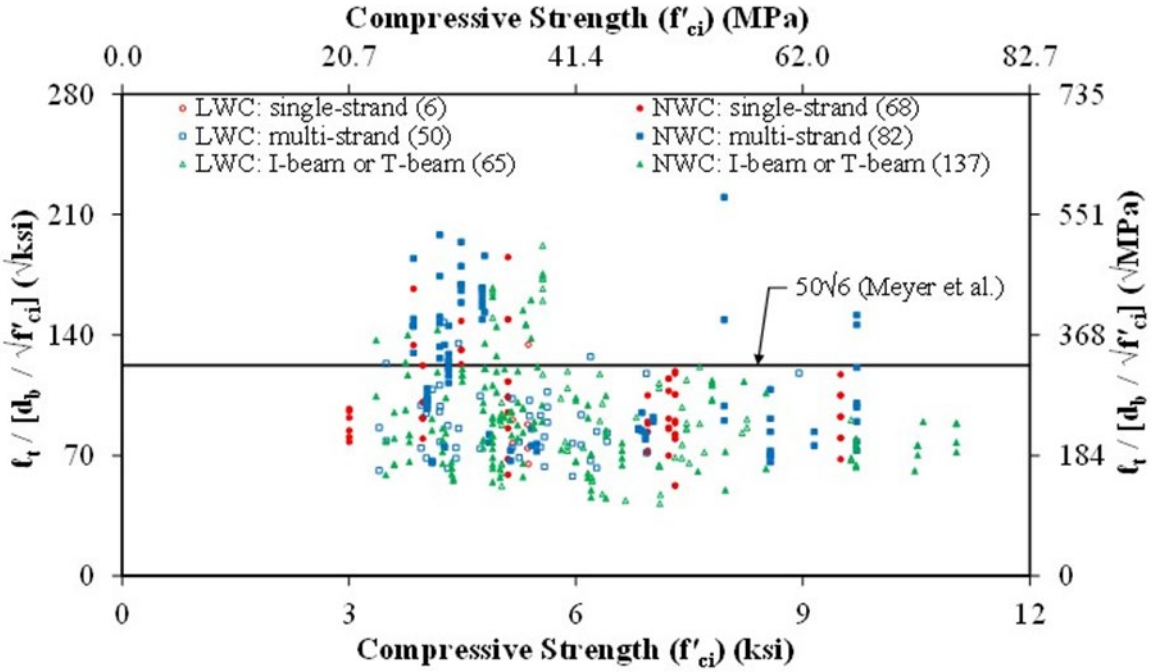


**Figure 72. Graph. Normalized Transfer Length ($\ell_t/[d_b/\sqrt{f'_{ci}}]$) Compared to Compressive Strength ($f'_{ci}$) by Specimen Type in the TFHRC Database.**

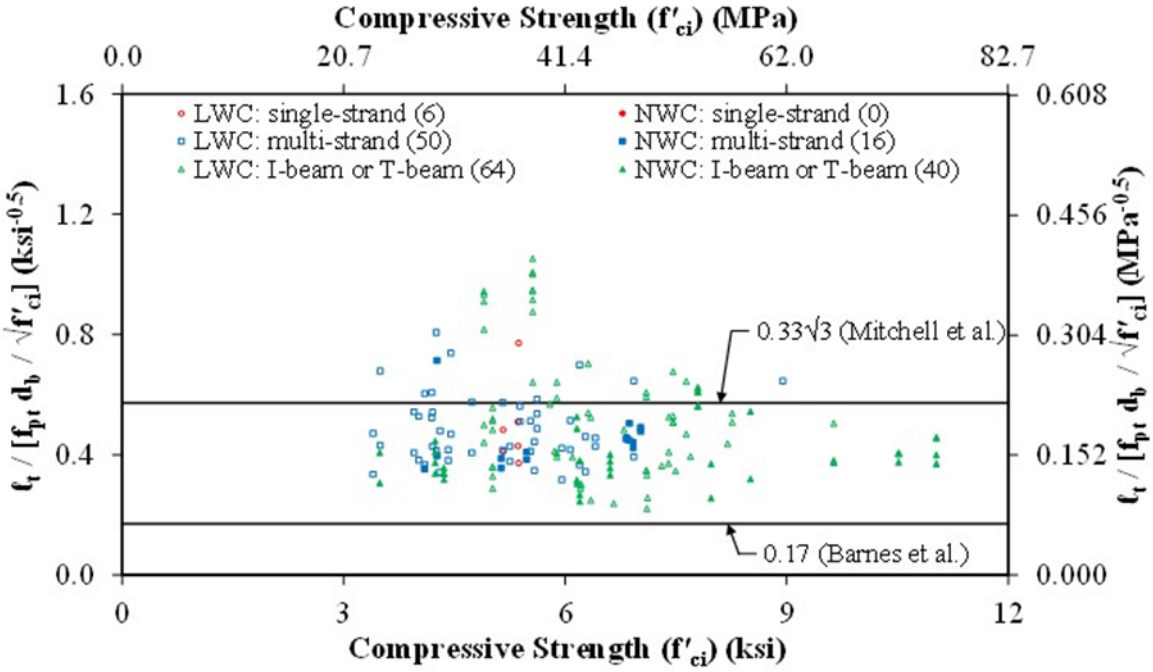


**Figure 73. Graph. Normalized Transfer Length ($\ell_t/[f_{pt}d_b/\sqrt{f'_{ci}}]$) Compared to Compressive Strength ($f'_{ci}$) by Specimen Type in the TFHRC Database.**

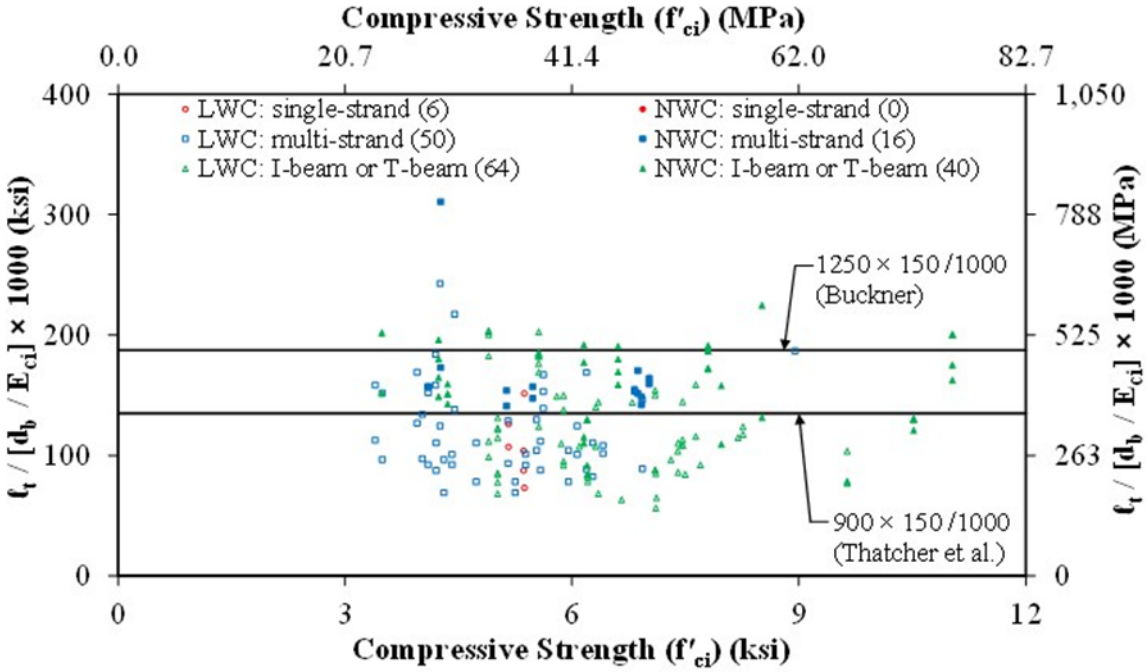


**Figure 74. Graph. Normalized Transfer Length ($\ell_t/[d_b/E_{ci}]$) Compared to Compressive Strength ($f'_{ci}$) by Specimen Type in the TFHRC Database.**

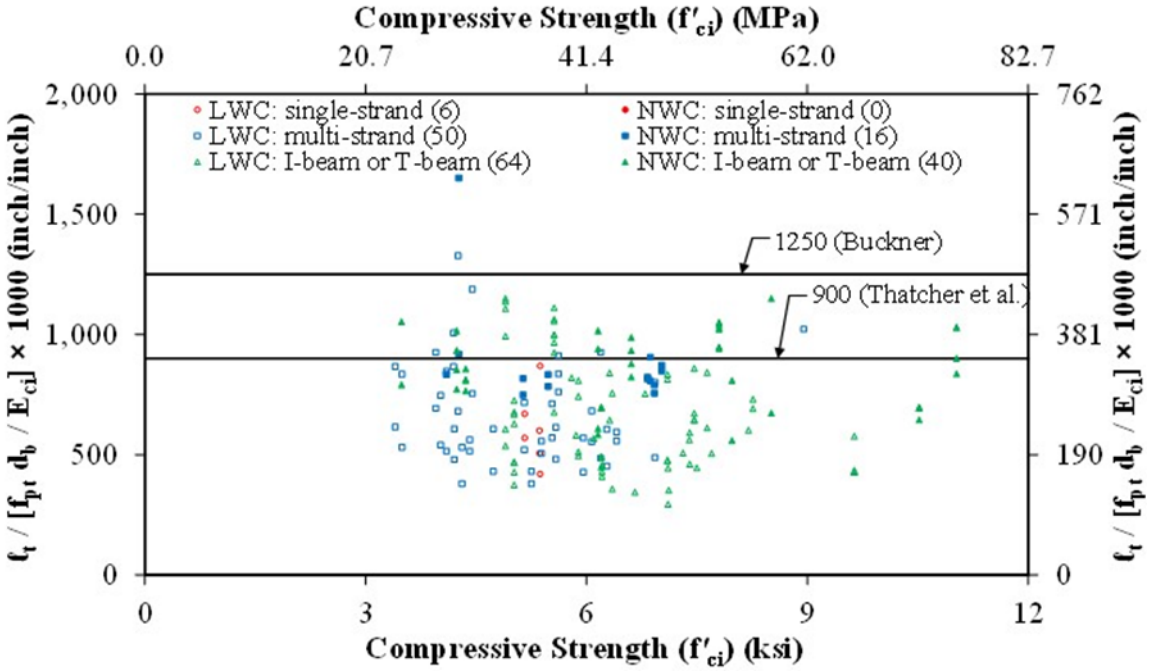


**Figure 75. Graph. Normalized Transfer Length ($\ell_t/[f_{pt}d_b/E_{ci}]$) Compared to Compressive Strength ($f'_{ci}$) by Specimen Type in the TFHRC Database.**

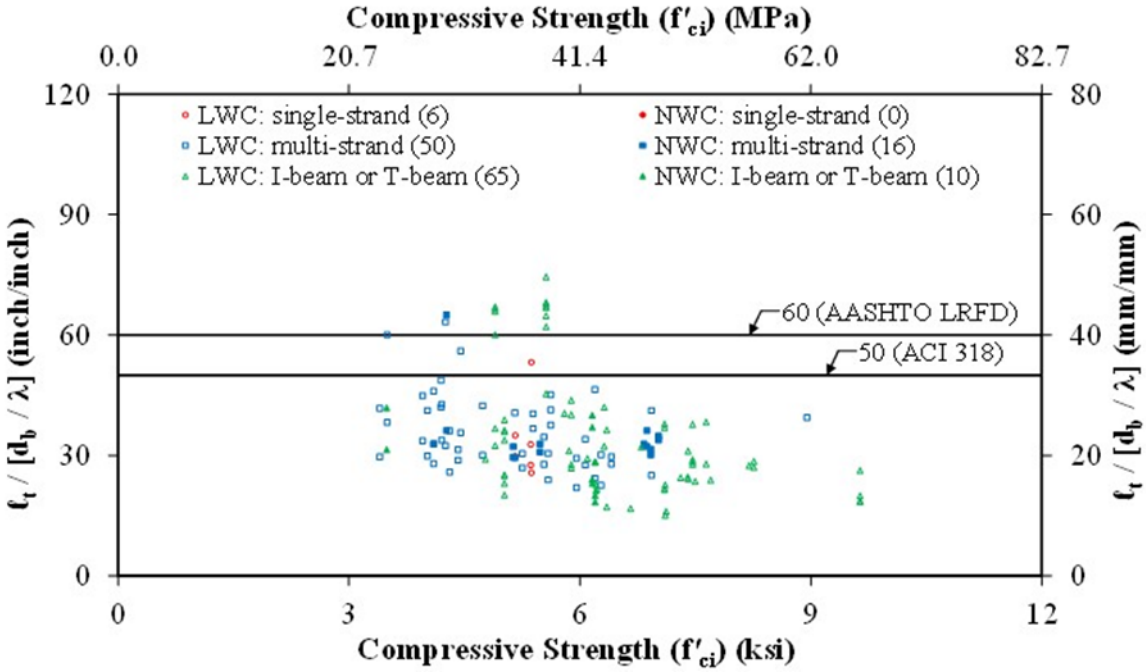


**Figure 76. Graph. Normalized Transfer Length ($\ell_t/[d_b/\lambda]$) Compared to Compressive Strength ($f'_{ci}$) by Specimen Type in the TFHRC Database.**

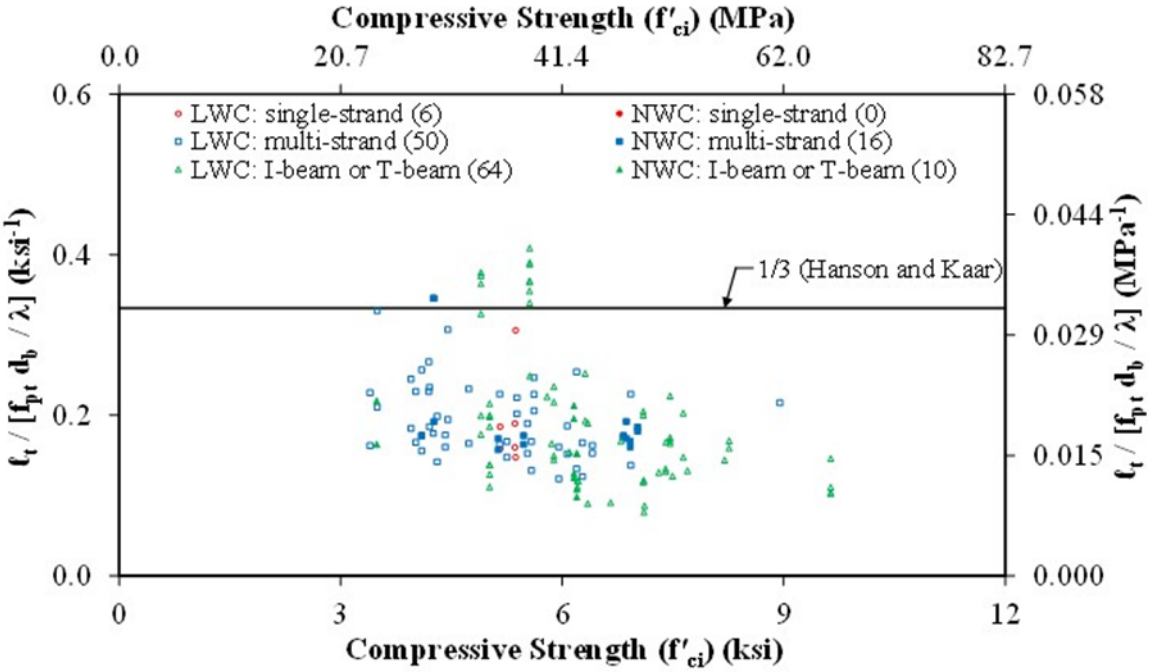


**Figure 77. Graph. Normalized Transfer Length ($\ell_t/[f_{pt}d_b/\lambda]$) Compared to Compressive Strength ($f'_{ci}$) by Specimen Type in the TFHRC Database.**

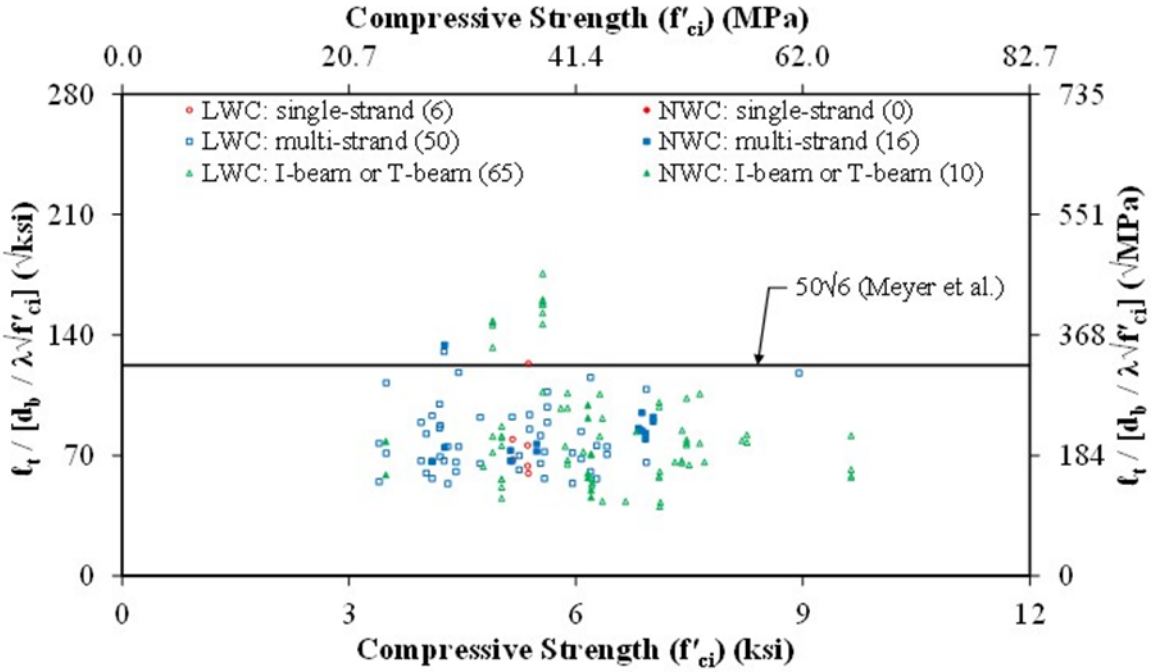


**Figure 78. Graph. Normalized Transfer Length ($\ell_t/[f_{pt}d_b/\lambda\sqrt{f'_{ci}}]$) Compared to Compressive Strength ($f'_{ci}$) by Specimen Type in the TFHRC Database.**

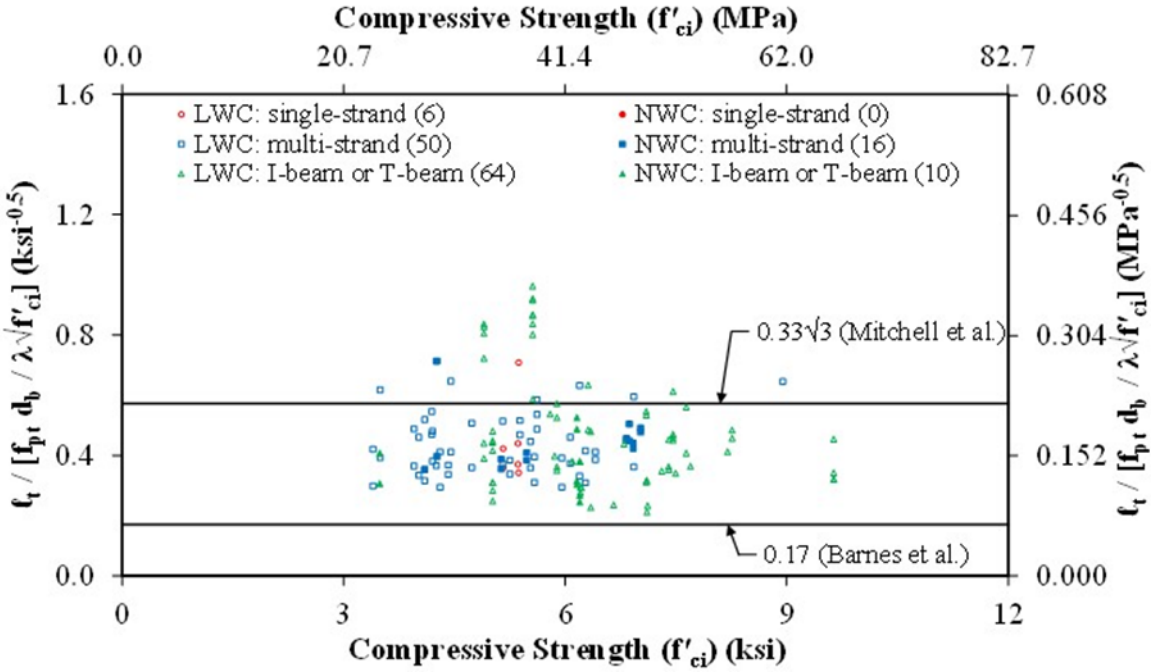


**Figure 79. Graph. Normalized Transfer Length ($\ell_t/[f_{pt}d_b/\lambda\sqrt{f'_{ci}}]$) Compared to Compressive Strength ($f'_{ci}$) by Specimen Type in the TFHRC Database.**

## ANALYSIS OF PARAMETERS USED TO NORMALIZE TRANSFER LENGTH

This section includes an evaluation of the parameters used to predict transfer length. The purpose of this evaluation is to determine which parameters and groups of parameters are the most useful in predicting transfer length. The individual parameters evaluated include concrete compressive strength ($f'_{ci}$) and elastic modulus ($E_{ci}$) at time of prestress transfer, strand prestress immediately after prestress transfer ($f_{pt}$), nominal strand diameter ($d_b$), and the λ-factor.

The measured transfer length ($\ell_t$) was assumed proportional to the normalizing parameters. For the general equation of a line given by Eq. 23, m is the slope, x represents the normalizing parameters and y represents the measured transfer length. The vertical axis intercept (b) is taken as zero. The resulting expression for a line is then given by Eq. 24 which can then be solved for the slope (m) as given in Eq. 25. This slope is determined for each measured transfer length. Based on this formulation, Figure 70 through Figure 79 are actually showing the slope on the vertical axis.

$$y = mx + b \quad \text{(Eq. 23)}$$

$$\ell_t = (m)(\text{Normalizing Parameters}) + 0 \quad \text{(Eq. 24)}$$

$$m = \frac{\ell_t}{\text{Normalizing Parameters}} \quad \text{(Eq. 25)}$$

The coefficient of determination ($R^2$) is a measure of the quality of a prediction expression. A value of 1.0 for $R^2$ would indicate that 100 percent of the variability in the data is accounted for in the prediction equation. A value of zero would indicate that using the mean of the data would equally account for the variability as the prediction equation. A negative value indicates that the prediction equation is less able to account for the variability than using the mean of the data. A larger value of $R^2$ indicates an improved prediction. A general expression for $R^2$ is given by Eq. 26.[46] In Eq. 26, $y_i$ is an individual value on the vertical axis, $\bar{y}$ is the mean of all of the $y_i$ values, and the predicted vertical-axis value corresponding to $y_i$ is $\hat{y}_i$.

$$R^2 = \frac{\sum(y_i - \bar{y})^2 - \sum(y_i - \hat{y}_i)^2}{\sum(y_i - \bar{y})^2} \quad \text{(Eq. 26)}$$

For this analysis, the expression used for $R^2$ is given by Eq. 27. The mean of the measured transfer lengths and the predicted transfer length are $\bar{\ell}_t$ and $\hat{\ell}_t$, respectively.

$$R^2 = \frac{\sum(\ell_t - \bar{\ell}_t)^2 - \sum(\ell_t - \hat{\ell}_t)^2}{\sum(\ell_t - \bar{\ell}_t)^2} \quad \text{(Eq. 27)}$$

The expression for the predicted transfer length is given by Eq. 28. The mean of the normalized transfer lengths shown in Figure 70 through Figure 79 is $\bar{m}$ (i.e., the mean slope). The mean

slope ($\bar{m}$) was determined for all of the slopes in a group of data normalized by the same parameters.

$$\hat{\ell}_t = (\bar{m})(\text{Normalizing Parameters}) \quad \text{(Eq. 28)}$$

The observed level of significance or p-value is the probability that the number of measured transfer lengths used to determine $R^2$ are as at least as extreme as transfer lengths that would be measured in a much larger set of data. The p-value can be used to determine whether the data set actually reflects the characteristics of the population (i.e., an infinitely large set of transfer length data).

The transfer length measurements have been separated by concrete mix type and specimen type resulting in a small number of samples for some groups of data. The Student t-distribution was used to account for the small amount of data in some groups. The significance test for $R^2$ used with the Student t-distribution is given by Eq. 29.[47] The p-value is then the two-tailed probability of having that Student t-value. The Student t distribution uses n – 1 degrees of freedom to determine the p-value, where n is the number of data values. A smaller p-value indicates stronger evidence that the data set reflects the population characteristics. A p-value less than the defined level of 0.01 indicates that the data set and $R^2$ value can be accepted.

$$t = \frac{\sqrt{R^2}}{\sqrt{\frac{1 - R^2}{n - 2}}} \quad \text{(Eq. 29)}$$

The results of the parameter analysis are given in Table 38 through Table 41. The following information is given for each combination of parameters: the mean slope ($\bar{m}$), the number of specimens with values for all of the parameters (No.), the coefficient of determination ($R^2$), the p-value, and the level of significance indicated by the p-value (Sig.). The $R^2$, p-value, and level of significance are not given for some combinations of parameters. These combinations have some specimens with missing parameter values. Smaller subsets of specimens were considered in order to analyze all of the parameter combinations. The p-value and level of significance was not given if the $R^2$ value was negative.

Table 38 gives the analysis for all of the LWC and NWC specimens together. For all the specimens, the $d_b/\sqrt{f'_{ci}}$ and $d_b/\lambda\sqrt{f'_{ci}}$ parameter combinations had that largest $R^2$ values at 0.293 and 0.247, respectively. The $R^2$ value for $d_b$ alone was only 0.039.

Adequate information was not reported in order for $f_{pt}$ to be determined for all specimens. An analysis for a subset of the LWC and NWC specimens with $f_{pt}$ values is given in Table 38. The largest $R^2$ values were 0.190 and 0.155 from the $d_b/\lambda\sqrt{f'_{ci}}$ and $d_b/\sqrt{f'_{ci}}$ parameter combinations. For the two parameter combinations with $\sqrt{f'_{ci}}$, the addition of $f_{pt}$ caused a decrease in the $R^2$ value. For the parameter group with $E_{ci}$, the addition of $f_{pt}$ caused an increase in the $R^2$ value.

Many of the NWC did not have a reported unit weight ($w_c$). In order to analyze LWC and NWC specimens with a reported $w_c$, a subset of specimens with both $w_c$ and $f_{pt}$ is given in Table 38. As a result, this subset is mostly LWC specimen. The parameter combinations with $E_{ci}$ and $\lambda\sqrt{f'_{ci}}$ had the largest values of $R^2$. For each parameter combination, the addition of $f_{pt}$ caused a decrease in the $R^2$ value, although for the combination with $E_{ci}$, the decrease due to $f_{pt}$ was much smaller.

Table 39 gives the analysis of the LWC specimens separated by specimen type. For the multi-strand rectangular specimens, the largest $R^2$ values were from the $d_b/\sqrt{f'_{ci}}$ and $d_b/\lambda\sqrt{f'_{ci}}$ parameter combinations. The $E_{ci}$ combinations for rectangular specimens had negative $R^2$ values. The largest $R^2$ values for the multi-strand I-beam or T-beam specimens were from the $E_{ci}$ parameter combinations. The combinations with $\sqrt{f'_{ci}}$ and $\lambda\sqrt{f'_{ci}}$ were considerably smaller.

The analysis of NWC specimens is given in Table 40 by specimen type. None of the specimens analyzed in this table had $f_{pt}$ values. A subset of NWC specimens with $f_{pt}$ values is given in Table 41. In Table 40, the parameter combination with $\sqrt{f'_{ci}}$ had the largest $R^2$ value regardless of specimen type. The $R^2$ values for single-strand and multi-strand rectangular specimens using the $\sqrt{f'_{ci}}$ parameter combination were 0.459 and 0.404, respectively.

Table 41 gives the analysis of a subset of NWC specimens with $f_{pt}$ values. This subset has multi-strand I-beam or T-beam specimens. The only parameter combination in this subset with a level of significance less than 0.01 contained $E_{ci}$. The $R^2$ value for the parameter combination containing $E_{ci}$ and $f_{pt}$ was slightly smaller than the combination without $f_{pt}$. Data subsets with only single-strand or multi-strand rectangular specimens were not given because these subsets did not contain enough specimens to have an adequate level of significance.

**Table 38. Parameter Analysis for Transfer Length Measurements on all LWC and NWC Specimens in the TFHRC Database.**

| Specimen Type | Parameter | Units | $\bar{m}^{\dagger}$ | No. | $R^2$ | p-value | Sig. |
|---|---|---|---|---|---|---|---|
| All LWC and NWC Tests | $d_b$ | (inch/inch) | 41.9 | 408 | 0.039 | 0.0001 | Yes |
| | $f_{pt}\, d_b$ | (inch/ksi) | 0.200 | 176 | -- | -- | -- |
| | $d_b / \sqrt{f'_{ci}}$ | (inch√ksi) | 97.3 | 408 | 0.293 | 0.0000 | Yes |
| | $f_{pt}\, d_b / \sqrt{f'_{ci}}$ | (inch/√ksi) | 0.480 | 176 | -- | -- | -- |
| | $d_b / E_{ci}$ | (inch×ksi) | 132,570 | 176 | -- | -- | -- |
| | $f_{pt}\, d_b / E_{ci}$ | (inch/inch) | 719 | 176 | -- | -- | -- |
| | $d_b / \lambda$ | (inch/inch) | 40.8 | 408 | -0.002 | -- | -- |
| | $f_{pt}\, d_b / \lambda$ | (inch/ksi) | 0.185 | 176 | -- | -- | -- |
| | $d_b / \lambda\sqrt{f'_{ci}}$ | (inch√ksi) | 94.7 | 408 | 0.247 | 0.0000 | Yes |
| | $f_{pt}\, d_b / \lambda\sqrt{f'_{ci}}$ | (inch/√ksi) | 0.446 | 176 | -- | -- | -- |
| LWC and NWC Tests: $f_{pt}$ subset | $d_b$ | (inch/inch) | 36.6 | 176 | -0.021 | -- | -- |
| | $f_{pt}\, d_b$ | (inch/ksi) | 0.200 | 176 | -0.087 | -- | -- |
| | $d_b / \sqrt{f'_{ci}}$ | (inch√ksi) | 88.0 | 176 | 0.155 | 0.0000 | Yes |
| | $f_{pt}\, d_b / \sqrt{f'_{ci}}$ | (inch/√ksi) | 0.480 | 176 | 0.098 | 0.0000 | Yes |
| | $d_b / E_{ci}$ | (inch×ksi) | 132,570 | 176 | 0.119 | 0.0000 | Yes |
| | $f_{pt}\, d_b / E_{ci}$ | (inch/inch) | 719 | 176 | 0.138 | 0.0000 | Yes |
| | $d_b / \lambda$ | (inch/inch) | 34.0 | 176 | 0.049 | 0.0032 | Yes |
| | $f_{pt}\, d_b / \lambda$ | (inch/ksi) | 0.185 | 176 | 0.004 | 0.4102 | No |
| | $d_b / \lambda\sqrt{f'_{ci}}$ | (inch√ksi) | 81.8 | 176 | 0.190 | 0.0000 | Yes |
| | $f_{pt}\, d_b / \lambda\sqrt{f'_{ci}}$ | (inch/√ksi) | 0.446 | 176 | 0.153 | 0.0000 | Yes |
| LWC and NWC Tests: $w_c$ and $f_{pt}$ subset[‡] | $d_b$ | (inch/inch) | 38.0 | 146 | 0.017 | 0.1220 | No |
| | $f_{pt}\, d_b$ | (inch/ksi) | 0.208 | 146 | -0.023 | -- | -- |
| | $d_b / \sqrt{f'_{ci}}$ | (inch√ksi) | 89.6 | 146 | 0.164 | 0.0000 | Yes |
| | $f_{pt}\, d_b / \sqrt{f'_{ci}}$ | (inch/√ksi) | 0.491 | 146 | 0.122 | 0.0000 | Yes |
| | $d_b / E_{ci}$ | (inch×ksi) | 125,840 | 146 | 0.167 | 0.0000 | Yes |
| | $f_{pt}\, d_b / E_{ci}$ | (inch/inch) | 688 | 146 | 0.167 | 0.0000 | Yes |
| | $d_b / \lambda$ | (inch/inch) | 34.8 | 146 | 0.053 | 0.0050 | Yes |
| | $f_{pt}\, d_b / \lambda$ | (inch/ksi) | 0.191 | 146 | 0.028 | 0.0452 | No |
| | $d_b / \lambda\sqrt{f'_{ci}}$ | (inch√ksi) | 82.2 | 146 | 0.185 | 0.0000 | Yes |
| | $f_{pt}\, d_b / \lambda\sqrt{f'_{ci}}$ | (inch/√ksi) | 0.450 | 146 | 0.156 | 0.0000 | Yes |

Notes:
[†] Mean of the normalized transfer lengths for the parameter combination
[‡] Includes 16 NWC multi-strand rectangular specimens and 10 multi-strand I-beam or T-beam specimens
Units: 1.0 inch = 25.4 mm, 1.0 ksi = 6.89 MPa

**Table 39. Parameter Analysis for Transfer Length Measurements on LWC Specimens in the TFHRC Database.**

| Specimen Type† | Parameter | Units | $\bar{m}$† | No. | $R^2$ | p-value | Sig. |
|---|---|---|---|---|---|---|---|
| Multi-strand rect.: LWC | $d_b$ | (inch/inch) | 39.6 | 50 | 0.027 | 0.2499 | No |
| | $f_{pt}\, d_b$ | (inch/ksi) | 0.218 | 50 | 0.031 | 0.2180 | No |
| | $d_b / \sqrt{f'_{ci}}$ | (inch√ksi) | 87.9 | 50 | 0.195 | 0.0013 | Yes |
| | $f_{pt}\, d_b / \sqrt{f'_{ci}}$ | (inch/√ksi) | 0.483 | 50 | 0.203 | 0.0010 | Yes |
| | $d_b / E_{ci}$ | (inch×ksi) | 120,890 | 50 | -0.340 | -- | -- |
| | $f_{pt}\, d_b / E_{ci}$ | (inch/inch) | 664 | 50 | -0.324 | -- | -- |
| | $d_b / \lambda$ | (inch/inch) | 35.7 | 50 | 0.029 | 0.2343 | No |
| | $f_{pt}\, d_b / \lambda$ | (inch/ksi) | 0.196 | 50 | 0.036 | 0.1884 | No |
| | $d_b / \lambda\sqrt{f'_{ci}}$ | (inch√ksi) | 79.4 | 50 | 0.152 | 0.0051 | Yes |
| | $f_{pt}\, d_b / \lambda\sqrt{f'_{ci}}$ | (inch/√ksi) | 0.436 | 50 | 0.163 | 0.0037 | Yes |
| Multiple-strand I-beam or T-beam: LWC | $d_b$ | (inch/inch) | 38.8 | 64 | -0.085 | -- | -- |
| | $f_{pt}\, d_b$ | (inch/ksi) | 0.214 | 64 | -0.129 | -- | -- |
| | $d_b / \sqrt{f'_{ci}}$ | (inch√ksi) | 96.1 | 64 | 0.115 | 0.0061 | Yes |
| | $f_{pt}\, d_b / \sqrt{f'_{ci}}$ | (inch/√ksi) | 0.530 | 64 | 0.067 | 0.0384 | No |
| | $d_b / E_{ci}$ | (inch×ksi) | 119,655 | 64 | 0.350 | 0.0000 | Yes |
| | $f_{pt}\, d_b / E_{ci}$ | (inch/inch) | 659 | 64 | 0.316 | 0.0000 | Yes |
| | $d_b / \lambda$ | (inch/inch) | 35.0 | 64 | -0.067 | -- | -- |
| | $f_{pt}\, d_b / \lambda$ | (inch/ksi) | 0.193 | 64 | -0.105 | -- | -- |
| | $d_b / \lambda\sqrt{f'_{ci}}$ | (inch√ksi) | 86.8 | 64 | 0.125 | 0.0042 | Yes |
| | $f_{pt}\, d_b / \lambda\sqrt{f'_{ci}}$ | (inch/√ksi) | 0.479 | 64 | 0.083 | 0.0212 | No |

Units: 1.0 inch = 25.4 mm, 1.0 ksi = 6.89 MPa, 0.001 kcf = 16.01 kg/m$^3$

**Table 40. Parameter Analysis for Transfer Length Measurements on NWC Specimens in the TFHRC Database.**

| Specimen Type† | Parameter | Units | $\bar{m}$† | No. | $R^2$ | p-value | Sig. |
|---|---|---|---|---|---|---|---|
| Single-strand rect.: NWC | $d_b$ | (inch/inch) | 42.1 | 68 | 0.118 | 0.0041 | Yes |
| | $f_{pt}\ d_b$ | (inch/ksi) | -- | 0 | -- | -- | -- |
| | $d_b / \sqrt{f'_{ci}}$ | (inch√ksi) | 98.3 | 68 | 0.459 | 0.0000 | Yes |
| | $f_{pt}\ d_b / \sqrt{f'_{ci}}$ | (inch/√ksi) | -- | 0 | -- | -- | -- |
| | $d_b / E_{ci}$ | (inch×ksi) | -- | 0 | -- | -- | -- |
| | $f_{pt}\ d_b / E_{ci}$ | (inch/inch) | -- | 0 | -- | -- | -- |
| | $d_b / \lambda$ | (inch/inch) | 42.1 | 68 | 0.118 | 0.0041 | Yes |
| | $f_{pt}\ d_b / \lambda$ | (inch/ksi) | -- | 0 | -- | -- | -- |
| | $d_b / \lambda\sqrt{f'_{ci}}$ | (inch√ksi) | 98.3 | 68 | 0.459 | 0.0000 | Yes |
| | $f_{pt}\ d_b / \lambda\sqrt{f'_{ci}}$ | (inch/√ksi) | -- | 0 | -- | -- | -- |
| Multi-strand rect.: NWC | $d_b$ | (inch/inch) | 51.5 | 82 | 0.098 | 0.0041 | Yes |
| | $f_{pt}\ d_b$ | (inch/ksi) | 0.185 | 16 | -- | -- | -- |
| | $d_b / \sqrt{f'_{ci}}$ | (inch√ksi) | 117.4 | 82 | 0.404 | 0.0000 | Yes |
| | $f_{pt}\ d_b / \sqrt{f'_{ci}}$ | (inch/√ksi) | 0.440 | 16 | -- | -- | -- |
| | $d_b / E_{ci}$ | (inch×ksi) | 165,000 | 16 | -- | -- | -- |
| | $f_{pt}\ d_b / E_{ci}$ | (inch/inch) | 877 | 16 | -- | -- | -- |
| | $d_b / \lambda$ | (inch/inch) | 51.5 | 82 | 0.098 | 0.0041 | Yes |
| | $f_{pt}\ d_b / \lambda$ | (inch/ksi) | 0.185 | 16 | -- | -- | -- |
| | $d_b / \lambda\sqrt{f'_{ci}}$ | (inch√ksi) | 117.4 | 82 | 0.404 | 0.0000 | Yes |
| | $f_{pt}\ d_b / \lambda\sqrt{f'_{ci}}$ | (inch/√ksi) | 0.440 | 16 | -- | -- | -- |
| Multiple-strand I-beam or T-beam: LWC | $d_b$ | (inch/inch) | 38.6 | 137 | -0.044 | -- | -- |
| | $f_{pt}\ d_b$ | (inch/ksi) | 0.157 | 40 | -- | -- | -- |
| | $d_b / \sqrt{f'_{ci}}$ | (inch√ksi) | 89.4 | 137 | 0.272 | 0.0000 | Yes |
| | $f_{pt}\ d_b / \sqrt{f'_{ci}}$ | (inch/√ksi) | 0.405 | 40 | -- | -- | -- |
| | $d_b / E_{ci}$ | (inch×ksi) | 158,531 | 40 | -- | -- | -- |
| | $f_{pt}\ d_b / E_{ci}$ | (inch/inch) | 831 | 40 | -- | -- | -- |
| | $d_b / \lambda$ | (inch/inch) | 38.6 | 137 | -0.044 | -- | -- |
| | $f_{pt}\ d_b / \lambda$ | (inch/ksi) | 0.157 | 40 | -- | -- | -- |
| | $d_b / \lambda\sqrt{f'_{ci}}$ | (inch√ksi) | 89.4 | 137 | 0.272 | 0.0000 | Yes |
| | $f_{pt}\ d_b / \lambda\sqrt{f'_{ci}}$ | (inch/√ksi) | 0.405 | 40 | -- | -- | -- |

Units: 1.0 inch = 25.4 mm, 1.0 ksi = 6.89 MPa, 0.001 kcf = 16.01 kg/m$^3$

**Table 41. Parameter Analysis for Transfer Length Measurements on NWC Specimens in the $f_{pt}$ Data Subset in the TFHRC Database.**

| Specimen Type | Parameter | Units | $\bar{m}$ | No. | $R^2$ | p-value | Sig. |
|---|---|---|---|---|---|---|---|
| Multiple-strand I-beam or T-beam: NWC $f_{pt}$ subset | $d_b$ | (inch/inch) | 29.8 | 40 | -0.016 | -- | -- |
| | $f_{pt}\ d_b$ | (inch/ksi) | 0.157 | 40 | -0.069 | -- | -- |
| | $d_b / \sqrt{f'_{ci}}$ | (inch$\sqrt{}$ksi) | 77.1 | 40 | 0.009 | 0.5584 | No |
| | $f_{pt}\ d_b / \sqrt{f'_{ci}}$ | (inch/$\sqrt{}$ksi) | 0.405 | 40 | -0.034 | -- | -- |
| | $d_b / E_{ci}$ | (inch×ksi) | 158,531 | 40 | 0.195 | 0.0044 | Yes |
| | $f_{pt}\ d_b / E_{ci}$ | (inch/inch) | 831 | 40 | 0.180 | 0.0064 | Yes |
| | $d_b / \lambda$ | (inch/inch) | 29.8 | 40 | -0.016 | -- | -- |
| | $f_{pt}\ d_b / \lambda$ | (inch/ksi) | 0.157 | 40 | -0.069 | -- | -- |
| | $d_b / \lambda\sqrt{f'_{ci}}$ | (inch$\sqrt{}$ksi) | 77.1 | 40 | 0.009 | 0.5584 | No |
| | $f_{pt}\ d_b / \lambda\sqrt{f'_{ci}}$ | (inch/$\sqrt{}$ksi) | 0.405 | 40 | -0.034 | -- | -- |

Units: 1.0 inch = 25.4 mm, 1.0 ksi = 6.89 MPa

This analysis of parameter combinations showed that certain parameters were better at predicting transfer length. The parameter $d_b$ alone gave consistently low $R^2$ values for LWC and NWC specimens, regardless of the subset of specimens. The parameter $\sqrt{f'_{ci}}$ gave large $R^2$ values for both LWC and NWC specimens. For most parameter combinations the inclusion of $f_{pt}$ reduced the $R^2$ values. The largest $R^2$ values for LWC specimens were from the $d_b/E_{ci}$ and $d_b/\lambda\sqrt{f'_{ci}}$ parameter combinations. Similar to the $d_b$ parameter alone for NWC specimens, the $d_b/\lambda$ parameter combination gave low $R^2$ values for LWC specimens.

## COMPARISONS WITH PREDICTED TRANSFER LENGTH

The following section discusses the test-to-prediction ratios for the specimens in the TFHRC Database. The measured transfer lengths were compared to the predicted transfer lengths using a test-to-prediction ratio with the measured $\ell_t$ being referred to as the "test."

### PUBLISHED EXPRESSIONS FOR TRANSFER LENGTH

The expressions used for predicting transfer length are from design specifications including the AASHTO Standard Specification (Eq. 1), the AASHTO LRFD Bridge Design Specification (Eq. 2), and the ACI 318-14 Building Code (Eq. 3). Predictive expressions from researchers include the ones by Meyer et al. (Eq. 8), Ramirez and Russell (Eq. 9), Mitchell et al. (Eq. 4), Barnes et al. (Eq. 10), Buckner (Eq. 6), and Thatcher et al. (Eq. 7).

Table 42 through Table 44 give the test-to-prediction ratios for predicting transfer length described previously in this report. The number of specimens (No.) with adequate information reported to calculate each parameter in the prediction expression is given for each expression. The mean ratio, COV of the ratios, maximum ratio, and minimum ratio are given for each expression. The COV is an indication of how close the individual transfer length values were to the mean transfer length and a smaller COV value indicates less scatter. The percent of test-to-prediction ratios less than 1.0 is also given. Ratios less than 1.0 indicate that the expression has underestimated the transfer length.

The test-to-prediction ratios for all of the LWC specimens and all of the NWC specimens are given in Table 42. For the LWC specimens, 99 percent of the ratios were less than 1.0 for Buckner expression and none of the measured transfer lenghts were below the prediction by the Barnes et al. expression. These two expressions effectively provided upper and lower bounds for the LWC data. Although the scatter in the data, as measured by the COV, was high for all nine expressions, the expressions that used $E_{ci}$ as a parameter had the lowest COV. For a more limited number of NWC specimens, the Buckner and Barnes et al. expressions are also effectively bounding expressions. The ACI 318 expression is also effectively an upper bound expression for the NWC data. For a larger group of NWC specimens, the Meyer et al. and Ramirez and Russell expressions had ratios that were less than 1.0 for 80 percent and 78 percent of the specimens, respectively. Both of these expressions used $\sqrt{f'_{ci}}$ as a parameter. The two AASHTO expressions had the highest amount of scatter in the data with a COV of 0.409 and the Buckner and Thatcher et al. expressions had the lowest amount of scatter with a COV of 0.218.

The test-to-prediction ratios are given by specimen type in Table 43 for LWC specimens and in Table 44 for NWC specimens. The ratios for the each LWC specimen type were similar to the ratios of all LWC specimens. The ratios for the ACI 318, Mitchell et al., and Buckner expressions were less than 1.0 for 94 percent of the limited number of NWC multi-strand rectangular specimens. For the NWC multi-strand I-beam or T-beam specimens, the 100 percent of the ratios were less than 1.0 for the ACI 318 and Buckner et all expressions. The Meyer et al.

and Ramirez and Russell expressions had ratios that were less than 1.0 for 91 percent and 88 percent, respectively, of the I-beam or T-beam specimens.

**Table 42. Test-to-Prediction Ratio of Transfer Length for LWC and NWC.**

| Specimen Type | Design Expression† | No. | Mean | COV | Max. | Min. | Percent < 1.0 |
|---|---|---|---|---|---|---|---|
| All LWC | AASHTO Std. | 139 | 0.776 | 0.369 | 1.628 | 0.315 | 85% |
| | AASHTO LRFD | 139 | 0.646 | 0.369 | 1.357 | 0.262 | 90% |
| | ACI 318 | 138 | 0.725 | 0.391 | 1.526 | 0.271 | 86% |
| | Meyer et al. | 121 | 0.752 | 0.345 | 1.567 | 0.343 | 87% |
| | Ramirez and Russell | 121 | 0.767 | 0.346 | 1.599 | 0.350 | 86% |
| | Mitchell et al. | 120 | 0.890 | 0.353 | 1.840 | 0.385 | 74% |
| | Barnes et al. | 120 | 2.992 | 0.353 | 6.186 | 1.294 | 0% |
| | Buckner | 138 | 0.519 | 0.327 | 1.062 | 0.235 | 99% |
| | Thatcher et al. | 138 | 0.721 | 0.327 | 1.475 | 0.327 | 87% |
| All NWC | AASHTO Std. | 316 | 0.886 | 0.409 | 2.080 | 0.353 | 66% |
| | AASHTO LRFD | 316 | 0.738 | 0.409 | 1.733 | 0.294 | 79% |
| | ACI 318 | 56 | 0.553 | 0.269 | 1.191 | 0.296 | 98% |
| | Meyer et al. | 287 | 0.813 | 0.324 | 1.797 | 0.368 | 80% |
| | Ramirez and Russell | 287 | 0.826 | 0.327 | 1.834 | 0.376 | 78% |
| | Mitchell et al. | 56 | 0.726 | 0.234 | 1.248 | 0.419 | 91% |
| | Barnes et al. | 56 | 2.440 | 0.234 | 4.196 | 1.410 | 0% |
| | Buckner | 56 | 0.676 | 0.218 | 1.321 | 0.352 | 98% |
| | Thatcher et al. | 56 | 0.938 | 0.218 | 1.835 | 0.489 | 64% |

Notes:

† AASHTO Standard Spec. (Eq. 1), AASHTO LRFD (Eq. 2), ACI 318 (Eq. 3), Meyer et al. (Eq. 8), Ramirez and Russell (Eq. 9), Mitchell et al. (Eq. 4), Barnes et al. (Eq. 10), Buckner (Eq. 6), Thatcher et al. (Eq. 7)

**Table 43. Test-to-Prediction Ratio of Transfer Length for LWC by Specimen Type.**

| Specimen Type | Design Expression† | No. | Mean | COV | Max. | Min. | Percent < 1.0 |
|---|---|---|---|---|---|---|---|
| Single-strand rect.: LWC | AASHTO Std. | 24 | 0.743 | 0.293 | 1.160 | 0.440 | 83% |
| | AASHTO LRFD | 24 | 0.619 | 0.293 | 0.967 | 0.367 | 100% |
| | ACI 318 | 24 | 0.692 | 0.292 | 1.122 | 0.411 | 88% |
| | Meyer et al. | 6 | 0.720 | 0.278 | 1.097 | 0.530 | 83% |
| | Ramirez and Russell | 6 | 0.735 | 0.278 | 1.120 | 0.541 | 83% |
| | Mitchell et al. | 6 | 0.868 | 0.290 | 1.351 | 0.652 | 83% |
| | Barnes et al. | 6 | 2.919 | 0.290 | 4.541 | 2.192 | 0% |
| | Buckner | 24 | 0.470 | 0.296 | 0.696 | 0.270 | 100% |
| | Thatcher et al. | 24 | 0.653 | 0.296 | 0.966 | 0.375 | 100% |
| Multi-strand I-beam or T-beam: LWC | AASHTO Std. | 50 | 0.793 | 0.260 | 1.430 | 0.473 | 88% |
| | AASHTO LRFD | 50 | 0.661 | 0.260 | 1.192 | 0.394 | 94% |
| | ACI 318 | 50 | 0.748 | 0.269 | 1.355 | 0.435 | 90% |
| | Meyer et al. | 50 | 0.718 | 0.233 | 1.204 | 0.472 | 92% |
| | Ramirez and Russell | 50 | 0.733 | 0.233 | 1.229 | 0.481 | 92% |
| | Mitchell et al. | 50 | 0.845 | 0.232 | 1.411 | 0.554 | 78% |
| | Barnes et al. | 50 | 2.843 | 0.232 | 4.745 | 1.863 | 0% |
| | Buckner | 50 | 0.531 | 0.312 | 1.062 | 0.304 | 98% |
| | Thatcher et al. | 50 | 0.738 | 0.312 | 1.475 | 0.422 | 86% |
| Multi-strand I-beam or T-beam: LWC | AASHTO Std. | 65 | 0.774 | 0.460 | 1.628 | 0.315 | 83% |
| | AASHTO LRFD | 65 | 0.645 | 0.460 | 1.357 | 0.262 | 83% |
| | ACI 318 | 64 | 0.721 | 0.496 | 1.526 | 0.271 | 83% |
| | Meyer et al. | 65 | 0.782 | 0.404 | 1.567 | 0.343 | 83% |
| | Ramirez and Russell | 65 | 0.796 | 0.406 | 1.599 | 0.350 | 82% |
| | Mitchell et al. | 64 | 0.927 | 0.415 | 1.840 | 0.385 | 70% |
| | Barnes et al. | 64 | 3.116 | 0.415 | 6.186 | 1.294 | 0% |
| | Buckner | 64 | 0.527 | 0.344 | 0.919 | 0.235 | 100% |
| | Thatcher et al. | 64 | 0.732 | 0.344 | 1.276 | 0.327 | 83% |

Notes:

† AASHTO Standard Spec. (Eq. 1), AASHTO LRFD (Eq. 2), ACI 318 (Eq. 3), Meyer et al. (Eq. 8), Ramirez and Russell (Eq. 9), Mitchell et al. (Eq. 4), Barnes et al. (Eq. 10), Buckner (Eq. 6), Thatcher et al. (Eq. 7)

**Table 44. Test-to-Prediction Ratio of Transfer Length for NWC by Specimen Type.**

| Specimen Type | Design Expression† | No. | Mean | COV | Max. | Min. | Percent < 1.0 |
|---|---|---|---|---|---|---|---|
| Single-strand rect.: NWC | AASHTO Std. | 89 | 0.961 | 0.380 | 2.080 | 0.387 | 60% |
| | AASHTO LRFD | 89 | 0.801 | 0.380 | 1.733 | 0.323 | 75% |
| | ACI 318 | 0 | -- | -- | -- | -- | -- |
| | Meyer et al. | 68 | 0.803 | 0.256 | 1.512 | 0.427 | 87% |
| | Ramirez and Russell | 68 | 0.817 | 0.257 | 1.543 | 0.436 | 85% |
| | Mitchell et al. | 0 | -- | -- | -- | -- | -- |
| | Barnes et al. | 0 | -- | -- | -- | -- | -- |
| | Buckner | 0 | -- | -- | -- | -- | -- |
| | Thatcher et al. | 0 | -- | -- | -- | -- | -- |
| Multi-strand rect.: NWC | AASHTO Std. | 82 | 1.030 | 0.412 | 1.933 | 0.452 | 50% |
| | AASHTO LRFD | 82 | 0.858 | 0.412 | 1.611 | 0.377 | 61% |
| | ACI 318 | 16 | 0.622 | 0.251 | 1.191 | 0.530 | 94% |
| | Meyer et al. | 82 | 0.959 | 0.333 | 1.797 | 0.540 | 57% |
| | Ramirez and Russell | 82 | 0.975 | 0.334 | 1.834 | 0.551 | 55% |
| | Mitchell et al. | 16 | 0.770 | 0.199 | 1.248 | 0.618 | 94% |
| | Barnes et al. | 16 | 2.589 | 0.199 | 4.196 | 2.078 | 0% |
| | Buckner | 16 | 0.702 | 0.241 | 1.321 | 0.599 | 94% |
| | Thatcher et al. | 16 | 0.975 | 0.241 | 1.835 | 0.833 | 81% |
| Multi-strand I-beam or T-beam: NWC | AASHTO Std. | 145 | 0.758 | 0.355 | 1.493 | 0.353 | 79% |
| | AASHTO LRFD | 145 | 0.631 | 0.355 | 1.244 | 0.294 | 92% |
| | ACI 318 | 40 | 0.525 | 0.263 | 0.779 | 0.296 | 100% |
| | Meyer et al. | 137 | 0.730 | 0.289 | 1.325 | 0.368 | 91% |
| | Ramirez and Russell | 137 | 0.740 | 0.294 | 1.353 | 0.376 | 88% |
| | Mitchell et al. | 40 | 0.708 | 0.247 | 1.065 | 0.419 | 90% |
| | Barnes et al. | 40 | 2.380 | 0.247 | 3.581 | 1.410 | 0% |
| | Buckner | 40 | 0.665 | 0.209 | 0.928 | 0.352 | 100% |
| | Thatcher et al. | 40 | 0.924 | 0.209 | 1.289 | 0.489 | 58% |

Notes:

† AASHTO Standard Spec. (Eq. 1), AASHTO LRFD (Eq. 2), ACI 318 (Eq. 3), Meyer et al. (Eq. 8), Ramirez and Russell (Eq. 9), Mitchell et al. (Eq. 4), Barnes et al. (Eq. 10), Buckner (Eq. 6), Thatcher et al. (Eq. 7)

The comparison of measured and predicted transfer lengths showed that some expressions were effective at predicting transfer length for both LWC and NWC specimens. The Buckner expression underestimated nearly all of the measured transfer lengths and was an effective upper bound. The Barnes et al. expression was an effective lower bound for both LWC and NWC as it overestimated all of the measured transfer lengths. The Meyer et al. and Ramirez and Russell expressions underestimated the transfer lengths of nearly all of the measured transfer lengths. The AASHTO LRFD expression underestimated nearly all of the transfer lengths of the LWC specimens, and the ACI 318 underestimated nearly all of the transfer lengths of the NWC specimens.

## POTENTIAL EXPRESSIONS FOR TRANSFER LENGTH

The results of the parameter analysis and test-to-prediction ratios of published expressions for predicting transfer length were used to develop several potential expressions for predicting the transfer length of LWC and NWC specimens. The parameter analysis showed that the $d_b/E_{ci}$ and $d_b/\lambda\sqrt{f'_{ci}}$ parameter combinations gave the best correlation to the transfer length measurements. The correlations that included the parameter $f_{pt}$ were not as strong as the parameter combinations without $f_{pt}$. The analysis of published prediction expressions showed that the Ramirez and Russell and Barnes et al. expressions were effective upper and lower bounds of the data.

Predictions of transfer length affect the design stress in pretensioned strand used in several different articles of the AASHTO LRFD Bridge Design Specifications. In Article 5.8 for Shear and Torsion, the transfer length affects the calculation of $f_{pc}$, $f_{cpe}$, $f_{po}$, and $V_p$. An underestimation of transfer length will result in a lower calculated shear resistance at the end of a member. In this case, underestimating the transfer length is conservative. In Article 5.9.4 for stress limits on concrete, an overestimation of the transfer length will result in larger calculated tensile and compressive stress in the end region of a member. In this case, overestimating the transfer length is conservative.

An expression for predicting transfer length that is an upper bound to the data will provide conservative estimates for determining the shear resistance at the end of a member. The expression for NWC concrete elastic modulus that was given in Commentary Article C5.4.2.4 in the 6$^{th}$ edition of the AASHTO LRFD Bridge Design Specifications[1] before the 2015 revisions of the 7$^{th}$ edition is given by Eq. 30. The expression can also be used for the elastic modulus at time of transfer ($E_{ci}$) for a given $f'_{ci}$. Solving Eq. 30 for $\sqrt{f'_{ci}}$ and substituting it into the expression for transfer length by Ramirez and Russell results in Eq. 31 after rounding. The lower limit of $40d_b$ corresponding to a compressive strength of 9 ksi (62 MPa) is maintained from Eq. 9. An alternative expression using the λ-factor with the Ramirez and Russell expression is given by Eq. 32. The expression by Ramirez and Russell, which was developed for NWC specimens, was used as the basis for the LWC expressions in an attempt to provide a smooth transition between the expressions for LWC and NWC.

$$E_c = 1820\sqrt{f'_c} \quad \text{(Eq. 30)}$$

$$\ell_t = \frac{220{,}000 d_b}{E_{ci}} \geq 40 d_b \quad \text{(Eq. 31)}$$

$$\ell_t = \frac{120 d_b}{\lambda\sqrt{f'_{ci}}} \geq 40 d_b \quad \text{(Eq. 32)}$$

A lower bound expression for predicting transfer length will provide conservative estimates of extreme fiber stresses for checking stress limits. Substituting Eq. 30 into the Barnes et al. expression given by Eq. 10 and assuming a stress of 180 ksi (1240 MPa) for $f_{pt}$ results in Eq. 33 after rounding down. A comparison of Eq. 31 and Eq. 33 shows that the lower bound expression is exactly 25 percent of the upper bound expression. Multiplying Eq. 32 by 0.25 results in Eq. 34, which is a lower bound expression that includes the λ-factor. The lower limit of $40d_b$ in Eq. 31 and Eq. 32 corresponding to a compressive strength of 9 ksi (62 MPa) was also multiplied by 0.25 which results in the $10d_b$ limit given in Eq. 33 and Eq. 34.

$$\ell_t = \frac{55{,}000 d_b}{E_{ci}} \geq 10 d_b \quad \text{(Eq. 33)}$$

$$\ell_t = \frac{30 d_b}{\lambda\sqrt{f'_{ci}}} \geq 10 d_b \quad \text{(Eq. 34)}$$

Table 45 through Table 47 give the test-to-prediction ratios determined using the four potential expressions. The ratios for the AASHTO LRFD expression are included as a comparison with current practice. The ratios for the Buckner expression are included because it was shown in the previous section that it was an upper bound for the LWC data. The Ramirez and Russell and Barnes et al. expressions are included because they are the basis for the potential expressions.

The test-to-prediction ratios are given in Table 45 for all of the LWC specimens. Potential upper bound Expression 1 using $E_{ci}$ gave similar predictions to the Buckner expression, with both having 99 percent of the specimens with a ratio less than 1.0. Both of the potential lower bound expressions overestimated the transfer lengths for all of the specimens (i.e., 0 percent less than 1.0). The maximum and minimum ratios for the lower bound Expression 3 using $E_{ci}$ were closer to 1.0 than the ratios for the Barnes et al. expression. This indicates that the potential expression does not excessively underestimate the transfer lengths by as much as the Barnes et al. expression. The potential expressions using the λ-factor were not as effective as using $E_{ci}$. More of the ratios were greater than 1.0 for the upper bound expression using the λ-factor. The lower bound expression using the λ-factor underestimated the ratios by a greater amount than the expression using $E_{ci}$.

Table 45 also gives the ratios for all of the NWC specimens. For the more limited number of NWC specimens with $E_{ci}$ values, 98 percent of the ratios determined using Expression 1 and the

Buckner expression were less than 1.0. The AASHTO LRFD expression and Ramirez and Russell expressions had 79 percent and 78 percent of their ratios less than 1.0.

Table 46 and Table 47 give the ratios determined using the potential expressions grouped by specimen type for LWC specimens and NWC specimens, respectively. The ratios for the multi-strand rectangular and multi-strand I-beam or T-beams were similar to the LWC data as a whole. The ratios determined using the potential expressions with $E_{ci}$ in Table 47 are shown for information purposes. The λ-factor for all of the NWC data is 1.0 so the potential U.B. expression is equal to the Ramirez and Russell expression. For the multi-strand I-beam or T-beam specimens, the Ramirez and Russell expression is an upper bound for 88 percent of the NWC data. This is similar to the AASHTO LRFD expression with 92 percent of the data with ratios less than 1.0.

**Table 45. Test-to-Prediction Ratio of Transfer Length for LWC and NWC using Potential Expressions for Upper and Lower Bounds.**

| Concrete Mix Type | Design Expression† | No. | Mean | COV | Max. | Min. | Percent < 1.0 |
|---|---|---|---|---|---|---|---|
| All LWC | U.B. Expr. 1 ($E_{ci}$) | 138 | 0.535 | 0.325 | 1.103 | 0.255 | 99% |
| | U.B. Expr. 2 (λ) | 121 | 0.693 | 0.348 | 1.464 | 0.336 | 89% |
| | L.B. Expr. 3 ($E_{ci}$) | 138 | 2.139 | 0.325 | 4.414 | 1.020 | 0% |
| | L.B. Expr. 4 (λ) | 121 | 2.771 | 0.348 | 5.854 | 1.343 | 0% |
| | AASHTO LRFD | 139 | 0.646 | 0.369 | 1.357 | 0.262 | 90% |
| | Buckner | 138 | 0.519 | 0.327 | 1.062 | 0.235 | 99% |
| | Ramirez and Russell | 121 | 0.767 | 0.346 | 1.599 | 0.350 | 86% |
| | Barnes et al. | 120 | 2.992 | 0.353 | 6.186 | 1.294 | 0% |
| All NWC | U.B. Expr. 1 ($E_{ci}$) | 56 | 0.699 | 0.222 | 1.412 | 0.381 | 98% |
| | U.B. Expr. 2 (λ) | 287 | 0.826 | 0.327 | 1.834 | 0.376 | 78% |
| | L.B. Expr. 3 ($E_{ci}$) | 56 | 2.798 | 0.222 | 5.649 | 1.523 | 0% |
| | L.B. Expr. 4 (λ) | 287 | 3.302 | 0.327 | 7.336 | 1.504 | 0% |
| | AASHTO LRFD | 316 | 0.738 | 0.409 | 1.733 | 0.294 | 79% |
| | Buckner | 56 | 0.676 | 0.218 | 1.321 | 0.352 | 98% |
| | Ramirez and Russell | 287 | 0.826 | 0.327 | 1.834 | 0.376 | 78% |
| | Barnes et al. | 56 | 2.440 | 0.234 | 4.196 | 1.410 | 0% |
| | Barnes et al. | 56 | 2.440 | 0.234 | 4.196 | 1.410 | 0% |

**Table 46. Test-to-Prediction Ratio of Transfer Length for LWC by Specimen Type using Potential Expressions for Upper and Lower Bounds.**

| Specimen Type | Design Expression† | No. | Mean | COV | Max. | Min. | Percent < 1.0 |
|---|---|---|---|---|---|---|---|
| Single-strand rect.: LWC | U.B. Expr. 1 ($E_{ci}$) | 24 | 0.479 | 0.303 | 0.688 | 0.273 | 100% |
| | U.B. Expr. 2 ($\lambda$) | 6 | 0.652 | 0.298 | 1.028 | 0.496 | 83% |
| | L.B. Expr. 3 ($E_{ci}$) | 24 | 1.918 | 0.303 | 2.752 | 1.092 | 0% |
| | L.B. Expr. 4 ($\lambda$) | 6 | 2.610 | 0.298 | 4.113 | 1.985 | 0% |
| | AASHTO LRFD | 24 | 0.619 | 0.293 | 0.967 | 0.367 | 100% |
| | Buckner | 24 | 0.470 | 0.296 | 0.696 | 0.270 | 100% |
| | Ramirez and Russell | 6 | 0.735 | 0.278 | 1.120 | 0.541 | 83% |
| | Barnes et al. | 6 | 2.919 | 0.290 | 4.541 | 2.192 | 0% |
| Multi-strand rect.: LWC | U.B. Expr. 1 ($E_{ci}$) | 50 | 0.549 | 0.315 | 1.103 | 0.314 | 98% |
| | U.B. Expr. 2 ($\lambda$) | 50 | 0.662 | 0.243 | 1.087 | 0.446 | 98% |
| | L.B. Expr. 3 ($E_{ci}$) | 50 | 2.198 | 0.315 | 4.414 | 1.255 | 0% |
| | L.B. Expr. 4 ($\lambda$) | 50 | 2.647 | 0.243 | 4.347 | 1.786 | 0% |
| | AASHTO LRFD | 50 | 0.661 | 0.260 | 1.192 | 0.394 | 94% |
| | Buckner | 50 | 0.531 | 0.312 | 1.062 | 0.304 | 98% |
| | Ramirez and Russell | 50 | 0.733 | 0.233 | 1.229 | 0.481 | 92% |
| | Barnes et al. | 50 | 2.843 | 0.232 | 4.745 | 1.863 | 0% |
| Multi-strand I-beam or T-beam: LWC | U.B. Expr. 1 ($E_{ci}$) | 64 | 0.544 | 0.335 | 0.925 | 0.255 | 100% |
| | U.B. Expr. 2 ($\lambda$) | 65 | 0.720 | 0.403 | 1.464 | 0.336 | 83% |
| | L.B. Expr. 3 ($E_{ci}$) | 64 | 2.176 | 0.335 | 3.702 | 1.020 | 0% |
| | L.B. Expr. 4 ($\lambda$) | 65 | 2.881 | 0.403 | 5.854 | 1.343 | 0% |
| | AASHTO LRFD | 65 | 0.645 | 0.460 | 1.357 | 0.262 | 83% |
| | Buckner | 64 | 0.527 | 0.344 | 0.919 | 0.235 | 100% |
| | Ramirez and Russell | 65 | 0.796 | 0.406 | 1.599 | 0.350 | 82% |
| | Barnes et al. | 64 | 3.116 | 0.415 | 6.186 | 1.294 | 0% |

Notes:

† Potential upper bound Expression 1 with $E_{ci}$ (Eq. 31), potential upper bound Expression 2 with $\lambda$ (Eq. 32), potential lower bound Expression 3 with $E_{ci}$ (Eq. 33), potential lower bound Expression 4 with $\lambda$ (Eq. 34), AASHTO LRFD (Eq. 2), Buckner (Eq. 6), Ramirez and Russell (Eq. 9), Barnes et al. (Eq. 10)

**Table 47. Test-to-Prediction Ratio of Transfer Length for NWC by Specimen Type using Potential Expressions for Upper and Lower Bounds.**

| Specimen Type | Design Expression† | No. | Mean | COV | Max. | Min. | Percent < 1.0 |
|---|---|---|---|---|---|---|---|
| Multi-strand rect.: NWC | U.B. Expr. 1 ($E_{ci}$) | 16 | 0.750 | 0.241 | 1.412 | 0.641 | 94% |
| | U.B. Expr. 2 ($\lambda$) | 82 | 0.975 | 0.334 | 1.834 | 0.551 | 55% |
| | L.B. Expr. 3 ($E_{ci}$) | 16 | 3.000 | 0.241 | 5.649 | 2.564 | 0% |
| | L.B. Expr. 4 ($\lambda$) | 82 | 3.901 | 0.334 | 7.336 | 2.205 | 0% |
| | AASHTO LRFD | 82 | 0.858 | 0.412 | 1.611 | 0.377 | 61% |
| | Buckner | 16 | 0.702 | 0.241 | 1.321 | 0.599 | 94% |
| | Ramirez and Russell | 82 | 0.975 | 0.334 | 1.834 | 0.551 | 55% |
| | Barnes et al. | 16 | 2.589 | 0.199 | 4.196 | 2.078 | 0% |
| Multi-strand I-beam or T-beam: NWC | U.B. Expr. 1 ($E_{ci}$) | 40 | 0.679 | 0.208 | 0.918 | 0.381 | 100% |
| | U.B. Expr. 2 ($\lambda$) | 137 | 0.740 | 0.294 | 1.353 | 0.376 | 88% |
| | L.B. Expr. 3 ($E_{ci}$) | 40 | 2.717 | 0.208 | 3.670 | 1.523 | 0% |
| | L.B. Expr. 4 ($\lambda$) | 137 | 2.962 | 0.294 | 5.411 | 1.504 | 0% |
| | AASHTO LRFD | 145 | 0.631 | 0.355 | 1.244 | 0.294 | 92% |
| | Buckner | 40 | 0.665 | 0.209 | 0.928 | 0.352 | 100% |
| | Ramirez and Russell | 137 | 0.740 | 0.294 | 1.353 | 0.376 | 88% |
| | Barnes et al. | 40 | 2.380 | 0.247 | 3.581 | 1.410 | 0% |

Notes:

† Potential upper bound Expression 1 with $E_{ci}$ (Eq. 31), potential upper bound Expression 2 with $\lambda$ (Eq. 32), potential lower bound Expression 3 with $E_{ci}$ (Eq. 33), potential lower bound Expression 4 with $\lambda$ (Eq. 34), AASHTO LRFD (Eq. 2), Buckner (Eq. 6), Ramirez and Russell (Eq. 9), Barnes et al. (Eq. 10)

## GRAPHICAL ANALYSIS OF NORMALIZED FLEXURAL BOND LENGTH

This section includes a comparison of the normalized flexural bond lengths for LWC and NWC specimens in the TFHRC Database. The purpose of the comparison is to examine the effect of different parameters on flexural bond length. Previous research has considered the following parameters to affect the transfer length of prestressing strand: concrete compressive strength ($f'_c$), strand prestress after all losses ($f_{pe}$), strand prestress at nominal flexural capacity ($f_{ps}$), and nominal strand diameter ($d_b$).[22,25,29,30] The concrete elastic modulus ($E_c$) and the λ-factor, given by Eq. 16, were used previously in this report as parameters in potential expressions to predict the transfer length. The parameters $E_c$ and λ-factor are used in potential expressions to predict flexural bond length in this section of the report.

Groups of parameters used to predict flexural bond length ($\ell_{fb}$) are evaluated graphically in Figure 80 through Figure 91. The figures are given in pairs: the first figure shows the data for LWC specimens and the second figure shows the NWC data. Each figure groups the data by specimen type and failure mode. Data shown in the figures represent tests that had both a measured transfer length and a tested embedment length. The flexural bond length was taken as the difference between the tested embedment length and the measured transfer length. The term "flexural bond length" refers to the bonded length of strand beyond the length required for the transfer length that is available to resist the additional strand stress caused by externally applied loads. The applied loads induce internal shear and bending moments in a beam and after cracking these internal forces induce stress in the strand. For the tests that had a reported transfer length and embedment length on the same specimen end, this information was used to determine the flexural bond length. For the specimens with only one reported transfer length, this transfer length was assumed to be valid at both specimen ends and was used to determine the flexural bond length. Some specimens had two reported transfer lengths, but did not indicate which transfer length measurement corresponded to the tested embedment length. For these tests, the mean of the two transfer lengths was used to determine the flexural bond length.

There is considerable scatter in the data shown in Figure 80 through Figure 91. Many of the NWC data points are high on the vertical axis because the embedment length test for these specimens was much longer than the predicted development length using any published expression. Most of the tests ending in bond failure form a horizontal band of data that are low on the vertical axis. There are several tests that ended in flexural failure that are below this band of bond failures. In the figures showing the LWC data, the rectangular specimens all have compressive strengths less than 9 ksi (62 MPa) and were tested over a wide range of embedment lengths. Most of the LWC data for I-beam or T-beam specimens have compressive strengths above 8 ksi (55 MPa) and were tested at longer embedment lengths. This may be due to the larger depth of the I-beam and T-beam specimens which frequently have full-scale standard AASHTO cross sections.

The expression for flexural bond included in the AASHTO LRFD Bridge Design Specifications is given by Eq. 19. It includes the parameters for strand diameter and strand stress. The

expression for flexural bond length proposed by Ramirez and Russell includes the parameters of stand diameter and concrete compressive strength and is given by Eq. 20. All three parameters are included Eq. 21, which is the expression proposed by Mitchell et al. for flexural bond length.

Figure 80 and Figure 81 show the flexural bond lengths compared to $(f_{ps}-f_{pe})d_b$ for LWC and NWC specimens, respectively. This group of parameters is used by the AASHTO LRFD Bridge Design Specifications. The prediction given by the AASHTO LRFD Bridge Design Specifications is indicated by the horizontal line at a value of 1. Specimens included in the figures had adequate information reported to calculate both $f_{ps}$ and $f_{pe}$. If available, a reported $E_{ci}$ was used to determine immediate prestress losses. Otherwise, $E_{ci}$ was determined using the expression in the AASHTO LRFD Bridge Design Specifications. Data points that are above the horizontal line were predicted to fail in flexure and data points below the line were predicted to fail in bond. The prediction given by the AASHTO LRFD Bridge Design Specifications was unconservative for tests ending in a bond failure that are above the horizontal line. The prediction given by the AASHTO LRFD Bridge Design Specifications was overly conservative for tests ending in a flexural failure that are below the horizontal line.

The flexural bond lengths are compared to $d_b/\sqrt{f'_c}$ in Figure 82 and Figure 83. The horizontal line at a value of 225 indicates the prediction given by the Ramirez and Russell expression. There are more specimens included in these figures because only the concrete compressive strength was needed for the prediction. Tests ending in bond failures that are above the horizontal line indicate an unconservative prediction.

The parameters $(f_{ps}-f_{pe})d_b/\sqrt{f'_c}$ are compared to flexural bond length in Figure 84 and Figure 85. The prediction by Mitchell et al. is indicated by the horizontal line at $\sqrt{4.5}$.

Figure 86 and Figure 87 show a comparison of the flexural bond lengths to $d_b/E_c$. Only specimens with a reported $E_c$ are shown in the figure. An expression for flexural bond length that includes $E_c$ was not found in the literature. An expression derived from the Ramirez and Russell expression is shown in the figures. The derived expression substitutes $E_c/1820$ for $\sqrt{f'_c}$ in the Ramirez and Russell expression.

Flexural bond lengths are compared to $(f_{ps}-f_{pe})d_b/E_c$ in Figure 88 and Figure 89. Only specimens with a reported $E_c$ are shown in the figure. An expression derived from the Ramirez and Russell expression is shown in the figures that includes a substitution of $E_c/1820$ for $\sqrt{f'_c}$ and an assumed $f_{ps}-f_{pe}$ of 90 ksi (620 MPa).

Figure 90 and Figure 91 show a comparison of the parameters that include the λ-factor to flexural bond length for LWC specimens only. The parameters compared to $\ell_{fb}$ are $\lambda\sqrt{f'_c}$ and $(f_{ps}-f_{pe})d_b/\lambda\sqrt{f'_c}$. The prediction given by Ramirez and Russell is shown in Figure 90 and in Figure 91 the prediction by Mitchell et al. is shown.

The considerable scatter in the data shown in Figure 80 through Figure 91 makes it difficult to draw strong conclusions from these figures. An ideal prediction expression would have all of the

tests ending in flexural failure above the horizontal prediction line and all of the bond failures below the line. As seen in the figures, none of the groups of normalizing parameters are able to accomplish this because of the scatter in the data. The approach taken in this research effort is to propose an expression that places strong emphasis on minimizing the number of tests ending in bond failure that are unconservatively predicted (i.e., above the horizontal line), while reducing the number flexural failures whose prediction is overly-conservative (i.e., under the horizontal line).

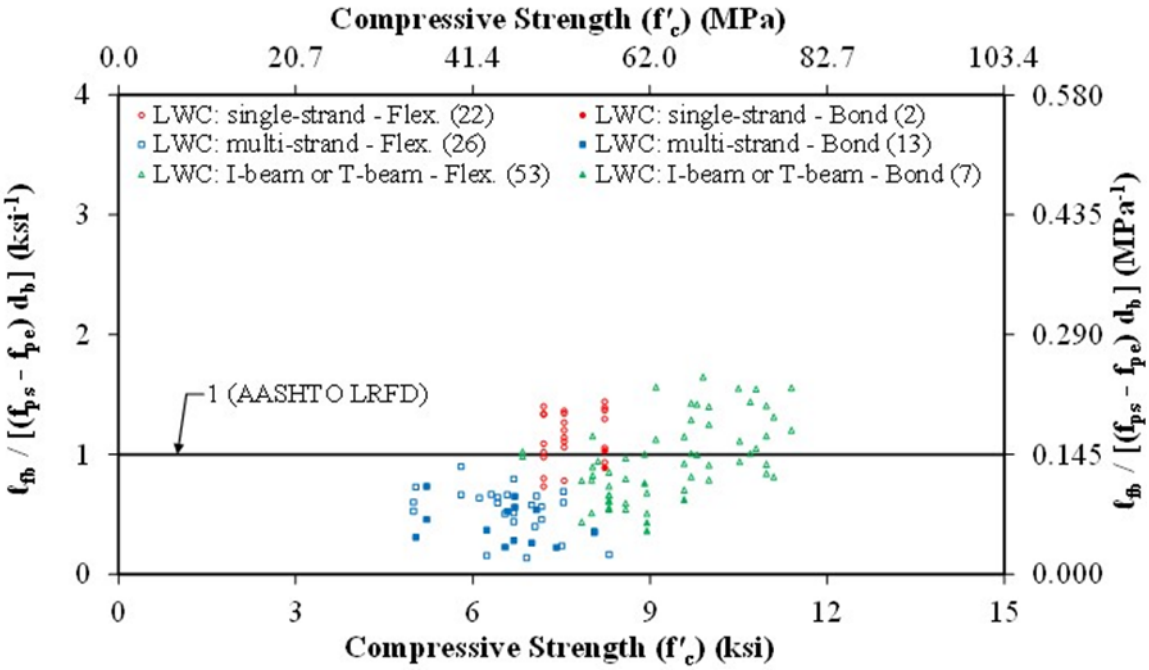


**Figure 80. Graph. Normalized Flexural Bond Length ($\ell_{fb}/[(f_{ps}-f_{pe})d_b]$) Compared to Compressive Strength ($f'_c$) by Specimen Type for LWC in the TFHRC Database.**

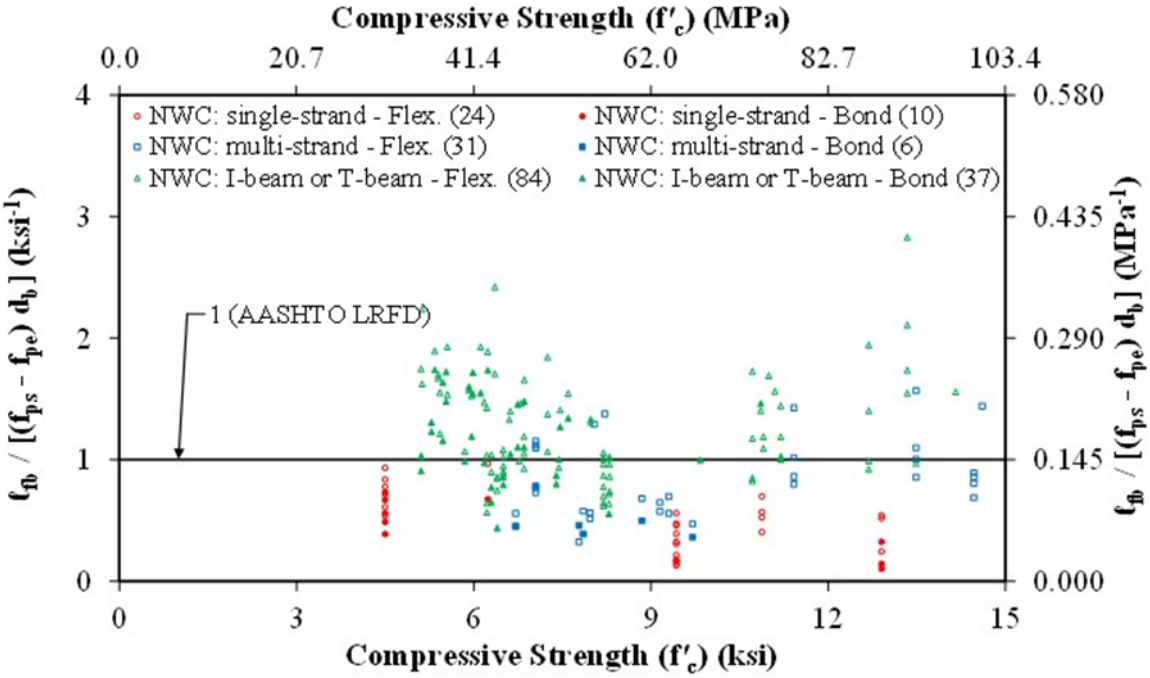


**Figure 81. Graph. Normalized Flexural Bond Length ($\ell_{fb}/[(f_{ps}-f_{pe})d_b]$) Compared to Compressive Strength ($f'_c$) by Specimen Type for NWC in the TFHRC Database.**

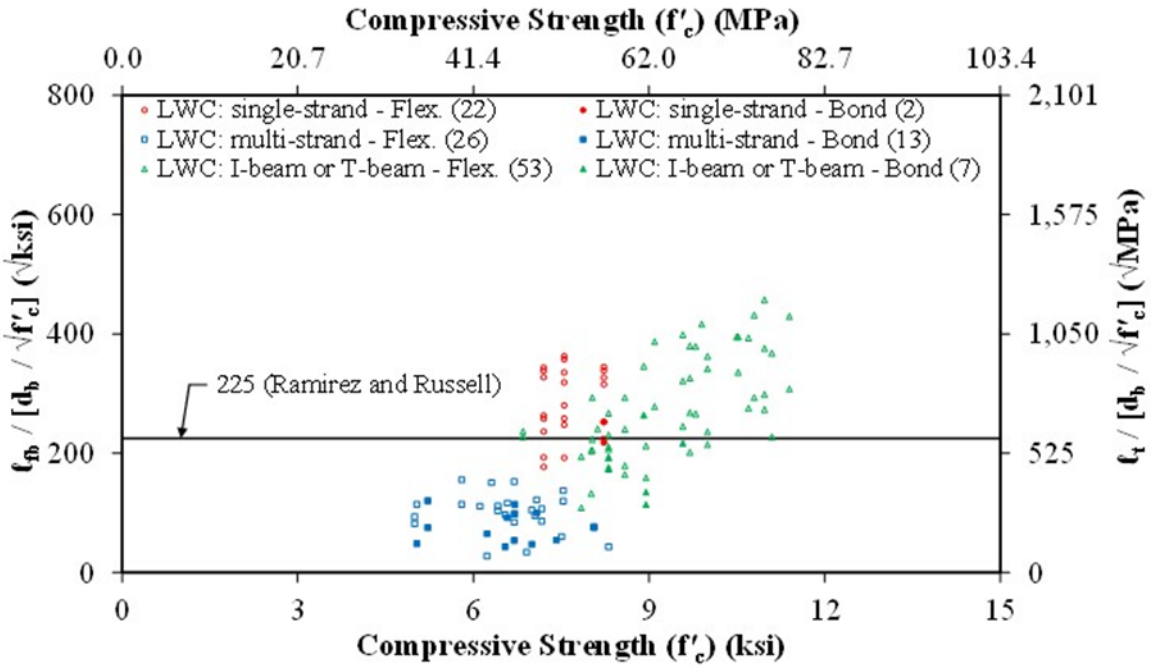


**Figure 82. Graph. Normalized Flexural Bond Length ($\ell_{fb}/[d_b/\sqrt{f'_c}]$) Compared to Compressive Strength ($f'_c$) by Specimen Type for LWC in the TFHRC Database.**

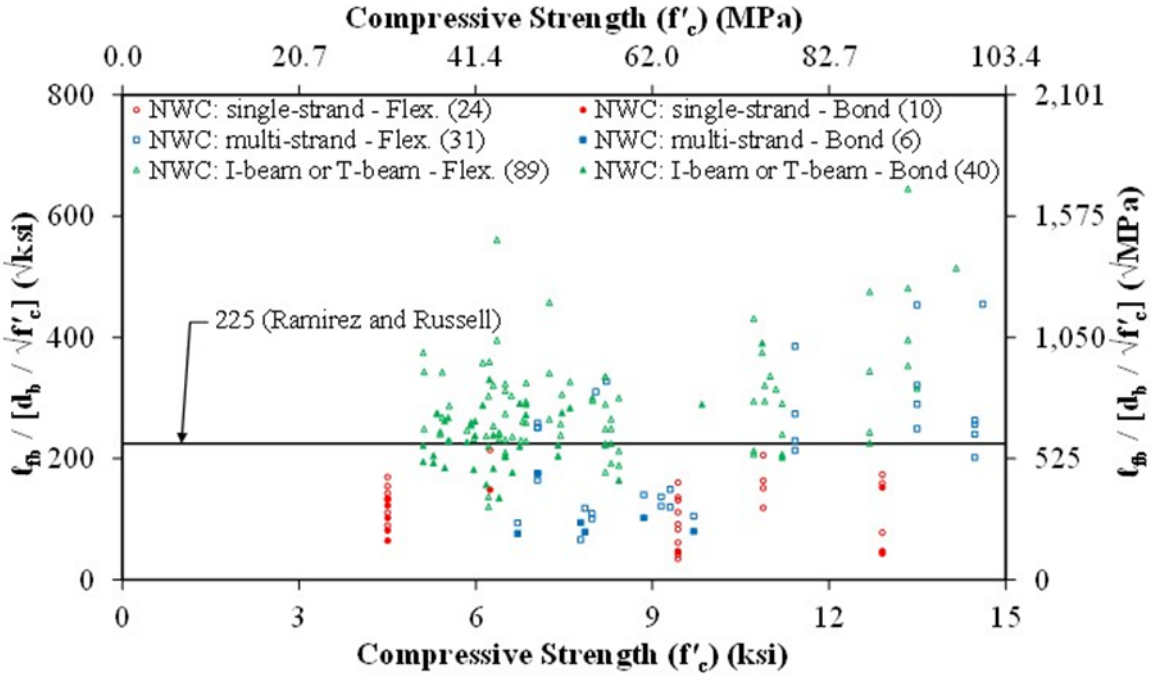


**Figure 83. Graph. Normalized Flexural Bond Length ($\ell_{fb}/[d_b/\sqrt{f'_c}]$) Compared to Compressive Strength ($f'_c$) by Specimen Type for NWC in the TFHRC Database.**

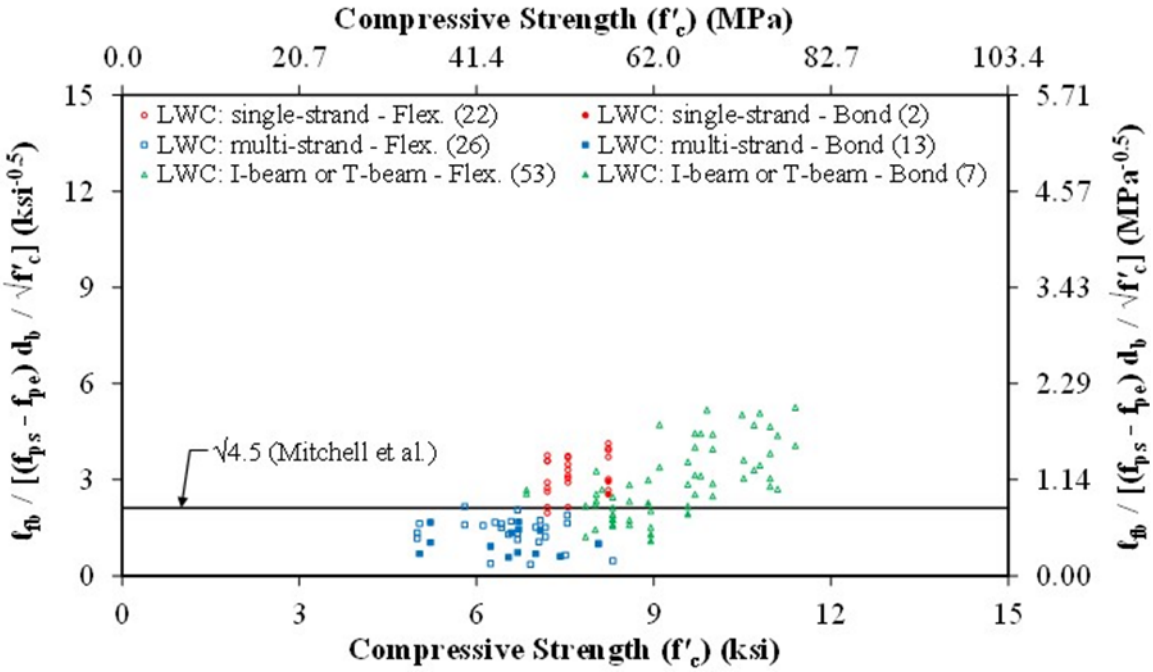


**Figure 84. Graph. Normalized Flexural Bond Length ($\ell_{fb}/[(f_{ps}-f_{pe})d_b/\sqrt{f'_c}]$) Compared to Compressive Strength ($f'_c$) by Specimen Type for LWC in the TFHRC Database.**

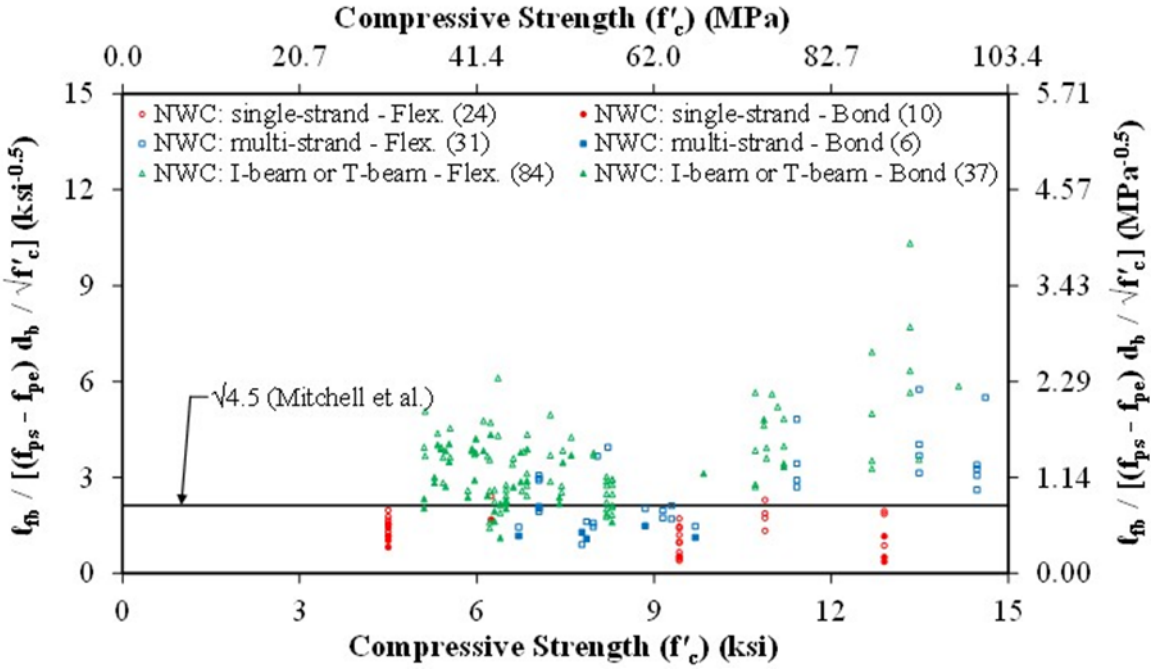


**Figure 85. Graph. Normalized Flexural Bond Length ($\ell_{fb}/[(f_{ps}-f_{pe})d_b/\sqrt{f'_c}]$) Compared to Compressive Strength ($f'_c$) by Specimen Type for NWC in the TFHRC Database.**

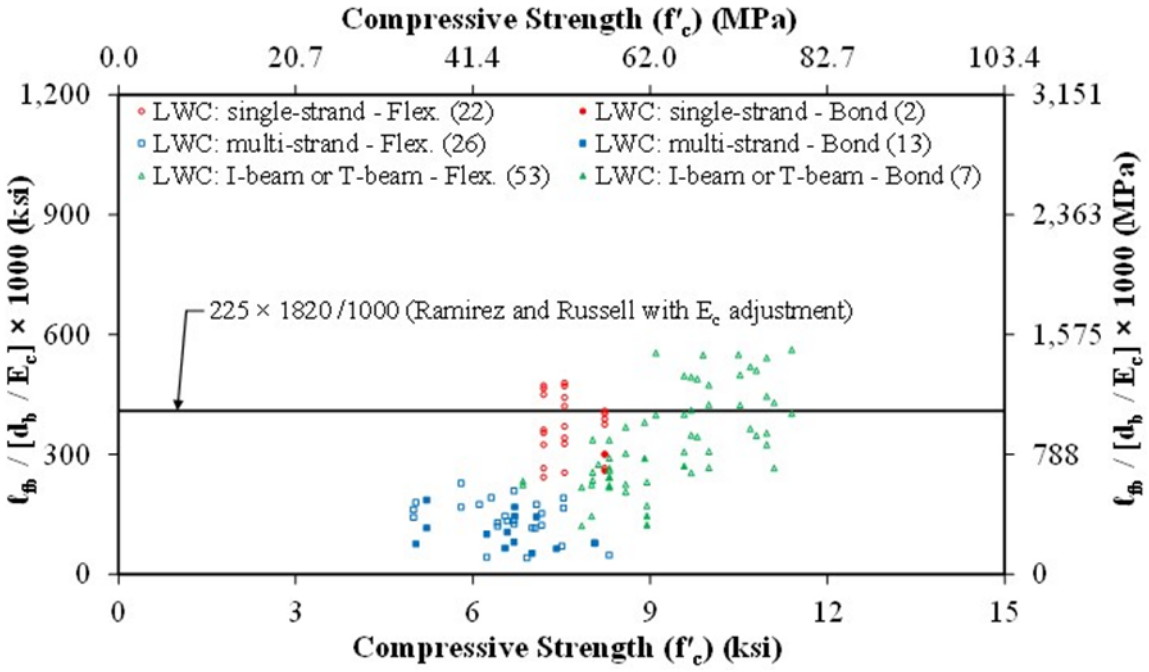


**Figure 86. Graph. Normalized Flexural Bond Length ($\ell_{fb}/[d_b/E_c]$) Compared to Compressive Strength ($f'_c$) by Specimen Type for LWC in the TFHRC Database.**

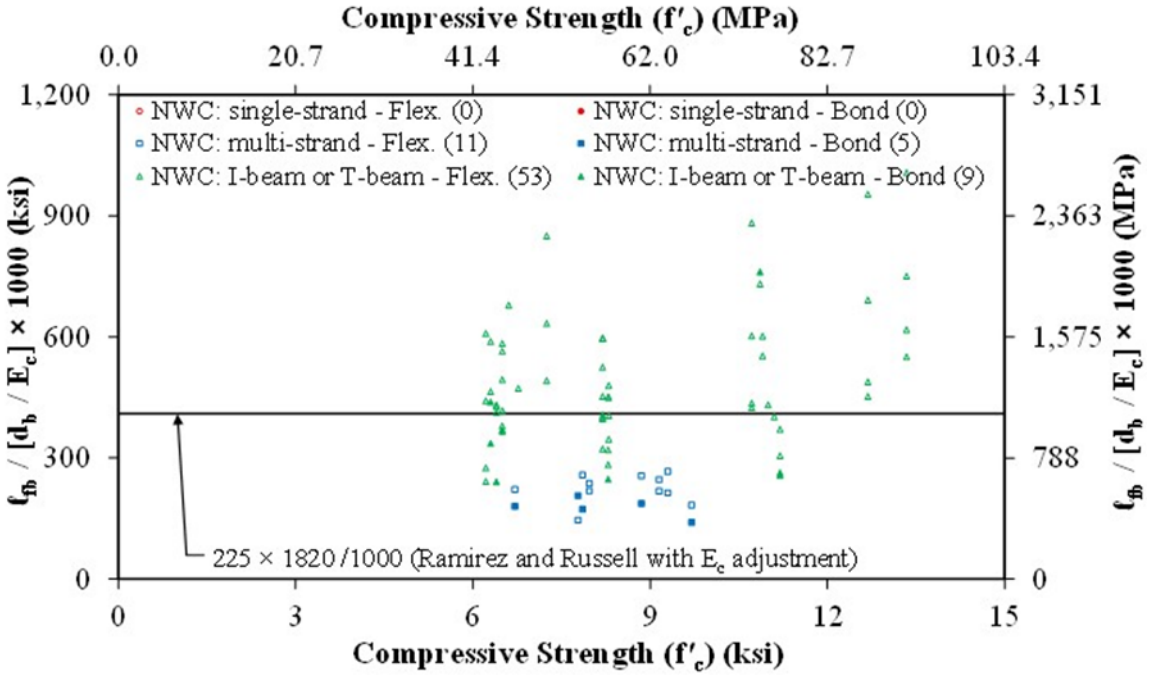


**Figure 87. Graph. Normalized Flexural Bond Length ($\ell_{fb}/[d_b/E_c]$) Compared to Compressive Strength ($f'_c$) by Specimen Type for NWC in the TFHRC Database.**

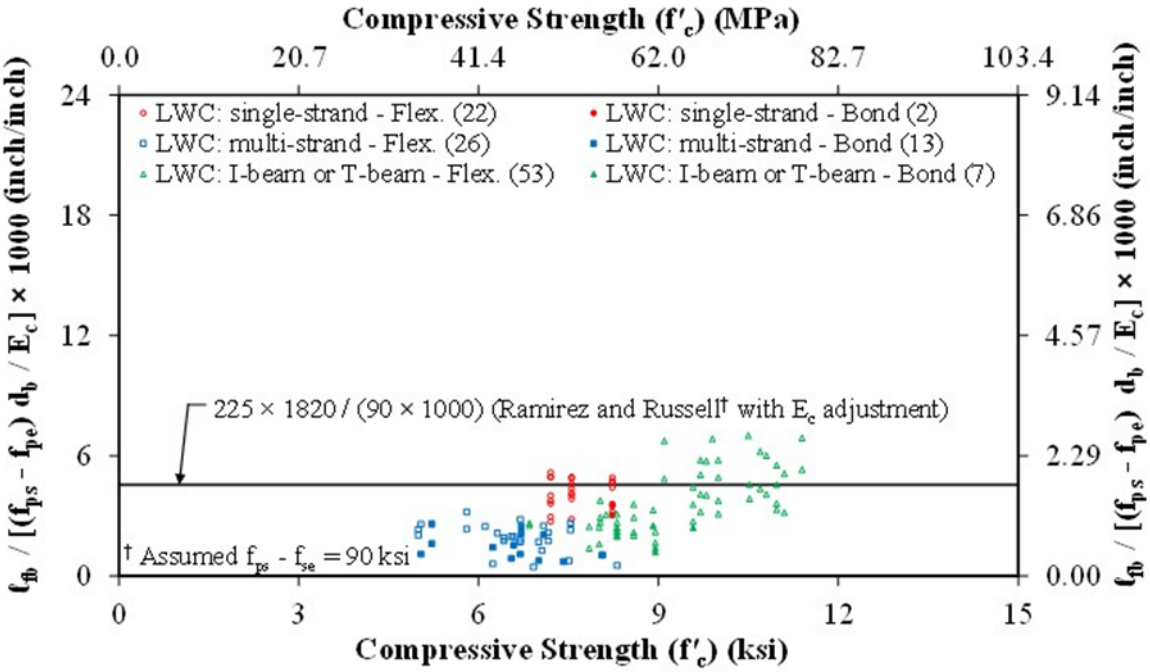


**Figure 88. Graph. Normalized Flexural Bond Length ($\ell_{fb}/[(f_{ps}-f_{pe})d_b/E_c]$) Compared to Compressive Strength ($f'_c$) by Specimen Type for LWC in the TFHRC Database.**

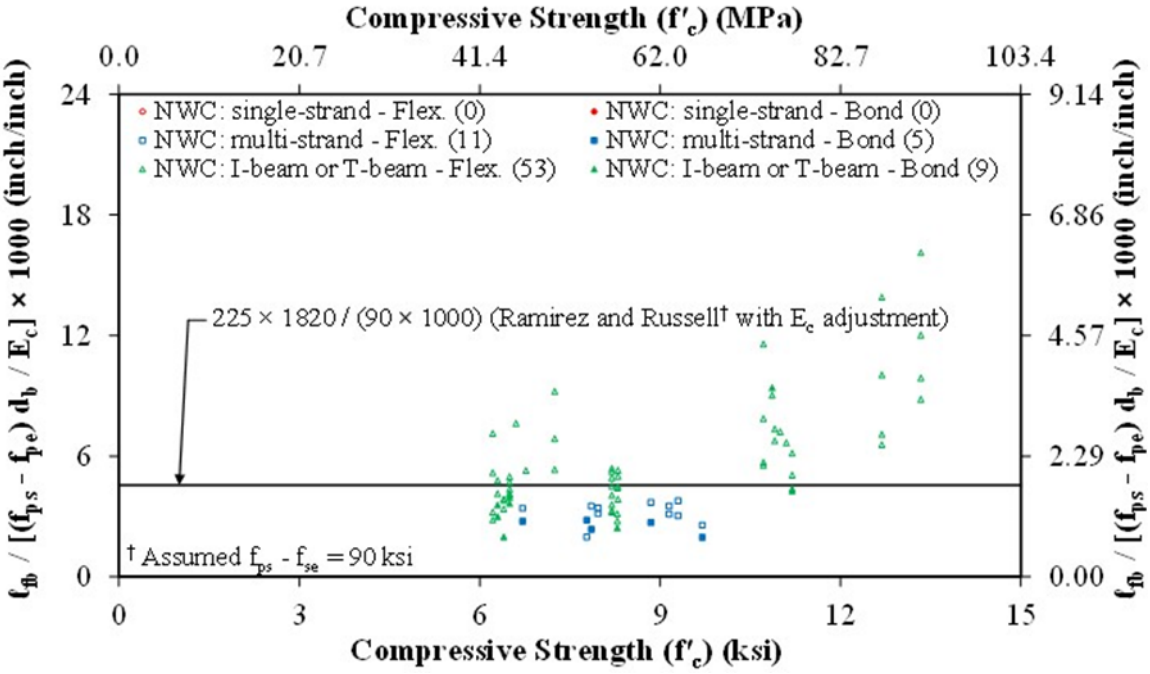


**Figure 89. Graph. Normalized Flexural Bond Length ($\ell_{fb}/[(f_{ps}-f_{pe})d_b/E_c]$) Compared to Compressive Strength ($f'_c$) by Specimen Type for NWC in the TFHRC Database.**

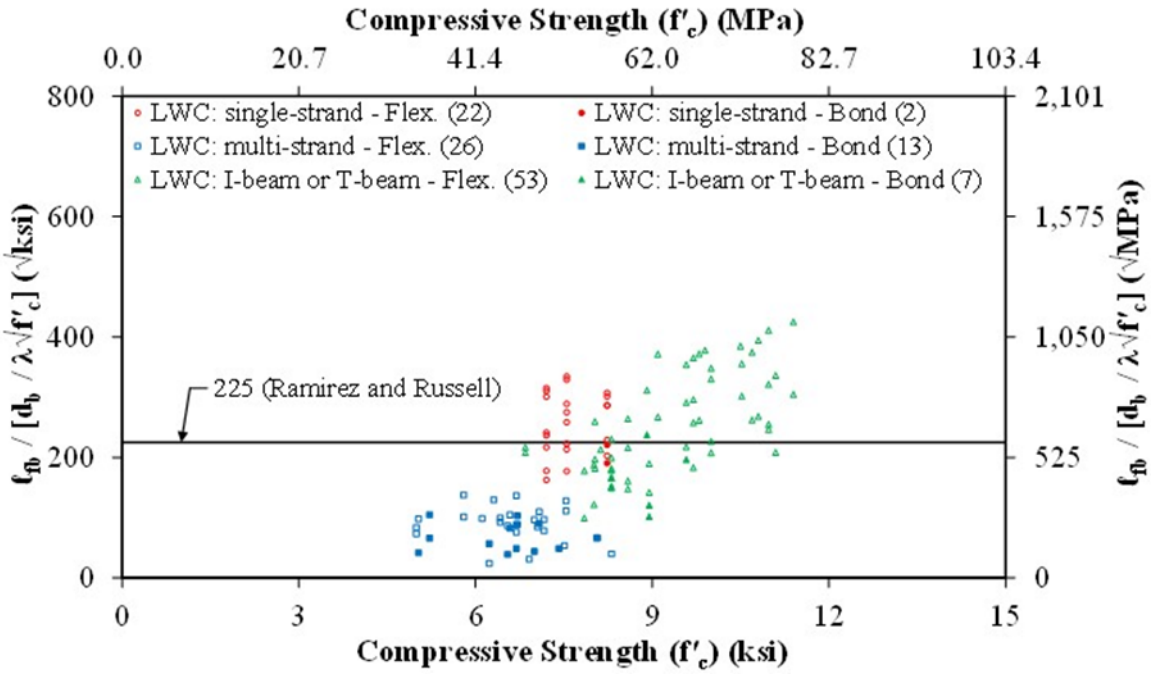


**Figure 90. Graph. Normalized Flexural Bond Length ($\ell_{fb}/[d_b/\lambda\sqrt{f'_c}]$) Compared to Compressive Strength ($f'_c$) by Specimen Type for LWC in the TFHRC Database.**

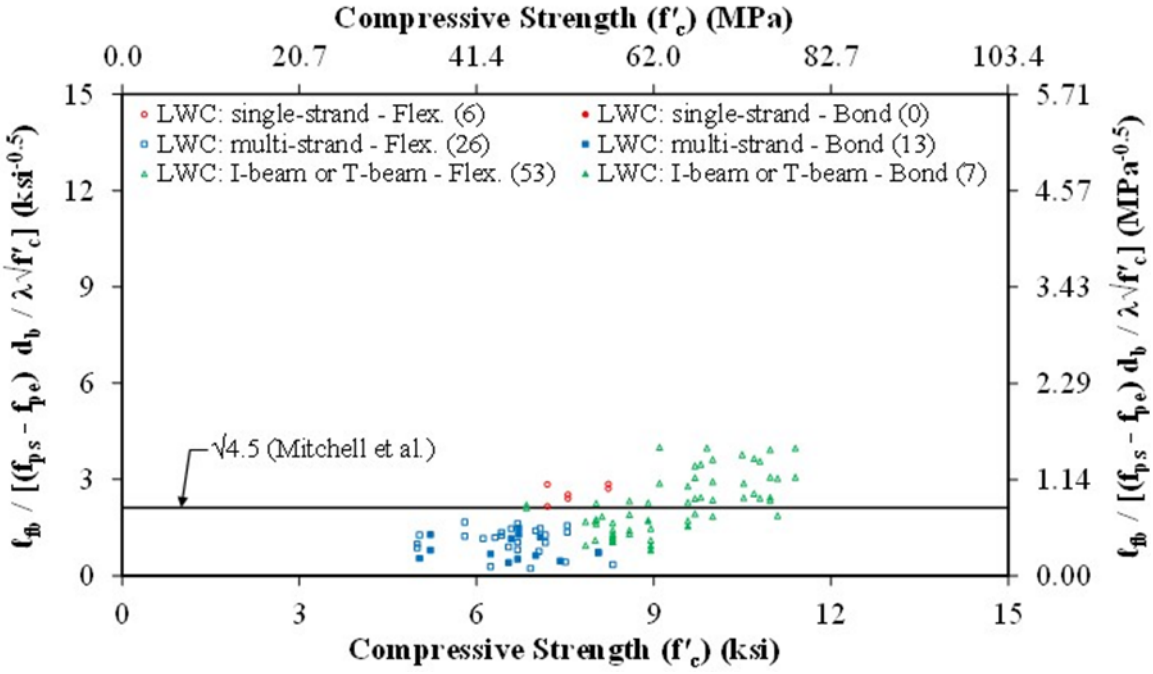


**Figure 91. Graph. Normalized Flexural Bond Length ($\ell_{fb}/[(f_{ps}-f_{pe})d_b/\lambda\sqrt{f'_c}]$) Compared to Compressive Strength ($f'_c$) by Specimen Type for LWC in the TFHRC Database.**

## COMPARISONS WITH PREDICTED FLEXURAL BOND LENGTH

The following section discusses the test-to-prediction ratios for the specimens in the TFHRC Database with both transfer length measurements and embedment length tests. The experimentally determined flexural bond lengths were compared to the predicted flexural bond lengths using a test-to-prediction ratio. The experimentally determined $\ell_{fb}$ is referred to as the "test."

### PUBLISHED EXPRESSIONS FOR FLEXURAL BOND LENGTH

The expressions used for predicting flexural bond length include the AASHTO LRFD Bridge Design Specifications expression (Eq. 19), the Ramirez and Russell expression (Eq. 20), and the Mitchell et al. expression (Eq. 21).

The test-to-predicted ratios for flexural bond length are given in Table 48. The table gives the ratios by concrete mix type and failure mode of the embedment length test. The number of specimens with adequate information reported to determine a predicted flexural bond length is given. For tests ending in a flexural failure, the minimum ratio and the percentage of specimens with ratios less than 1.0 is given. Specimens ending in a flexural failure with a test-to-prediction ratio less than 1.0 have an overly-conservative prediction. Prediction expressions with a high percentage of ratios less than 1.0 indicate that the expression requires longer embedment lengths than necessary to achieve a flexural failure. For embedment length tests ending in a bond failure, the maximum ratio and the percentage of tests with ratios greater than 1.0 is given. Ratios greater than 1.0 for tests ending in bond failures indicate that the prediction expression has made an unconservative prediction.

The test-to-prediction ratios of flexural bond length for LWC specimens are given in Table 48. For tests ending in bond failure, the AASTHO LRFD expression had the smallest percentage of ratios greater than 1.0 and the Mitchell et al. expression had the largest percentage. For tests ending in flexural failure, the AASHTO LRFD expression had the largest percentage of ratios greater than 1.0 and the Mitchell et al. expression had the smallest percentage.

Table 48 gives the test-to-prediction ratios of flexural bond length for NWC specimens. The Ramirez and Russell expression had a smaller percentage of unconservative estimates of flexural bond length (i.e., smaller percent of ratios greater than 1.0 for tests ending in bond failures) than the expression in the AASHTO LRFD Specifications. Mitchell et al. expressions had a larger percentage of unconservative estimates of flexural bond length than either the Ramirez and Russell expression or the AASHTO LRFD expression.

**Table 48. Test-to-Prediction Ratio of Flexural Bond Length by Concrete Mixture Type.**

| | | Flexural Failures | | | Bond Failures | | |
|---|---|---|---|---|---|---|---|
| **Concrete Mix Type** | **Design Expression†** | **No.** | **Min.** | **Percent ≤ 1.0** | **No.** | **Max.** | **Percent > 1.0** |
| All LWC | AASHTO LRFD | 101 | 0.137 | 59% | 22 | 1.029 | 5% |
| | Ramirez and Russell | 101 | 0.122 | 45% | 22 | 1.172 | 9% |
| | Mitchell et al. | 101 | 0.170 | 36% | 22 | 1.392 | 14% |
| | Expr. 1 ($\Delta f_p$ and $E_c$) | 101 | 0.095 | 77% | 22 | 0.763 | 0% |
| | Expr. 2 ($\Delta f_p$ and $\lambda$) | 101 | 0.125 | 70% | 22 | 0.900 | 0% |
| | Expr. 3 ($\lambda\sqrt{f'_c}$) | 101 | 0.107 | 54% | 22 | 1.055 | 5% |
| | Expr. 4 ($\Delta f_p$ and $\lambda\sqrt{f'_c}$) | 101 | 0.154 | 45% | 22 | 1.218 | 9% |
| | Expr. 5 ($\Delta f_p$ and $\lambda\sqrt{f'_c}$) | 101 | 0.131 | 53% | 22 | 1.033 | 5% |
| All NWC | AASHTO LRFD | 139 | 0.129 | 52% | 53 | 1.739 | 45% |
| | Ramirez and Russell | 144 | 0.155 | 37% | 56 | 1.820 | 39% |
| | Mitchell et al. | 139 | 0.187 | 31% | 53 | 2.269 | 58% |
| | Expr. 1 ($\Delta f_p$ and $E_c$) | 64 | 0.429 | 47% | 14 | 2.040 | 7% |
| | Expr. 2 ($\Delta f_p$ and $\lambda$) | 139 | 0.129 | 52% | 53 | 1.739 | 45% |
| | Expr. 3 ($\lambda\sqrt{f'_c}$) | 144 | 0.155 | 37% | 56 | 1.988 | 39% |
| | Expr. 4 ($\Delta f_p$ and $\lambda\sqrt{f'_c}$) | 139 | 0.187 | 31% | 53 | 2.269 | 58% |
| | Expr. 5 ($\Delta f_p$ and $\lambda\sqrt{f'_c}$) | 139 | 0.158 | 40% | 53 | 1.925 | 47% |

Notes:

† AASHTO LRFD (Eq. 19), Ramirez and Russell (Eq. 20), Mitchell et al. (Eq. 21), Potential Expression 1 (Eq. 35), Potential Expression 2 (Eq. 36), Potential Expression 3 (Eq. 37), Potential Expression 4 (Eq. 38), Potential Expression 5 (Eq. 39); $\Delta f_p$ indicates $f_{ps}$-$f_{pe}$

## POTENTIAL EXPRESSIONS FOR FLEXURAL BOND LENGTH

Several potential expressions were developed for flexural bond length. These expressions introduce the use of concrete elastic modulus ($E_c$) and the λ-factor with the previously used parameters of $f_{ps}$, $f_{pe}$, and $d_b$.

Five potential expressions for predicting the flexural bond length of LWC were developed. The potential expressions for LWC were based on the Ramirez and Russell expression and Mitchell et al. expression that were originally developed using data from NWC specimens. The NWC expressions were used as the basis for the LWC expressions in an attempt to provide a smooth transition between the expressions for LWC and NWC. The Potential Expression 1 is given by Eq. 35 and was derived by substituting $\sqrt{f'_c}$ with $E_c/1820$ in the Ramirez and Russell expression, multiplying it by $(f_{ps}-f_{pe})/90$, and then rounding up. The mean $f_{ps}-f_{pe}$ for the LWC multi-strand I-beam or T-beam specimens was approximately 90 ksi (62 MPa).

Potential Expression 2 is given by Eq. 36 and is the flexural bond length portion of the AASHTO LRFD Bridge Design Specifications expression for development length divided by the λ-factor. Potential Expression 3 also includes the λ-factor and is given by Eq. 37. This expression is simply the Ramirez and Russell expression with the $\sqrt{f'_c}$ term multiplied by the λ-factor, but without the inequality to limit compressive strength. The λ-factor was included in the Mitchell et al. expression to give Potential Expression 4 (Eq. 38). The Ramirez and Russell expression was multiplied by $(f_{ps}-f_{pe})/90$ and then rounded to give Eq. 39, which is Potential Expression 5. Potential Expression 5 predicts flexural bond lengths that are 18 percent longer than Potential Expression 4.

$$\ell_{fb} = \frac{4600(f_{ps} - f_{pe})d_b}{E_c} \quad \text{(Eq. 35)}$$

$$\ell_{fb} = \frac{(f_{ps} - f_{pe})d_b}{\lambda} \quad \text{(Eq. 36)}$$

$$\ell_{fb} = \frac{225 d_b}{\lambda\sqrt{f'_c}} \quad \text{(Eq. 37)}$$

$$\ell_{fb} = \frac{\sqrt{4.5}(f_{ps} - f_{pe})d_b}{\lambda\sqrt{f'_c}} \quad \text{(Eq. 38)}$$

$$\ell_{fb} = \frac{2.5(f_{ps} - f_{pe})d_b}{\lambda\sqrt{f'_c}} \quad \text{(Eq. 39)}$$

The test-to-prediction ratios determined for the LWC specimens using the five potential expressions are given in Table 48. Potential Expressions 1 and 2, which included $E_c$ and the λ-factor, respectively, gave conservative predictions for all of the tests ending in bond failure.

Potential Expressions 1 and 2 also gave a larger percentage of overly-conservative predictions for the specimens ending in flexural failure than the AASHTO LRFD Bridge Design Specifications expression. Potential Expression 3, which included the λ-factor and $\sqrt{f'_c}$, gave unconservative predictions for 5 percent of the specimens ending in bond failure. For specimens ending in a flexural failure, Potential Expression 3 had a smaller percentage of specimens with overly conservative ratios (i.e., with ratios less than or equal to 1.0), but some tests had very large predicted flexural bond lengths (i.e., a low minimum ratio). Potential Expression 4 had ratios similar to the Ramirez and Russell expression and Potential Expression 5 had ratios similar to the AASHTO LRFD Bridge Design Specifications expression.

The test-to-predicted flexural bond length is given in Table 48 for the NWC specimens. The ratios for the potential expressions are given for informational purposes only. Potential Expression 1 includes $E_c$ and for the limited number NWC specimens with a reported $E_c$, the percentage of unconservative predictions for tests ending in bond failure were considerably less than the AASHTO LRFD Bridge Design Specifications expression.

## COMPARISONS WITH PREDICTED DEVELOPMENT LENGTH

The following section discusses the test-to-prediction ratios for the specimens in the TFHRC Database with embedment length tests. The experimentally determined development lengths (i.e., the tested strand embedment length) were compared to the predicted development lengths using a test-to-prediction ratio. The tested embedment length is referred to as the "test."

### PUBLISHED EXPRESSIONS FOR DEVELOPMENT LENGTH

The expressions used for predicting flexural bond length include the AASHTO LRFD Bridge Design Specifications expression (Eq. 12) with the κ-factor taken as 1.0, the Ramirez and Russell expression (Eq. 13), and the Mitchell et al. expression (Eq. 15).

The test-to-prediction ratios for development length are given in Table 49 through Table 51. Table 49 gives the ratios for all LWC specimens and all NWC specimens. The AASHTO LRFD Bridge Design Specifications expression gave conservative predictions of development length for all of the LWC specimens. The other two published expressions gave a few unconservative predictions of development length for specimens ending in bond failure. All three published prediction expressions gave a considerable number of unconservative predictions of development length for NWC specimens ending in bond failure. For both the LWC and NWC specimens, the Mitchell et al. expression had a higher percentage of unconservative predictions than the AASHTO LRFD Bridge Design Specifications expression for tests ending in bond failure. The Ramirez and Russell expression had a higher percentage of unconservative predictions than the AASHTO LRFD Bridge Design Specifications expression for LWC specimens, but a lower percentage for the NWC specimens. Table 50 for LWC specimens and Table 51 for NWC

specimens show that the unconservative predictions for the three expressions were from tests on multi-strand I-beam or T-beam specimens and not from rectangular specimens.

**Table 49. Test-to-Prediction Ratio of Development Length by Concrete Mixture Type.**

| | | Flexural Failures | | | Bond Failures | | |
|---|---|---|---|---|---|---|---|
| **Concrete Mix Type** | **Design Expression†** | **No.** | **Min.** | **Percent ≤ 1.0** | **No.** | **Max.** | **Percent > 1.0** |
| All LWC | AASHTO LRFD | 120 | 0.373 | 73% | 27 | 0.949 | 0% |
| | Ramirez and Russell | 104 | 0.367 | 46% | 25 | 1.096 | 12% |
| | Mitchell et al. | 104 | 0.416 | 35% | 25 | 1.245 | 16% |
| | Expr. 1.: $\ell_t(E_c)$, $\ell_{fb}(E_c)$ | 117 | 0.237 | 91% | 26 | 0.930 | 0% |
| | Expr. 2: $\ell_t(E_c)$, $\ell_{fb}$(LRFD) | 117 | 0.289 | 81% | 26 | 0.947 | 0% |
| | Expr. 3: $\ell_t(\lambda\sqrt{f'_c})$, $\ell_{fb}(\lambda)$ | 104 | 0.314 | 75% | 25 | 0.987 | 0% |
| | Expr. 4: $\ell_t(\lambda\sqrt{f'_c})$, $\ell_{fb}$(LRFD) | 104 | 0.332 | 68% | 25 | 0.987 | 0% |
| All NWC | AASHTO LRFD | 144 | 0.305 | 65% | 55 | 1.595 | 44% |
| | Ramirez and Russell | 144 | 0.374 | 53% | 55 | 1.432 | 33% |
| | Mitchell et al. | 144 | 0.439 | 38% | 55 | 1.712 | 55% |
| | Expr. 1.: $\ell_t(E_c)$, $\ell_{fb}(E_c)$ | 46 | 0.558 | 54% | 9 | 1.579 | 11% |
| | Expr. 2: $\ell_t(E_c)$, $\ell_{fb}$(LRFD) | 46 | 0.473 | 63% | 9 | 1.279 | 11% |
| | Expr. 3: $\ell_t(\lambda\sqrt{f'_c})$, $\ell_{fb}(\lambda)$ | 144 | 0.321 | 63% | 55 | 1.432 | 45% |
| | Expr. 4: $\ell_t(\lambda\sqrt{f'_c})$, $\ell_{fb}$(LRFD) | 144 | 0.321 | 63% | 55 | 1.432 | 45% |

Notes:

†AASHTO LRFD (Eq. 12) with the κ-factor taken as 1.0, Ramirez and Russell (Eq. 13), Mitchell et al. (Eq. 15), Potential Expression 1 (Eq. 40), Potential Expression 2 (Eq. 41), Potential Expression 3 (Eq. 42), Potential Expression 4 (Eq. 43)

**Table 50. Test-to-Prediction Ratio of Development Length for LWC by Specimen Type.**

| | | Flexural Failures | | | Bond Failures | | |
|---|---|---|---|---|---|---|---|
| **Specimen Type** | **Design Expression†** | **No.** | **Min.** | **Percent ≤ 1.0** | **No.** | **Max.** | **Percent > 1.0** |
| Single-strand rect.: LWC | AASHTO LRFD | 34 | 0.866 | 47% | 2 | 0.881 | 0% |
| | Ramirez and Russell | 18 | 1.078 | 0% | 0 | -- | -- |
| | Mitchell et al. | 18 | 1.309 | 0% | 0 | -- | -- |
| | Expr. 1.: $\ell_t(E_c)$, $\ell_{fb}(E_c)$ | 34 | 0.631 | 82% | 2 | 0.670 | 0% |
| | Expr. 2: $\ell_t(E_c)$, $\ell_{fb}$(LRFD) | 34 | 0.711 | 59% | 2 | 0.798 | 0% |
| | Expr. 3: $\ell_t(\lambda\sqrt{f'_c})$, $\ell_{fb}(\lambda)$ | 18 | 0.896 | 33% | 0 | -- | -- |
| | Expr. 4: $\ell_t(\lambda\sqrt{f'_c})$, $\ell_{fb}$(LRFD) | 18 | 0.984 | 11% | 0 | -- | -- |
| Multi-strand rect.: LWC | AASHTO LRFD | 26 | 0.373 | 100% | 14 | 0.705 | 0% |
| | Ramirez and Russell | 26 | 0.367 | 100% | 14 | 0.559 | 0% |
| | Mitchell et al. | 26 | 0.416 | 100% | 14 | 0.775 | 0% |
| | Expr. 1.: $\ell_t(E_c)$, $\ell_{fb}(E_c)$ | 26 | 0.237 | 100% | 14 | 0.508 | 0% |
| | Expr. 2: $\ell_t(E_c)$, $\ell_{fb}$(LRFD) | 26 | 0.289 | 100% | 14 | 0.581 | 0% |
| | Expr. 3: $\ell_t(\lambda\sqrt{f'_c})$, $\ell_{fb}(\lambda)$ | 26 | 0.314 | 100% | 14 | 0.587 | 0% |
| | Expr. 4: $\ell_t(\lambda\sqrt{f'_c})$, $\ell_{fb}$(LRFD) | 26 | 0.332 | 100% | 14 | 0.623 | 0% |
| Multi-strand I-beam or T-beam: LWC | AASHTO LRFD | 60 | 0.500 | 75% | 11 | 0.949 | 0% |
| | Ramirez and Russell | 60 | 0.657 | 37% | 11 | 1.096 | 27% |
| | Mitchell et al. | 60 | 0.700 | 17% | 11 | 1.245 | 36% |
| | Expr. 1.: $\ell_t(E_c)$, $\ell_{fb}(E_c)$ | 57 | 0.423 | 93% | 10 | 0.930 | 0% |
| | Expr. 2: $\ell_t(E_c)$, $\ell_{fb}$(LRFD) | 57 | 0.490 | 86% | 10 | 0.947 | 0% |
| | Expr. 3: $\ell_t(\lambda\sqrt{f'_c})$, $\ell_{fb}(\lambda)$ | 60 | 0.486 | 77% | 11 | 0.987 | 0% |
| | Expr. 4: $\ell_t(\lambda\sqrt{f'_c})$, $\ell_{fb}$(LRFD) | 60 | 0.522 | 72% | 11 | 0.987 | 0% |

Notes:

†AASHTO LRFD (Eq. 12) with the κ-factor taken as 1.0, Ramirez and Russell (Eq. 13), Mitchell et al. (Eq. 15), Potential Expression 1 (Eq. 40), Potential Expression 2 (Eq. 41), Potential Expression 3 (Eq. 42), Potential Expression 4 (Eq. 43)

**Table 51. Test-to-Prediction Ratio of Development Length for NWC by Specimen Type.**

| | | Flexural Failures | | | Bond Failures | | |
|---|---|---|---|---|---|---|---|
| **Specimen Type** | **Design Expression†** | **No.** | **Min.** | **Percent ≤ 1.0** | **No.** | **Max.** | **Percent > 1.0** |
| Single-strand rect.: NWC | AASHTO LRFD | 24 | 0.305 | 100% | 10 | 0.829 | 0% |
| | Ramirez and Russell | 24 | 0.374 | 100% | 10 | 0.699 | 0% |
| | Mitchell et al. | 24 | 0.439 | 92% | 10 | 0.829 | 0% |
| | Expr. 1.: $\ell_t(E_c)$, $\ell_{fb}(E_c)$ | 0 | -- | -- | 0 | -- | -- |
| | Expr. 2: $\ell_t(E_c)$, $\ell_{fb}$(LRFD) | 0 | -- | -- | 0 | -- | -- |
| | Expr. 3: $\ell_t(\lambda\sqrt{f'_c})$, $\ell_{fb}(\lambda)$ | 24 | 0.321 | 100% | 10 | 0.733 | 0% |
| | Expr. 4: $\ell_t(\lambda\sqrt{f'_c})$, $\ell_{fb}$(LRFD) | 24 | 0.321 | 100% | 10 | 0.733 | 0% |
| Multi-strand rect.: NWC | AASHTO LRFD | 31 | 0.443 | 71% | 6 | 0.825 | 0% |
| | Ramirez and Russell | 31 | 0.405 | 52% | 6 | 0.803 | 0% |
| | Mitchell et al. | 31 | 0.519 | 42% | 6 | 0.953 | 0% |
| | Expr. 1.: $\ell_t(E_c)$, $\ell_{fb}(E_c)$ | 11 | 0.558 | 100% | 5 | 0.962 | 0% |
| | Expr. 2: $\ell_t(E_c)$, $\ell_{fb}$(LRFD) | 11 | 0.473 | 100% | 5 | 0.782 | 0% |
| | Expr. 3: $\ell_t(\lambda\sqrt{f'_c})$, $\ell_{fb}(\lambda)$ | 31 | 0.426 | 71% | 6 | 0.803 | 0% |
| | Expr. 4: $\ell_t(\lambda\sqrt{f'_c})$, $\ell_{fb}$(LRFD) | 31 | 0.426 | 71% | 6 | 0.803 | 0% |
| Multi-strand I-beam or T-beam: NWC | AASHTO LRFD | 89 | 0.585 | 54% | 39 | 1.595 | 62% |
| | Ramirez and Russell | 89 | 0.606 | 40% | 39 | 1.432 | 46% |
| | Mitchell et al. | 89 | 0.712 | 22% | 39 | 1.712 | 77% |
| | Expr. 1.: $\ell_t(E_c)$, $\ell_{fb}(E_c)$ | 35 | 0.599 | 40% | 4 | 1.579 | 25% |
| | Expr. 2: $\ell_t(E_c)$, $\ell_{fb}$(LRFD) | 35 | 0.622 | 51% | 4 | 1.279 | 25% |
| | Expr. 3: $\ell_t(\lambda\sqrt{f'_c})$, $\ell_{fb}(\lambda)$ | 89 | 0.621 | 51% | 39 | 1.432 | 64% |
| | Expr. 4: $\ell_t(\lambda\sqrt{f'_c})$, $\ell_{fb}$(LRFD) | 89 | 0.621 | 51% | 39 | 1.432 | 64% |

Notes:

†AASHTO LRFD (Eq. 12) with the κ-factor taken as 1.0, Ramirez and Russell (Eq. 13), Mitchell et al. (Eq. 15), Potential Expression 1 (Eq. 40), Potential Expression 2 (Eq. 41), Potential Expression 3 (Eq. 42), Potential Expression 4 (Eq. 43)

## POTENTIAL EXPRESSIONS FOR DEVELOPMENT LENGTH

Several potential expressions were created to predict strand development length. These expressions introduce the use of concrete elastic modulus ($E_c$) and the λ-factor with the previously used parameters of $f_{ps}$, $f_{pe}$, and $d_b$. In previous sections of this report, the $E_c$ and λ-factor parameters were used in potential expressions to predict transfer length and flexural bond length.

Prediction expressions for flexural bond length that have parameters for LWC members that are similar to parameters for NWC members should be easier for designers to use than substantially different expressions. From Table 48, the Ramirez and Russell expression gave similar ratios for LWC specimens and uses the $d_b/\sqrt{f'_c}$ term not in the AASHTO LRFD Bridge Design Specifications expression. Also, excluding the $(f_{ps}-f_{pe})$ parameter from the flexural bond length term implies that in order to develop a larger strand stress a longer length of bond is not necessarily required to ensure that a bond failure does not occur at nominal flexural capacity. For this reason, potential expressions for development length did not include a flexural bond length term that were a multiple of $d_b/\sqrt{f'_c}$. The AASHTO LRFD Bridge Design Specifications expression, the Mitchell et al. expression, and Potential Expressions 2, 4, and 5 for flexural bond length all included the term $(f_{ps}-f_{pe})/d_b$. The potential expressions for development length include the $(f_{ps}-f_{pe})/d_b$ term.

Four potential expressions for predicting the development length of LWC were evaluated. The first two expressions included the concrete elastic modulus and the second two included the λ-factor. In each pair of expressions, the first expression included concrete elastic modulus or the λ-factor in the flexural bond length term, and the second expression used the flexural bond length term from the AASHTO LRFD Bridge Design Specifications. Potential Expressions 1 and 2, given by Eq. 40 and Eq. 41, include the transfer length term based on concrete elastic modulus given by Eq. 31. The transfer length term given by Eq. 34 includes the λ-factor and is used in Potential Expressions 3 and 4. Potential Expressions 3 and 4 are given by Eq. 42 and Eq. 43. The calculations of test-to-prediction ratios included an inequality to limit the effect of concrete strength of $40d_b$ on the transfer length term of the potential expressions.

$$\ell_d = \frac{220{,}000 d_b}{E_{ci}} + \frac{4600\left(f_{ps} - f_{pe}\right)d_b}{E_c} \quad \text{(Eq. 40)}$$

$$\ell_d = \frac{220{,}000 d_b}{E_{ci}} + \left(f_{ps} - f_{pe}\right)d_b \quad \text{(Eq. 41)}$$

$$\ell_d = \frac{120 d_b}{\lambda\sqrt{f'_c}} + \frac{\left(f_{ps} - f_{pe}\right)d_b}{\lambda} \quad \text{(Eq. 42)}$$

$$\ell_d = \frac{120 d_b}{\lambda\sqrt{f'_c}} + \left(f_{ps} - f_{pe}\right)d_b \quad \text{(Eq. 43)}$$

The test-to-prediction ratios for development length determined using the four potential expressions are given in Table 49 for LWC and NWC specimens. For LWC specimens, all four expressions gave conservative predictions of development length. For NWC specimens, Potential Expressions 1 and 2 gave fewer unconservative predictions than the AASHTO LRFD expression and Potential Expressions 3 and 4 gave a similar number of unconservative predictions as the AASHTO LRFD expression. From Table 51, the unconservative test results were from multi-strand I-beam or T-beam specimens.

In Table 49, a comparison of Potential Expression 2 with Potential Expression 1 for LWC specimens shows that while the percentage of conservatively predicted specimens ending in bond failure is the same, the percentage of overly-conservative predictions for specimens ending in flexural failure is less. This indicates that Potential Expression 2 provided the same level of conservatism for predicting the bond failures without being as overly-conservative on flexural failures. Similar observations can be made in a comparison of Potential Expression 4 with Potential Expression 3 for LWC specimens.

## CALCULATED DEVELOPMENT LENGTH USING KAPPA-FACTOR

The AASHTO LRFD Bridge Design Specifications[1] use the κ-factor to provide additional safety for the "worst-case characteristics of strands shipped prior to 1997." Article 5.11.4.2 defines the κ-factor as 1.0 for members with a depth less than or equal to 24 inches (610 mm) and 1.6 for members with a depth greater than 24 inches (610 mm). As given in Table 49, the expression for predicting development length in the AASHTO LRFD Bridge Design Specifications was unconservative for 44 percent of the NWC specimens that failed in bond.

Table 52 gives the test-to-prediction ratios determined using the κ-factor multiplied by the AASHTO LRFD Bridge Design Specifications expression, Potential Expression 2, and Potential Expression 4. For NWC specimens, 4 percent of the predicted ratios determined using the AASHTO LRFD Bridge Design Specifications were still unconservative, even using the κ-factor. Potential Expression 2 had conservative predictions for all of the specimens that failed in bond. Potential Expression 4 had a slightly larger number of unconservative predictions as compared to the AASHTO LRFD Bridge Design Specifications expression. All of the unconservative predictions had a depth less than or equal to 24 inch (610 mm), so the κ-factor was equal to 1.0.

**Table 52. Test-to-Prediction Ratio of Development Length using the κ-factor by Concrete Mixture Type.**

| | | Flexural Failures | | | Bond Failures | | |
|---|---|---|---|---|---|---|---|
| **Specimen Type** | **Design Expression†** | **No.** | **Min.** | **Percent ≤ 1.0** | **No.** | **Max.** | **Percent > 1.0** |
| All LWC | AASHTO LRFD | 120 | 0.373 | 85% | 27 | 0.949 | 0% |
| | Expr. 2: $\ell_t(E_c)$, $\ell_{fb}$(LRFD) | 117 | 0.289 | 87% | 26 | 0.947 | 0% |
| | Expr. 4: $\ell_t(\lambda\sqrt{f'_c})$, $\ell_{fb}$(LRFD) | 104 | 0.332 | 84% | 25 | 0.987 | 0% |
| All NWC | AASHTO LRFD | 144 | 0.305 | 85% | 55 | 1.173 | 4% |
| | Expr. 2: $\ell_t(E_c)$, $\ell_{fb}$(LRFD) | 46 | 0.425 | 89% | 9 | 0.933 | 0% |
| | Expr. 4: $\ell_t(\lambda\sqrt{f'_c})$, $\ell_{fb}$(LRFD) | 144 | 0.321 | 84% | 55 | 1.224 | 7% |

Notes:
†AASHTO LRFD (Eq. 12) with the κ-factor determined using Article 5.11.4.2, Potential Expression 2 (Eq. 41), Potential Expression 4 (Eq. 43)

COMPARISON OF CALCULATED DEVELOPMENT LENGTH

The development lengths predicted by the Ramirez and Russell expression, Potential Expression 2, and Potential Expression 4 were compared to the prediction given by the AASHTO LRFD Bridge Design Specifications in Table 53 and Table 54. For each expression, the ratio of the predicted development length was determined. In Table 53 the ratios for all of the specimens are given. The ratios were grouped by failure mode of the embedment length test in Table 54. The number of specimens, the minimum ratio, maximum ratio, and mean ratio were given. A ratio greater than 1.0 indicates the development length determined by the potential expression was longer than the development length determined by the AASHTO LRFD Bridge Design Specifications expression.

As given in Table 53, the mean increase for LWC specimens would be 10 percent using Potential Expression 2 and less than 1 percent using Potential Expression 4. For NWC specimens, the mean predicted development length would be reduced using Potential Expression 2 or 4.

For the potential expressions, the largest increase in predicted development for the LWC specimens is 29 percent by Potential Expression 2. For the NWC specimens, the largest increase is 13 percent by Potential Expression 4. Both of these increases are for specimens in the TFHRC Database.

The Ramirez and Russell expression, which had a mean reduction of predicted transfer lengths for all of the NWC specimens, had a maximum increase of 81 percent. This increase is the largest of the three expressions compared in Table 53. From Table 54 this increase in predicted development length applies to specimens that failed in bond and specimens that failed in flexure.

This large increase in predicted development length accounts for the reduced number of unconservative predictions of bond failure given in Table 49.

**Table 53. Ratio of Predicted Development Length for LWC and NWC.**

| Concrete Mix Type† | Ratio of Predicted Development Length† | No. | Max. | Min. | Mean |
|---|---|---|---|---|---|
| All LWC | $\ell_{d,\text{Ramirez and Russell}} / \ell_{d,\text{LRFD}}$ | 129 | 1.370 | 0.687 | 0.929 |
| | $\ell_{d,\text{Expr.2}} / \ell_{d,\text{LRFD}}$ | 143 | 1.293 | 0.888 | 1.102 |
| | $\ell_{d,\text{Expr.4}} / \ell_{d,\text{LRFD}}$ | 129 | 1.178 | 0.842 | 1.003 |
| All NWC | $\ell_{d,\text{Ramirez and Russell}} / \ell_{d,\text{LRFD}}$ | 199 | 1.364 | 0.635 | 0.954 |
| | $\ell_{d,\text{Expr.2}} / \ell_{d,\text{LRFD}}$ | 55 | 0.945 | 0.844 | 0.911 |
| | $\ell_{d,\text{Expr.4}} / \ell_{d,\text{LRFD}}$ | 199 | 1.131 | 0.844 | 0.968 |

Notes:
†AASHTO LRFD (Eq. 12) with the κ-factor taken as 1.0, Ramirez and Russell (Eq. 13), Potential Expression 2 (Eq. 41), Potential Expression 4 (Eq. 43)

**Table 54. Ratio of Predicted Development Length by Failure Type.**

| Concrete Mixture Type | Ratio of Predicted Development Length† | Flexural Failures | | | | Bond Failures | | | |
|---|---|---|---|---|---|---|---|---|---|
| | | No. | Max. | Min. | Mean | No. | Max. | Min. | Mean |
| All LWC | $\ell_{d,\text{Ramirez and Russell}} / \ell_{d,\text{LRFD}}$ | 104 | 1.370 | 0.687 | 0.911 | 25 | 1.316 | 0.716 | 1.004 |
| | $\ell_{d,\text{Expr.2}} / \ell_{d,\text{LRFD}}$ | 117 | 1.293 | 0.888 | 1.100 | 25 | 1.285 | 1.003 | 1.113 |
| | $\ell_{d,\text{Expr.4}} / \ell_{d,\text{LRFD}}$ | 104 | 1.178 | 0.842 | 0.994 | 25 | 1.145 | 0.954 | 1.039 |
| All NWC | $\ell_{d,\text{Ramirez and Russell}} / \ell_{d,\text{LRFD}}$ | 144 | 1.292 | 0.687 | 0.919 | 55 | 1.364 | 0.635 | 1.046 |
| | $\ell_{d,\text{Expr.2}} / \ell_{d,\text{LRFD}}$ | 46 | 0.945 | 0.844 | 0.908 | 9 | 0.942 | 0.856 | 0.923 |
| | $\ell_{d,\text{Expr.4}} / \ell_{d,\text{LRFD}}$ | 144 | 1.131 | 0.844 | 0.955 | 55 | 1.131 | 0.864 | 1.003 |

Notes:
†AASHTO LRFD (Eq. 12) with the κ-factor taken as 1.0, Ramirez and Russell (Eq. 13), Potential Expression 2 (Eq. 41), Potential Expression 4 (Eq. 43)

## SUMMARY OF THE TRANSFER AND DEVELOPMENT LENGTH ANALYSIS

Transfer length measurements and development length test results were collected into the TFHRC Database. The transfer length measurements, flexural bond length, and development length was analyzed and compared to published prediction expressions and additional expressions (i.e., "potential expressions") that were developed as part of this research effort. The published expressions and potential expressions that gave the best predictions are summarized at the end of this section and will be proposed as prediction expressions for inclusion in the AASHTO LRFD Bridge Design Specifications.

### TRANSFER LENGTH

A graphical analysis was performed that plotted compressive strength versus normalized transfer length. The overall trend of the data was that normalized transfer length decreases slightly as compressive strength increases. The downward trend of transfer length with increasing compressive strength was no longer apparent when the parameter $\sqrt{f'_{ci}}$ was included as a normalizing parameter. The use of $f_{pt}$ with $E_{ci}$ or the $\lambda$-factor was better able to reduce the number of overestimated of transfer lengths for the LWC specimens.

The analysis of parameter combinations for predicting transfer length showed that certain parameters were better at predicting transfer length. The parameter $d_b$ alone, which is used in the current expression in the AASHTO LRFD Bridge Design Specifications, gave a poor correlation with transfer length for both LWC and NWC specimens. The parameter $\sqrt{f'_{ci}}$ gave a strong correlation with transfer length for both LWC and NWC specimens. For most parameter combinations the inclusion of $f_{pt}$ reduced the strength of the correlation. The best correlation for LWC specimens were from the $d_b/E_{ci}$ and $d_b/\lambda\sqrt{f'_{ci}}$ parameter combinations.

The comparison of measured and predicted transfer lengths showed that published expressions were more effective at predicting transfer length for both LWC and NWC specimens. The Buckner expression underestimated nearly all of the measured transfer lengths. The Barnes et al. expression overestimated all of the measured transfer lengths for both LWC and NWC. The AASHTO LRFD Bridge Design Specifications expression, Meyer et al. expression, and Ramirez and Russell expression underestimated almost as many transfer lengths for the LWC specimens as the Buckner expression. The ACI 318 expression underestimated nearly all of the transfer lengths for the NWC specimens.

Four potential expressions were developed and compared to measured transfer lengths. Two of the potential expressions were intended to overestimate the transfer lengths and act as upper bound expressions. The other two potential expressions were intended to act as lower bound expressions and underestimate the transfer lengths. The upper bound expression using $E_{ci}$ overestimated nearly all of the measured transfer lengths for both the LWC and NWC specimens. The upper bound expression using the $\lambda$-factor was not as effective as the expression using $E_{ci}$. Both lower bound expressions were able to overestimate all of the LWC and NWC

data. For the LWC specimens, the lower bound expression using $E_{ci}$ gave test-to-prediction ratio closer to 1.0 than the published lower bound expression by Barnes et al. This indicates that the lower bound expression using $E_{ci}$ gave a better prediction as it was not as overly-conservative as the Barnes et al. expression.

## FLEXURAL BOND LENGTH

A graphical analysis of flexural bond lengths was performed. The normalized flexural bond lengths were compared to compressive strength. The considerable scatter in the data made it difficult to draw strong conclusions from the figures. None of the groups of normalizing parameters are able to conservatively predict all of the tests ending in a bond failure and also not be overly conservative for tests ending in flexural failure. The approach taken in this research effort is to propose an expression that places strong emphasis on minimizing the number of tests ending in bond failure that are unconservative predicted, while reducing the number flexural failures whose prediction is overly-conservative.

An analysis of flexural bond length predictions using published expressions showed that the AASHTO LRFD Bridge Design Specifications expression and the Ramirez and Russell expression had the same small percentage of unconservative predictions for tests on LWC specimens ending in bond failure. The Mitchell et al. expression had a slightly higher number of unconservative predictions.

The analysis of flexural bond length predictions using potential expressions showed that the expression using $E_c$ had no unconservative predictions for LWC specimens. The potential expressions that included the $\lambda$-factor had the same number or a fewer number of unconservative predictions than the AASHTO LRFD Bridge Design Specifications expression depending upon the other parameters in the expression.

## DEVELOPMENT LENGTH

The development length tests in the database were compared to published expressions for predicting development length. The AASHTO LRFD Bridge Design Specifications expression did not have any unconservative predictions of bond failure for LWC specimens. The Ramirez and Russell expression and Mitchell et al. expression all had a few unconservative predictions of development length for LWC specimens ending in a bond failure. The number of NWC specimens with unconservative predictions was considerably higher. By including the $\kappa$-factor in the expressions for development length, number of unconservative predictions of bond failure by the AASHTO LRFD Bridge Design Specifications expression was considerably reduced.

Potential expressions for predicting development length were also compared to the development length tests in the database. None of the potential expressions had any unconservative predictions of development length for LWC specimens ending in bond failure. The development lengths predicted using Potential Expression 2 and 4 were compared to the development length predicted using the AASHTO LRFD Bridge Design Specifications expression. For the LWC specimens in

the TFHRC Database, the mean development length predicted by Potential Expression 2 was 10 percent longer than the AASHTO LRFD Bridge Design Specifications prediction. The mean development length predicted by Potential Expression 4 was similar to the AASHTO LRFD Bridge Design Specifications prediction. The maximum increase in the development length predicted by the potential expressions when compared to the AASHTO LRFD Bridge Design Specifications prediction was 29 percent for the LWC specimens (i.e., for Potential Expression 2) and 13 percent for the NWC specimens (i.e., for Potential Expression 4).

The development length predicted using the Ramirez and Russell expression was also compared to the AASHTO LRFD Bridge Design Specifications prediction. The mean development length predicted by the Ramirez and Russell expression for NWC specimens was 4 percent less than the AASHTO LRFD Bridge Design Specifications prediction. For some NWC specimens in the TFHRC Database, the Ramirez and Russell expression predicted a 36 percent longer development length than the AASHTO LRFD Bridge Design Specifications expression. This significant increase in predicted development length accounts for the reduced number of unconservative predictions of bond failures by the Ramirez and Russell expression.

## PROPOSED EXPRESSIONS FOR TRANSFER AND DEVELOPMENT LENGTH

A new methodology is proposed for predicting the transfer and development length of prestressing strand. Upper and lower bound expressions are proposed for predicting transfer length and separate expressions are proposed for LWC and NWC members. A new expression for predicting development length is proposed. The transfer length term in the development length expression is consistent with the upper bound expression for transfer length.

### *Transfer Length*

New expressions are proposed for predicting the transfer length of prestressing strand. The AASHTO LRFD Bridge Design Specifications uses the simple expression given by Eq. 2 to predict transfer length. This expression was originally intended as a prediction of the mean transfer length for a group of transfer length measurements. The proposed philosophy is to use two expressions to predict transfer length. One expression will overestimate the transfer length and is intended to be conservative when determining the strand stress in provisions that calculate nominal shear resistance. The second expression is intended to underestimate the transfer length and be conservative when determining the strand stress in provisions that calculate the extreme fiber stresses. Another aspect of the proposed expressions for transfer length is that separate expressions for LWC members and NWC members are proposed.

The proposed expressions for predicting the transfer length of LWC members are given by Eq. 31 and Eq. 33. For NWC members, Eq. 9 and Eq. 44 are proposed. The transfer length predicted by Eq. 31 and Eq. 9 should be used to determine the $f_{pc}$, $f_{cpe}$, $f_{po}$, and $V_p$ terms in Article 5.8 relating to nominal resistance for shear and torsion. The transfer length used for determining fiber stresses that can be compared to the stress limits of Article 5.9.4 should be predicted by Eq. 33 and Eq. 44.

$$\ell_t = \frac{30d_b}{\sqrt{f'_{ci}}} \geq 10d_b \quad \text{(Eq. 44)}$$

Figure 92 and Figure 93 compare the predicted transfer length determined using the AASHTO LRFD Bridge Design Specifications expression and the proposed expressions. The measured transfer length is compared to the prediction given by the simple $60d_b$ expression in the AASHTO LRFD Bridge Design Specifications in Figure 92. A diagonal line in the figure indicates the prediction. The LWC specimens are shown in series by specimens with measured $E_{ci}$ values and a specimen without an $E_{ci}$ value. The series for the NWC specimens are specimens with a measured $f'_{ci}$ value and specimens without an $f'_{ci}$ value. The specimens were grouped to allow a direct comparison with the specimens in Figure 92. The AASHTO LRFD Bridge Design Specifications expression underestimates the transfer length of 10 percent of the LWC specimens and 21 percent of the NWC specimens. This indicates that when the transfer length is used to determine the strand prestress for the calculation of nominal resistance, the transfer length predicted by the AASHTO LRFD Bridge Design Specifications expression is unconservative for 10 percent of the LWC specimens and 21 percent of the NWC specimens. The rest of the transfer lengths are overestimated indicating that when the AASHTO LRFD Bridge Design Specifications expression for transfer length is used to determine concrete fiber stresses at a member end-region, the transfer length is unconservative for 90 percent of the LWC specimens and 79 percent of the NWC specimens.

In Figure 93 the measured transfer lengths are compared to the transfer lengths predicted by the proposed expressions. The data for LWC specimens with an $E_{ci}$ value and NWC specimens with an $f'_{ci}$ value are shown. The two diagonal lines in Figure 93 show the prediction given by the upper and lower bound expressions, respectively. The proposed expressions are unconservative for only 1 percent of LWC specimens and 15 percent of NWC when the transfer length is used to calculate nominal resistance and is not unconservative for any of specimens when used to determine concrete fiber stresses at member end-regions.

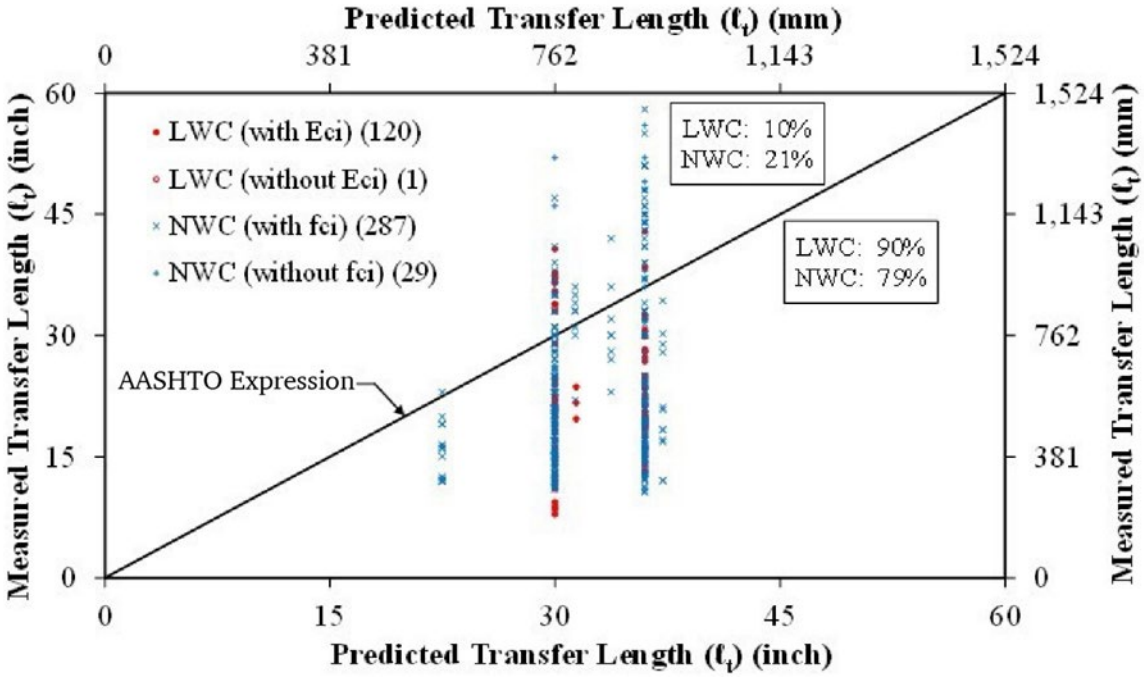


**Figure 92. Graph. Measured Transfer Length ($\ell_t$) Compared to Transfer Length Predicted by AASHTO Expression for Specimens in the TFHRC Database.**

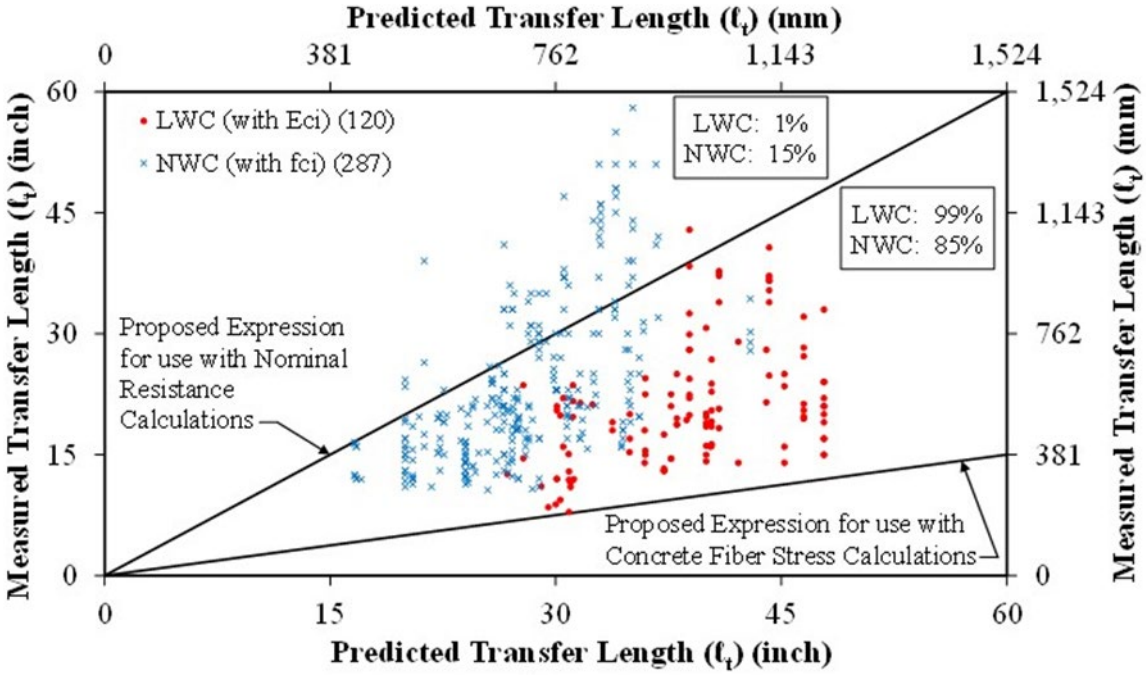


**Figure 93. Graph. Measured Transfer Length ($\ell_t$) Compared to Transfer Length Predicted by Proposed Expressions for Specimens in the TFHRC Database.**

***Development Length***

The AASHTO LRFD Bridge Design Specifications expression for development length uses Eq. 3 instead of Eq. 2 as the expression for the transfer length term. The proposed development length expression includes the transfer length expression used in other articles. The proposed expression uses the upper bound transfer length expression and is intended to provide a conservative estimate of the transfer length.

The proposed expression for the development length is given by Eq. 45. For LWC members, Eq. 45 is equivalent to Potential Expression 2 multiplied by the κ-factor. The $\ell_t$ term in Eq. 45 is given by Eq. 31. For NWC members the $\ell_t$ term in Eq. 45 is given by Eq. 32 and Eq. 45 is equivalent to Potential Expression 4 multiplied by the κ-factor.

$$\ell_d = \kappa\left[\ell_t + \left(f_{ps} - f_{pe}\right)d_b\right] \quad \text{(Eq. 45)}$$

Figure 94 through Figure 97 compare the predicted development length determined using the AASHTO LRFD Bridge Design Specifications expression and the proposed expressions. The embedment lengths for specimens with a depth less than or equal to 24 inches (610 mm) (i.e., κ-factor of 1.0) are shown in Figure 94 and Figure 95. Figure 96 and Figure 97 show the embedment lengths for specimens with a depth greater than 24 inches (610 mm) (i.e., κ-factor of 1.6). Each figure shows the embedment lengths in series by concrete type (i.e, LWC or NWC) and failure type (i.e., flexural failure or bond failure). A diagonal line in each figure indicates the prediction given by either the AASHTO LRFD expression or the proposed expressions. The percent of specimens ending in bond failure that were unconservatively underestimated is indicated in each for for the LWC specimens and NWC specimens. The percent of specimens ending in a flexural failure that were overestimated by the expressions is also indicated.

The embedment length is compared to the prediction given by the expression in the AASHTO LRFD Bridge Design Specifications in Figure 94 and Figure 96. The AASHTO LRFD Bridge Design Specifications expression gave conservative predictions of development length for all of the LWC specimens, unconservative estimates for 6 percent of the NWC specimens. Overly-conservative estimates for LWC and NWC specimens ending in flexural failure were 80 percent and 78 percent, respectively, for specimens with a depth of 24 inch (610 mm) or less. Nearly all of the specimens ending in flexural failure that had a depth greater than 24 inch (610 mm) were overestimated.

Figure 95 and Figure 97 compare the tested embedment length to the development length predicted by the proposed expression. The proposed expression gave conservative predictions of development length for all of the LWC specimens. The proposed expression had a similar percentage of unconservative predictions of bond failure and overly-conservative estimates of development length for flexural failure as the AASHTO LRFD Bridge Design Specifications expression.

There are several advantages of using the proposed expression for development length over the current expression in the AASHTO LRFD Bridge Design Specifications. From Table 53, the mean predicted development length for NWC using the proposed expression is 3 percent less than using the AASHTO LRFD Bridge Design Specifications expression, with a similar level of conservatism. In the proposed expressions, the transfer length term used in the development length expression is consistent with the transfer length expression used for nominal resistance, whereas in the AASHTO LRFD Bridge Design Specifications expression it is inconsistent. By including the transfer length term, the development length expression includes the beneficial effect of increased concrete strength on the development length.

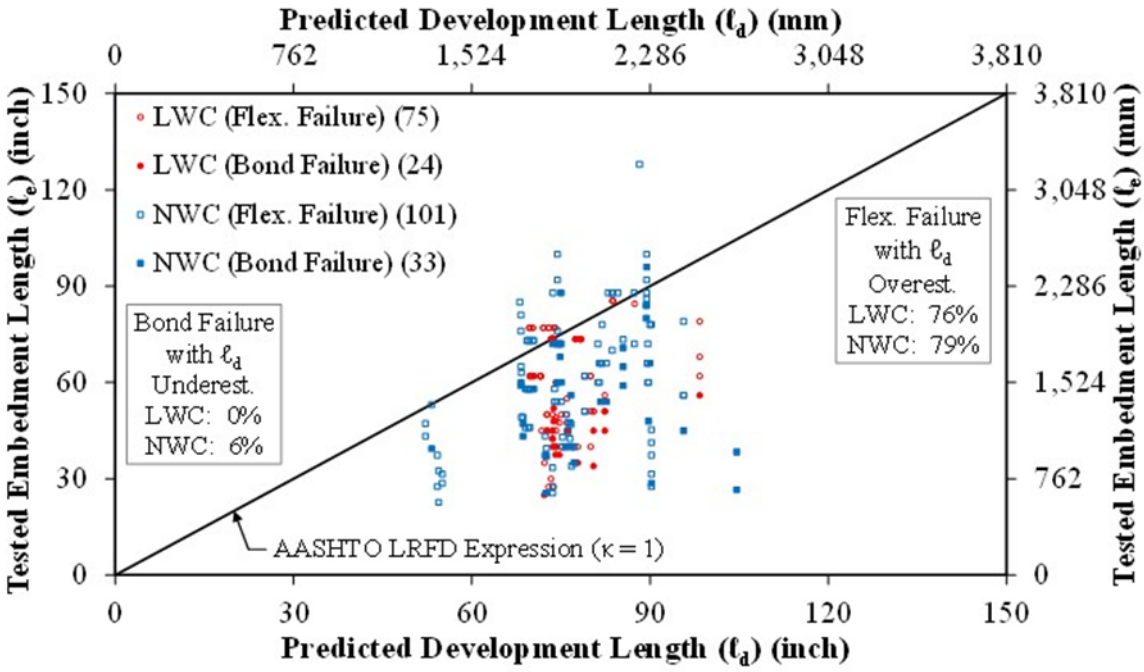


**Figure 94. Graph. Tested Embedment Length Compared to Development Length Predicted by AASHTO Expression for Specimens with κ = 1.0 in the TFHRC Database.**

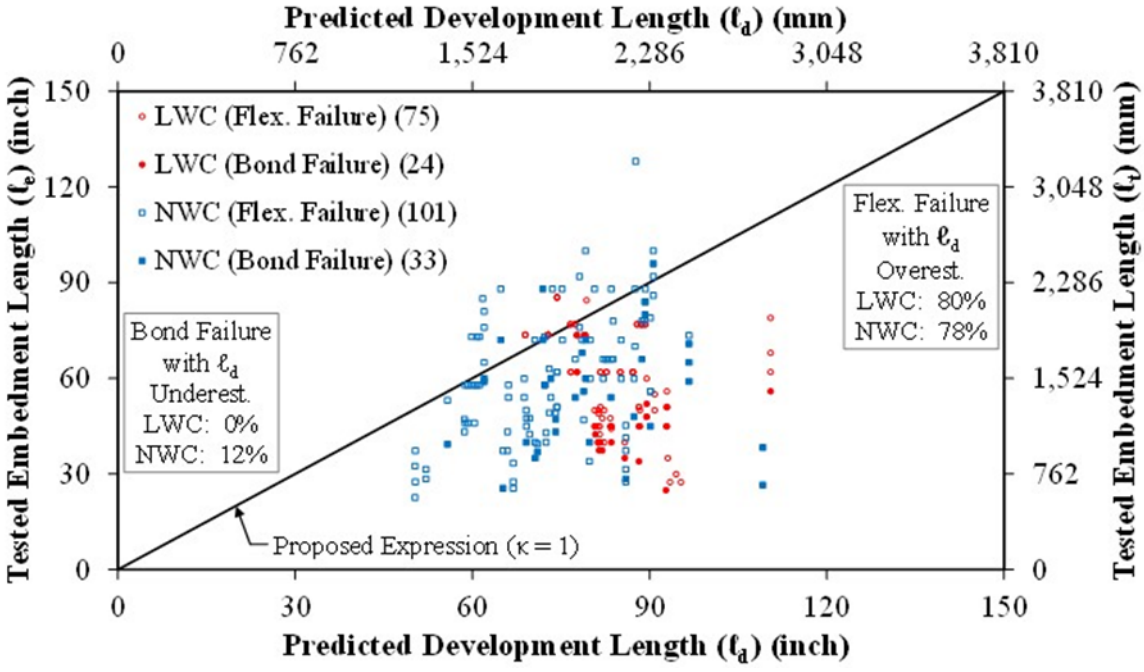


**Figure 95. Graph. Tested Embedment Length Compared to Development Length Predicted by Proposed Expression for Specimens with κ = 1.0 in the TFHRC Database.**

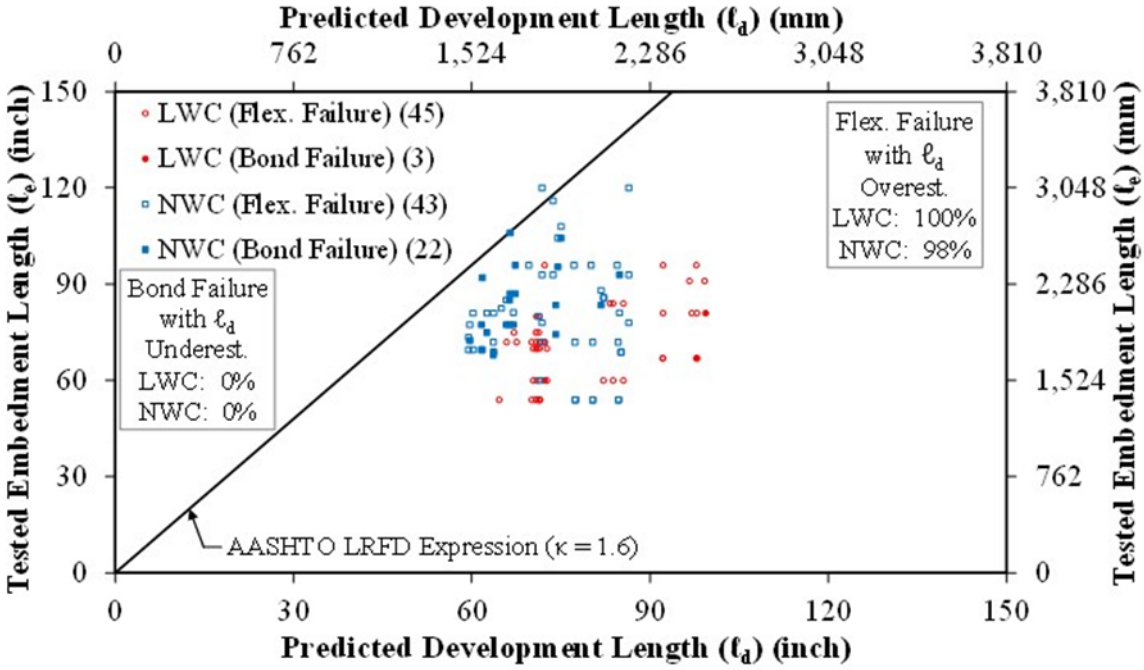


**Figure 96. Graph. Tested Embedment Length Compared to Development Length Predicted by AASHTO Expression for Specimens with κ = 1.6 in the TFHRC Database.**

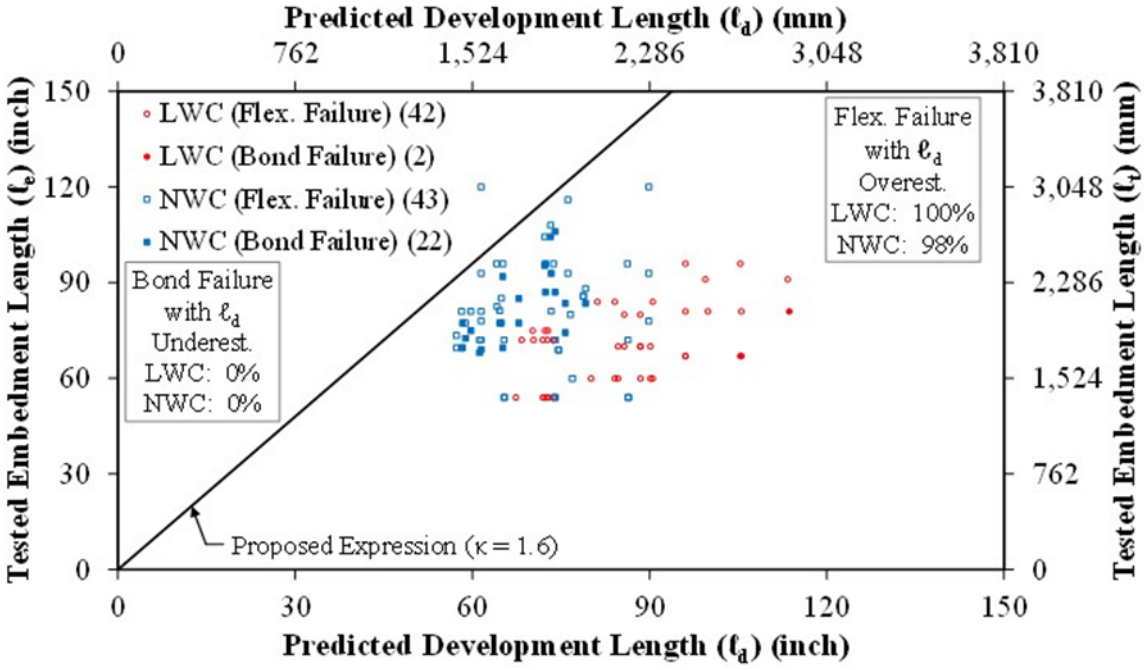


**Figure 97. Graph. Tested Embedment Length Compared to Development Length Predicted by Proposed Expression for Specimens with κ = 1.6 in the TFHRC Database.**

***Design Stress in the Pretensioned Strand***

The use of the proposed expression for transfer length requires a change to the expressions for the design stress in the pretensioned strand. The proposed expression for the design stress from the point where bonding commences to the end of the transfer length is given by Eq. 46. The proposed strand stress from the end of the transfer length to the end of the development of the strand is given by Eq. 47.

$$f_{px} = \frac{f_{pe}\ell_{px}}{\ell_t} \quad \text{(Eq. 46)}$$

$$f_{px} = f_{pe} + \frac{\ell_{px} - \ell_t}{\ell_d - \ell_t}\left(f_{ps} - f_{pe}\right) \quad \text{(Eq. 47)}$$

# CHAPTER 6. PRELIMINARY RECOMMENDATIONS FOR AASHTO LRFD SPECIFICATIONS

## INTRODUCTION

This chapter summarizes several preliminary recommended changes to the AASHTO LRFD Specifications. These recommended changes regarding strand bond build upon previous recommendations that were adopted by the AASHTO Subcommittee on Bridges and Structures (SCOBS) T-10 and were first introduced in the 2015 Interim Revisions.[11] The adopted changes included the definition of LWC and an expression for predicting concrete elastic modulus. The basis for these changes were previously described in a related document concerning the mechanical properties of LWC and are presented again for clarity.[8] Additional recommended changes to the AASHTO LRFD Bridge Design Specifications that are based upon the analysis described in this document are presented in this chapter. These additional recommendations are built upon the two previous recommendations.

The three changes to the AASHTO LRFD Bridge Design Specifications recommended in this chapter are in regards to the bond of prestressing strand in LWC members and NWC members. The first recommended change involves new and separate transfer length expressions for LWC members and NWC members. Another change involves adding the new transfer length expressions to the expression for development length. The final recommended change involves adding the new transfer length expression to the strand design stress expressions.

This document described transfer length measurements on 18 LWC prestress girders and development length tests on 12 of those girders that were conducted at TFHRC. Additional transfer length measurements and development length tests on LWC specimens and NWC specimens were found in the literature.[51-76] The recommended changes to the AASHTO LRFD Bridge Design Specifications were validated using the specimens from the TFHRC Database.

## NEW DEFINITION FOR LWC

The definition for lightweight concrete in the AASHTO LRFD Specifications[7] is in Article 5.2 and states the following:

> *Lightweight Concrete* – Concrete containing lightweight aggregate conforming to AASHTO M 195 and having an equilibrium density not exceeding 0.135 kcf, as determined by ASTM C567.

The previous LWC definition limited the unit weight for LWC to 0.120 kcf (1920 kg/m$^3$) and included definitions for sand-lightweight and all-lightweight concrete.[1] The new definition for LWC expanded the range of unit weights and eliminates the definitions for terms relating to the constituent materials in LWC.

The term "air-dry unit weight" was used in the previous definition; however this term is not found in ASTM C567 (Standard Test Method for Determining Density of Structural Lightweight Concrete).[50] The AASHTO LRFD term "air-dry unit weight" is interpreted to be equivalent to the ASTM C567 term "equilibrium density."

## NEW EXPRESSION FOR MODULUS OF ELASTICITY

The new expression for modulus of elasticity in the AASHTO LRFD Bridge Design Specifications[7] is in Article 5.4.2.4 and states the following:

> In the absence of measured data, the modulus of elasticity, $E_c$, for concretes with unit weights between 0.090 and 0.155 kcf and specified compressive strengths up to 15.0 ksi may be taken as:

$$E_c = 120{,}000\, K_1\, w_c^{2.0}\, f'^{0.33}_c \qquad (5.4.2.4\text{-}1)$$

The derivation for this expression for $E_c$ is described previously in another document.[8]

## PROPOSED EXPRESSIONS FOR STRAND TRANSFER LENGTH

The expression for transfer length in the AASHTO LRFD Bridge Design Specifications[7] is in the text of Article 5.9.4.3.1 which states the following:

> For the purpose of this Article, the transfer length may be taken as 60 strand diameters and the development length shall be taken as specified in Article 5.9.4.3.2.

The proposed definition of transfer length would have separate expressions for NWC and LWC. The expression for NWC was developed by Ramirez and Russell[30] as part of NCHRP Project 12-60. The expression for LWC is derived by substituting and expression for the concrete elastic modulus ($E_c$) into the Ramirez and Russell expression. The proposed text for the transfer length ($\ell_t$) expressions is as follows:

> For the purpose of this Article, the transfer length and the development length shall be taken as specified in Article 5.9.4.3.2.
>
> The transfer length of pretensioning strand from the point bonding commences shall be taken as:
>
> For normal weight concrete:

$$\ell_t = 120\, d_b / \sqrt{f'_{ci}} \geq 40\, d_b \qquad (5.9.4.3.2\text{-}1)$$

For lightweight concrete:

$$\ell_t = 220{,}000\, d_b / E_{ci} \geq 40\, d_b \qquad (5.9.4.3.2\text{-}2)$$

where:

$E_{ci}$ = modulus of elasticity of concrete at prestress transfer, may be determined using Eq. 5.4.2.4-1 unless specified

The transfer length determined by Eqs. 5.9.4.3.2-1 and 5.9.4.3.2-2 shall be multiplied by 0.25 when used to calculate the concrete extreme fiber stresses in Article 5.9.2.3

These expressions are intended to provide conservative over-estimates of the transfer length when the prestressing force is used to determine nominal resistance. The 0.25 factor used in the determination of concrete fiber stresses is intended to provide conservative under-estimates of the transfer length. The modulus of elasticity may be calculated using the specified concrete compressive strength and specified unit weight. Alternatively, the modulus of elasticity may be directly specified by the designer.

In Figure 98 the measured transfer lengths are compared to the transfer lengths predicted by the proposed expressions. The data for LWC specimens with an $E_{ci}$ value and NWC specimens with an $f'_{ci}$ value are shown. The two diagonal lines in Figure 98 show the prediction given by the upper and lower bound expressions, respectively. An overestimate of transfer length is conservative when the transfer length is used to determine the strand prestress for the calculation of nominal resistance. When transfer length is used to determine concrete fiber stresses at a member end-region, an underestimation of transfer length is conservative. The proposed expressions are unconservative for only 1 percent of LWC specimens and 15 percent of NWC when the transfer length is used to calculate nominal resistance and is not unconservative for any of specimens when used to determine concrete fiber stresses at member end-regions.

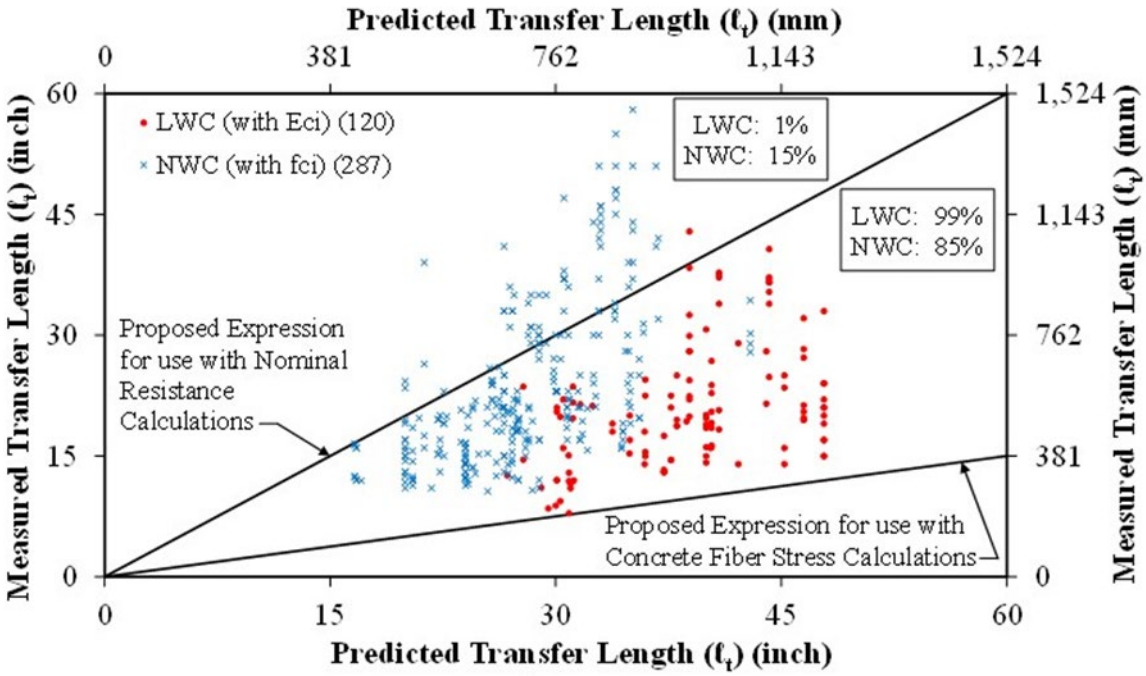


**Figure 98. Graph. Measured Transfer Length Compared to Transfer Length Predicted by the Proposed Expressions.**

## PROPOSED DESIGN EXPRESSION FOR STRAND DEVELOPMENT LENGTH

The proposed change to the development length expressions is to replace the transfer length term with the new definition of transfer length. The proposed text for the development length ($\ell_d$) expression is as follows:

> Pretensioning strand shall be bonded beyond the section required to develop $f_{ps}$ for a development length, $\ell_d$, in in., where $\ell_d$ shall satisfy:
>
> $$\ell_d \geq \kappa \left[\ell_t + (f_{ps} - f_{pe})\, d_b\right] \qquad (5.9.4.3.2\text{-}3)$$
>
> where:
>
> $\ell_t$ = transfer length determined using Eqs. 5.9.4.3.2-1 and 5.9.4.3.2-2

Figure 99 and Figure 100 compare the tested embedment length to the development length predicted by the proposed expression. Figure 99 shows the data specimens with a depth less than or equal to 24 inches (610 mm) (i.e., κ-factor of 1.0) and Figure 100 shows the data for specimens with a depth greater than 24 inches (610 mm) (i.e., κ-factor of 1.6). The LWC specimens and NWC specimens are differentiated as specimens ending in flexural failure and specimens ending in bond failure. Diagonal lines in the figure indicate the predicted development length. The proposed expression gave conservative predictions of development length for all of the LWC specimens. The proposed expression gave unconservative estimates of development

length for 12 percent of the NWC specimens when the κ-factor was taken as 1.0 and there were not any unconservative estimates when the κ-factor was taken as 1.6. The κ-factor was determined using the AASHTO LRFD Bridge Design Specifications.[7]

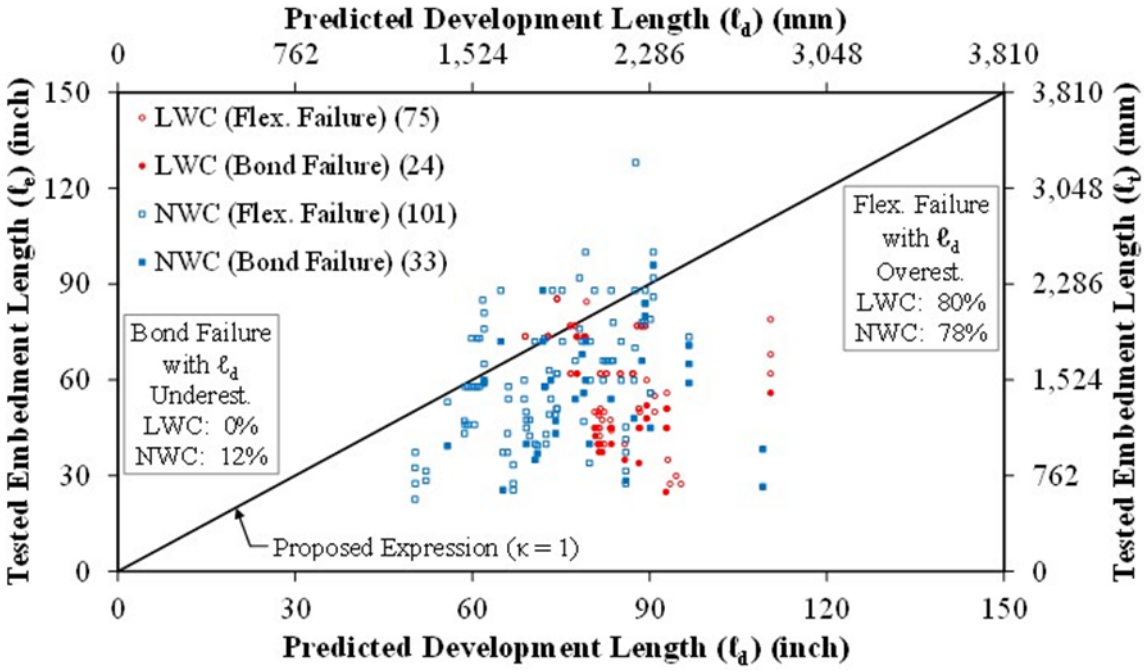


**Figure 99. Graph. Tested Embedment Length Compared to Development Length Predicted by Proposed Expression for Specimens with 24 inch Depth or Less.**

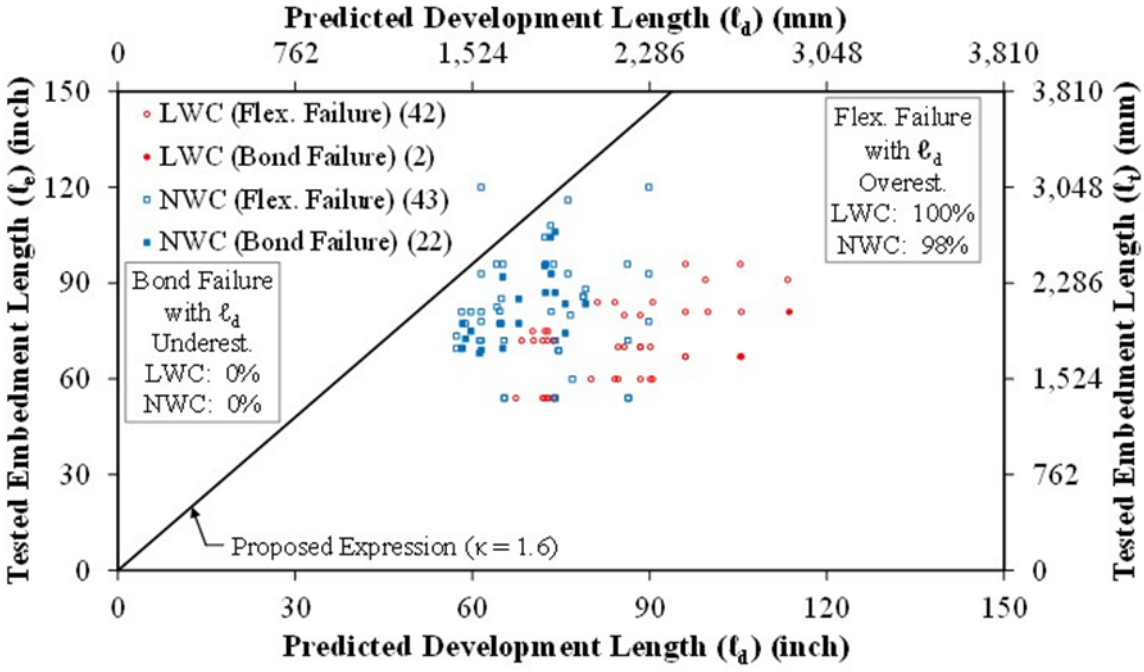


**Figure 100. Graph. Tested Embedment Length Compared to Development Length Predicted by Proposed Expression for Specimens with greater than 24 inch Depth.**

**PROPOSED DESIGN EXPRESSION FOR STRAND DESIGN STRESS**

The existing definition for transfer length is embedded in the expressions for strand design stress. The proposed change replaces the existing definition of transfer length with the new definition. The proposed text for the strand design stress ($f_{px}$) expression is as follows:

From the point where bonding commences to the end of transfer length:

$$f_{px} = f_{pe}\, \ell_{px} / \ell_t \qquad (5.9.4.3.2\text{-}4)$$

From the end of the transfer length and to the end of the development of the strand:

$$f_{px} = f_{pe} + [(\ell_{px} - \ell_t) / (\ell_d - \ell_t)]\, (f_{ps} - f_{pe}) \qquad (5.9.4.3.2\text{-}5)$$

# CHAPTER 7. CONCLUDING REMARKS

## INTRODUCTION

This document describes transfer length measurements on 30 LWC prestressed girders, development length tests on 12 LWC prestressed girders, describes a strand bond database, and presents potential revisions to the AASHTO LRFD Specifications relating to the transfer and development length of LWC and NWC. The proposed design expressions for transfer length and development length of prestressing strand were compared to tested values in a database including over 150 LWC specimens and over 350 NWC specimens that was collected as part of this research effort. A description of the database and the development and evaluation of prediction expressions is included in this document.

## SUMMARY OF EXPERIMENTAL RESULTS

The experimental research conducted at TFHRC investigated the bond performance of prestressing strand in high-strength LWC. The strand transfer length was measured on 18 prestressed girders and the strand development length was evaluated using 24 tests on the end-regions of 12 prestressed girders. Key test parameters included the lightweight aggregate, the size of the strand, the number of strand, the amount of shear reinforcement, and the girder depth. Three different concrete mix designs using three different lightweight aggregates were used. The mix designs included two expanded shales and one expanded slate. The concrete mixes used a blend of lightweight and normal-weight coarse aggregate and normal-weight sand. The design compressive strength ranged from 6 to 10 ksi (41 to 69 MPa) and the target unit weight ranged from 0.126 to 0.130 kcf (2020 to 2080 kg/m$^3$). The resulting concrete had a range in 28-day compressive strength of 8.6 to 9.7 ksi (59.3 to 66.9 MPa) and an air-dry density range of 0.125 to 0.132 kcf (2000 to 2110 kg/m$^3$).

The transfer length measurements were made on a total of 18 girders. The transfer length of each girder was determined from concrete surface strain measurements. Concrete strain profiles were determined from the strain measurements and the 95 percent Average Maximum Strain Method was used to determine the transfer length. A 53 percent increase in the mean transfer length was observed for girders with a 25 percent increase in stirrup spacing. As expected, the mean transfer length of girders with 0.6 inch (15 mm) nominal diameter strand was 33 percent longer than the mean transfer length of girders with 0.5 inch (13 mm) nominal diameter strand. The mean ratio of the long-term to immediately measured transfer lengths was 1.01 indicating only a slight increase in transfer length with time.

The development length was evaluated using 24 tests on the end-regions of 12 girders. Girder end tests on two of the three specimens with the larger number of strand (Girder Design 2) ended in a shear failure. This indicates that these specimens had a strand development length longer than the tested embedment length which was approximately 70 percent of the development

length determined using the AASHTO LRFD Bridge Design Specifications.[7] The remaining girder end tests resulted in flexural failures. Six of these tests had a strand slip greater than 0.010 inch (0.25 mm), which is the amount of slip considered to indicate a significant amount of slip.

## SUMMARY OF THE STRAND BOND DATABASE ANALYSIS

The measured transfer lengths in the database were analyzed using three methods: graphical analysis, statistical parameter analysis, and comparison with prediction expressions.

A graphical analysis was performed that plotted compressive strength versus normalized transfer length. The overall trend of the data was that normalized transfer length decreases slightly as compressive strength increases. The downward trend of transfer length with increasing compressive strength was no longer apparent when the parameter $\sqrt{f'_{ci}}$ was included as a normalizing parameter.

The analysis of parameter combinations for predicting transfer length showed that certain parameters were better at predicting transfer length. The parameter $d_b$ alone, which is used in the current expression in the AASHTO LRFD Bridge Design Specifications[7], gave a poor correlation with transfer length for both LWC and NWC specimens. The parameter $\sqrt{f'_{ci}}$ gave a strong correlation with transfer length for both LWC and NWC specimens. For most parameter combinations the inclusion of $f_{pt}$ reduced the strength of the correlation. The best correlation for LWC specimens were from the $d_b/E_{ci}$ and $d_b/\lambda\sqrt{f'_{ci}}$ parameter combinations.

The comparison of measured and predicted transfer lengths showed that published expressions were more effective at predicting transfer length for both LWC and NWC specimens. The Buckner expression underestimated nearly all of the measured transfer lengths. The Barnes et al. expression overestimated all of the measured transfer lengths for both LWC and NWC. The AASHTO LRFD Bridge Design Specifications expression, Meyer et al. expression, and Ramirez and Russell expression underestimated almost as many transfer lengths for the LWC specimens as the Buckner expression. The ACI 318 expression underestimated nearly all of the transfer lengths for the NWC specimens.

The development length tests in the database were compared to published expressions for predicting development length. The AASHTO LRFD Bridge Design Specifications expression did not have any unconservative predictions of bond failure for LWC specimens. The Ramirez and Russell expression and Mitchell et al. expression all had a few unconservative predictions of development length for LWC specimens ending in a bond failure. The number of NWC specimens with unconservative predictions was considerably higher. By including the κ-factor in the expressions for development length, number of unconservative predictions of bond failure by the AASHTO LRFD Bridge Design Specifications expression was considerably reduced.

Potential expressions for predicting development length were also compared to the development length tests in the database. None of the potential expressions had any unconservative predictions

of development length for LWC specimens ending in bond failure. The development lengths predicted using Potential Expression 2 and 4 were compared to the development length predicted using the AASHTO LRFD expression. For the LWC specimens in the TFHRC Database, the mean development length predicted by Potential Expression 2 was 10 percent longer than the AASHTO LRFD prediction. The mean development length predicted by Potential Expression 4 was similar to the AASHTO LRFD Bridge Design Specifications prediction. The maximum increase in the development length predicted by the potential expressions when compared to the AASHTO LRFD prediction was 29 percent for the LWC specimens (i.e., for Potential Expression 2) and 13 percent for the NWC specimens (i.e., for Potential Expression 4).

## PRELIMINARY RECOMMENDATIONS

A new methodology is proposed for predicting the transfer and development length of prestressing strand. Upper and lower bound expressions are proposed for predicting transfer length and separate expressions are proposed for LWC and NWC members. A new expression for predicting development length is proposed. The transfer length term in the development length expression is consistent with the upper bound expression for transfer length.

New expressions are proposed for predicting the transfer length of prestressing strand. The AASHTO LRFD Bridge Design Specifications[7] uses a simple expression to predict transfer length. This expression was originally intended as a prediction of the mean transfer length for a group of transfer length measurements. The proposed philosophy is to use two expressions to predict transfer length. One expression will overestimate the transfer length and is intended to be conservative when determining the strand stress in provisions that calculate nominal shear resistance. The second expression is intended to underestimate the transfer length and be conservative when determining the strand stress in provisions that calculate the extreme fiber stresses. Another aspect of the proposed expressions for transfer length is that separate expressions LWC members and NWC members are proposed.

The AASHTO LRFD Bridge Design Specifications' expression underestimates the transfer length of 10 percent of the LWC specimens and 21 percent of the NWC specimens. This indicates that when the transfer length is used to determine the strand prestress for the calculation of nominal resistance, the transfer length predicted by the AASHTO LRFD expression is unconservative for 10 percent of the LWC specimens and 21 percent of the NWC specimens. The rest of the transfer lengths are overestimated indicating that when the AASHTO LRFD Bridge Design Specifications' expression for transfer length is used to determine concrete fiber stresses at a member end-region, the transfer length is unconservative for 90 percent of the LWC specimens and 79 percent of the NWC specimens. The proposed expressions are unconservative for only 1 percent of LWC specimens and 15 percent of NWC when the transfer length is used to calculate nominal resistance and is not unconservative for any of specimens when used to determine concrete fiber stresses at member end-regions.

Using a κ-factor of 1.0, the AASHTO LRFD Bridge Design Specifications' expression gave conservative predictions of development length for all of the LWC specimens, but unconservative estimates for 44 percent of the NWC specimens. Using the κ-factor defined in the AASHTO LRFD Bridge Design Specifications, the expression still gave unconservative predictions for 4 percent of specimens. The proposed expression gave conservative predictions of development length for all of the LWC specimens. The proposed expression had a similar number of unconservative predictions of bond failure as the AASHTO LRFD Bridge Design Specifications' expression.

There are several advantages of using the proposed expression for development length over the current expression in the AASHTO LRFD Bridge Design Specifications. The mean predicted development length for NWC using the proposed expression is 3 percent less than using the AASHTO LRFD Bridge Design Specifications expression, with a similar level of conservatism. In the proposed expressions, the transfer length term used in the development length expression is consistent with the transfer length expression used for nominal resistance, whereas in the AASHTO LRFD Bridge Design Specifications it is inconsistent. By including the transfer length term, the development length expression includes the beneficial effect of increased concrete strength on the development length.

## CONCLUDING REMARKS

Future phases of this research compilation and analysis effort will include synthesis of past work on structural performance of LWC. The test results will be compared to the prediction expressions for nominal resistance in the AASHTO LRFD Specifications incorporating appropriate proposed revisions for LWC mechanical properties.

## ACKNOWLEDGMENTS

This document presents results from a research program and is intended to both facilitate broader understanding of the performance of lightweight concrete and to assist AASHTO SCOBS T-10 as they consider relevant revisions to Section 5 of the AASHTO LRFD Bridge Design Specifications.[1] It does not constitute a policy statement from FHWA. Additionally, the publication of this article does not necessarily indicate approval or endorsement of the findings, opinions, conclusions, or recommendations either inferred or specifically expressed herein by FHWA or the United States Government. This document was created by PSI on behalf of FHWA as part of contract DTFH61-10-D-00017.

The authors would like to acknowledge the work of the T-10 Ad-hoc Group on LWC Revisions to AASHTO LRFD Bridge Design Specifications for their assistance, helpful comments, and suggestions during the analysis and compilation of these results. The work of Matthew Swenty, who greatly assisted with the collection of the transfer and development length database, is

gratefully acknowledged by the authors. The authors would also like to gratefully acknowledge the TFHRC library staff who assisted in the collection of hundreds of articles relating to LWC.

# REFERENCES

## INTRODUCTION

This chapter gives the references for the document in three parts. The first part consists of general references cited in the document text. The second and third part consists of references for the transfer and development length data used in the TFHRC Database with LWC specimens and NWC specimens, respectively.

## GENERAL REFERENCES


1. AASHTO (2012), “AASHTO LRFD Bridge Design Specifications, Customary U.S. Units,” American Association of State Highway and Transportation Officials, Sixth Edition.
2. ACI Committee 213 (1967), "Guide for Structural Lightweight Aggregate Concrete," ACI Journal, Vol. 64, No. 8, American Concrete Institute, August, pp. 433-469.
3. Hanson, J.A. (1961), "Tensile Strength and Diagonal Tension Resistance of Structural Lightweight Concrete," ACI Journal Proceedings, Vol. 58, No. 1, American Concrete Institute, July, pp. 1-40.
4. Ivey, D.L. and Buth, E. (1966), "Splitting Tension Test of Structural Lightweight Concrete," ASTM Journal of Materials, Vol. 1, No.4, pp. 859-871.
5. Pauw, A. (1960), "Static Modulus of Elasticity of Concrete as Affected by Density," ACI Journal, Vol. 57, No. 6, American Concrete Institute, December, pp. 679-687.
6. Russell, H. (2007), "Synthesis of research and Provisions Regarding the Use of Lightweight concrete in Highway bridges," Report No. FHWA-HRT-07-053, Federal Highway Administration report, Washington, DC, August.
7. AASHTO (2017), “AASHTO LRFD Bridge Design Specifications,” American Association of State Highway and Transportation Officials, Eighth Edition
8. Greene, G.G. and Graybeal, B.A. (2013), “Lightweight Concrete: Mechanical Properties,” Report No. FHWA-HRT-13-062, Federal Highway Administration report, Washington, DC, June.
9. Greene, G.G. and Graybeal, B.A. (2014), “Lightweight Concrete: Development of Mild Steel in Tension,” Report No. FHWA-HRT-14-029, Federal Highway Administration report, Washington, DC, January.
10. Greene, G.G. and Graybeal, B.A. (2014), “Lightweight Concrete: Shear Performance,” Report No. FHWA-HRT-15-022, Federal Highway Administration report, Washington, DC, April.
11. AASHTO (2014), “AASHTO LRFD Bridge Design Specifications, Customary U.S. Units,” American Association of State Highway and Transportation Officials, Seventh Edition, with 2015 Interim Revisions.
12. ACI Committee 213 (2003), “Guide for Structural Lightweight Aggregate Concrete,” ACI 213R-03, American Concrete Institute, Farmington Hills, MI.

13. Barnes, R.W., Burnes, N.H., and Kreger, M.E. (1999), "Development Length of 0.6-Inch Prestressing Strand in Standard I-Shaped Pretensioned Concrete Beams," Report No. FHWA/TX-02/1388-1, Center for Transportation Research, University of Texas at Austin, Austin, TX, 338 pp.

14. Barnes, R.W., Grove, J.W., and Burns, N.H. (2003), "Experimental Assessment of Factors Affecting Transfer Length," ACI Structural Journal, Vol. 100, No. 6, American Concrete Institute, November-December, pp. 740-748.

15. Janney, J.R. (1954), "Nature of Bond in Pretensioned Prestressed Concrete," ACI Journal, Vol. 50, No. 8, American Concrete Institute, April, 717-736.

16. Hanson, N.W. and Kaar, P.H. (1959), "Flexural Bond Tests of Pretensioned Prestressed Beams," ACI Journal, Vol. 55, No. 7, American Concrete Institute, January, pp. 783-802.

17. Hoyer, E. and Friedrick, E. (1939), "Beitrag Zur Frage Der Haftspannung in Eisenbetonbauteilen" ("Contribution to the Question of Bond Stress in Reinforced Concrete Elements"), Beton und Eisen, Vol. 38, March 20 [in German]

18. Stocker, M.F. and Sozen, M.A. (1970), "Investigation of Prestressed Concrete for Highway Bridges – Part V: Bond Characteristics of Prestressing Strand," Bulletin 503, Engineering Experiment Station, University of Illinois-Urbana, Urbana, IL.

19. Russell, B.W. and Burns, N.H. (1993), "Design Guidelines for Transfer, Development and Debonding of Large Diameter Seven Wire Strands in Pretensioned Concrete Girders," Report TX-93/1250-5F, Center for Transportation Research, University of Texas at Austin, Austin, TX, January, 300 pp.

20. Buckner, C.D. (1994), "An Analysis of Transfer and Development Lengths for Pretensioned Concrete Structures," Report No. FHWA-RD-94-049, McLean, Virginia, Federal Highway Administration, December, 108 pp.

21. Zia, P. and Mostafa, T. (1977), "Development Length of Prestressing Strands," PCI Journal, Vol. 22, No. 5, Precast/Prestressed Concrete Institute, September-October, pp. 54-65.

22. Mitchell, D., Cook, W.D., Khan, A.A., and Tham, T. (1993), "Influence of High Strength Concrete on Transfer and Development Length of Pretensioning Strand," PCI Journal, Vol. 38, No. 3, Precast/Prestressed Concrete Institute, May-June, pp. 52-66.

23. Base, G. D. (1957), "Some Tests on the Effect of Time on Transmission Length," Research Report No. 5, Magazine of Concrete Research, Vol. 9, No. 26, August, pp. 73-82.

24. Thatcher, D.B., Heffinton, J.A., Kolozs, R.T., Sylva, G.S., Breen, J.E., and Burns, N.H. (2002), "Structural Lightweight Concrete Prestressed Girders and Panels," Report TX-02/1852-1, Center for Transportation Research, University of Texas at Austin, Austin, TX, January, 208 pp.

25. Meyer, K.F, Kahn, L.F., Lai, J.S., and Kurtis, K.E. (2002), "Transfer and Development Length of High-Strength Lightweight Concrete Precast Prestressed Bridge Girders," Task Report 5, Georgia Institute of Technology, Atlanta, Georgia, June, 617 pp.

26. Cousins, T., Roberts-Wollmann, C., Brown, M.C. (2013), "High-Performance/High-Strength Lightweight Concrete for Bridge Girders and Decks, NCHRP Report 733," NCHRP Project 18-15, Transportation Research Board.

27. AASHTO (1996), "Standard Specifications for Highway Bridges," American Association of State Highway and Transportation Officials, 16th Edition.

28. ACI Committee 318 (2014), “Building Code Requirements for Reinforced Concrete (ACI 318-14) and Commentary,” American Concrete Institute, Farmington Hills, MI.

29. Mattock, A. H. (1962), “Proposed Redraft of Section 2611 – Bond, of the Proposed Revision of Building Code Requirements for Reinforced Concrete (ACI 318-56),” ACI Committee 323 Correspondence, October.

30. Ramirez, J.A., and Russell, B.W. (2008), "Transfer, Development, and Splice Length for Strand/Reinforcement in High-Strength Concrete, NCHRP Report 603," NCHRP Project 12-60, Transportation Research Board.

31. Cousins, T.E. and Nassar, A. (2003), “Investigation of Transfer Length, Development Length, Flexural Strength, and Prestress Losses in Lightweight Prestressed Concrete Girders,” Final Report (VTRC 03-CR20), Virginia Transportation Research Council, Charlottesville, VA, April, 44 pp.

32. Peterman, R., Ramirez, J., and Olek, J. (1999), “Evaluation of Strand Transfer and Development Lengths in Pretensioned Girders with Semi-Lightweight Concrete,” Report IN/JTRP-99/3, Purdue University, West Lafayette, IN, July, 193 pp.

33. ACI Committee 408 (2003), "Bond and Development of Straight Reinforcing Bars in Tension," ACI 408R-03, American Concrete Institute, Farmington Hills, MI.

34. Burge, T.A. (1983), "High-Strength Lightweight Concrete with Silica Fume," SP79, Fly Ash, Silica Fume, Slag and Other Mineral By-Products in Concrete, V.M. Malhotra editor, American Concrete Institute, pp. 731-745.

35. Seabrook, P.I. and Wilson, H.S. (1988), "High Strength Lightweight Concrete for use in Offshore Structures: Utilization of Fly Ash and Silica Fume," International Journal of Cement Composites and Lightweight Concrete, Vol. 10, No. 3, August, pp. 183-192.

36. Yeginobali, A., Sobolev, K.G., Soboleva, S.V., Tokyay, M. (1998), "High Strength Natural Lightweight Aggregate Concrete with Silica Fume," ACI SP 178-38, American Concrete Institute, May, 739-758.

37. Greene, G. and Graybeal, B. (2008), “FHWA Research Program on Lightweight High-Performance Concrete – Transfer Length,” PCI National Bridge Conference, Orlando, Florida, October, 16 pp.

38. ASTM C31 (2006), “Standard Practice for Making and Curing Concrete Test Specimens in the Field,” American Society for Testing and Materials Standard Practice C39, Philadelphia, PA.

39. ASTM C39 (2001), “Standard Test Method for Compressive Strength of Cylindrical Concrete Specimens,” American Society for Testing and Materials Standard Practice C39, Philadelphia, PA.

40. ASTM C496 (2002), “Standard Test Method for Splitting Tensile Strength of Cylindrical Concrete Specimens,” American Society for Testing and Materials Standard Practice C496, Philadelphia, PA.

41. ASTM C469 (2002), “Standard Test Method for Static Modulus of Elasticity and Poisson’s Ratio of Concrete in Compression,” American Society for Testing and Materials Standard Practice C469, Philadelphia, PA.

42. Bresler, B., and MacGregor, J.G. (1967), "Review of Concrete Beams Failing in Shear," Journal of Structural Division, ASCE, Vol. 93, No. ST1, February, pp. 343-372.

43. Ivey, D.L., and Buth, E. (1967), "Shear Capacity of Lightweight Concrete Beams," ACI Journal, Vol. 64, No. 10, American Concrete Institute, October, pp. 634-643.

44. Slate, F.O., Nilson, A.H., and Martinez, S. (1986), "Mechanical Properties of High-Strength Lightweight Concrete," ACI Journal, Vol. 83, American Concrete Institute, July-August, pp. 606-613.

45. Rizkalla, S., Mirmiran, A., Zia, P., Russell, H., Mast, R. (2007), "Application of the LRFD Bridge Design Specifications to High-Strength Structural Concrete: Flexure and Compression Provisions, NCHRP Report 595," NCHRP Project 12-64, Transportation Research Board.

46. Vardeman, Stephen B., and Jobe, Marcus J. (2001), Basic Engineering Data Collection and Analysis, Duxbury, Thomson Learning, Pacific Grove, CA.

47. Lowry, R. (2012), Concepts and Applications of Inferential Statistics, http://vassarstats.net/textbook/index.html

48. Shahawy, M.A., Issa, M., and Batchelor, B. (1992), "Strand Transfer Lengths in Full-Scale AASHTO Prestressed Concrete Girders," PCI Journal, Vol. 37, No. 3, Precast/Prestressed Concrete Institute, May-June, pp. 84-96.

49. Dill, J.C., "Development Length of 0.6-inch Diameter Prestressing Strand in High-Performance Concrete," Masters Thesis, Georgia Institute of Technology, Atlanta, GA, May, 322 pp.

50. ASTM C567 (2005), "Standard Test Method for Determining Density of Structural Lightweight Concrete," American Society for Testing and Materials Standard Practice C567, Philadelphia, PA.

## REFERENCES FOR LWC SPECIMENS IN TFHRC DATABASE

51. Cousins, T.E. and Nassar, A. (2003), "Investigation of Transfer Length, Development Length, Flexural Strength, and Prestress Losses in Lightweight Prestressed Concrete Girders," Final Report (VTRC 03-CR20), Virginia Transportation Research Council, Charlottesville, VA, April, 44 pp.

52. Cousins, T., Roberts-Wollmann, C., Brown, M.C. (2013), "High-Performance/High-Strength Lightweight Concrete for Bridge Girders and Decks, NCHRP Report 733," NCHRP Project 18-15, Transportation Research Board.

53. Floyd, R. and Hale, M.H. (2012), "Performance of Prestressed Girders Cast with LWSCC," Mack-Blackwell Rural Transportation Center, University of Arkansas, Fayetteville, AR, August, 506 pp.

54. Greene, G.G. and Graybeal, B.A. (2014), "Lightweight Concrete: Shear Performance," Report No. FHWA-HRT-15-022, Federal Highway Administration report, Washington, DC, April.

55. Greene, G.G. and Graybeal, B.A. ([2015]), "Lightweight Concrete: Transfer and Development Length of Prestressing Strands," Report No. FHWA-HRT-15-[XXX], Federal Highway Administration report, Washington, DC, [April].

56. Meyer, K.F., Kahn, L.F., Lai, J.S., and Kurtis, K.E. (2002), "Transfer and Development Length of High Strength Lightweight Concrete Precast Prestressed Bridge Girders," Georgia Dept. of Trans., GDOT Research Project No. 2004, Task 5 Report, June.

57. Perkins, J. (2006), "Concrete Fluidity Effects on Bond of Prestressed Tendons for Lightweight Bridge Girders," Masters Thesis, Kansas State University, Manhattan, KS, 199 pp.

58. Peterman, R., Ramirez, J., and Olek, J. (1999), "Evaluation of Strand Transfer and Development Lengths in Pretensioned Girders with Semi-Lightweight Concrete," *Report IN/JTRP-99/3*, Purdue University, West Lafayette, IN, July, 193 pp.

59. Thatcher, D.B., Heffinton, J.A., Kolozs, R.T., Sylva, G.S., Breen, J.E., and Burns, N.H. (2002), "Structural Lightweight Concrete Prestressed Girders and Panels," Report TX-02/1852-1, Center for Transportation Research, University of Texas at Austin, Austin, TX, January, 208 pp.

60. Ward, D. (2010), "Performance of Prestressed Double-Tee Beams Cast with Lightweight Self-Consolidating Concrete," Masters Thesis, University of Arkansas, Fayetteville, AR, May, 133 pp.

61. Ziehl, P.H., Rizos, D.C., Caicedo, J.M., Barrios, F., Howard, R.B., and Colmorgan, A.S. (2009), "Investigation of Performance and Benefits of Lightweight SCC Prestressed Concrete Bridge Girders and SCC Materials", Report No. FHWA-SC-09-02/CEE-SG-0662-01, Department of Civil and Environmental Engineering, University of South Carolina, Columbia, SC, October, 182 pp.

## REFERENCES FOR NWC SPECIMENS IN TFHRC DATABASE

62. Barnes, R.W., Burnes, N.H., and Kreger, M.E. (1999), "Development Length of 0.6-Inch Prestressing Strand in Standard I-Shaped Pretensioned Concrete Beams," Report No. FHWA/TX-02/1388-1, Center for Transportation Research, University of Texas at Austin, Austin, TX, 338 pp

63. Braun, M.O. (2002), "Bond Behavior of 15.2 mm (0.6-inch) Diameter Prestressing Strands in San Angelo Bridge Research Beams," Masters Thesis, University of Texas at Austin, Austin, TX, December, 162 pp.

64. Castrodale, R.W. (1988), "A Study of Pretensioned High Strength Concrete Girders in Composite Highway Bridge," Ph.D. Dissertation, University of Texas at Austin, Austin, TX, May, 697 pp.

65. Cousins, T.E. and Nassar, A. (2003), "Investigation of Transfer Length, Development Length, Flexural Strength, and Prestress Losses in Lightweight Prestressed Concrete Girders," Final Report (VTRC 03-CR20), Virginia Transportation Research Council, Charlottesville, VA, April, 44 pp.

66. Cousins, T., Roberts-Wollmann, C., Brown, M.C. (2013), "High-Performance/High-Strength Lightweight Concrete for Bridge Girders and Decks, NCHRP Report 733," NCHRP Project 18-15, Transportation Research Board.

67. Deatherage, J.H., Burdette, E.G., and Chew C.K. (1994), "Development Length and Lateral Spacing Requirements of Prestressing Strand for Prestressed Concrete Bridge Girders," PCI Journal, Vol. 39, No. 1, Precast/Prestressed Concrete Institute, January-February, pp. 70-83.

68. Floyd, R. and Hale, M.H. (2012), "Performance of Prestressed Girders Cast with LWSCC," Mack-Blackwell Rural Transportation Center, University of Arkansas, Fayetteville, AR, August, 506 pp.

69. Kahn, L.K., Dill, J.C., and Reutlinger, C.G. (2002), "Transfer and Development Length of 15-mm Strand in High Performance Concrete Girders," Journal of Structural Engineering, ASCE, Vol. 128, No. 7, July, pp. 913-921.

70. Mitchell, D., Cook, W.D., Khan, A.A., and Tham, T. (1993), "Influence of High Strength Concrete on Transfer and Development Length of Pretensioning Strand," PCI Journal, Vol. 38, No. 3, Precast/Prestressed Concrete Institute, May-June, pp. 52-66.

71. Ozyildirim, C. and Gomez, J.P. (1999), "High-Performance Concrete in a Bridge in Richlands, Virginia," Report VTRC 00-R6, Virginia Transportation Research Council, Charlottesville, VA, September, 44 pp.

72. Ramirez, J.A., and Russell, B.W. (2008), "Transfer, Development, and Splice Length for Strand/Reinforcement in High-Strength Concrete, NCHRP Report 603," NCHRP Project 12-60, Transportation Research Board.

73. Roberts-Wollmann, C., Cousins, T., Carroll, C. (2009), "Grade 300 Prestressing Strand and the Effects of Vertical Casting Position," Report VTRC 10-CR2, Virginia Transportation Research Council, Charlottesville, VA, September, 37 pp.

74. Russell, B.W. and Burns, N.H. (1993), "Design Guidelines for Transfer, Development and Debonding of Large Diameter Seven Wire Strands in Pretensioned Concrete Girders," Report TX-93/1250-5F, Center for Transportation Research, University of Texas at Austin, Austin, TX, January, 300 pp.

75. Shing, P.B., Cooke, D.E., Frangopol, D.M., Leonard, M.A., McMullen, M.L., and Hutter, W. (2000), "Strand Development and Transfer Length Tests on High Performance Concrete Box Girders," PCI Journal, Vol. 45, No. 5, Precast/Prestressed Concrete Institute, September-October, pp. 96-109.

76. Thatcher, D.B., Heffinton, J.A., Kolozs, R.T., Sylva, G.S., Breen, J.E., and Burns, N.H. (2002), "Structural Lightweight Concrete Prestressed Girders and Panels," Report TX-02/1852-1, Center for Transportation Research, University of Texas at Austin, Austin, TX, January, 208 pp.

# APPENDIX A

This appendix contains a table and figures with material test data from the reinforcing bars used in the LWC girders tested at TFHRC as part of the investigation of transfer and development length of prestressing strand in LWC. The tensile data includes yield and ultimate strength, and stress-strain relationship of the mechanical tests.

**Table 55. Reinforcing Bar Mechanical Properties.**

| Tensile Test | Girder Design No. | Coupon | Bar Type | Bar Size | Yield Strength† (ksi) | Ultimate Strength (ksi) |
|---|---|---|---|---|---|---|
| 5-1 | 1 - 4 | 1 | Stirrup | 5 | 76.6 | 116.3 |
| 5-2 | 1 - 4 | 2 | Stirrup | 5 | 73.5 | 113.7 |
| 5-3 | 1 - 4 | 3 | Stirrup | 5 | 69.8 | 110.1 |
| 5-4 | 1 - 4 | 4 | Stirrup | 5 | 71.2 | 112.4 |
| 1-end | 1 - 4 | 1 | End Long.‡ | 6 | 65.2 | 105.6 |
| 3-end | 1 - 4 | 2 | End Long.‡ | 6 | 66.4 | 107.1 |
| 4-conf-1 | All | 1 | Confinement‡ | 4 | 65.5 | 106.5 |
| 4-conf-2 | All | 2 | Confinement‡ | 4 | 66.1 | 107.7 |

Notes:
† Calculated using 0.2 percent offset method
‡ End longitudinal reinforcement (Art. 5.8.3.5); confinement reinforcement (5.10.10.2)
Units: 1.0 ksi = 6.89 MPa

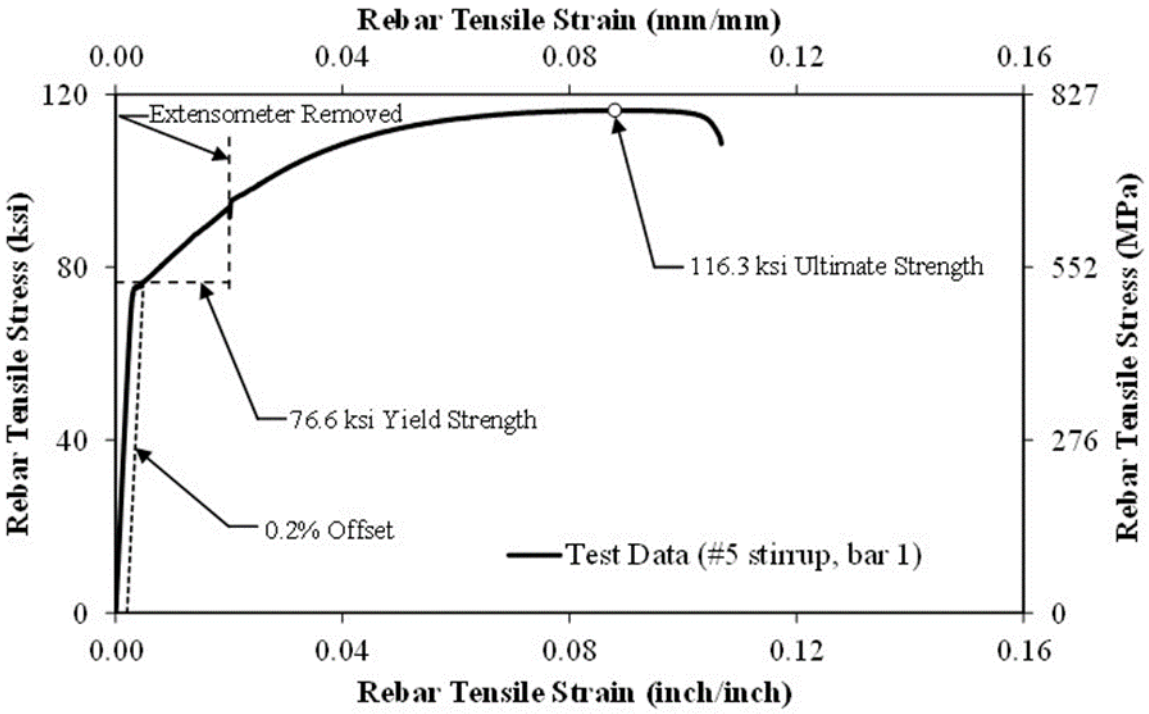


**Figure 101. Graph. Measured Stress-Strain Relationship for #5 Stirrup Reinforcing Bar for Girder Design 1–4 – Coupon 1.**

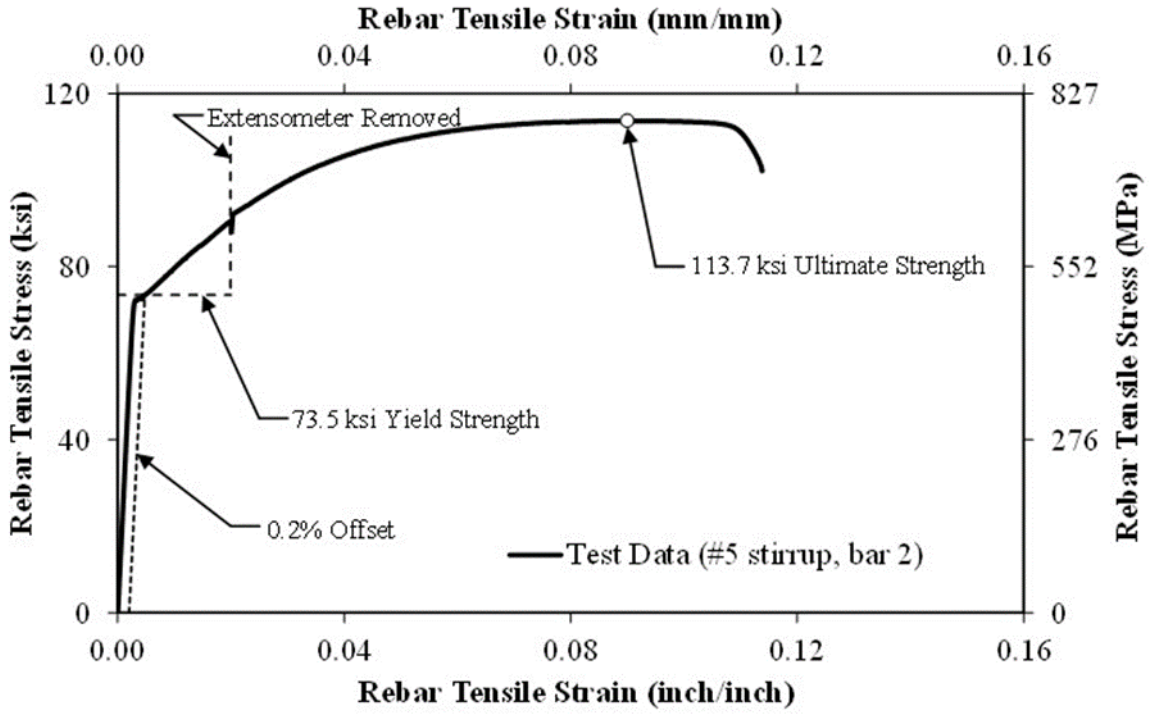


**Figure 102. Graph. Measured Stress-Strain Relationship for #5 Stirrup Reinforcing Bar for Girder Design 1–4 – Coupon 2.**

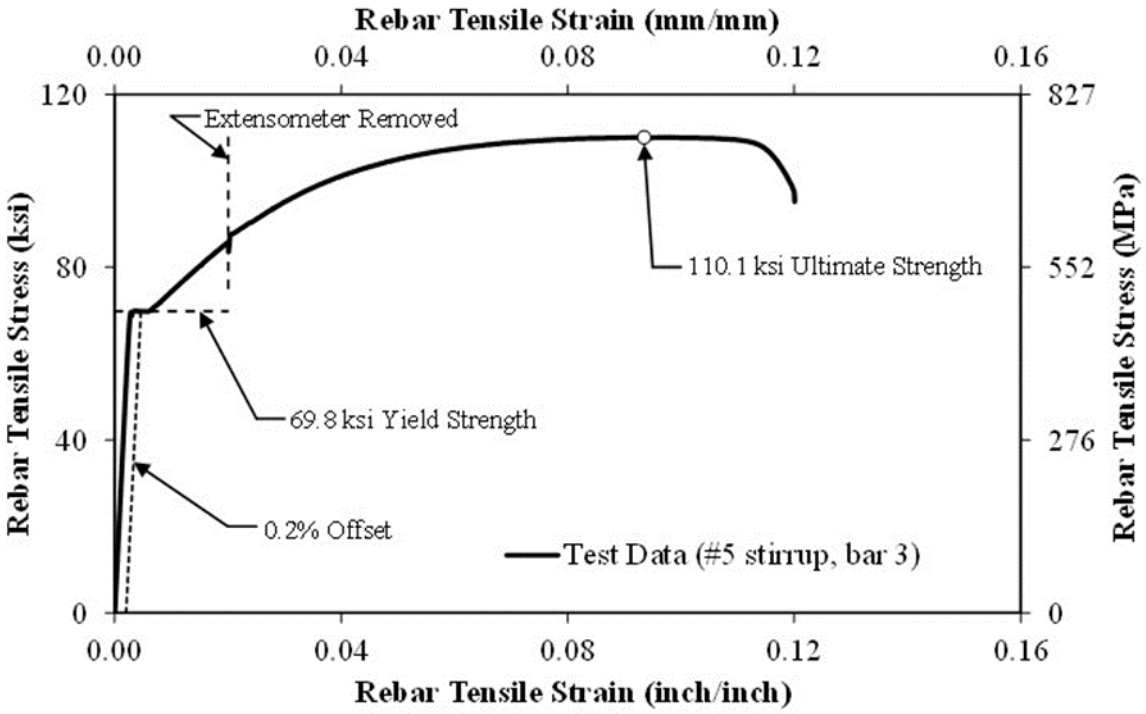


**Figure 103. Graph. Measured Stress-Strain Relationship for #5 Stirrup Reinforcing Bar for Girder Design 1–4 – Coupon 3.**

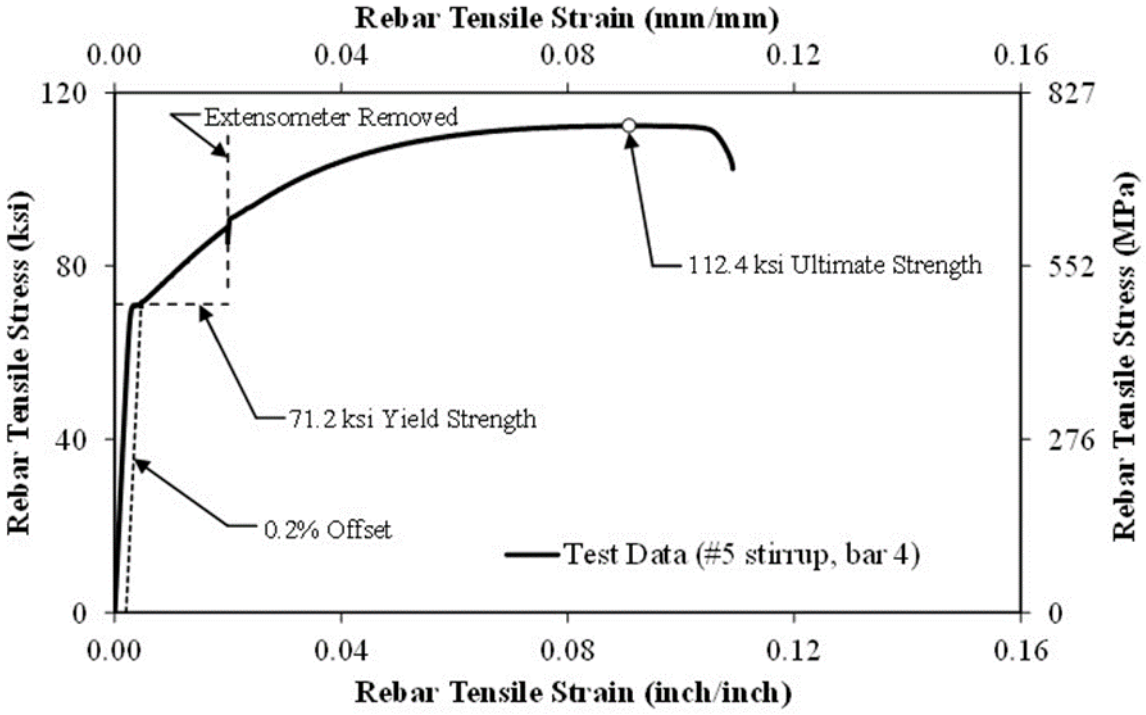


**Figure 104. Graph. Measured Stress-Strain Relationship for #5 Stirrup Reinforcing Bar for Girder Design 1–4 – Coupon 4.**

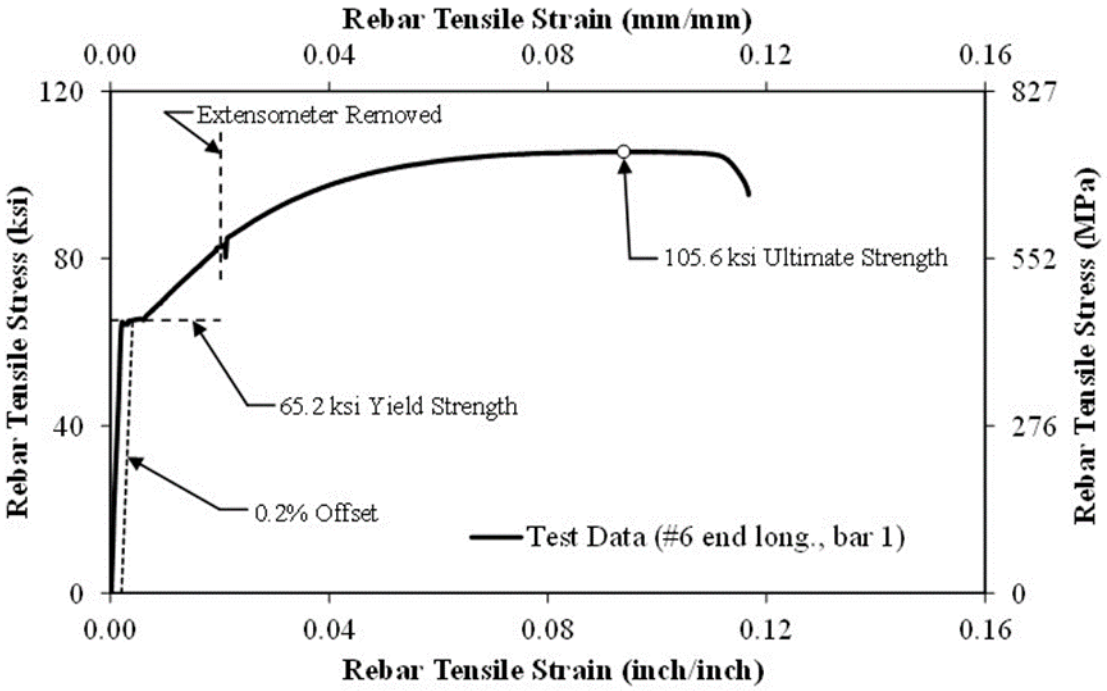


**Figure 105. Graph. Measured Stress-Strain Relationship for #6 End Longitudinal Reinforcing Bar for Girder Design 1–4 – Coupon 1.**

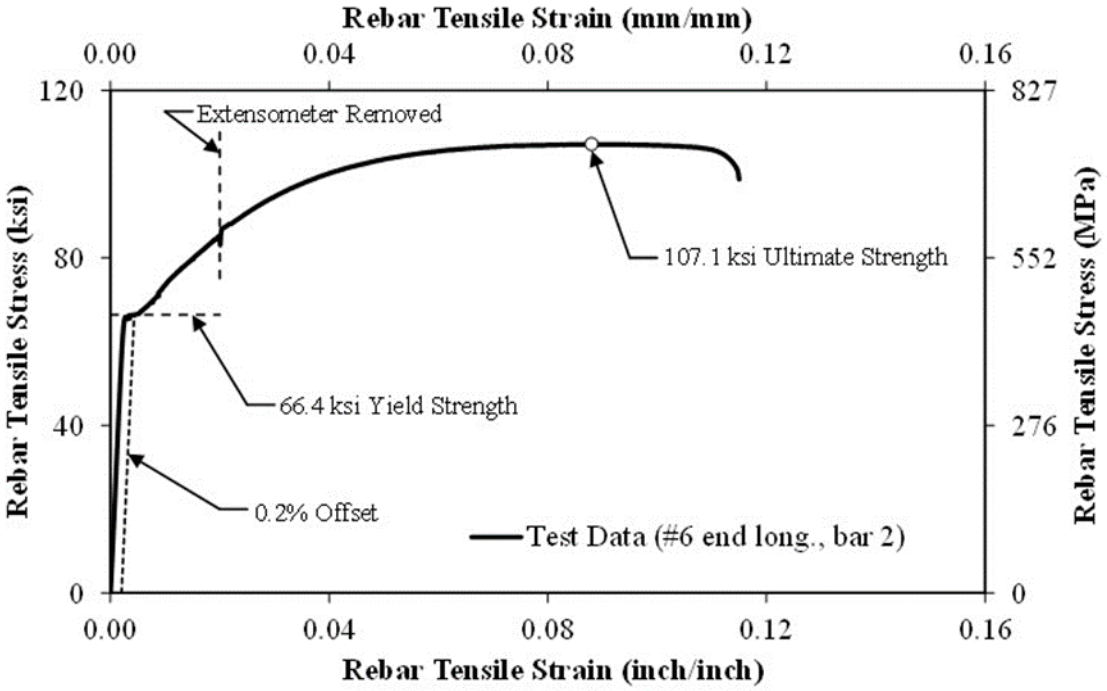


**Figure 106. Graph. Measured Stress-Strain Relationship for #6 End Longitudinal Reinforcing Bar for Girder Design 1–4 – Coupon 2.**

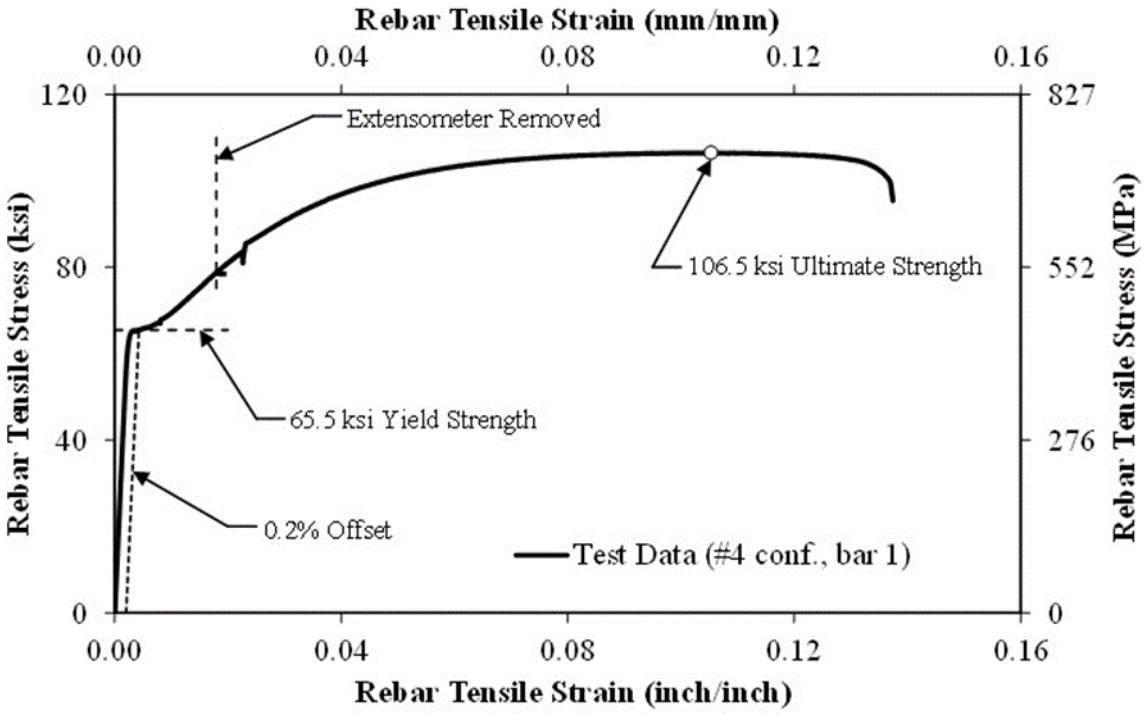


**Figure 107. Graph. Measured Stress-Strain Relationship for #4 End Confinement Reinforcing Bar for Girder Design 1–4 – Coupon 1.**

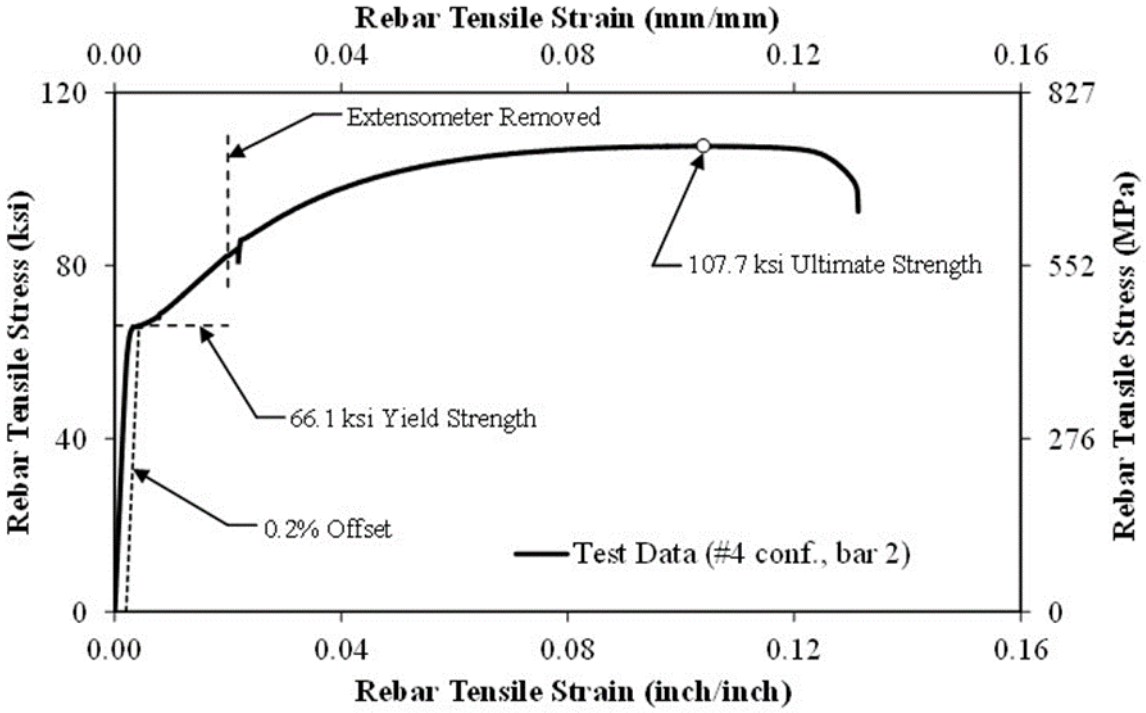


**Figure 108. Graph. Measured Stress-Strain Relationship for #6 End Confinement Reinforcing Bar for Girder Design 1–4 – Coupon 2.**

# APPENDIX B

This appendix contains tables that list the LWC specimens in the TFHRC Database. Specimens with measurements at both ends are indicated with the suffix "_1st" or "_2nd," respectively.

**Table 56. List of LWC Specimens with Transfer Length Measurements in the TFHRC Database.**

| Reference | Specimen Names |
|---|---|
| Cousins and Nassar (2003) | LW8000IV-4A/B |
| Cousins, Roberts-Wollmann, Brown (2013), and Cross (2012) | 1.LW1.5A_1st, 1.LW1.5A_2nd, 1.LW1.5B_1st, 1.LW1.5B_2nd, 2.LWC3.5A_1st, 2.LWC3.5A_2nd, 2.LWC3.5B_1st, 2.LWC3.5B_2nd, 2.LWC3.6A_1st, 2.LWC3.6A_2nd, 2.LWC3.6B_1st, 2.LWC3.6B_2nd, 3.LWC2.5A_1st, 3.LWC2.5A_2nd, 3.LWC2.5B_1st, 3.LWC2.5B_2nd |
| Floyd and Hale (2012) | NSC-1D, NSC-1, NSC-2D, NSC-2, NSC-3D, NSC-3, NSC-4D, NSC-4, NSS-1D, NSS-1, NSS-2D, NSS-2, NSS-3D, NSS-3, NSS-4D, NSS-4, NSS-5D, NSS-5, HSC-1D, HSC-1, HSC-2D, HSC-2, HSC-3D, HSC-3, HSC-4D, HSC-4, HSS-1D, HSS-1, HSS-2D, HSS-2, HSS-3D, HSS-3, HSS-4D, HSS-4 |
| Greene and Graybeal (2013), shear | C8D, A9L, B8D, A8D, B9L, C9L |
| Greene and Graybeal (2014), Lt-Ld | C3L, C1L, C2L, B4L, A4L, C4L, A3L, B3L, A1L, B1L, A2L, B2D |
| Meyer, K.F., Kahn, L.F., Lai, J.S., and Kurtis, K.E. (2002) | G1A-E, G1A-W, G1B-E, G1B-W, G1C-E, G1C-W, G2A-E, G2A-W, G2B-E, G2B-W, G2C-E, G2C-W |
| Perkins (2006) | KC-9_100Ld_1st, KC-9_100Ld_2nd, KC-9_80Ld_1st, KC-9_80Ld_2nd, KC-3_100Ld_1st, KC-3_100Ld_2nd, KC-3_80Ld_1st, KC-3_80Ld_2nd, MQ-9_100Ld_1st, MQ-9_100Ld_2nd, MQ-9_80Ld_1st, MQ-9_80Ld_2nd, MQ-3_100Ld_1st, MQ-3_100Ld_2nd, MQ-3_80Ld_1st, MQ-3_80Ld_2nd, STA-9_100Ld_1st, STA-9_100Ld_2nd, STA-9_80Ld_1st, STA-9_80Ld_2nd, STA-3_100Ld_1st, STA-3_100Ld_2nd, STA-3_80Ld_1st, STA-3_80Ld_2nd |
| Peterman, Ramirez, Olek (1999) | 7SLW-FWC, 7SLW-IST, 7SLW-IST, 10SLW-0.6 |
| Thatcher, Heffinton, Kolozs, Sylva, Breen, and Burns (2001) | LW6000-20-N, LW6000-20-S, LW6000-1-N, LW6000-1-S, LW6000-2-N, LW6000-2-S, LW8000-20-N, LW8000-20-S, LW8000-1-N, LW8000-1-S, LW8000-2-N, LW8000-2-S, LW8000-3-N, LW8000-3-S |
| Ward (2010) | LWSCC 1_1st, LWSCC 1_2nd, LWSCC 2_1st, LWSCC 2_2nd, LWSCC 3_1st, LWSCC 3_2nd, LWSCC 4_1st, LWSCC 4_2nd, LWSCC 5_1st, LWSCC 5_2nd, LWSCC 6_1st, LWSCC 6_2nd |
| Ziehl, Rizos, Caicedo, Barrios, Howard, Colmorgan (2009) | SCLC, SCLC, HESLC, HESLC |

**Table 57. List of LWC Specimens with Development Length Tests in the TFHRC Database.**

| Reference | Specimen Names |
|---|---|
| Cousins and Nassar (2003) | LW8000II-1A, LW8000II-1B, LW8000II-2C, LW8000II-2D |
| Cousins, Roberts-Wollmann, Brown (2013) | 1.LW1.5A_1st, 1.LW1.5A_2nd, 1.LW1.5B_1st, 1.LW1.5B_2nd, 2.LWC3.5A_1st, 2.LWC3.5A_2nd, 2.LWC3.5B_1st, 2.LWC3.5B_2nd, 2.LWC3.6A_1st, 2.LWC3.6A_2nd, 2.LWC3.6B_1st, 2.LWC3.6B _2nd, 3.LWC2.5A_1st, 3.LWC2.5A_2nd, 3.LWC2.5B_1st, 3.LWC2.5B_2nd |
| Floyd and Hale (2012) | NSC-1_1st, NSC-1_2nd, NSC-2_1st, NSC-2_2nd, NSC-3_1st, NSC-3_2nd, NSC-4_1st, NSC-4_2nd, NSS-1_1st, NSS-1_2nd, NSS-2_1st, NSS-2_2nd, NSS-3_1st, NSS-3_2nd, NSS-4_1st, NSS-4_2nd, NSS-5_1st, NSS-5_2nd, HSC-1_1st, HSC-1_2nd, HSC-2_1st, HSC-2_2nd, HSC-3_1st, HSC-3_2nd, HSC-4_1st, HSC-4_2nd, HSS-1_1st, HSS-1_2nd, HSS-2_1st, HSS-2_2nd, HSS-3_1st, HSS-3_2nd, HSS-4_1st, HSS-4_2nd |
| Greene and Graybeal (2014), Lt-Ld | C3L, C1L, C2L, C1D, C3D, B4L, A4L, C4L, A4D, C4D, B4D, A3L, B3L, A1L, B1L, A2L, A3D, B3D, A1D, B1D, B2D, B2L |
| Meyer, K.F., Kahn, L.F., Lai, J.S., and Kurtis, K.E. (2002) | G1A-E, G1A-W, G1B-E, G1B-W, G1C-E, G1C-W, G2A-E, G2A-W, G2B-E, G2B-W, G2C-E, G2C-W |
| Perkins (2006) | KC-9_100Ld_1st, KC-9_100Ld_2nd, KC-9_80Ld_1st, KC-9_80Ld_2nd, KC-3_100Ld_1st, KC-3_100Ld_2nd, KC-3_80Ld_1st, KC-3_80Ld_2nd, MQ-9_100Ld_1st, MQ-9_100Ld_2nd, MQ-9_80Ld_1st, MQ-9_80Ld_2nd, MQ-3_100Ld_1st, MQ-3_100Ld_2nd, MQ-3_80Ld_1st, MQ-3_80Ld_2nd, STA-9_100Ld_1st, STA-9_100Ld_2nd, STA-9_80Ld_1st, STA-9_80Ld_2nd, STA-3_100Ld_1st, STA-3_100Ld_2nd, STA-3_80Ld_1st, STA-3_80Ld_2nd |
| Peterman, Ramirez, Olek (1999) | 7SLW-FWC-1S, 7SLW-FWC-1L, 7SLW-FWC-2S, 7SLW-FWC-3S, 7SLW-FWC-3L, 7SLW-IST-2S, 7SLW-IST-2L, 7SLW-IST-3S, 7SLW-IST-3L, 10SLW-0.6-1S, 10SLW-0.6-3S, 10SLW-0.6-2L, T-Beam IST1, T-Beam IST2, T-Beam FWC, 10 ksi T-Beam, T-Beam FWC-3", T-Beam FWC-6", T-Beam FWC-15" |
| Thatcher, Heffinton, Kolozs, Sylva, Breen, and Burns (2001) | LW6000-1-N, LW6000-1-S, LW6000-2-N, LW6000-2-S, LW8000-1-N, LW8000-1-S, LW8000-2-N, LW8000-2-S, LW8000-3-N, LW8000-3-S |
| Ward (2010) | LWSCC 1, LWSCC 2, LWSCC 3, LWSCC 4, LWSCC 5, LWSCC 6 |

# APPENDIX C

This appendix contains tables that list the NWC specimens in the TFHRC Database. Specimens with measurements at both ends are indicated with the suffix "_1st" or "_2nd," respectively.

**Table 58. List of NWC Specimens with Transfer Length Measurements in the TFHRC Database.**

| Reference | Specimen Names |
|---|---|
| Barnes, Burns, and Kreger (1999) | L0B-A-96, L0B-B-72, L0B-C-54H, L0B-D-54, M0B-A-96, M0B-B-72, M0B-C-54H, M0B-D-54, H0B-A-96, H0B-B-72, H0B-C-54H, H0B-D-54 |
| Braun (2002) | H1S, H1N, H2S, H2N, N1S, N1N, N2S, N2N |
| Castrodale (1988) | 5G-4-1, 5G-4-1, 5G-4-2, 5G-4-2, 5S-4-1, 5S-4-1, 5S-4-2, 5S-4-2, 10G-4-1, 10G-4-1, 10G-4-2, 10G-4-2, 10S-4-1, 10S-4-1, 10S-4-2, 10S-4-2, 5G-6-1, 5G-6-1, 5G-6-2, 5G-6-2, 5S-6-2, 5S-6-2 |
| Cousins, Roberts-Wollmann, Brown (2013) | 1.NW1.5A_1st, 1.NW1.5A_2nd, 1.NW1.5B_1st, 1.NW1.5B_2nd, 3.NWC1.6A_1st, 3.NWC1.6A_2nd, 3.NWC1.6B_1st, 3.NWC1.6B_2nd |
| Deatherage, Burdette, and Chew (1994) | 5-1-EXT, 5-1-INT, 5-2-EXT, 5-2-INT, 5-3-EXT, 5-3-INT, 5-4-EXT, 5-4-INT, 5-SWAI-EAST, 5-SWAI-WEST, 5-UWR-EAST, 5-UWR-WEST, 5-FWC-EAST, 5-FWC-WEST, 5-ASW-EAST, 5-ASW-WEST, 5S-1-EXT, 5S-1-INT, 5S-2-EXT, 5S-2-INT, 5S-3-EXT, 5S-3-INT, 5S-4-EXT, 5S-4-INT, 916-1-EXT, 916-1-INT, 916-2-EXT, 916-2-INT, 916-3-EXT, 916-3-INT, 916-4-EXT, 916-4-INT, 6-1-EXT, 6-1-INT, 6-2-EXT, 6-2-INT, 6-3-EXT, 6-3-INT, 6-4-EXT, 6-4-INT |
| Floyd and Hale (2012) | NSL-1D, NSL-1, NSL-2D, NSL-2, NSL-3D, NSL-3, NSL-4D, NSL-4, HSL-1D, HSL-1, HSL-2D, HSL-2, HSL-3D, HSL-3, HSL-4D, HSL-4 |
| Kahn, Dill, and Reutlinger (2002) | G2AN, G2AS, G2BN, G2BS, G4AN, G4AS, GRBN, G4BS |
| Mitchell, Cook, Khan, and Tham (1993) | 9.5/31-1200, 9.5/43-1350, 9.5/43-1350, 9.5/43-1000, 9.5/43-1000, 9.5/65-800, 9.5/75-950, 9.5/75-950, 9.5/75-700, 9.5/75-700, 9.5/89-825, 9.5/89-825, 9.5/89-575, 9.5/89-575, 13/31-1200, 13/43-1600, 13/43-1600, 13/43-1250, 13/43-1250, 13/65-850, 13/75-1100, 13/75-1100, 13/75-950, 13/75-950, 13/89-950, 13/89-950, 13/89-650, 13/89-650, 16/31-1865, 16/31-1865, 16/31-1500, 16/31-1500, 16/65-1150, 16/65-1150, 16/65-725, 16/65-725, 16/89-975, 16/89-975, 16/89-675, 16/89-675 |
| Ozyildirim and Gomez (1999) | 1 end A, 1 end B, 2 end A, 2 end B, A Live, A Dead, B Live, B Dead, C Live, C Dead |
| Ramirez and Russell (2008) | RB4-5-1_North, RB4-5-1_South, RA6A-5-1_North, RA6A-5-1_South, RA8-5-1_North, RA8-5-1_South, RA8-5-1-T_North, RA8-5-1-T_South, RA10-5-1_North, RA10-5-1_South, RA10-5-1-T_North, RA10-5-1-T_South, RD4-5-1_North, RD4-5-1_South, RD6A-5-1_North, RD6A-5-1_South, RD8-5-1_North, RD8-5-1_South, RD8-1-T_North, RD8-1-T_South, RD10-5-1_North, RD10-5-1_South, RD10-5-1-T_North, RD10-5-1-T_South, RA4-6-1_North, RA4-6-1_South, RA6-6-1_North, RA6-6-1_South, RA8-6-1_North, RA8-6-1_South, RA10-6-1_North, RA10-6-1_South, IB6-5-1_North, IB10-5-1_North, ID6-5-1_North, ID10-5-1_North, IA6-6-2_North, IA6-6-2_South, IA10-6-1_North, IA10-6-2_North |

**Table 58 (continued). List of NWC Specimens with Transfer Length Measurements in the TFHRC Database.**

| Reference | Specimen Names |
|---|---|
| Roberts-Wollmann, Cousins, Carroll (2009) | 1.270.5N.R_1st, 1.270.5N.R_2nd, 2.270.5N.R_1st, 2.270.5N.R_2nd, 3.270.5S.R_1st, 3.270.5S.R_2nd, 4.270.5S.R_1st, 4.270.5S.R_2nd, 5.270.5S.R_1st, 5.270.5S.R_2nd, 6.270.5S.R_1st, 6.270.5S.R_2nd, 1.300.5N.R, 2.300.5N.R_1st, 2.300.5N.R_2nd, 3.300.5S.R_1st, 3.300.5S.R_2nd, 4.300.5S.R_1st, 4.300.5S.R_2nd, 5.300.5S.R_1st, 5.300.5S.R_2nd, 6.270.6N.R_1st, 6.270.6N.R_2nd |
| Russell and Burns (1993) | SS150-3_cut, SS150-3_dead, SS150-4_cut, SS150-4_dead, SS150-5_cut, SS150-5_dead, SS150-6_cut, SS150-6_dead, SS160-1_cut, SS160-2_dead, SS160-3_dead, SS160-4_cut, SS160-4_dead, SS160-5_cut, SS160-5_dead, SS160-6_cut, SS160-6_dead, SS160-7_cut, SS160-7_dead, SS160-8_cut, SS160-8_dead, FC150-11_north, FC150-11_south, FC150-12_north, FC150-12_south, FC160-12_north, FC160-12_south, FC350-1_north, FC350-1_south, FC350-2_north, FC350-2_south, FCT350-3_north, FCT350-3_south, FCT350-4_north, FCT350-4_south, FC550-1_north, FC550-1_south, FCT550-2_north, FCT550-2_south, FC550-3_north, FC550-3_south, FC360-1_north, FC360-1_south, FC360-2_north, FC360-2_south, FCT360-3_north, FCT360-3_south, FCT360-4_north, FCT360-4_south, FC362-11_north, FC362-11_south, FCT362-12_north, FCT362-12_south, FC362-13_north, FC362-13_south, FC560-1_north, FC560-1_south, FCT560-2_north, FCT560-2_south, FC560-3_north, FC560-3_south, FA550-1_north, FA550-1_south, FA550-2_north, FA550-2_south, FA550-3_north, FA550-3_south, FA550-4_north, FA550-4_south, FA460-1_north, FA460-1_south, FA460-2_north, FA460-2_south, FA460-3_north, FA460-3_south, FA460-F4_north, FA460-F4_south, FA460-5_north, FA460-5_south, FA460-6_north, FA460-6_south |
| Shing, Cooke, Frangopol, Leonard, McMullen, and Hutter (2000) | 1-E, 1-W, 2-E, 2-W, 3-E, 3-W |
| Thatcher, Heffinton, Kolozs, Sylva, Breen, and Burns (2001) | NW6000-1-N, NW6000-1-S |

**Table 59. List of NWC Specimens with Development Length Tests in the TFHRC Database.**

| Reference | Specimen Names |
|---|---|
| Barnes, Burns, and Kreger (1999) | L0B-A-96, L0B-B-72, L0B-C-54H, L0B-D-54, M0B-A-96, M0B-B-72, M0B-C-54H, M0B-D-54, H0B-A-96, H0B-B-72, H0B-C-54H, H0B-D-54 |
| Braun (2002) | H1S, H1N, H2S, H2N, N1S, N1N, N2S |
| Cousins and Nassar (2003) | LW8000II-3B |
| Cousins, Roberts-Wollmann, Brown (2013) and Cross (2012) | 1.NW1.5A_1st, 1.NW1.5A_2nd, 1.NW1.5B_1st, 1.NW1.5B_2nd, 3.NWC1.6A_1st, 3.NWC1.6A_2nd, 3.NWC1.6B_1st, 3.NWC1.6B_2nd |
| Deatherage, Burdette, and Chew (1994) | 5-1-EXT, 5-1-INT, 5-2-EXT, 5-2-INT, 5-3-EXT, 5-3-INT, 5-4-EXT, 5-4-INT, 5-SWAI-EAST, 5-SWAI-WEST, 5-UWR-EAST, 5-UWR-WEST, 5-FWC-EAST, 5-FWC-WEST, 5-ASW-EAST, 5-ASW-WEST, 5S-1-EXT, 5S-1-INT, 5S-2-INT, 5S-3-EXT, 5S-3-INT, 5S-4-EXT, 5S-4-INT, 916-1-EXT, 916-1-INT, 916-2-EXT, 916-2-INT, 916-3-EXT, 916-3-INT, 916-4-EXT, 916-4-INT, 6-1-EXT, 6-1-INT, 6-2-EXT, 6-2-INT, 6-3-EXT, 6-3-INT, 6-4-EXT, 6-4-INT |
| Floyd and Hale (2012) | NSL-1D, NSL-1, NSL-2D, NSL-2, NSL-3D, NSL-3, NSL-4D, NSL-4, HSL-1D, HSL-1, HSL-2D, HSL-2, HSL-3D, HSL-3, HSL-4D, HSL-4 |
| Kahn, Dill, and Reutlinger (2002) | G2AN, G2AS, G2BN, G2BS, G4AN, G4AS, GRBN, G4BS |
| Mitchell, Cook, Khan, and Tham (1993) | 9.5/31-1200, 9.5/31-1100, 9.4/43-1350, 9.5/43-1000, 9.5/65-800, 9.5/65-725, 9.5/75-950, 9.5/75-700, 9.5/89-825, 9.5/89-575, 13/31-1250, 13/31-1200, 13/31-1100, 13/43-1600, 13/43-1250, 13/65-850, 13/65-700, 13/65-650, 13/75-1100, 13/75-950, 13/89-950, 13/89-650, 16/31-1865, 16/31-1800, 16/31-1650, 16/31-1500, 16/65-1150, 16/65-1050, 16/65-950, 16/65-800, 16/65-700, 16/65-725, 16/89-975, 16/89-675 |
| Ozyildirim and Gomez (1999) | 1 end A, 1 end B, 2 end A, 2 end B |
| Ramirez and Russell (2008) | RB4-5-1_North, RB4-5-1_South, RA6A-5-1_North, RA6A-5-1_South, RA8-5-1_North, RA8-5-1_South, RA10-5-1_North, RA10-5-1_South, RD4-5-1_North, RD4-5-1_South, RD6A-5-1_North, RD6A-5-1_South, RD8-5-1_North, RD8-5-1_South, RD10-5-1_North, RD10-5-1_South, RA4-6-1_North, RA4-6-1_South, RA6-6-1_North, RA8-6-1_North, RA10-6-1_North, IB6-5-1_South, IB10-5-1_North, IB10-5-1_South, ID6-5-1_North, ID6-5-1_South, ID10-5-1_North, ID10-5-1_South, IA10-6-1_South, IA10-6-2_S |
| Roberts-Wollmann, Cousins, Carroll (2009) | 1.270.5N.R_1st, 1.270.5N.R_2nd, 2.270.5N.R_1st, 2.270.5N.R_2nd, 3.270.5S.R_1st, 3.270.5S.R_2nd, 4.270.5S.R_1st, 4.270.5S.R_2nd, 5.270.5S.R_1st, 5.270.5S.R_2nd, 6.270.5S.R_1st, 6.270.5S.R_2nd, 1.300.5N.R, 2.300.5N.R_1st, 2.300.5N.R_2nd, 3.300.5S.R_1st, 3.300.5S.R_2nd, 4.300.5S.R_1st, 4.300.5S.R_2nd, 5.300.5S.R_1st, 5.300.5S.R_2nd, 6.270.6N.R_1st, 6.270.6N.R_2nd |

**Table 59 (continued). List of NWC Specimens with Development Length Tests in the TFHRC Database.**

| Reference | Specimen Names |
|---|---|
| Russell and Burns (1993) | FA550-1B, FA550-1C, FA550-2A, FA550-3A, FA550-3B, FA550-4A, FA550-4B, FA460-1A, FA460-1B, FA460-2A, FA460-2B, FA460-3A, FA460-3B, FA460-5A, FA460-5B, FA460-6A, FA460-6B |
| Shing, Cooke, Frangopol, Leonard, McMullen, and Hutter (2000) | 1-E, 1-W, 2-E, 2-W, 3-E, 3-W |
| Thatcher, Heffinton, Kolozs, Sylva, Breen, and Burns (2001) | NW6000-1-N, NW6000-1-S |

# APPENDIX D

This appendix contains detailed results of the 24 development length tests on high-strength LWC prestressed girders that were tested at TFHRC. Tables for each test give information about the girder geometry and reinforcement, material properties, test setup, and measured transfer length. The tables also give the applied load, internal shear force, measured deflection, and measured reinforcement strain, strand slip, and deck strain. A figure shows the applied average shear stress versus measured deflection. The measured concrete surface strain at each end, the smoothed concrete surface strain, the 95 percent average maximum strain, and the transfer length determined from the measured strain is shown in a figure. Additional figures show the measured strain in the girder end reinforcement, measured longitudinal strain, measured transverse strain, and measured crack angles. Photographs show the girder before ultimate, after ultimate, and the failure mode.

The research data contained in this appendix has not been published. A draft copy of this appendix is available in hardcopy by contacting Benjamin Graybeal at Benjamin.Graybeal@dot.gov.

# APPENDIX E

This appendix contains the drawings of the TFHRC prestressed concrete girders that were given to the beam fabricator.

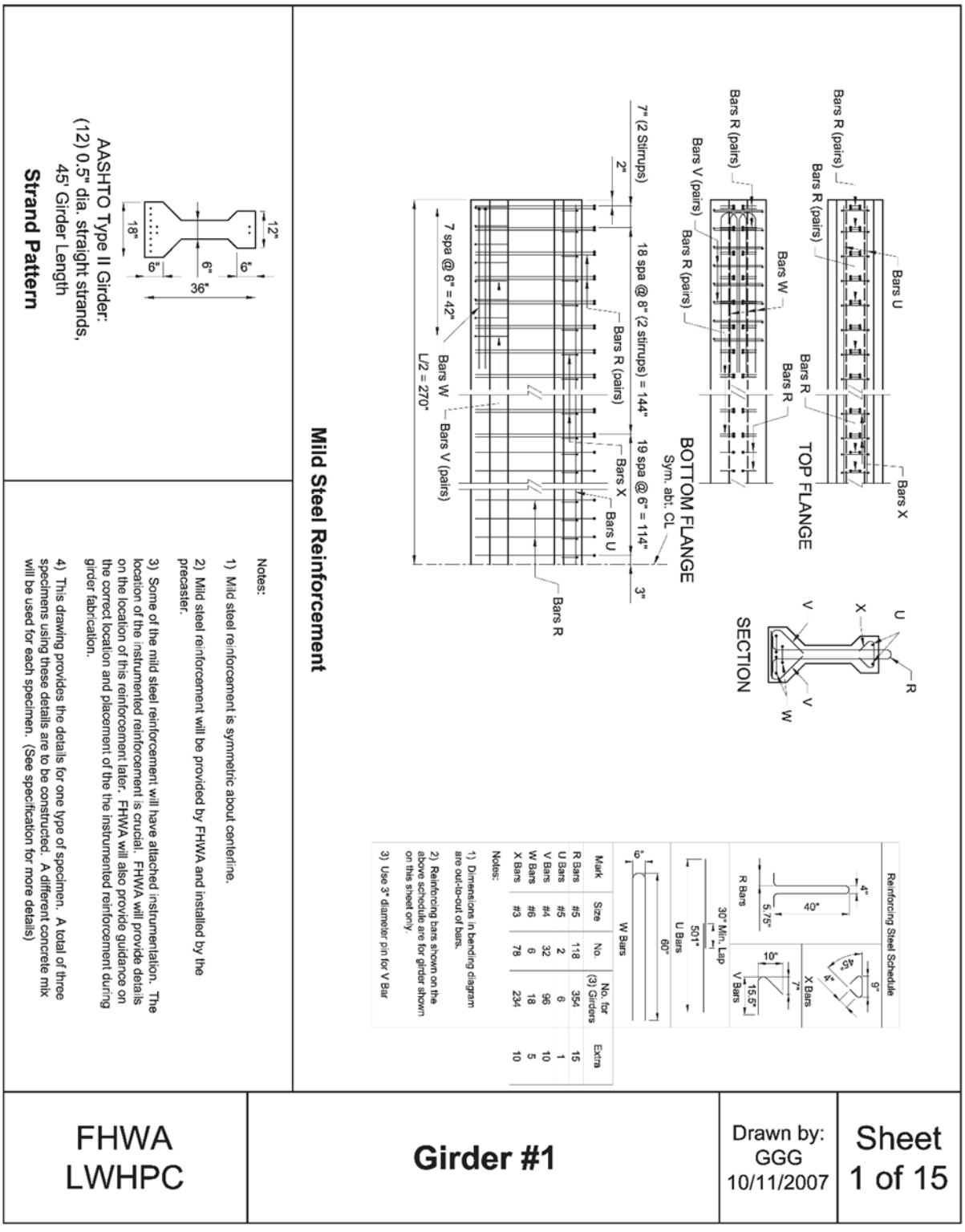


**Figure 109. Illustration. Drawing of girder design 1.**

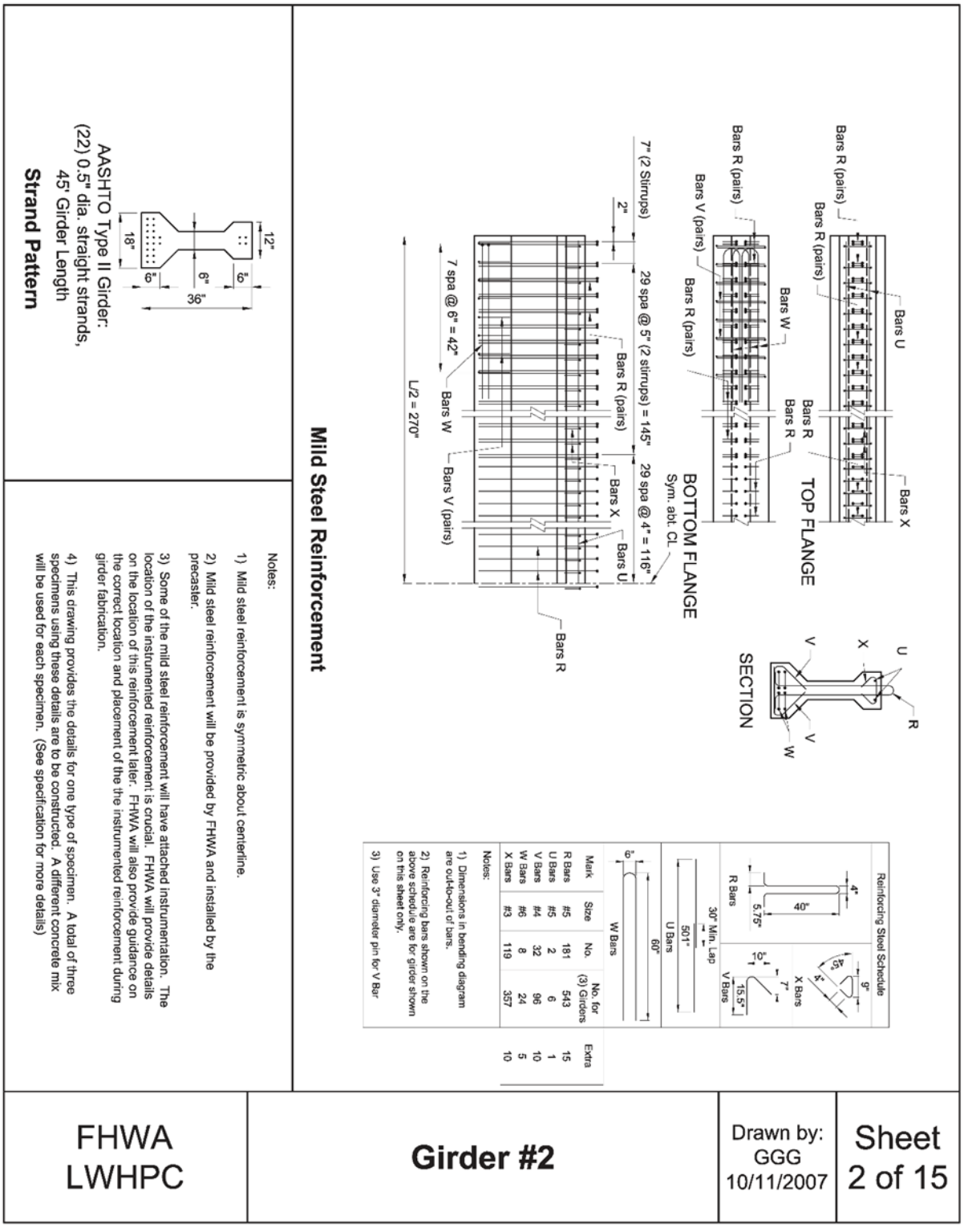


**Figure 110. Illustration. Drawing of girder design 2.**

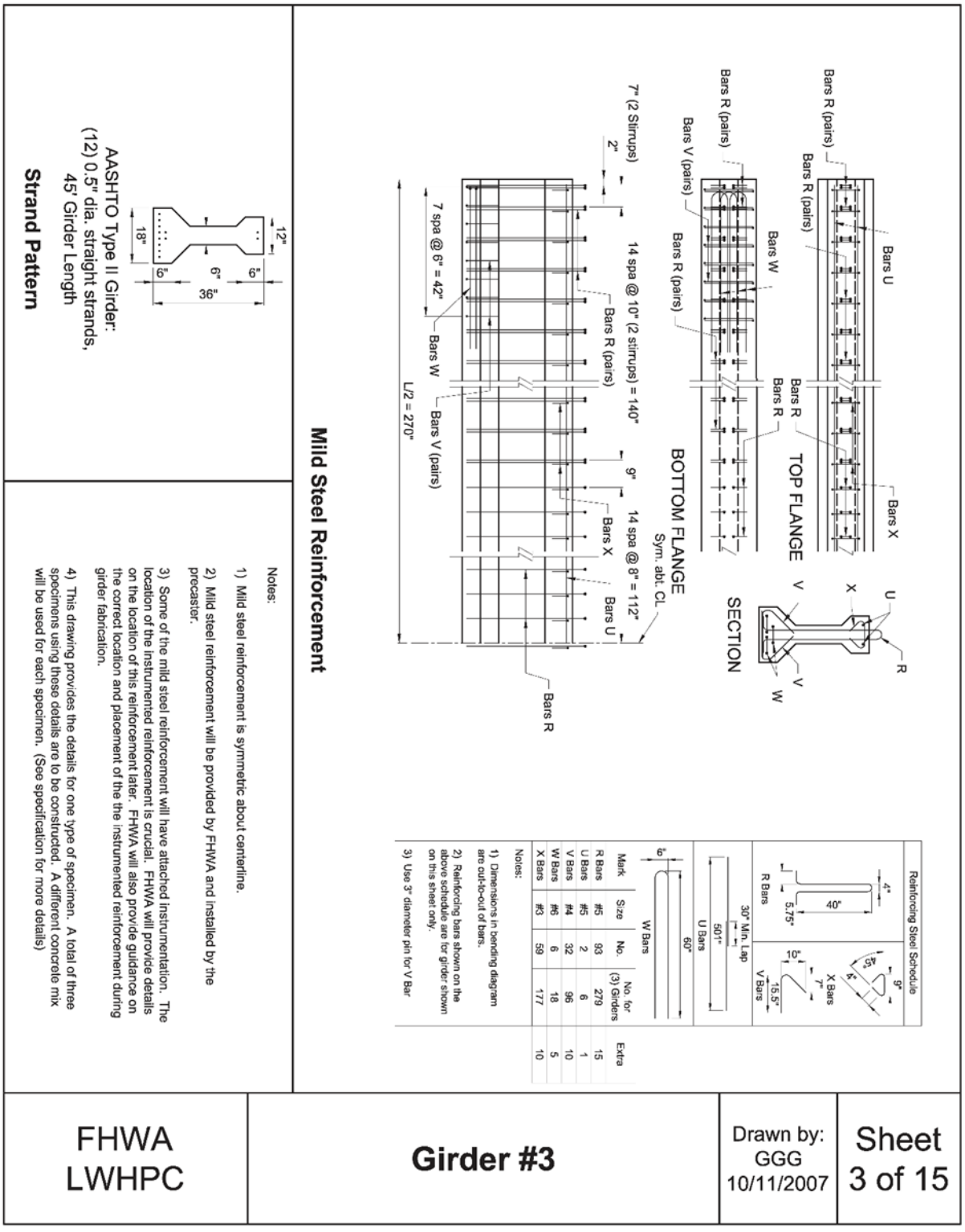


**Figure 111. Illustration. Drawing of girder design 3.**

**Figure 112. Illustration. Drawing of girder design 4.**

Publication FHWA-HIF-19-018
HRDI-40/2-19(WEB)EHIF